Optical, Nonlinear Optical and Semiconducting Molecular Materials Based on Remote Functionalized Chromophores and Polyelectrolyte Templated Molecules and Polymers

A Thesis Submitted for the Degree of
DOCTOR OF PHILOSOPHY

by

Jayanty Subbalakshmi

School of Chemistry
University of Hyderabad
Hyderabad 500 046
INDIA

September 2003

Dedicated   to

My Parents & Husband

CONTENTS

DECLARATION

I hereby declare that the matter embodied in this thesis is the result of investigations carried out by me in the School of Chemistry, University of Hyderabad, Hyderabad under the supervision of Prof. T. P. Radhakrishnan.

In keeping with the general practice of reporting scientific observations, due acknowledgements have been made wherever the work described is based on the findings of other investigators.

Jayanty Subbalakshmi

CERTIFICATE

This is to certify that the work described in this thesis entitled **"Optical, Nonlinear Optical and Semiconducting Molecular Materials Based on Remote Functionalized Chromophores and Polyelectrolyte Templated Molecules and Polymers"** has been carried out by Jayanty Subbalakshmi, under my supervision and the same has not been submitted elsewhere for any degree.

Prof. T. P. Radhakrishnan
(Thesis Supervisor)

Dean
School of Chemistry
University of Hyderabad
DEAN
School of Chemistry
University of Hyd.
Hyderabad-46.

ACKNOWLEDGEMENTS

I take this opportunity to express profound respect and a deep sense of gratitude to *my guru,* Prof. T. P. Radhakrishnan. Without his constant guidance, encouragement and above all his cooperation, the thesis would not have taken this shape. I am indebted to him for the freedom he gave me in carrying out my research and the time he spent in trying to explain various facts and concepts. His commitment to the work with a great sense of dedication, motivation, discipline and patience are highly admirable and very inspiring.

I thank Prof. E. D. Jemmis, Dean School of Chemistry, former Deans and other faculty members of the school for their support and help on various occasions. I thank Prof. D. Narayana Rao, School of Physics for his help. I thank all my M. Phil. teachers at the School of Chemistry for their wonderful teaching from which I have benefited very much. Special thanks are due to Prof. Kumaraswamy and Prof. Bhaskar Maiya. I thank DST for the National Single Crystal X-ray Diffractometer Facility at our School and CSIR for the financial support.

I am deeply indebted to all my teachers in school and college, especially Dr. G. S. Moses, Late Dr. Krishnamacharyulu, Sambasivarao garu and Mrs. Vijayalakshmi for their encouragement and affection.

I also thank all the non-teaching staff for their assistance in carrying out my research. The assistance of Raghavaiah, Dr. Manjunadh, Mr. Murthy, Mrs. Asia, Mr. Vincent are gratefully appreciated. I thank Dr. P. Sharma for help with some of the computations.

It is a great pleasure to thank my seniors Dr. S. Prasanna, Dr. M. Ravi, Dr. B. L. V. Prasad, Dr. Sonika Sharma and Dr. G. K. Prasad for their help and cooperation. My special thanks to Dr. Palas gangopadhyay for his support and timely help during his stay. I especially thank Philip and Sharat for extending their cooperation and help during my thesis work. Thanks to Prakash, Shatabdi, Srinivas, Prem, Joseph, Manoj and other laser

labmates for their cooperation. I am extremely thankful to Dr. Sailaja, Aparna and Padmaja for making my stay in the campus a memorable one.

I am at a loss of words to thank my parents, my in-laws for their love, affection, care and unstinting support. I thank my mother-in-law, for her timely help. I also thank my sister, brother-in-law, brother and sister-in-law for their constant support. I would like to include Maithili, Chandu, Srivani and Rohit for the moments of joy we shared together. I am grateful to all my relatives for their constant encouragement. I am sincerely thankful to my husband for his love, cooperation, understanding, patience and moral support through out my research work which has helped in the successful completion of this thesis.

I thank all my friends Sudha, Kavitha, Rama, Aruna, Visweshwar, Venu, Reddy, Sastry, Srihari, Srinivas, Praveen, Sankaran, Satyen and other friends in the School for helping me always.

Jayanty Subbalakshmi

COMMON ABBREVIATIONS

AM1	Austin Model 1
br	broad
CD	circular dichroism
CI	configuration interaction
COSMO	conductor-like screening model
CT	charge transfer
d	doublet
D, A	donor, acceptor
DADQ	diaminodicyanoquinodimethane
DDQ	2,3-dichloro-5,6-dicyano-1,4-benzoquinone
dec.	decomposition
Iod	iodide
LB	Langmuir-Blodgett
m	multiplet
M.P.	melting point
NIR	near ir
NLO	nonlinear optical
PANI	polyaniline
Pic	picrate
PSS	poly(4-styrenesulfonate)
PVA	polyvinyl alcohol
s	singlet
SHG	second harmonic generation
t	triplet
TCNQ	tetracyanoquinodimethane
Tos	tosylate
TPA	terephthalic acid
TTF	tetrathiafulvalene

CHAPTER 1

Introduction

1.1   MOLECULAR MATERIALS

The latter half of the last century has witnessed a steady growth of the field of molecular materials culminating in their current status as promising candidates for a wide spectrum of technologies in this century. The defining characteristic of molecular materials[1] is their constitution - molecules or molecular ions are their building blocks as opposed to atoms and ions in the traditional solid state. Polymeric materials built from macromolecules can also be classified as belonging to the general family of molecular materials. Molecular materials represent a fundamental and significant departure from the traditional routes of materials fabrication, affording greater flexibility and versatility. They also possess unique electronic, magnetic or optical features opening up the possibility of realizing a vast range of novel applications.

Molecular materials are rather unique in the sense that when dissolved in appropriate solvents, melted or sublimed they break down into their constituents which retain to a large extent the characteristics they exhibited in the solid state. Traditional solids like inorganic salts, metal oxides, covalent solids, metals and alloys, on the other hand, exhibit vastly different characteristics in the bulk state compared to their constituent atoms or ions. It is natural that nanoscale materials[2] which are at the focus of extensive scientific and technological research today, show stark differences from the atomic and bulk limits in the case of metals and semiconductors, whereas in the case of molecular materials, the supramolecular clusters[3] represent a smooth transition from the molecular to the bulk material. Molecular materials utilize, in addition to ionic and covalent interactions, a wide variety of relatively weaker interactions such as H-bonds, *n*-stacking and dispersion forces not found elsewhere in conventional solid state materials[14] (Fig. 1.1). The nature of the forces in the molecular materials may however be quite different from that in other solids. For example the electrostatic interactions in ionic solids like sodium chloride are very strong owing to the point charges involved, whereas in ionic molecular solids, such interactions are much weaker due to the smearing out of the charge on the molecular ions. Covalent interactions in solids like silicon or graphite extend throughout the solid, whereas in molecular materials, they are confined to the intramolecular level; polymers[5] represent the state between the two extremes.
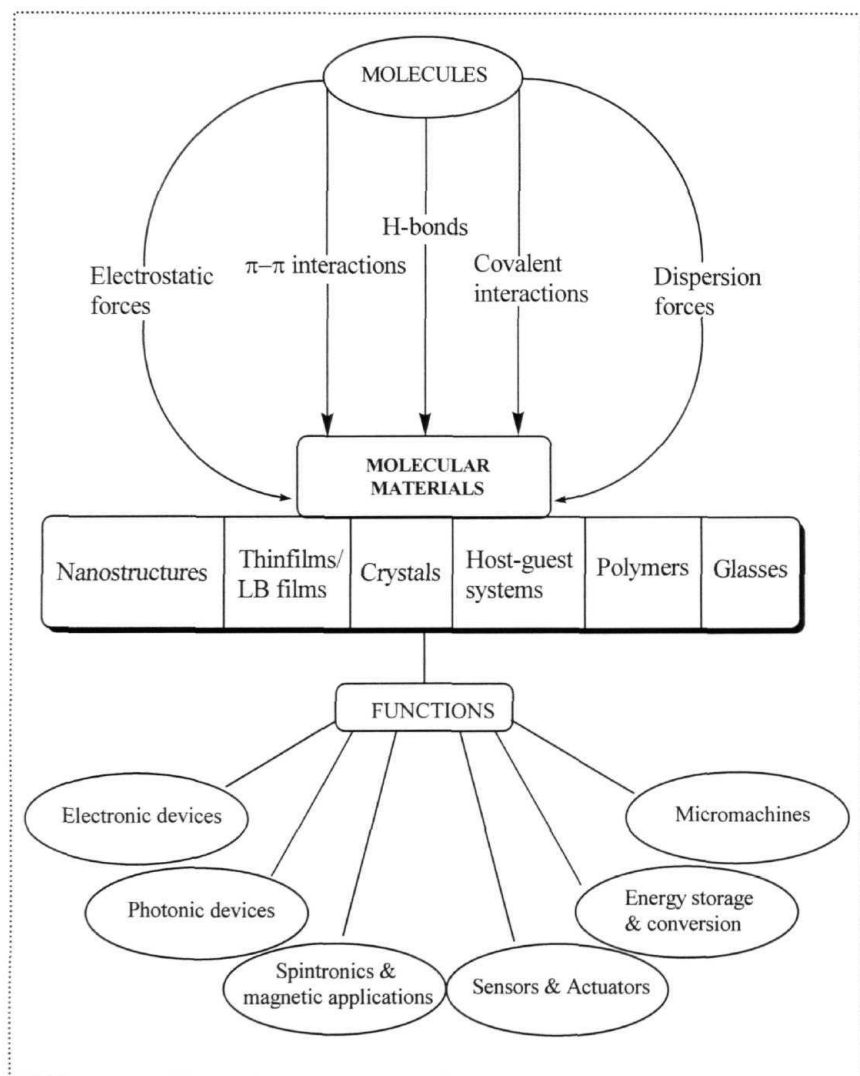
Figure 1.1 *A schematic diagram describing the organization and functions of molecular materials.*

Development of molecular materials

There exists a close parallel between the evolution of materials and human civilization. In fact the nomenclature denoting the progress of civilization is intimately linked to the nature of materials that were developed through the course of history. The stone age was followed by the copper, bronze and iron ages and the period we live in is often called the 'plastic age'. The materials fabrication techniques reflect the progress of technology. Starting with crude mechanical approaches to materials structuring, more sophisticated thermal, electrical, chemical and electrochemical techniques have evolved. Assembly of materials at the atomic and molecular level we witness today is the next link in the logical evolution of materials fabrication. Molecular materials therefore represent one of the prime examples of the 'state of the art'.

Liquid crystals discovered in 1888 are perhaps the first examples of molecular materials which found extensive technological application.[6] Discovery of the twisted nematic effect in 1969 in cyanobiphenyls and terphenyls have led to the wide application of liquid crystals in display technology. Their sensitivity towards electric field has been exploited in a variety of ways to fabricate switches and other devices. A variety of luminescent materials were discovered in the 1960's marking the development of novel optical materials. Since the advent of lasers in the 1960's extensive research has been carried out in the field of optical and non-linear optical (NLO) materials. In 1966 Sorokin and Lankard demonstrated the first dye laser[7,8] and observed stimulated emission from alcoholic phthalocyanine dye pumped with ruby laser. The development of dye lasers and the role of fluorescent dyes and pigments have been described by Schafer[7] and Maeda.[8] The demonstration of the nonlinear optical phenomenon of second harmonic generation (SHG) in single crystal quartz by Franken and co-workers,[9] and phase matched SHG in KDP crystals by Geordamine[10] and Maker and co-workers[11] laid the basis for modern nonlinear optics. Rentzepis and Pao[12] in 1964 observed SHG in benzopyrene, the first instance in a molecular system. The potential of organics was revealed by studies on hexamethylenetetramine,[13] hippuric acid, benzil[14] and urea.[15,16] In 1968 a systematic approach was developed to quantify and classify SHG in organic and inorganic compounds by Kurtz and Perry.[15] In the 1970's the analysis of nonlinear interference pattern in crystals was developed by Jerphagnon et al[17] and electric field

induced second harmonic generation was developed by Hauchecorne and coworkers[18] which showed the possibility of measuring individual molecular nonlinearities in solutions.[19]   Several books and reviews have appeared which deal with the theory, structural characteristics and applications of nonlinear optical molecules and **materials**.[20-3] Organic molecules and polymers are of great importance in the area of optoelectronics and **photonics**.[23,24] It is believed that future information technology will be largely based on photonics, wherein photons instead of electrons will be used to acquire, transmit and store information. **Photorefractive**[25] and photoconductive [6] materials are actively being explored for various applications in information processing and technology.

Fabrication of the first transistor in 1948, discovery of superconductivity[27] in 1911 and the explanation of the amazing phenomenon in 1957 marked the development of a new era in the history of materials. The pace at which new developments took place in fundamental physics and chemistry was reflected in the fabrication of novel materials. The growth of electronic industry propelled primarily by the advances in semiconductor physics[28] made unprecedented and challenging demands on the specificity and precision of materials properties. In the latter half of the twentieth century emergence of electronic information technology led to new requirements of materials for application such as transistor based information processing, semiconductor based signal transmission, optical storage devices, fast optical switches and sensors which have also contributed to the progress of communication devices.

The first molecular conductor was synthesized in 1842 by Knop by oxidizing the metal complex $K_2(Pt(CN)_4)$[29] with bromine, though the conducting property of this material was perhaps not realized at that time. The development of purely organic conductors containing no metal atoms/ions is quite fascinating. In the early 1950's Japanese researchers observed that **perylene-bromine** complex[30] showed a low electrical resistivity of about 8 Ωcm, a rather unexpected property for an organic solid. After the synthesis of **tetracyanoquinodimethane** (TCNQ) in 1962[31] many of its salts were shown to exhibit electrical conductivity. Following the synthesis of tetrathiafulvalene (TTF) in 1970,[32] many of its halides yielded conducting materials.[33] TTF-TCNQ prepared in 1973, exhibited a room temperature conductivity of 10^3 S/cm. Several metal complexes and phthalocyanines show metallic conductivities.

In 1980 Bechgaard and coworkers demonstrated superconductivity in molecular materials based on bis(tetramethyltetraselenafulvalene) hexafluorophosphate $(TMTSF)_2PF_6$ under 6.5 kPa pressure. $(TMTSF)_2ClO_4$ was the first molecular material to show superconductivity at ambient pressure.[34] In 1984, another chemical modification of TTF, bis(ethylenedithiotetrathiafulvalene) (BEDT-TTF) led to superconductors of the type $(BEDT-TTF)_2X$, where X^- is I_3^- or inorganic anions.[35,36] Alkali metal salts of buckministerfullerene,[37] such as K_3C_{60} entered the world of superconductors in 1994. Conjugated polymers form an important class of semiconductors today. Starting from the early study of aniline black in the year 1834, the modern era began with the discovery of conduction in doped polyacetylene in 1977. Currently, it is an area of intense basic research and technology development.

Magnetic materials are largely based on the compounds and alloys of elements such as iron, cobalt, nickel and gadolinium which are themselves ferromagnetic in the pure state. Later, magnetic materials based on coordination polymers and molecular systems in which metal ion serves as the source of magnetic moment were discovered. The charge transfer complex of decamethylferrocene and tetracyanoethylene (TCNE) was the first molecular material that showed ferromagnetic phase transition with a $T_C \sim$ 4.8 K. *p*-nitrophenylnitronylnitroxide was the first purely organic ferromagnet to be synthesized. Molecular magnetic materials are potential candidates to develop magnetic, electromagnetic and magneto-optic devices. Though molecular magnets[38] based on organic polymers and charge transfer complexes continues to fascinate materials chemists, a well characterized ambient temperature organic polymer ferromagnet is yet to be realized. Currently there is considerable excitement about the development of the so-called single molecule magnets.[38,39]

Multidisciplinary activities involving chemists, physicists, biologists and engineers have led to the emergence of a wide spectrum of novel materials with desired properties. The quest for miniaturization appears to be heading to its logical conclusion through the development of molecular devices. There are several reports of single molecules functioning as active devices carrying out a wide variety of optical, electrical, and mechanical functions. The fantastic list of functional molecular scale devices include rectifiers,[40] switches,[41] gates,[42] wires,[43] shuttles,[44] brakes,[45] ratchets[46] and gears.[47]

Fabrication of molecular materials

The design and fabrication of molecular materials effectively exploits the enormous power and flexibility of synthetic chemistry to tailor specific molecular structures and hence the desired molecular materials. The fundamental differences between the route to molecular materials and conventional approaches to materials is schematized in Fig. 1.2. Traditionally materials are fabricated from suitable precursor materials employing techniques such as ceramics methods, melt-quench processes, vapor deposition, sol-gel and so on methods.[2,48] In the case of molecular materials on the other hand a well defined intermediate stage is involved which is simply the molecule or
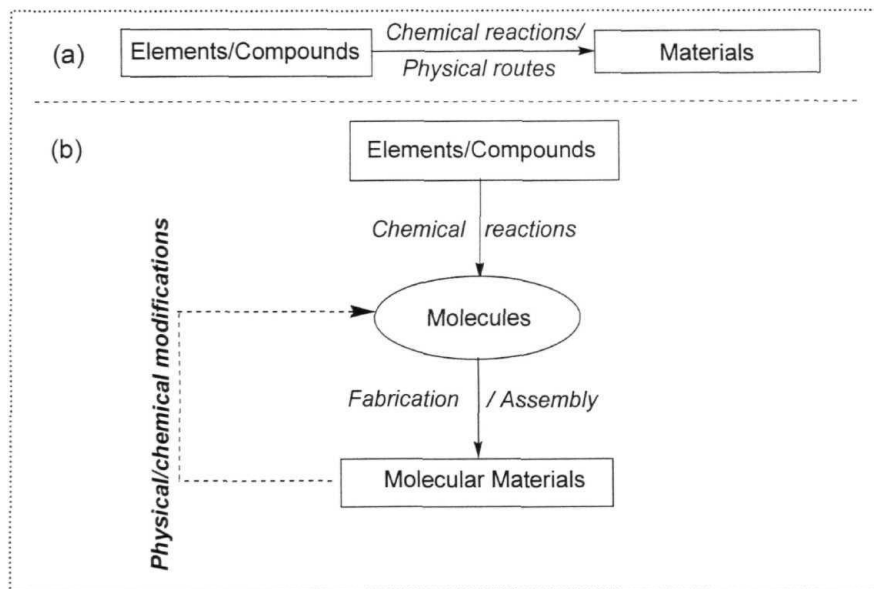

Figure 1.2 *Schematic representation of the (a) traditional approach to materials fabrication compared to the (b) two level synthesis of molecular materials.*

molecular ion and which effectively separates the chemical reaction from the material fabrication process. The property of the molecule is determined by its structure resulting from the chemical reactions employed for its synthesis while the property of the fabricated materials depends on the property of the molecules and the way they are organized in the bulk. The molecules can be identified and studied using a variety of spectroscopic and analytical tools. This provides a synthetic approach for the design of molecular materials. Design of molecular materials[1] involves molecular recognition[49] and organization thus leading to the construction of supramolecular systems.[3] The iterative way of realizing the property of tailored molecular materials provides a unique handle to fine tune the materials properties.

Crystallization from organic or aqueous solvent medium is perhaps the most common technique for the fabrication of molecular materials.[3] Electrocrystallization is popular in the case of conductors and superconductors. In this technique the molecule is oxidized or reduced in the presence of appropriate counterions. Since simple crystallization does not provide much control on the final bulk organization, alternative techniques which involve directed assembly of molecular materials are often adopted. They include methods such as electric field poling,[51] Langmuir-Blodgett technique[52] and layer by layer assembly.[53] Spin and dip coating, sol-gel processing[48] and chemical or physical vapor deposition[54] are other approaches resorted to. The intermediate stage involved in the synthesis of molecular materials provides a systematic control in the assembly of the bulk material and the realization of the materials properties.

1.2 MOLECULAR OPTICAL MATERIALS

Dyes and pigments

Substances that are used to color materials are broadly divided into two classes-dyes and pigments.[55] Dyes are soluble substances commonly used to color items such as utensils, paper, plastic and leather. Certain classes of dyes are made insoluble by a chemical process after they penetrate into the material being dyed. Pigments are colored

solids, practically insoluble in most of the solvents and exist as particles when dispersed in paints, lacquers, inks, paper, plastics and rubber. Triphenylmethane dyes are some of the early synthetic dyes developed and form an important class of commercial dyes and pigments. Photophysical and photochemical properties of triphenylmethane dyes in solid state and solution have been discussed by Duxbury and coworkers. In recent years carbides, nitrides and carboxynitrides of transition metal compounds as well as diamond-like carbon films have been extensively investigated for decorative applications.[57] Organic dye-metal oxide composite thin films possessing good mechanical properties and showing strong selective absorption in the visible range are important candidates for future applications. Bottcher and coworkers[58] were the first to report on the preparation of mixtures called norganics of organic merocyanine dye and inorganic materials for spectral sensitization in photography. Organic dyes have attracted considerable attention in the field of diodes and laser optical storage devices. The use of cyanine and phthalocyanine dyes in commercial recordable compact discs (CD-R) have facilitated the use of shorter wavelength (635-650 nm) laser beams in place of the traditional 780 nm lasers. Metallized thiazolyl dyes[59] are often used as recording materials. Optical fibre based chemical sensors exhibiting strong optical response have attracted increasing interest in recent years owing to their immunity to electrical noise, ease of miniaturization and possibility of application in real time monitoring and remote sensing. Some ultra violet dyes incorporated in solid polymer electrodes (PVA/H_3PO_4) and certain NIR dyes are promising candidates for optical humidity and integrated optical sensing.

The prime concerns in dye chemistry are color control (tuning the wavelength of absorption and emission) and thermal and photostability. Dyes find application in electronic devices, lasers, liquid crystal displays, electrochromic systems,[7,8] optical switches,[61] solar cells[62] and nonlinear optical devices.[21,63] Crystal violet, cyanine,[64] molecules based on squarine templates,[65] benzolothiazolium[66] and salts of N-methyl-pyridinium,[67] several of them in the form of LB films, have demonstrated stronger upconversion of fluorescence emission than common organic dyes such as rhodamine. Several of them also exhibit strong nonlinear optical responses due to the large molecular hyperpolarizabilities. Phthalocyanine base dyes have attracted considerable attention due to the ease of synthesis.

Quinacridone, coumarines and pyrrolopyrroles are some of the famous industrial pigments. Quinacridone and pyrrolopyrroles belong to the group of carbonyl pigments and are some of the oldest known and most important colorants. Fluorescent pigments for paints are commonly dyes embedded in a plastic matrix. Zinc oxide is the most common, one of the longest known and widely used white inorganic pigment. New colored compounds have now been prepared using zinc oxide as the base and these can be used as pigments for coloring plastics and paints.[68] Colored oxides produced through solid state reaction with mixed oxides[69] are potential inorganic pigments which are environmentally friendly.

Laser dyes

After the demonstration of the dye laser in 1966 by Sorokin and Lankard, Schafer and coworkers[70] and Spaeth and Bortfeld[71] observed the dye laser action in cyanine dye. In 1967 a flashlamp-pumped dye laser was developed and both xanthene dyes and coumarin derivatives showed efficient laser action. Various classes of laser dyes have been developed to cover the wide spectral range from IR to UV. A continuous wave rhodamine 6G dye laser using an argon ion laser as a pumping source was demonstrated in 1970. The first experiment on tuning and condensation of lasing spectrum of a dye laser was made by Soffer and McFarland.[72] Dye lasers have contributed greatly to the progress in laser spectroscopy and laser chemistry. A wide variety of organic compounds with complex chemical structures are used as the active medium in current dye lasers.[7] Although dyes usually imply colored substances, many colorless, but fluorescent organic materials are also used for dye lasers. The lasing compounds are classified according to their chemical structure. A compilation of 30 famous dyes have been published by Kauffman.[73]

Until recently liquid dye lasers were the main systems used to achieve tunability in the visible range and the only choice for commercial lasers. But in the last few years intensive efforts have been devoted to produce embeddings of organic dyes in various solid materials such as polymers, silica gels, xerogels, alumina gels, ormosils and composite glass with a view to replace liquid dye lasers. Solid state dye lasers are

attractive due to their nonvolatile, nonflammable and nontoxic nature, the compact size and stability. Photostability is a feature of prime importance in selecting a laser dye. Pyrylimide dyes,[74] spiro type molecules,[75] electroluminescent oxadiazole dimers[76] and polyurethanes with pendant nitrostilbene units[77] are important candidate systems.

Photoluminescent *materials*

Organic luminescent materials have been surveyed in various books.[78,79] Fluorescent molecules and materials are of great interest in a wide variety of applications. They are potential candidates for display devices and are some of the most popular choices for sensor applications. Molecular recognition events which trigger fluorescence response are effectively exploited in chemical and biological applications. Families of molecules which exhibit efficient fluorescence include aromatic hydrocarbons and their derivatives, azomethines, azines, several five and six membered heterocycle derivatives, carbonyl compounds and metal complexes with a wide range of organic ligands.   A variety of nanomaterials, polymers, sol-gel systems etc. also display strong fluorescence.[2,78]   A wide variety of molecules used as fluorescent and phosphorescent probes in biological applications are listed below since they can form the basis for the development of novel luminescent materials.

Well known phosphorescent molecules include proteins such as hemeprotein, probes like tryptophan and erythrosine, 4,4'-dimethoxybenzophenone (DMOBP), 2,2,2-triphenylacetophenone   (TPAP)   and   heavy   metal   complexes   such   as 2,3,4,7,8,12,13,17,18-octaethyl-12H,23H-porphine platinum (II) (PtOEP) and *fac*-tris(2-phenylpyridine)iridium (Ir(PPy)3).[80] Fluorescence probes are useful in the trace analysis of substances in biological systems and therefore have become very useful in the detection of drugs in blood or other fluids. Extensive research in biology and medicine make use of fluorescent materials.   1-dimethylaminonaphthalene-5-sulfochloride (DANSYL chloride)[78,79] is used as a tracer for proteins. Fluorescamine is an even better tracer since it fluoresces only after combining with amino acids and proteins and not as isolated species in solution. Fluorescein and its derivatives are the most widely used diagnostic tools which can be injected into the body; their luminescence demonstrates the

patency of blood vessels, blood supply to various parts of grafted skin, the boundaries of affected area etc. Fluorescein and rhodamine derivatives were used as antibody tracers; recently, substituted stilbenes, derivatives of dichlorotriazine and pyrene are also being used for this purpose. In addition to acridine orange, ethidium bromide, quinacrine and mithramycin are capable of binding to DNA; hence they find application in staining nucleic acids. DANSYL chloride and fluorescamine are used in quantitative determination of proteins and amino acids. Acridine orange is the most popular fluorophore used in determining the DNA to RNA ratio within a single cell as well as in the study of the activation of chromatin in various processes. Acridine orange, rivanol, proflavin, primulin and many other fluorophores are used for direct tracing of antibodies and labeling of cells. Proflavine and ethidium bromide have been used as probes of nucleic acid structure.[81] Thiazole orange is used in the characterization of long wavelength probes for DNA sequencing. Photodynamic therapy is a new modality for the treatment of cancer[82] and current research in this field is also concerned with the design of molecules which potentially bind DNA and cleave the duplex under illumination with visible light. DNA intercalators such as adriamycin and daunomycin and complexes such as cis-platin are strongly mutagenic in nature which stop the replication and transcription of the DNA resulting in promising chemotherapeutic activity.[83] NIR dyes are used for clinical sensing. Fluorescent probes are extensively used in the study of cell membranes; their charge, potential and viscosity give us an idea about the presence of cholesterol and the mobility of cancer cells. In addition to the above described systems several strongly intercalating metal complexes of platinum and ruthenium can act as luminescent markers for DNA[84] and foot printing applications.

Electroluminescent materials

Electroluminescence (EL) is a phenomenon with wide application in the areas of illumination and display technology. It shares some similarities with the familiar process of photoluminescence. In photoluminescence, light (typically in the ultraviolet range) excites a molecule or material which in turn relaxes by emission of visible light. In electroluminescent materials, an applied electric field generates the excited state or exciton which decays emitting the visible light. This phenomenon was first discovered in

inorganic materials in 1936 when Destriau et al observed high field electroluminescence from a zinc phosphor powder dispersed in an insulator and sandwiched between two electrodes. In the early 1960's General Electric introduced commercially available light emitting diodes (LED) based on the inorganic semiconductor GaAsP.[85] Since the energy of the emitted photons and therefore the color of the LED is determined by the energy gap of the semiconducting material in the active region, early LED's emitted only red. The development of new materials granted access to colors other than red and made blue, orange, yellow and green as well as infrared accessible. Electroluminescence in organic compounds was first demonstrated by Pope et al,[86] Helfrich and Schneider[87] and Mehl and Bucher.[88] In the late 1980's Tang and Van Slyke[89] as well as Saito and Tsutsui,[90] revived the search on electroluminescence of molecular materials, developing a new generation of LED with organic fluorescent dyes. Organic light emitting diodes (OLED) are obtained by placing charge-transporting and electroluminescent material between two electrodes (one of them being transparent) and applying a suitable bias.

Electroluminescence in semiconductor devices arises from the electron impact excitation of luminescent centers, for example the manganese or terbium ions doped in ZnS. On the other hand, EL in molecular systems arises from the recombination of electrons and holes injected into the material from the cathode and anode respectively. The energy gap between the HUMO and the LUMO controls the emission color. Strong EL arises from efficient charge carrier transport and high fluorescence efficiency. Voltage required to drive the luminescence is generally low in the case of molecular materials, especially when fabricated in the form of thin films. Most of the current EL devices run on DC voltage but recent experiments show that some organic polymer EL devices can be run on AC voltage as well, enlarging the scope of these materials for practical applications.   The efficiency of electroluminescence goes down if recombination of electrons and holes takes place too close to the electrodes. Special multilayer thin film assemblies are often fabricated to ensure that the recombination takes place away from the electrodes and efficient luminescence occurs. Excellent reviews of organic electroluminescent materials and devices may be found in Refs. 91 and 92. The progress in thin film electroluminescent devices has been reviewed by Tsutsui.[93]

Molecular materials for electroluminescence devices are often classified into three catagories according to their structure : (i) organic dyes (no metal atom), (ii) chelate metal complexes[94] and (iii) conjugated polymers. Fig. 1.3 provides a schematic view of the scope of inorganic and organic molecular EL materials. Some of the common organic EL dyes are based on derivatives of oxadiazole, phthaloperinone, quinacridone and pyrazoline. Electroluminescence in derivatized organic molecules containing donor-acceptor groups has been reported recently.[95] An interesting family of materials being explored is based on spirosystems such as spirolinked quarterphenyl and higher analogues. They show high quantum yield (nearly 60 %) for blue photoluminescence. The spiro linkage apparently leads to high quality amorphous materials with high glass transition temperatures.[75] Important properties of organic dyes include high fluorescent quantum yield, ease of film formation by vapor deposition, possibility of obtaining high levels of purity and flexible molecular design. On the other hand there are several problems with the use of organic dyes such as easy crystallization after film formation and the occasional production of exciplexes. The chelate complexes commonly employed in EL applications include those of aluminium and zinc with ligands such as

Organics		**Inorganics**	
Fluorescent dyes	Conjugated polymers	Doped Semiconductors Eg. ZnS : Mn	Semiconductors j Eg. GaAs
Large area application		Small (mm^2) ! area application \	

Figure 1.3 *The wider scope of molecular materials over inorganic semiconductor materials in electroluminescent device application (adapted from Ref. 91).*

8-hydroxyquinoline, 2-methyl-8-hydroxyquinoline, 7-n-propyl-8-hydroxyquinoline, 2-(2-hydroxyphenyl)-5-phenyloxadiazole (ODZ), **1-phenyl-2-(2-hydroxyphenyl)** benzimid-azole (BIZ)[76,80] The most widely used electron transport and emitting material is AlQ$_3$, as it is easily synthesized and purified, avoids exciplex formations and is thermally and morphologically stable when evaporated into films. Since the functioning of molecular organic devices is affected by crystallization in the amorphous thin films, special efforts have gone into the design of amorphous EL materials.

Polymeric EL materials is a fast expanding field or research. ' This fundamental contribution to the evolution of OLED came from Friend and coworkers in 1990.[96] They replaced the fluorescent dyes and inorganic semiconductors which require expensive and technologically inconvenient vapor deposition methods for fabrication, by the highly fluorescent conjugated polymer, poly(p-phenylenevinylene) (PPV) as the active material in a single layer OLED. Conjugated polymers derive their semiconducting properties from the π electrons delocalized along the polymer chain; the delocalized valence π and conduction π^* wave functions support the mobile charge carriers. PPV and its derivatives are some of the most promising conjugated polymers for EL applications. PPV produces intense yellow green luminescence (> 100 candela/m^2) at driving DC voltages typically below 10 V. Doped ZnS on the other hand, normally require voltages of the order of 100 V. Organic EL devices based on polymeric materials have been reported using conjugated polymers such as polyphenylenes, polyalkylfluorene, polyalkyl thiophenes and polyvinyl carbazole. The main advantage of polymers is the ease of film formation by casting and the absence of crystallization in the cast films. However their purification is generally not simple. The external quantum efficiency (number of photons per electron injected) of commercial inorganic LED's remains close to 1% after several decades of development whereas in less than a couple of decades, OLED's have reached comparable or better efficiency. The other advantages they offer are the low threshold voltages, possibility for large area application and the light weight and mechanical properties of plastics. Synthetic manipulations can be easily carried out on conjugated polymers providing control on the HOMO-LUMO gap and hence on the color of the electroluminescence. An important advantage of polymer LED's is the flexibility of fabrication modes.[98] Polymers can be processed into several forms such as solid films, solutions and gels.[99] Polyaniline as a hole injecting material

and polyethylene terephthalate as substrate have been used in the fabrication of flexible light emitting diodes.[100] Polymers with substituted diphenylamino groups have been reported to have excellent emissive capability. Several novel benzene derivatives have been synthesized and used as hole blockers applicable in blue-violet emitting fluorescent and green emitting phosphorescent EL devices.[101]

Electroluminescent devices with multilayered structures composed of two or three vaccum sublimed dye films[102] exhibit high device performances. There has been considerable effort to develop efficient hole transport materials for multilayer OLED's since the discovery of triaryl amines with biphenyl center core as hole transport layer which improved the electroluminescence and operational stability of OLED's. Several systems like biphenyldiamine derivatives, amorphous spiro-linked systems, triphenylene derivatives, vanadyl phthalocyanines and crosslinkable polymers have been developed. Conjugated molecules containing cyano substituents are known to achieve desirable luminescence property and good electron injection/transport ability. The potential of molecular and polymeric EL devices for extensive commercial application is bright indeed.

1.3   MOLECULAR NONLINEAR OPTICAL MATERIALS

Basic concepts of nonlinear optics

The electric field of an electromagnetic radiation typically in the range of optical frequencies induces electronic polarization in a molecule or material, with which it interacts. The dipole moment induced per unit volume is called polarization. At low electric fields, the polarization, P is linearly related to the field E by the proportionality constant $\chi^{(1)}$, the linear electric susceptibility tensor (Fig. 1.4). At high fields typically those associated with lasers, contribution of the nonlinear (second and higher order) terms become significant and P varies nonlinearly with E.[22] Higher order susceptibilities $\chi^{(n)}$ (n >1) are inherently smaller than $\chi^{(1)}$ and their magnitudes get smaller with

increasing n. The polarization in a bulk material along the direction i can be represented as:

$$P_i = \chi_{ij}^{(1)} E_j + \chi_{ijk}^{(2)} E_j E_k + \chi_{ijkl}^{(3)} E_j E_k E_l + ...$$

(1.1)
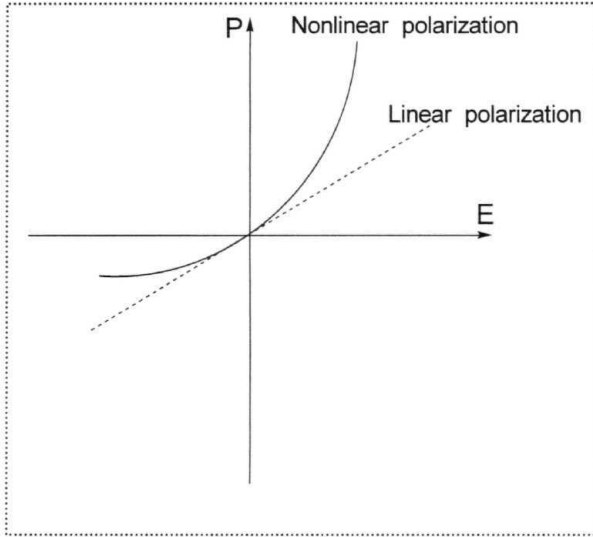
Figure 1.4 *Nonlinear polarization at high electric fields; the linearity at low fields is shown using the dashed line.*

In Eqn. 1.1 the indices $i,j,$ k and l refer to the coordinate framework of the bulk material. The polarization at the molecular level, ρ_i similarly depends on the molecular polarizability, a and hyperpolarizabilities, β, γ etc as given in Eqn. 1.2.

$$\rho_i = \alpha_{ij} E_j + \beta_{ijk} E_j E_k + \gamma_{ijkl} E_j E_k E_l + ...$$

(1.2)

The coefficients $\chi^{(n)}$ in Eqn. 1.1 as well as a, β, y etc in Eqn. 1.2 are tensorial quantities. The phenomenon of frequency doubling or second harmonic generation, a quadratic

nonlinear optical (NLO) effect can be visualized as follows. If the applied electric field has frequency, ω and can be represented as $\sin(\omega t)$, the quadratic term will have a 2ω dependence as seen in Eqn. 1.3.

$$
\begin{aligned}
E &\propto \sin \omega t \\
E^2 &\propto \sin^2 \omega t \ \left(= \frac{1}{2}(1 - \cos 2\omega t)\right)
\end{aligned}
\tag{1.3}
$$

Eqns. 1.1 and 1.2 show that there is an important symmetry constraint for observing second harmonic generation or any even order NLO effect. In systems having a centre of symmetry, reversal of the electric field would exactly reverse the polarization, *ie,* P(-E) = -P(E). From Eqn. 1.1 it can be seen that this is possible if and only if all terms with even powers of E become zero. This implies that the even order coefficients such as β, 5 etc and $\chi^{(2)}$, $\chi^{(4)}$ etc. are strictly zero. In a noncentric system, no such equality exists and generally, P(-E) $\neq$ -P(E). This implies that quadratic or any other even order effect are possible only in noncentrosymmetric molecules or materials.

*Materials **for** second harmonic generation (SHG)*

Materials developed initially for NLO applications were largely based on inorganic systems. Ferroelectric materials lacking a centre of symmetry were prime candidates for the quadratic effects. The popular materials used for second order NLO applications are inorganic crystals such as potassium dihydrogen phosphate (KDP),[103] lithium niobate $(LiNbO_3)$[104] and β-barium borate (BBO).[105] NLO effects in inorganic materials based on ionic solids arise primarily due to the ionic polarization and hence are relatively slow. Since the responses are due to bulk effects, decomposition of the NLO coefficients in terms of atomic/ionic contributions is not straight forward. Molecular materials on the other hand, with their relatively lower refractive indices, exhibit faster NLO responses and the NLO effects can be conveniently analyzed in terms of the molecular contributions and the impact of the intermolecular organization. If molecules with large (3 values are aligned so that their hyperpolarizabilities add up constructively, the assembly leads to noncentric materials with appreciable NLO response.

There has been a growing interest in developing π-conjugated organic molecules for nonlinear optical application. Considerable effort has gone into overcoming the limitations of organic materials such as low thermal and mechanical stability, so that they can compete with inorganic materials which at present dominate the area of technological applications. The physical mechanism of charge transfer that leads to the nonlinear optical effect in organic molecules possessing a 'donor-conjugating unit-acceptor'(D-π-A) framework, can be understood in terms of the Mulliken resonance structures illustrated in Fig. 1.5. When the molecule is subjected to an applied field parallel to the dipolar axis, the electronic polarization response will be unsymmetric as a result of the cooperative influence of the donor and acceptor groups; this can be contrasted with the symmetric response of an unsubstituted benzene (broken line). The asymmetry in the polarization gives rise to the harmonic frequencies of the field radiated by the molecular dipole oscillations. These simple considerations have led to the developments of a vast number of organic molecular crystals and polymers as candidates for NLO applications. The D-π-A system leads to high second order nonlinear optical response.

The quadratic NLO molecules are mostly based on donor-acceptor substituted aromatics. Some of the extensively studied classes of NLO chromophores of this type are 1,4-substituted benzenes and stilbenes,[106,107] 4-nitroanilines and 4-(N,N-dimethylamino)-4'-nitrostilbene (DANS).[108] Dulcic and Sauteret [109] were the first to
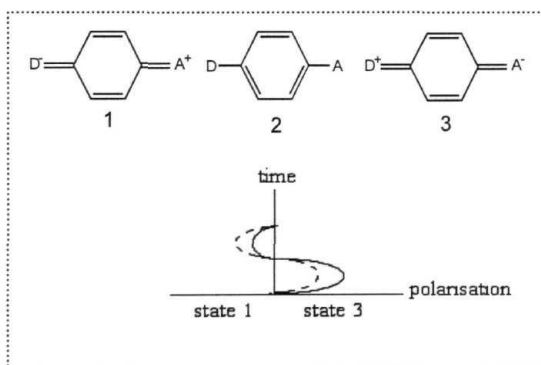
Figure 1.5 *Origin of nonlinear polarization in a donor-acceptor substituted benzene. The broken line represents the response of unsubstituted benzene.*

study the substituent effect in para disubstituted benzene derivatives and Oudar and Leperson reported on the effect of conjugation length by using stilbene in the place of the benzene system.[110] Since then several systematic investigations have been carried out on the structure-property relationship of NLO chromophores. Compounds with conjugating bridges such as tolans,[107] diazostilbenes,[111] polyenes,[112][113] polyphenylenes,[114] as well as heteroaromatic 5- or 6- membered rings like thiophenes and azoles[115] have been investigated. Other systems studied include organometallic compounds[11] and calixarenes.[117] In order to overcome the problem of absorption at 2ω, Mignani and coworkers have developed an interesting approach of linking donor and acceptor groups through s-p conjugative units, such as silanes, oligo-silanes and poly-silanes. A variety of salts especially with pyridinium and stilbazolium cations have been studied for their second order NLO properties.

Since D-π-A type systems often tend to prefer centrosymmetric organization in the bulk, there has been considerable interest in exploring octupolar molecules.[119] Recently there have also been reports on novel NLO chromophores with through space or through σ-bond (as opposed to π conjugative) interactions between the donor and acceptor groups which show improved absorption characteristics.[120] There is also growing interest in chromophores organized as mesoscopic and crystalline superstructures; the significance of their helical organization for enhanced nonlinearity has been discussed.[121]

Molecular hyperpolarizability

The first hyperpolarizability, β quantifies the second order NLO effect at the molecular level. Several theoretical methodologies are available to compute molecular hyperpolarizabilities. Two approaches[122] are often employed to compute (3: (i) generalized finite field elaborations in which the perturbation due to the field is explicitly included in the Hamiltonian (the finite field (FF) and coupled perturbed Hartree-Fock (CPHF) method) and (ii) perturbative schemes in which the calculations are carried out on the free (independent of field) molecules and the response involves the coupling of excited states (the sum-over-states (SOS) method). The CPHF method is equivalent to

the time dependent Hartree-Fock approximation (TDHF) for static calculations. The semiempirical AM1/TDHF method incorporated in the MOPAC93 programme package provides a convenient and quick solution for the prediction of (3 of organic molecules. The simplest model to take into account the contribution of charge transfer resonance within a molecule to the first hyperpolarizability is the two-level model proposed by Oudar and Chemla.[108,123] An increased p is often accompanied by a red shift in the absorption spectrum due to a larger conjugation length or lower energy charge transfer between the donor and acceptor substituents.[124]

Experimental determination of molecular hyperpolarizability is often carried out in the solution phase. Since molecular motion in solution leads to an average centre of symmetry, high electric fields are applied to break the symmetry of the isotropic solution in the approach called electric field induced second harmonic generation (EFISHG).[125] In another technique called the hyper-Rayleigh scattering (HRS),[126] local anisotropy within the solution is used to produce incoherent harmonic scattering which allows determination of the p. The latter technique is applicable to charged and octupolar compounds that are not amenable to EFISHG studies. Molecular β values can be related to the bulk crystal NLO coefficients through the oriented gas model.[127]

Noncentrosymmetric organization of molecules in materials

As noted earlier, dipolar molecules often show a predilection towards centrosymmetric organization in the bulk. In fact, an examination of the Cambridge Crystallographic Database shows that typically 70-80% of the molecular crystals belong to centrosymmetric space groups. Different strategies have been developed to obtain noncentrosymmetric organizations. (i) Inclusion of chirality,[11] ' (ii) exploitation of weak as well as strong intermolecular forces[129] and (iii) incorporation of alkyl chains of appropriate length[130] are some of the approaches developed for molecular crystals. Other strategies include, (i) electric field poling of polymer films containing the NLO-phores,[51] (ii) fabrication of X and Z type LB films,[52] (iii) formation of host-guest systems,[131] (iv) sol-gel synthesis[53] and (v) salt formation.[132]
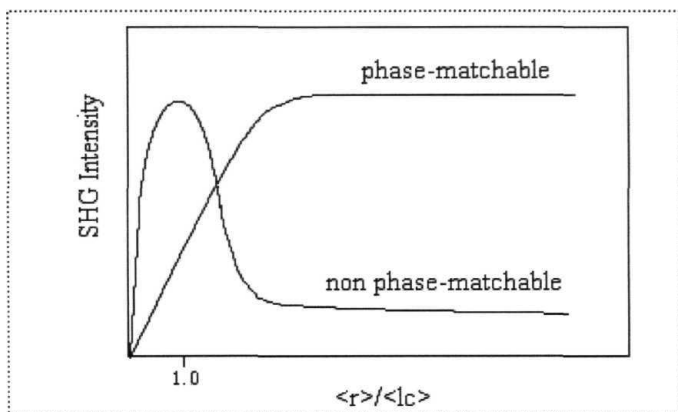
Figure 1.6 *The dependence of SHG intensity on the average particle size, <r> for phase-matchable and non phase-matchable materials; $<l_c>$ is the average coherence length.*

The Kurtz-Perry powder technique[15] is a convenient and simple method for screening large sets of microcrystalline materials for SHG activity. It involves the determination of the variation of SHG intensity with the average particle size of the microcrystalline powder as illustrated in Fig. 1.6 for phase-matchable and non phase-matchable materials. The salient feature to be noted here is that for particle sizes much greater than the average SHG interaction length (*ie.* to the right of <r> = $<l_c>$), the SHG intensity, $I_{2\omega}$ for phase-matchable materials reaches a saturation value and is independent of the particle size whereas $I_{2\omega}$ for non phase-matchable materials decreases with increasing particle size and becomes negligible or undetectable at large sizes. Materials which are phase-matchable include $LiNbO_3$, urea, 4-nitrophenyl-*S*-prolinol (NPP) and 2-Methyl-4-nitroaniline (MNA). The powder technique is a reliable tool for establishing the presence or absence of centre of symmetry in the crystal lattice. However one should exercise caution in using this technique, since factors such as changes of chemical composition on powdering the crystals (for example by loss of solvate molecules[133]) and modification of surface features are known to cause artifacts.

Diaminodicyanoquinodimethanes

Diaminodicyanoquinodimethanes (DADQ) are easily synthesized from tetracyanoquinodimethanes (TCNQ) by treatment with primary or secondary amines.[134] DADQ's are highly versatile push-pull molecules with a strongly zwitterionic structure. (Fig. 1.7). Several families of DADQ's have been investigated in our laboratory over the past few years, because of their interesting quadratic nonlinear optical properties.[135]
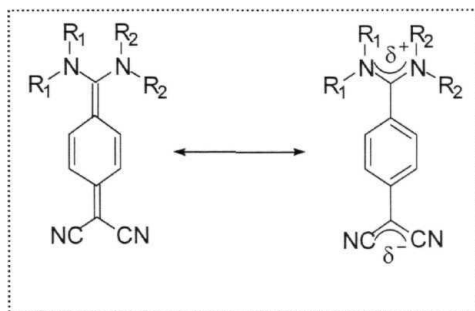
Figure 1.7 *Structure of diaminodicyanoquinodimethanes (DADQ's).*

Semiempirical computational studies have shown that they possess large molecular hyperpolarizabilities in spite of the relatively small size of the **chromophore**.[136] These studies also provided insight into the influence of the molecular structure on the molecular nonlinear response. Inclusion of chirality and **intermolecular** H-bonds have been effectively used in developing DADQ systems showing strong SHG in the solid state. Introduction of **alkyl** chain on the **amino** end of diaminodicyanoquinodimethanes was shown to be an interesting novel strategy to control centrosymmetric **and** noncentrosymmetric lattice formation and hence SHG activity.[130] Ampiphiles based on DADQ's and their LB films have also been investigated in our laboratory.[137] We present in Chapters 2 and 3, a variety of novel optical and nonlinear optical materials based on DADQ's, in which the molecular assembly and materials property are strongly influenced by functionalities attached remotely from the **π-electron** chromophore unit.

1.4 MOLECULAR CONDUCTING MATERIALS

Materials are often classified into the three broad categories of insulators, semiconductors, and conductors based on their electrical conductivity behavior. Substances which offer strong resistance to the flow of electrons are insulators. Their conductivity is typically less than 10^{-6}-10^{-8} S/cm. Most organic solids and polymers are insulators; polymers such as teflon or bakelite are some of the best electrical insulators. Those materials which show very low resistance to electrical transport are the conductors. Their conductivity is 10^5-10^6 S/cm or higher. Metallic conductivity is marked by an increase with decrease of temperature. Metals and their alloys are some of the best conductors. However several molecular materials based on charge transfer complexes and doped 7r-conjugated polymers show appreciable conductivity. They are called synthetic metals,[138] as they are prepared through normal organic synthesis protocols. Materials which show partial resistance to electron transport are the semiconductors. They behave as insulators at absolute zero of temperature, and at finite temperatures show conductivity intermediate between metals and insulators. The room temperature conductivity of semiconductors are typically of the order of 10^{-5} to 10^2 S/cm. Their conductivity increases with increasing temperature. Classic examples of semiconductors include silicon, germanium and gallium arsenide. Many molecular crystals and *n*-conjugated polymers show conductivity typical of semiconductors.

The band theory of solids provides a convenient framework to understand and explain the conductivity behavior of materials. Appreciable overlap between the wave functions of large number of atoms in the solid leads to the formation of energy bands. Depending on the atomic energy levels from which they are constructed and the extent of overlap, the bands would show different widths and forbidden energy regions between them. The resulting band structure and the electron count, leads to the following situations : (i) the highest energy electrons (Fermi electrons) occupying a partially filled band (metals) or (ii) completely filled and empty bands with an energy gap in between. The latter situation leads to insulating or semiconducting behavior depending on whether the energy gap is large or small compared to thermal energy. The bands in molecular charge transfer complexes are expected to be generally narrow and best explained as an intermediate regime between the valence band and molecular orbital limits.[139] Electronic

structure of conducting polymers are best explained using polyacetylene as a model system.[138,140] In a regular all *trans*-polyacetylene, the band picture predicts a half-filled conduction band and hence metallic behavior. However, due to the one-dimensional nature, the polymer undergoes Peierl's dimerization opening up a gap at the Fermi level. This leads to the observed semiconducting nature of pure polyacetylene. Doping introduces a wide range of charge carriers leading to enhanced conductivity in the conjugated polymer.

Organic charge transfer complexes

Perylene-bromine[30] is perhaps the earliest organic material in which enhanced electrical conductivity was observed. As mentioned in Sec. 1.1, synthesis of the strong *n*-electron acceptor, TCNQ[31] led to the development of a large number of semiconducting charge transfer complexes. The earliest and the most studied among organic metals is TTF-TCNQ which shows metallic conductivity down to ~ 60 K. The high conductivity of TTF-TCNQ arises due to the segregated stacks of donor and acceptor molecules with short inter-layer distances as well as their partial ionicity. The extent of charge transfer leads to 'neutral' or 'ionic' ground states for the charge transfer complexes. A 'partially ionic' state leading to fractional oxidation state allows unactivated electron transport along the π-stacked structures and high electrical conductivity.

Some of the well known π-electron donor and π-electron acceptor organic molecules which have been used to prepare conducting or semiconducting charge transfer complexes are shown in Figs. 1.8 and 1.9 respectively. Molecules like, N,N,N',N' tetramethyl-*p*-phenylenediamine (TMPD), tetrakis(dimethylamino)ethylene (TDAE), tetramethyltetraselenafulvalene (TMTSF) and bis(ethylenedithio)tetrathiafulvalene (BEDT-TTF)[141] are very good π-electron donors and possess ionization potential of ~ 6-7 eV. Charge transfer complexes based on TMTSF and BEDT-TTF and several of their derivatives show superconductivity at low temperatures. Molecules like tetracyanoethylene (TCNE), tertracyanoquinodimethane (TCNQ) and dicyanoquinodiimine (DCNQI) are very good it-electron acceptors with electron effinities ~ 3-4 eV. Various heterocyclic analogues of TCNQ, generally called as hetero-TCNQ's,[142] are of interest because they engage in strong intermolecular interactions and
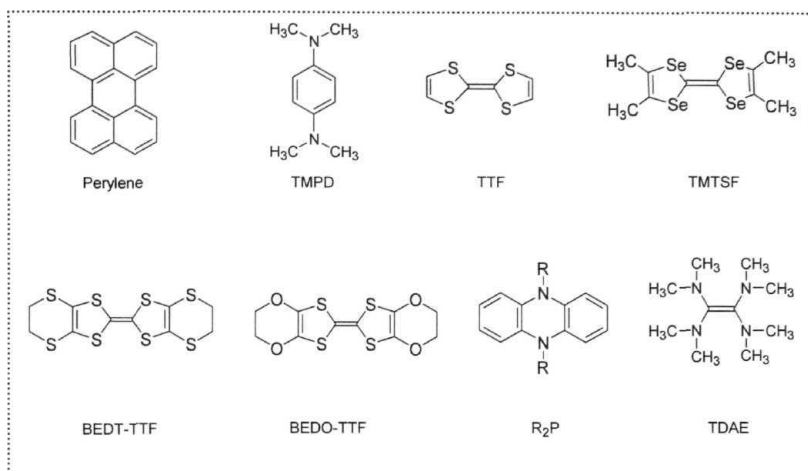
Figure 1.8 *Molecular structures of π-electron donors.*
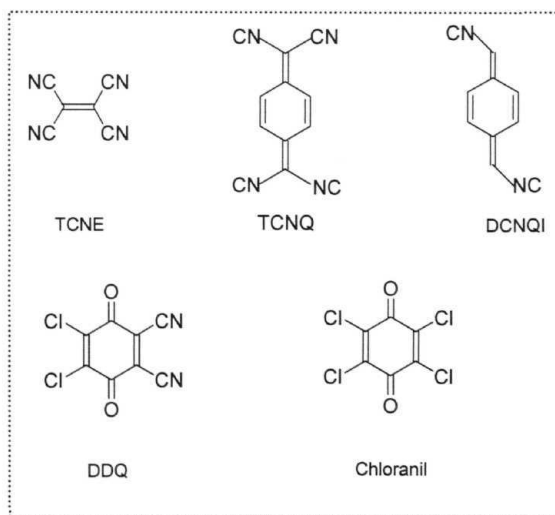
Figure 1.9 *Molecular structures of π-electron acceptors.*

possess reduced on-site Coulombic repulsion. In spite of the lack of superconductivity in their salts and complexes, derivatives of TCNQ and DCNQI, have been the focus of extensive synthetic efforts because of the variety of conducting materials that could be fabricated using them. Advances related to these significant acceptor molecules and other cyano compounds have been reviewed recently.[143] Several charge transfer salts of TCNQ have been investigated for **magnetic**[144] and conducting **properties.**[145] Functionalized electron acceptor TCNAQ has been utilized in the synthesis of new D-σ-A compounds.[146] A comparison of TCNQ and $TCNQF_4$ based complexes and their properties has been presented by Azcondo *et al.*[147] The clathrate compounds of H2TCNDQ are expected to have both electron acceptor and proton donor **capability.**[148]

TTF and related molecules have been the prime focus of a majority of organic conductor and superconductor **research.**[138,149] Recent developments in the **functionalization**[150] of TTF have enabled these units to be covalently linked to **macromolecular**[151] systems. New architectures and interesting redox activity have been realized with the synthesis of polymeric TTF's. Extended π-electron donors are important systems in modern TTF chemistry.[152] Fused[153] and halogenated TTF's[154] have provided useful input for structure-property relationships. Dimeric and oligomeric TTF's[155,156] are also being extensively studied. An excellent review on TTF has been published recently.[157] In spite of several advantages possessed by conducting charge transfer complexes and ion radical salts, these materials tend to be brittle and unprocessable. In principle this problem can be overcome by incorporating them in polymers where the charge transfer complexes form part of the main chain or the side chains.

Conjugated polymers

Prior to the discovery of conducting **polymers**[158] in the 1970's, polymer science and technology was largely based on saturated polymers. Saturated polymers like polyethylene are insulators and consequently do not show any special electronic or optical properties. Conjugated polymers on the other hand possess overlapping π-orbitals leading to extended 71-electron delocalization. The resulting band structure bestows

semiconducting or metallic properties on these materials. The classic case of polyacetylene $(CH)_n$ has been noted earlier. Conjugated polymers with chain structures and extended π-electron conjugation can be considered as quasi one dimensional conductors.[159] The conductivity of the conjugated polymers are usually very sensitive to the extent of electron or hole doping. The structures of some of the common conducting polymers are shown in Fig 1.10. Polymers such as poly vinyl ferrocene, poly vinyl carbazole and tetrathiafulvalene substituted polystyrene[160] are called redox polymers and can be subjected to doping. However they are less suitable for electrical conduction.
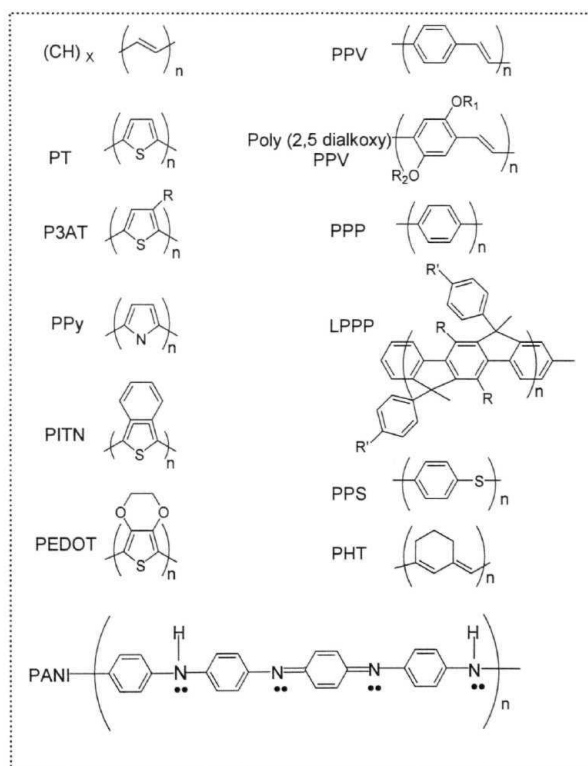
Figure 1.10 *Molecular structures of some of the well known conjugated polymers (adapted from Ref.138).*

Conducting polymers combine many of the electrical and optical properties of metals and semiconductors and the mechanical attributes of conventional plastics. Thus they are unique materials poised for major applications in the current and future technologies. We have discussed in Section 1.2, the electroluminescence of conducting polymers. The electrical conductivity of these polymers arise due to a variety of nonlinear excitations such as solitons, polarons and bipolarons generated by chain relaxation or deformation as well as doping.[159] One of the important features of these materials is the feasibility of fine-tuning the conductivity by controlling the doping levels. This has significant implications for applications of conducting polymers as sensor elements. Conducting polymers find application in other areas as well, such as electromagnetic radiation shields, anticorrosion coatings, smart windows and solid electrolytes.

Polyanilines

Polyaniline (PANI) is one of the most easily synthesized, thermally and environmentally stable conducting polymer. Its versatility stems from the possibility of controlling its electrical and optical characteristics through proton doping. PANI is also probably the oldest known conjugated organic polymer. It was prepared in 1834 by treating aniline with concentrated sulfuric acid. The product was an ill-defined, black, amorphous powder, aniline black.[161] From 1980's PANI has been synthesized chemically electrochemically and its electrochromic[162] characteristics in aqueous and nonaqueous solutions have been extensively investigated. It exists in five different forms (Fig. 1.11) ranging from the fully reduced leucoemeraldine to the fully oxidized pernigraniline. Protonation of the emeraldine base yields the famous 'emeraldine salt' state which is the conducting form of PANI. Molecular weights of polyanilines generally range from 2500 - 6000 g/mol; high molecular weight polyanilines have also been reported.

Oligoanilines provide useful insight into structure-property relationships. Wudl and Heeger have synthesized phenyl capped octaniline[163] which showed the same conductivity as the normal polyaniline. N-methyl substituted oligoanilines have also been synthesized. Recently Buchwald and coworkers have used palladium catalyzed
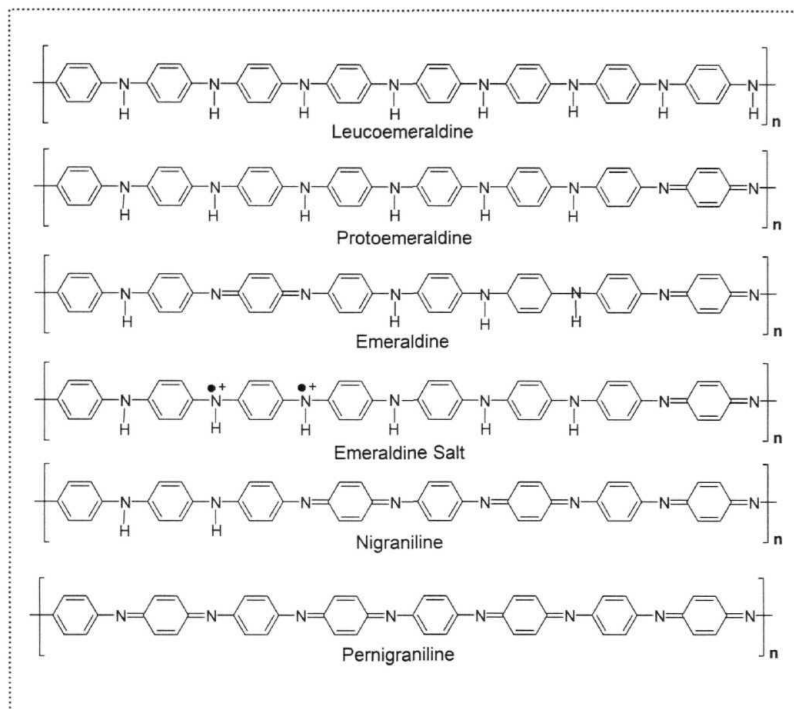
Figure 1.11 *Various states of polyaniline.*

coupling of aryl bromides and arylamines in conjugation with protective groups to synthesize oligoanilines of upto 24 units.[164]   Self-doped conducting polyaniline with improved solubility is obtained by sulfonation of the aromatic units with fuming sulfuric acid.[165]   It shows a conductivity of 0.1 S/cm which is independent of the pH.   Recently Mullen *et al.* have synthesized hybrid structures[166] of polyphenylene sulfide and polyaniline which exhibit excellent solubility in various organic solvents.   Because of their electron rich character they are being tested as hole transport layers in LED's.

Research on PANI has been extensive and multifaceted. It has been the subject of fundamental studies as well as a wide range of applications. An exhaustive review of all the work on this fascinating material is beyond the scope of this brief overview. We list a few of the recent exciting investigations. Polyaniline has been deposited on self assembled monolayers for micron scale patterning.[167] PANI-PVA composite films[168] have been utilized in humidity sensing; at high humidity polyaniline existed in the emeraldine salt form and transformed into a non-conducting base form with decreasing environmental humidity. The conductivity of novel poly aniline-inorganic salt composites[169] have been analyzed via percolation theory. Nanocomposites with transition metal oxides[170] prepared by direct intercalation methods possess good electrical conductivity. Nanoscopic polyaniline particles with good crystallinity have been successfully synthesized in water-oil emulsion.[171] Novel polyaniline nanotubules have been used as second order template[172] by encapsulating iron nanowires and their magnetic behavior has been investigated. Polyaniline nanowires were obtained by electropolymerization of liquid crystalline phases[173] and chiral polyaniline nanotubes were obtained by template-free methods.[174] Polyaniline - metal chelate blends synthesized recently[175] are promising candidates for cathodes in lithium batteries. Realization of good solubility and processability along with high conductivity continues to be a challenge in the research on polyanilines. Our efforts in this direction will be discussed in Chapter 4.

1.5   LAYOUT OF THE THESIS

We are interested in the electronic and optical properties of organic molecular and polymeric materials. As discussed in Sec. 1.3, zwitterionic push-pull molecules based on diaminodicyanoquinodimethanes have been investigated previously in our laboratory, because of their quadratic nonlinear optical properties. This family of molecules exhibit interesting structural control of electronic properties which in turn, impact upon their materials properties. We have now focussed on the question of controlling their assembly through functional groups attached remotely from the π-electron framework that is responsible for their optical characteristics. This led to the discovery of a variety

of interesting phenomena and the fabrication of novel optical and nonlinear optical materials. We have extended this logic to the control of molecular assembly through the utilization of template structures and the fabrication of semiconducting molecular and polymeric materials providing insight into the correlation of molecular organization and materials attributes. The thesis is organized in five chapters. The basic concepts of molecular materials and an overview of optical, nonlinear optical and conducting molecular materials are already covered in the previous sections in this Chapter. We summarize below, the salient features of the remaining chapters.

Chapter 2

In their electronic ground state, the zwitterionic push-pull molecules, diaminodicyanoquinodimethanes (DADQ's), exhibit a large dihedral twist between the diaminomethylene unit and the benzenoid ring plane. The molecular twist has significant impact on the linear and nonlinear optical properties of these materials. After a brief introduction in Sec. 2.1, we present in Sec. 2.2, a semiempirical computational investigation combined with crystallographic examination which we have carried out to model these push-pull quinonoid structures, leading to the concept of a 'molecule-in-a-crystal'. The optimized twist angle, θ of these molecules are found to sensitively depend on the dielectric constant, ε employed in the solvation subroutine in the calculation. The ε required to reproduce the experimental twist angles from crystal structure analysis could be qualitatively related to conventional intermolecular interactions such as H-bonds and electrostatic forces. This study demonstrates the utility of a standard solvation model in mimicking the molecular microenvironment in crystals. We have used this approach in several instances later in the thesis.

The optical and electronic properties of DADQ's are primarily controlled by the π-electron structure. However molecular assembly can be controlled and fine tuned by remote functional groups such as amines, not in conjugation with the π-electron framework. Sec. 2.3 presents a study on a novel situation involving solid state charge transfer promoted by the remote functionality which acts as an anchoring agent. Charge transfer complex formation observed exclusively in the solid state, between the

ᴊush-pull molecule 7,7-bis(piperazino)-8,8 dicyanoquinodimethane (BPDQ) acid is shown to be a two-component analogue of the Kofler's ternary ᴜ   The secondary amine moiety of the piperazine units plays the role of the anchoring agent.   Computational studies provide insight into the nature of the charge transfer interaction.   Synthesis and investigation of a new family of DADQ molecules possessing remote amino functionalities, exhibiting enhanced fluorescence in the solid state and in polymer films is presented in Sec. 2.4.   The critical role of the remote functionality and molecular twist is analyzed through crystallographic and computational studies and the reversible switching of the enhanced fluorescence in a doped polymer film triggered by solvent vapors is demonstrated.

Chapter 3

Sec. 3.1 introduces previous studies in our laboratory which have demonstrated the large hyperpolarizability of DADQ's and their potential application as quadratic NLO materials.   Subsequently we present novel modes by which noncentrosymmetric SHG active materials were obtained in remote functionalized DADQ's and their derivatives. In Sec. 3.2 we demonstrate a simple approach to the modification of crystal architecture using remote functionalities and the fabrication of noncentrosymmetric and SHG active cocrystals. Structural characterization of centrosymmetric crystals of *7,7-bis(N,N-*dimethylethylenediamino)-8,8-dicyanoquinodimethane and its SHG active complex with terephthalic acid, are presented. Sec. 3.3 highlights a novel derivative of DADQ obtained through a simple synthetic modification of remote functionalized systems.   7-(N,N-dimethylpiperazinium)-7-oxo-8,8-dicyanoquinodimethane   is   found   to   exhibit spontaneous resolution in crystals.   This conformationally chiral molecule engages in strong H-bonding and electrostatic interactions leading to the formation of interesting helical superstructures along the three crystallographic axes. The concomitant formation of the helical motifs expresses the homochirality of the molecular assembly leading to the spontaneous resolution in this material.   The moderate SHG exhibited by the microcrystalline material is also presented.

Chapter 4

In the study of remote functionalized DADQ's showing enhanced light emission discussed in Sec. 2.4, we used polyelectrolytes as templates to organize some of the ionic **chromophores**. We have considered the utilization of polyelectrolyte templates in the fabrication of molecular and polymeric conductors as well. After a brief introduction in Sec. 4.1 we present in Sec. 4.2, the development of a simple and convenient protocol for the synthesis of poly(4-styrenesulfonate) templated polyaniline in the form of practically useful stable aqueous colloidal solutions. Good quality films were fabricated by forming composites with trace amounts of polyvinylalcohol (PVA). Investigation of the submicron and nano level morphological features in the film revealed interesting dependence on the template molecular weight and the amount of PVA additive. The dependence of the film conductivity on the template polymer molecular weight revealed in our studies suggests that the latter is a novel design element for conducting polyaniline. Sec. 4.3 presents the synthesis of a new class of molecular materials which incorporate tetrathiafulvalene (TTF) and polyionic polymers such as poly(4-**styrenesulfonate)** and poly(vinylsulfate). Enhancement of the conductivity by $\sim10^2$ -10^4 over the starting TTF salt based on small anion is demonstrated. We also present a brief investigation of the interesting 'core-sheath' crystal structure and **semiconductivity** of a TTF complex based on a symmetric counterion.

Chapter 5

In Sec. 5.1 we provide an overview of the various investigations presented in the thesis. The highlights of the work include : (i) a new methodology to model **molecule-in-a-crystal** allowing critical solid state effects on molecular geometry and electronic properties to be assessed, (ii) development of a variety of optical materials based on remote functionalized DADQ's exhibiting novel charge transfer complex **formation,** enhanced fluorescence in the solid state, spontaneous resolution through helical assembly and second harmonic generation, and (iii) fabrication of polyelectrolyte templated molecular and polymeric semiconductors. Directions for further explorations in this area of research are outlined in Sec. 5.2.

REFERENCES

1. Simon, J.; Bassoul, P. *Design of Molecular Materials: Supramolecular Engineering,* John Wiley: Chichester, 2000.

2. (a) Klabunde, K. J. *Nanoscale Materials in Chemistry,* John Wiley: New York, 2001; (b) Rao, C. N. R.; Cheetham, A. K. *J. Mater. Chem.* **2001,***11,* 2887; (c) Nalwa, H. S. (Ed.) *Handbook of Nanostructured Materials and Nanotechnology, Vols. 1-5,* Academic Press, New York, 2000.

3. (a) Lehn, J. -M. *Supramolecular Chemistry* : *Concepts and Perspectives,* VCH: Weinheim, 1995; (b) Steed, J. W.; Atwood, J. L. *Supramolecular Chemistry,* John Wiley: Chichester, 2000.

4. Desiraju, G. R. *Crystal Engineering: The Design of Organic Solids,* Elsevier, Amsterdam, 1989.

5. (a) Seymour, R. B; Carraher.Jr. C. E. *Polymer Chemistry,* Marcel Dekker Inc, New York, 1981; (b) Cowie, J. M. G. *Polymers: Chemistry & Physics of Modern Materials,* 2nd Edn, Chapman & Hall, London, 1991.

6. (a) Demus, D.; Goodby, J.; Gray, G. W.; Spiess, H. -W.; Vill,V. (Eds.) *Physical Properties of Liquid Crystals,* Wiley-VCH: Weinheim, 1999; (b) Bahadur, B. *Liquid Crystals: Applications and Uses, Vol. 3,* World Scientific Publishing Co. Pte. Ltd. Singapore, 1992.

7. Schafer, E. P.; Maeda, M. *Dye Lasers,* Springer-Verlag, Berlin, 1990.

8. Maeda, M. *Laser Dyes: Properties of Organic Compounds for Dye Lasers,* Academic Press Inc, New York, 1984.

9. Franken, P. A.; Hill, A.E.; Peters, C.W.; Weinreich, G. *Phys. Rev. Lett.* **1961,** *6,* 118.

10. Giordmaine, J. A. *Phys. Rev. Lett.* **1962,** *8,* 19.

11. Maker, P. D.; Terhune, R. W.; Nisenhoff, M.; Savage, C. M. *Phys. Rev. Lett.* **1964,5,21.**

12. Rentzepis, P. M.; Pao, Y. H. *Appl. Phys. Lett.* **1964,** *5,* 156.

13. Heilmeier, G. H.; Ockman, N.; Braunstein, R.; Kramer, D.A. *Appl. Phys. Lett.* **1964,** 5, 228.

14. Gott. J. R *J. Phys. B* **1971,** *4,* 116.

15. Kurtz, S. K.; Perry, T. T. *J. Appl. Phys.* **1968,** *39,* 3798.

16.   Zyss, J.; Berthier, G. *J. Chem. Phys.* **1982,** *77,* 3635.

17.   (a) Jerphagnon, J.; Kurtz, S. K. J. *Appl. Phys.* **1970,** *41,* 1667; (b) Jerphagnon, J.; Kurtz, S. K. *Phys. Rev. B* **1970**, *1*, 1739.

18.   Hauchecorne, G.; Kerherve, F.; Mayer, G. *J. Phys.* **1971,** *32,* 47.

19.   Levine, B. F. *Chem. Phys. Lett.* **1976,** *37,* 516.

20. (a) Chemla, D. S.; Zyss, J. (Eds.) *Nonlinear Optical Properties of Organic Molecules and Crystals, Vols.* 7-2, Academic Press, Orlando, 1987; (b) Giinter, P. *Nonlinear Optical Effects and Materials, Springer Series in Optical Sciences, Vol. 72,* Springer-Verlag, Heidelberg, 2000.

21.   Williams, D. J. *Angew. Chem. Int. Ed. Engl.* **1984,** *23,* 690.

22.   Kanis, D. R.; Ratner, M. A.; Marks, T. J. *Chem. Rev.* **1994,** *94,* 195.

23. (a) Messier, J.; Kajzar, F.; Prasad, P. (Eds.) *Organic Molecules for Nonlinear Optics and Photonics, Vol. 194,* Kluwer Academic Publishers, Nato ASI Series, Dordrecht, 1991; (b) Wolff, J. J.; Wortmann, R. *Adv. Phys. Org. Chem.* **1999,** *32,* 121.

24. (a) Wang, C.P. *Polymers for Photonic and Electronic Applications,* Academic Press, London, 1993; (b) Prasad, P. N.; Williams, D. J. *Introduction to Nonlinear Optical Effects in Molecules and Polymers,* John Wiley: New York, 1991.

25.   (a) Moerner, W. E.; Silence, S .M. *Chem. Rev.* **1994,** *94,* 127; (b) Zhang, Y.; Wada, T.; Sasabe, H. *J. Mater. Chem.* **1998,** *8,* 809.

26.   Law, K.Y. *Chem. Rev.* **1993,** *93,* 449.

27. Poople Jr, C. P. *Handbook of Superconductivity,* Academic Press, New York, 2000.

28. (a) Enderlein, R.; Horing, N. J. M. *Fundamentals of Semiconductor Physics and Devices,* World Scientific Publishing Co. Pte. Ltd. Singapore, 1997; (b) Wenckebach, W. T. *Essentials of Semiconductor Physics,* John Wiley: Chichester, 1999.

29.   (a) Bruce, D.W.; O'Hare, D. (Eds.) *Inorganic Materials,* John Wiley: Chichester, 1992; (b) Knop, W. *Justus Leibigs. Ann. Chem.* **1842,** *43,* 111.

30.   Akamatu, H.; Inokuchi, H.; Matsunaga, Y. *Nature* **1954**, *173*, 168.

31.   (a) Wudl, F. *Acc. Chem. Res.* **1984**, *17*, 227; (b)Williams, J. M.; Beno, M. A.; Wang, H. H.; Leung, P. C. W.; Emge, T. J.; Geiser, U.; Carlson, K. D. *Acc. Chem.*

Res. **1985,** *18,* 261; (c) Kristenmacher, T. J.; Philips, T. E.; Cowan, D. O. *Acta Crystallogr. B* **1974,** *30,* 763.

32.   Wudl, F.; Smith, G. M; Hufnagel, E. J. *J. Chem. Soc. Chem. Commun.* **1970,** 1453.

33.   Scott, B. A.; Placa., S. J. L.; Torrance, J. B.; Silverman, B. D.; Welber, B. *J. Am. Chem. Soc.* 1977,20,6631.

34.   Bechgaard, K.; Carneiro, K.; Rasmussen, F. B.; Olsen., M.; Rindorf. G.; Jacobsen, C. S.; Pederson, H. J.; Scott, J. C. *J. Am .Chem. Soc.* **1981**, *103*, 2440.

35.   (a) Parkin, S. S.; Engler, E. M.; Schumaker, R. R.; Lagier, R.; Lee, V. Y.; Scott, J. C; Greene, R. L. *Phys. Rev. Lett.* **1983,** *50,* 270; (b) Williams, J. M.; Emge, T. J.; Wang, H. H.; Beno, M. A.; Coops, P. T.; Hall, L. N.; Carlson, K. D.; Crabtree, G. W. *Inorg. Chem.* **1984,** *23,* 2558.

36.   Urayama, H.; Yamochi, H.; Saito, G.; Nozawa, K.; Sugano, T.; Kinoshita, M.; Sato, S.; Oshima, K.; Kawamoto, A.; Tanaka, J. *Chem. Lett.* **1988,** 55.

37.   (a) Hebard, A. F.; Rosseinsky, M. J.; Haddon, R. C; Murphy, D. W.; Glarum, S, H.; Palstra, T. T. M.; Ramirez, A. P.; Kortan, A. R. *Nature* **1991,** 550, 600; (b) Holczer, K.; Klein, O.; Huang, S. M.; Kaner, R. B.; Fu, K. J.; Whetten, R. L.; Diederich, F. *Science* **1991,** *252,* 1154; (c) Haddon, R. C. *Acc. Chem. Res.* **1992,** *25,* 127; (d) Prato. M. *J. Mater. Chem.* **1997,** 7, 1097.

38.   (a) Gatteschi, D.; Kahn, O.; Miller, J. S.; Palacio, F. (Eds.) *Magnetic Molecular Materials,* NATO Series *Vol. 198,* Kluwer Academic Publishers, Dordrecht, 1991; (b) Miller, J. S.; Drillon, M. *Magnetism: Molecules to Materials,* Wiley-VCH: Weinheim,2001.

39.   Gatteschi, D. *J. Alloys. Comp.* **2001,** *317-318*, 8.

40.   (a) Metzger, R. M. *Acc. Chem. Res.* **1999,** *32,* 950; (b) Ashwell,G. J.; Gandolfo, D. S. *J. Mater. Chem.* **2002,** *12*, 411; (c) Ashwell,G. J.; Gandolfo, D. S.; Hamilton, R. *J. Mater. Chem.* **2002,** *12*, 416; (d) Martin, A. S.; Sambles, J. R.; Ashwell, G. J. *Phy. Rev. Lett.* 1993, *70,* 218.

41.   (a) Fabbrizzi, L.; Licchelli, M.; Pallavicini, P. *Acc. Chem. Res.* **1999,** *32,* **846; (b)** Pease, A. R.; Jeppesen, J. O.; Stoddart, J. F.; Lou, Y.; Collier, C. P.; Heath, J. R. *Acc. Chem. Res.* **2001,** *34,* 433.

42.   (a) De Silva, A. P.; Gunaratne, H. Q. N.; McCoy, C. P. *Nature* **1993,** *364*, 42; (b) Credi, A; Balzani, V.; Langford, S. J.; Stoddart, J. F. *J. Am. Chem. Soc.* **1997,**

119, 2679; (c) De Silva. A P.; McClenagham, N. D. *J. Am. Chem. Soc.* **2000, 122,** 3965; (d) Gunnlaugsson, T.; Danail,D. A. M.;Parker, D. *Chem. Commun.* **2000,** 93; (e) Rong, D.; Mallouk, T. E. *Inorg. Chem.* **1993,** *32,* 1454.

43. (a) Davis, W. B.; Svec, W. A.; Ratner, M. A.; Wasielewski, M. R. *Nature* **1998,** *396,* 60; (b) Bumm, L. A.; Arnold, J. J.; Cygan, M. T.; Dunbar, T. D.; Burgin, T. P.; Jones, L.; Allara, D. L.; Tour, J. M.; Weiss, P. S. *Science* **1996,** *271,* 1705; (c) Barigelletti, F.; Flamigni, L. *Chem. Soc. Rev.* **2000,** *29,* 1.

44. Bissell, R. A.; Cordova, E.; Kaifer, A. E.; Stoddart, J. F. *Nature* **1994,** *369,* 133.

45. Kelly, T. R.; Bowyer, M. C; Bhaskar, K. V.; Bebbington, D.; Garcia, A.; Lang, F.; Kim,M. H.; Jette, M. P. *J. Am. Chem. Soc.* **1994**, *116*, 3657.

46. Kelly, T. R.; Tellitu, I.; Sestelo, J. P. *Angew. Chem. Int. Ed. Engl.* **1997,** *36,* 1866.

47. Clayden, J.; Pink, J. H. *Angew. Chem. Int. Ed. Engl.* **1998,** *37,* 1937.

48. (a) Hench, L. L.; West, J. K. *Chem. Rev.* **1990,** *90,* 33; (b) Gesser, H. D.; Goswami, P. C. *Chem. Rev.* **1989,** *89,* 765; (c) Rao, C. N. R.; Gopalakrishnan, J. *New Directions in Solid State Materials,* Cambridge Univeristy Press, Cambridge, 1986.

49. Maeda, M; Bartsch, R. A. *Molecular and Ionic Recognition with Imprinted Polymers,* ACS Symposium Series, Oxford University Press, Oxford, 1998.

50. Hulliger, J. *Angew. Chem. Int. Ed. Engl.* **1994,** 53, 143.

51. (a) Burland, D. M.;Miller, R.D.; Walsh, C.A. *Chem. Rev.* **1994,** *94,* 31; (b) *Poled Polymers and their Applications to SHG and EO Devices,* Miyata, S.; Sasabe, H. (Eds.) Gorden and Breach Science Publishers: Amsterdam, 1997.

52. (a) Ashwell, G. J.; Jackson, D. P.; Crossland, W. A. *Nature* **1994,** *368,* 438; (b) Ashwell, G. J.; Jefferies, G, George, C. D.; Ranjan, R.; Charters, R. B.; Tatam, R. P. *J. Mater. Chem.* **1996,** 6, 131.

53. (a) Lvov, Y.; Ariga, K.; Onda, M.; Ichinose, I.; Kunitake, T. *Colloids and surfaces A* **1999**, *146*, 337; (b) Cui, X.; Pei, R.; Wang, Z.; Yang, F.; Ma, Y.; Dong, S.; Yang, X. *Biosensors & Bioelectronics* **2003**, *18*, 59; (c) Park, S. Y.; Rubner, M. F.; Mayes, A. M. *Langmuir* **2002**, *18*, 9600; (d) Ulman, A. *Chem. Rev.* **1996,96,1533.**

54. **Forrest,** S. **R.** *Chem. Rev.* **1997,** *97,* 1793.

55. MacAdam, D. L. *Theory of Color and its Applications,* Springer Series in Optical Sciences, *Vol. 19,* Springer-Verlag, Heidelberg, 1979.

56.   Duxbury, D. F. *Chem. Rev.* **1993,** *93*, 381.

57.   Jager, S. *Thin Solid Films* **1996,** *286,* 154.

58. Hertz, O.; Bottcher, H.; Fischer, U. *Thin Solid Films.* **1991,***199,* 153.

59.   Wang, S.; Shen, S.; Xu, H.; Gu, D.; Yin, J.; Dong, X. *Mater. Sci. & Engg. B* **2001,** *79,* 45.

60.   (a) Somani, P. R.; Viswanath, A. K.; Aiyer R. C; Radhakrishnan, S. *Organic Electronics* **2001,** *2,* 83; (b) Citterio, D.; Jenny, L.; Rasonyi, S.; Spichiger, U. E. *Sens. Actuators B* **1997,** *38-39,* 202.

61.   Marder, S. R.; Kippelen, B.; Jen, A. K. -Y.; Peyghambarian, N. *Nature* **1997,** 388, 845.

62.   Bach, U.; Lupo, D.; Comte, P.; Moser, J. E.; Weissortel ,F.; Salbeck, J.; Sprietzer, H.; Grätzel, M. *Nature* **1998,** *395,* 533.

63.   (a) Wurthner, F.; Yao, S.; Debaerdemaeker, T.; Wortmann, R. *J. Am. Chem. Soc.* **2002,** *124,* 9431; (b) Tirelli, N.; Altomare, A.; Solaro, R.; Ciardelli, F.; Follonier, S.; Bosshard, Ch.; Giinter, P. *Polymer* **2000,** *41,* 415.

64.   (a) Kato, K.; Shinbo, K.; Obata, K.; Kaneko, F. *Synth. Met.* **2000,** *111-112,* 615; (b) Kirstein, S.; Mohwald, H. *Chem. Phys. Lett.* **1992,** *189,* **408.**

65.   (a) Ashwell. G. J.; Jefferies, G.; Hamilton, D. G.; Lynch. D.E.; Roberts, M. P. S.; Bahra, G. S.; Brown, C. R. *Nature* **1995,** *375,* 385; (b) Petermann, R.; Tian, M.; Tatsuura, S.; Furuki, M. *Dyes and Pigments* **2003,** *57,* 43.

66.   Ashwell, G. J.; Handa, T.; Jefferies, G.; Hamilton. D. *Colloids and Surfaces A* **1995,** *102*, 133.

67.   Zhou G.; Wang, X.; Wang, D.; Wang, C; Shao, Z.; Fang, Q.; Jiang, M. *Optics Commun.* **2001,** *190*, 345.

68.   (a) Sulcova, P.; Trojan, M. *Dyes and Pigments* **1998,** *4,* 83; (b) Sulcova, P.; Trojan, M. *Dyes and Pigments* **1998,** *36,* 287.

69.   Gonzalvo, B.; Romero, J.; Fernandez, F.; Torralvo, M. J. *J. Alloys Compds.* **2001,** *323,* 372.

70.   Schafer, F. P.; Schmidt, W.; Volze, J. *Appl. Phys. Lett.* **1966,** *9,* 306.

71.   Spaeth, M. L.; Bortfeld, D. P. *Appl. Phys. Lett.* **1966,** *9,* 179.

72.   Soffer, B. H.; McFarland, B. B. *Appl. Phys. Lett.* **1967,** *10,* 266.

73.   Kauffman, J. M. *Appl. Opt.* **1980,** *19*, 3431.

74.   Gvishi, R.; Reisfeld, R.; Burshtein, Z. *Chem. Phys. Lett.* **1993,** *213,* 338.

75.   (a) Johansson, N.; Salbeck, J.; Bauer, J.; Weissortel, F.; Bröms, P.; Andersson, A; Salaneck, W. R. *Adv. Mater.* **1998,***10,* 1136; (b) Salbeck, J.; Bauer, J.; Weissortel, F. *Polymer Preprints* **1997,** *38,* 349; (c) Salbeck, J.; Weissortel, F. *Macromol. Symp.* **1997**, *125*, 121; (d) Johansson, N.; Dos Santos, D. A.; Guo, S.; Cornil, J.; Fahlman, M.; Salbeck, J.; Schenk, H.; Arwin, H.; Bredas, J. L.; Salanek, W. R. *J. Chem. Phys.* **1997,** 707, 2542; (e) Spreitzer, H.; Schenk, H.; Salbeck, J.; Weissoertel, F.; Riel, H.; Reiss, W. *SPIE Proceedings*,Denver, 1999; (f) Weinfurtner, K. H; Weissortel, F.; Harmgarth, G.; Salbeck, J. in *SPIE Proceedings,* p.40, San Diego, 1998.

76.   Hamada, Y.; Adachi, C; Tsutsui, T.; Saito, S. *Jpn. J. Appl. Phys.* **1992,** *31,* 1812.

77.   Jeong, H.; Zou, D.; Tsutsui, T. *Mol. Cryst. Liq. Cryst.* **1999,** *327,* 185.

78.   (a) Krasovitskii, B. M.; Bolotin, B. M. *Organic Luminescent Materials,* VCH: Weiheim, 1988; (b) Miyata, S.; Nalwa, H. S. (Eds.) *Organic Electroluminescent Materials and Devices,* Gordon and Breach: Amsterdam, 1997.

79.   Lackowicz, J. R. *Principles of Fluorescence Spectroscopy,* 2nd Edn. Kluwer Academic/ Plenum Publishers, New York, 1999.

80.   (a) Hung, L. S.; Chen, C. H. *Mater. Sci. Engg.* **2002,** *R39,* 143; (b) Shirota, Y. *J. Mater. Chem.* **2000,** *10, 1.*

81.   (a) Waring, M. *J. Mol. Biol.* **1970,** *54,* 247; (b) Lawrence, J. J. Daune, M. *Biochemistry* **1976,** 75, 3301.

82.   Henderson, B. W.; Dougherty, T. J. (Eds.) *Photodynamic Therapy: Basic Principles and Clinical Applications,* Marcel Dekker, New York, 1992.

83.   Weidle, S. *Proc. Med. Chem.* **1979**, *16*, 151.

84.   Friedman, A. E.; Chambron, J. C; Sauvage, J. P.; Turro, N. J.; Barton, J. K. *J. Am. Chem. Soc.* **1990,** 772, 4960.

85.   Holonyak, J. R. N.; Bevacqua, S. F. *Appl. Phys. Lett.* **1962,** 7, 82.

86.   Pope, M.; Kallmann, H. P.; Magnante, P. *J. Chem. Phys.* **1963,** *38,* 2042.

87.   (a) Helfrich, W.; Schneider, W. G. *Phys. Rev. Lett.* **1965,** *14,* 229; (b) Helfrich, W.; Schneider, W. G. *J. Chem. Phys.* **1965,** *44,* 2902.

88.   Mehl, W.; Bucher, W. *Z. Phys. Chem.* **1965,** *47,* 76.

89.   Tang, C. W.; Van Slyke, S. A. *Appl. Phys. Lett,* **1987,** 57, 913.

90.   Adachi, C; Tsutsui, T.; Saito, S. *Appl. Phys. Lett* **1990,** 56, **799.**

91.   Salbeck, J. *Ber. Bunsenges. Phys. Chem.* **1996**, *100*, 1667.

92.   (a) Sheats, J. R.; Antoniadis, H.; Hueschen, M.; Leonard, W.; Miller, J.; Moon, R.; Roitman, D.; Stocking, A. *Science* **1996**, *273,* 884; (b) Mitschke, U.; Bauerle, P. *J. Mater. Chem.* **2000**, *10,* 1471; (c) Tang, C. W.; Van Slyke, S. A.; Chen, C. H. *J. Appl. Phys.* **1989**, *65,* 3610; (d) Ono, Y. A. *Annu. Rev. Mater. Sci.* **1997**, *27,* 283.

93.   Tutsui, T. *Mater. Res. Bull.* **1997**, *22,* 39.

94.   Hamada, Y. *IEEE Trans. Electron. Dev.* **1997**, *44,* 1208.

95.   Patra, A.; Pan, M.; Friend, C. S.; Lin, T. C; Cartwright, A. N.; Prasad, P. N.; Burzynski, R. *Chem. Mater.* **2002**, *14*, 4044.

96.   (a) Sheats, J. R.; Chang, Y. L.; Roitman, D. B.; Stocking, A. *Acc. Chem. Res.* **1999**. *32,* 193; (b) Friend, R. H.; Gymer, R. W.; Holmes, A. B.; Burroughes, J. H.; Marks, R. N.; Taliani, C; Bradley, D. D. C; Santos, D. A. D.; Bredas, J. L.; Lögdlund, M.; Salaneck, W. R. *Nature* **1999**, *397,* 121.

97.   (a) Kraft, A.; Grimsdale, A. C; Holmes, A. B. *Angew. Chem. Int. Ed. Engl.* **1998**, *37,* 402; (b) Burroughes, J. H.; Bradley, D. D. C; Brown, A. R.; Marks, R. N.; Mackey, K.; Friend; R. H.; Burns, P. L.; Holmes, A. B. *Nature* **1990**, *347,* 539.

98.   Kasim, R. K.; Pomerantz, M.; Elsenbaumer, R. L. *Chem. Mater.* **1998**, *10*, 235.

99.   Chang, S. C; Yang, Y. *Appl. Phys. Lett,* **1999**, *75,* 2713.

100.   Gustafsson, G.; Cao, Y.; Treacy, G. M.; Klavetter, F.; Colaneri, N.; Heeger, A. J. *Nature* **1992**, *357, All.*

101.   Okumoto, K.; Shirota, Y. *Chem. Mater.* **2003**, *15,* 699.

102.   Tsutsui, T.; Aminaka, E.; Lin, C. P.; Kim, D. -U. *Phil. Trans. R. Soc. Lond. A* 1997,555,801.

103.   Shen, H. Y.; Zhou, Y. P.; Lin, W. X.; Zeng, Z. D.; Zeng, R. R.; Yu, G. F.; Huang, C. H.; Jiang, A. D.; Jia, S. Q.; Shen, D. Z. *IEEE J. Quant. Electron.* **1992**, *28,* 48.

104.   Smith, R. G.; Geusic, J. E.; Levinstein, H. J.; Rubin, J. J.; Singh, S.; Uitert, L. G. V. *Appl. Phys. Lett.* **1968**, *12*, 308.

105.   Lin, S.; Wu, B.; Xie, F.; Chen, C. *Appl. Phys. Lett.* **1991**, *59,* 1541.

106.   Cheng, L. -T.; Tarn, W.; Stevenson,S. H.; Meredith G .R,.;Rikken, G.; Marder, S. R. *J. Chem. Phys.* **1991**, *95* ,10631.

107.   Cheng, L. -T.; Tam, W.; Marder, S. R.; Steigman, A. E.; Rikken, G.; Spangler, C. W. *J. Chem. Phys.* **1991**, *95* ,10643.

108. (a) Oudar, J. L. *J. Chem. Phys*. **1977,** *67,* 446; (b) Levine, B. F. *J. Chem. Phys.* 1975,65, 115.

109. Dulcic, A.; Sauteret, C. *J. Chem. Phys.* **1978,** *69,* 3453.

110. Oudar, J. L.; Leperson, H. *Opt. Commun.* **1975,** 75, 258.

111. (a) Katz, H. E.; Singer, K. D.; Sohn, J. E.; Dirk, C. W.; King, L. A.; Gordon, H. M. *J. Am. Chem. Soc.* **1987,***109,* 6561; (b) Singer, K. D.; Sohn, J. E.; King, L. A.; Gordon, H. M.; Katz, H. E.; Dirk, C. W. *J. Opt. Soc. Am. B* **1989,** *6,* 1339.

112. Eaton, D. F. *Science* **991,** *253,* 281.

113. (a) Blanchard-Desce, M.; Wortmann, R.; Lebus, S.; Lehn, J. M.; Kramer, P. *Chem. Phys. Lett.* **1995,** *243,* 526; (b) Marder, S. R.; Cheng, L. T.; Tiemann, B. G.; Friedli, A. C; Blanchard-Desce, M; Perry, J. W.; Skindhøj, J. *Science* **1994,** 265,511.

114. Morley, J. O.; Docherty, V.J.; Pugh, D. *J. Chem. Soc. Perkin. Trans. II* **1987,** 1351.

115. (a) Miller, R. D.; Lee, V. Y.; Moylan, C. R. *Chem. Mater.* **1994,** *6,* 1023; (b) Dirk, C. W.; Katz, H. E.; Schilling, M. L.; King, L. A. *Chem. Mater.* **1990,** *2,* 700.

116. (a) Long, N. J. *Angew. Chem. Int. Ed. Engl.* **1995,** *34,* 21; (b) Bella, S. D. *Chem. Soc. Rev.* **2001,** *30,* 355; (c) Torre, G. D. L.; Vazquez, P.; Lopez, F. A.; Torres, T. *J. Mater. Chem.* **1998,** *8,* 1671.

117. (a) Kelderman, E.; Starmans, W. A. J.; van Duynhoven. J. P. M ; Verboom, W.; Engbersen, J. F. J.; Reinhoudt, D. N.; Derhaeg, L.; Verbiest, T.; Clays, K.; Persoons, A. *Chem. Mater.* **1994,** *6,* 412; (b) Kelderman, E; Derhaeg, L.; Heesink, G. J. T.; Verboom, W.; Engbersen, J. F. J.; van Hulst, N. F. Persoons, A.; Reinhoudt, D. N. *Angew. Chem. Int. Ed. Engl.* **1992,** *31,* 1075.

118. (a) Mignani, G.; Barzoukas, M; Zyss, J.; Soula, G.; Balegroune, F.; Grandjean, D.; Josse, D. *Organometallics*. **1991,** *10,* 3660; (b) Mignani, G.; Kramer, A.; Puccetti, G.; Ledoux, I.; Soula, G.; Zyss, J.; Meyrueix, R. *Organometallics.* **1990,** *9,* 2640.

119. (a) Verbiest, T.; Clays, K.; Samyn, C; Wolff, J.; Reinhoudt, D.; Persoons, A. *J. Am. Chem. Soc.* **1994,** *116,* 9320; (b) Ray, P. C; Das, P. K. *Chem. Phys. Lett.* **1995,** *244,* 153; (c) Zyss. J.; Ledoux, I. *Chem. Rev.* **1994,** *94,* **77.**

120. Bahl, A.; Grahn, W.; Stadler, S.; Feiner, F.; Bourhill, G.; Brauchle.; Reisner, A.; Jones, P. G. *Angew. Chem. Int. Ed. Engl.* **1995,** *34,* 1485.

121.   (a) Verbiest, T.; van Elshocht, S.; Kauranen, M; Hellemans, L.; Snauwaert, J.; Nuckolls, C; Katz, J. T.; Persoons, A. *Science* **1998,** *282,* 913; **(b)** Gangopadhyay, P.; Radhakrishnan, T. P. *Angew. Chem. Int. Ed.* **2001,** *40,* 2451.

122.   (a) Kurtz, H. A.; Stewart, J. J.; Dieter, K. M. *J. Comput. Chem.* **1990,** *11,* 82; (b) Jain, M.; Chandrasekhar, J. *J. Phys. Chem.* **1993,** *97,* 4044.

123.   Oudar, J. L.; Chemla, J. S. *J. Chem. Phys.* **1977,** *66,* 2664.

124.   Verbiest, T.; Houbrechts, S.; Kauranen, M.; Clays, K.; Persoons, A. *J. Mater. Chem.* **1997,** 7,2175.

125.   (a) Levine, B. F.; Bethea, C. G. *J. Chem. Phys.* **1975,** *63*, 2666; (b) Singer, K. D.; Sohn, J. E.; King, L. A.; Gordon, H. M.; Katz, H. E.; Dirk, C. W. *J. Opt. Soc. Am. B* **1989,** *6,* 1339.

126.   (a) Kielich, S.; Lalane, J. R.; Martin, F. B. *Phys. Rev. Lett.* **1971,** *26,* 1295; (b) Clays, K.; Persoons, A. *Phys. Rev. Lett.* **1991,** *66,* 2980.

127.   Zyss, J.; Oudar, J. L.; *Phys. Rev. A* **1982,** *26,* 2028.

128.   (a) Reichoff. K.; Peticolas. W. F. *Science* **1965**, *147*, 611; (b) Ukachi, T.; Shigemoto, T.; Komatsu, H.; Sugiyama, T. *J. Opt. Soc. Am. B* **1993,** *10,* 1372.

129.   (a) Etter, M. C. *Acc. Chem. Res.* **1990,** *23,* 120; (b) Russell, V. A.; Ward, M. D. *Chem. Mater.* **1996,** *8,* 1654; (c) Lipscomb, G. F.; Garito, A. F.; Narang, R. S. J. *Chem. Phys.* **1981,** *75,* 1509; (d) Lipscomb, G. F.; Garito, A. F.; Narang, R. S. *Appl. Phys. Lett.* **1981,** *38,* 663; (e) Twieg, R.; Azema, A.; Jain, K.; Cheng, Y. Y. *Chem. Phys. Lett.* **1982,** *92,* 208; (f) Levine, B. F.; Bethea, C. G.; Thurmond, C. D.; Lynch, R. T.; Bernstein, J. *J. Appl. Phys.* **1979,** 50, 2523; (g) Zerkowski, J. A.; MacDonald, J. C; Whitesides, G. M. *Chem. Mater.* **1994,** *6,* 1250; (h) Sarma, J. A. R. P.; Rao, J. L.; Bhanuprakash, K. *Chem. Mater.* **1995,** 7, 1843; (i) Bernstein, J.; Davis, R. E.; Shimoni, L.; Chang, N. L. *Angew. Chem. Int. Ed. Engl.* **1995,** *34,* 1555; (j) Sarma, J. A. R. P.; Allen, F. H.; Hoy, V. J.; Howard, J. A. K.; Thaimattam, R.; Biradha, K.; Desiraju, G. R. *Chem. Commun.* **1997,** 101.

130.   (a) Gangopadyay, P.; Rao, S. V.; Rao, D. N.; Radhakrishnan, T. P.; *J. Mater. Chem.* **1999,** *9,* 1699; (b) Gangopadyay, P.; Sharma, S.; Rao, A. J.; Rao, D. N, Cohen, S.; Agranat, I.; Radhakrishnan, T. P. *Chem. Mater.* **1999,** *11,* 466; (c) Sharma, S.; Radhakrishnan, T. P. *Mol. Cryst. Liq. Cryst.* **1999,** *338,* 257; (d) Gangopadyay, P.; Radhakrishnan, T. P. *Chem. Mater.* **2000**, *12* , 3362.

131. (a) Ramamurty, V.; Eaton, D. F. *Chem. Mater.* 1994, *6*, 137; (b) Weissbuch, I.; Lahav, M.; Leiserowitz, L.; Meredith, G. R.; Vanherzeele, H. *Chem. Mater.* 1989, *1*, 114; (c) Cox, S. D.; Gier, T. E.; Stucky, G. D. *Chem. Mater.* 1990, *2*, 609.

132. Marder, S. R.; Perry, J. W.; Yakymyshyn, C. P. *Chem. Mater.* **1994**, *6*, 1137.

133. Ravi, M; Rao, D. N.; Cohen, S.; Agranat, I.; Radhakrishnan, T. P. *J. Mater. Chem.* 1996, 6, 1853.

134. Hertler, L. R.; Hartzler, H. D.; Acker, D. S.; Benson, R. E. *J. Am. Chem. Soc.* 1962, *84*, 3387.

135. (a) Ravi, M. *Ph. D. Thesis,* University of Hyderabad, 1997; (b) Gangopadhyay, P. *Ph. D. Thesis,* University of Hyderabad, 2002.

136. Gangopadhyay, P.; Ravi, M.; Radhakrishnan, T. P. *Ind. J. Chem.* 2000, *A39*, 106.

137. Sharma, S. *Ph. D. Thesis,* University of Hyderabad, 2002.

138. Bernier, P.; Lerant , S.; Bidan, G. *Advances in synthetic metals: Twenty Years of Progress in Science and Technology,* Elsevier Science, Amsterdam, 1999.

139. Torrance, J. B. *Acc. Chem. Res.* 1979, *12*, 79.

140. Curran, S.; Stark-hauser, A.; Roth, S. in *Hand Book of Organic Conductive Molecules and Polymers,* Nalwa, H. S. (Ed.) *Vol. 2,* p. 1, John Wiley: Chichester, 1997.

141. (a) Parkin, S. S. P.; Engler, E. M.; Schumaker, R. R.; Lagier, R.; Lee, V. Y.; Scott, J. C; Greene, R. L. *Phys. Rev. Lett.* 1983, *50*, 270; (b) Moustarder, S. L.; Hudhomme, P.; Durand, C; Mercier, N.; Azcondo, M. T.; Delhaes, P.; Riou, A.; Gorgues, A. *J. Mater. Chem.* **2000**, *10*, 617; (c) Naito, T.; Inabe, T.; Takeda, K.; Awaga, K.; Akutagawa, T.; Hasegawa, T.; Nakamura, T.; Kakiuchi, T.; Sawa, H.; Tamamoto, T.; Tajima, H. *J. Mater. Chem.* 2001, *11*, 2221.

142. Ogura, F.; Otsubo, T. in *Handbook of Organic Conductive Molecules and Polymers,* Nalwa, H. S. (Ed.) *Vol. 1,* p.229, John Wiley: Chichester, 1997.

143. (a) Martin. N.; Segura, J. L.; Seoane, C. *J. Mater. Chem.* **1997**, 7, 1661; (b) Yamashita, Y.; Tomura. M. *J. Mater. Chem.* **1998**, *8*, 1933.

144. (a) Bigoli, F.; Deplano, P.; Devillanova, A. F.; Girlando, A.; Lippolis, V.; Mercuri, M. L.; Pellinghelli, M. -A.; Trogu, E. *J. Mater. Chem.* **1998**, *8*, 1145; (b) Ito, A.; Saito, T.; Ota, K. I.; Miura, T.; Misaki. Y.; Tanaka, K. Yamabe, T. *J. Mater. Chem.* **1998**, *8*, 1799.

145. (a) Brook, D. J. R.; Koch, T. H. *J. Mater. Chem.* **1997,** 7, 2381; (b) Fox, J. R.; Foxman, B. M.; Guarrera, D.; Miller, J. S.; Calabrese, J. C; Reis, A. H. Jr. *J. Mater. Chem.* **1996,** *6,* 1627.

146. Miguel, P. D.; Bryce, M. R.; Goldenberg, L. M.; Beeby, A.; Khodorkovsky, V.; Shapiro, L.; Neimz, A.; Cuello, A. O.; Rotello, V. *J. Mater. Chem.* **1998,** *8,* 71.

147. Azcondo, M. T.; Ballester, L.; Golhen, S.; Gutierrez, A.; Ouahab, L.; Delhaes, P. *J. Mater. Chem.* **1999,** *9,* 12376.

148. Nishimura, K.; Khasanov, S. S.; Saito, G. *J. Mater. Chem.* **2002,** *12,* 1693.

149. (a) Metzger, R. M.; Day, P.; Papavassiliou, G. C. (Eds.) *Low Dimensional Systems and Molecular Electronics.* NATO Series *Vol. 128*, Plenum Press, New York, 1990; (b) Papavassiliou, G. C; Terzis, A.; Delhaes, P. in *HandBook of Organic Conductive Molecules and Polymers,* Nalwa, H. S. (Ed.) *Vol.* 7, p. 151, John Wiley: Chichester, 1997.

150. (a) Moore, A. J.; Bryce, M. R. *J. Chem. Soc. Chem. Commn.* **1991,** 1638; (b) Bryce, M. R. *J. Mater. Chem.* **2000**, *10*, 589; (c) Bras, Y. L.; Sallé, M.; Leriche, P.; Mingotaud, C.; Richomme, P.; Møller, J. *J. Mater. Chem.* **1997,** 7, 2393.

151. (a) Bryce, M. R.; Devenport, W.; Goldenberg, L. M.; Wang, C. *Chem. Commn.* **1998,** 945; (b) Wang, C; Bryce, M. R.; Batsanov, A. S.; Goldenberg, L. M.; Howard, J. A. K. *J. Mater. Chem.* **1997,** 7, 1189.

152. Roncali, J. *J. Mater. Chem.* **1997,** 7, 2307.

153. Jigami, T.; Kodani, M.; Murakami, S.; Takimiya, S.; Aso, Y.; Otsubo, T. *J. Mater. Chem.* **2001**, *11*, 1026.

154. Batsanov, A. S.; Bryce, M. R.; Chesney, A.; Howard, J. A. K.; John, D. E.; Moore, A. J.; Wood, C. L.; Gershtenman, H.; Becker, J. Y.; Khodorkhovsky, V. Y.; Ellern, A.; Bernstein, J.; Perepichka, 1. F.; Rotello, V.; Gray, M.; Cuello, A. O. *J. Mater. Chem.* **2001,** *11,* 2181.

155. Bryce, M. R; Marshallsay, G. J.; Moore, A. J. *J. Org. chem.* **1992,** *57,* 4859.

156. Iyoda, M.; Ogura, E.; Hara, K.; Kuwatani, Y.; Nishikawa, H.; Sato, T.; Kikuchi, K.; Mori, T. *J. Mater. Chem.* **1999,** *9,* 335.

157. Segura, J. L.; Martin, N. *Angew. Chem. Int. Ed. Engl.* **2001,** *40,* 1372.

158. (a) Nalwa, H. S. (Ed.) *Hand Book of Organic Conductive Molecules and Polymers, Vols. 1-4,* John Wiley: Chichester, 1997; (b) Chandrasekhar, P.

Conducting Polymers: Fundamentals and Applications, Kluwer Academic publishers, Norwell, 1999.

159. (a) Roth, S. *One Dimensional Metals : Physics and Material Science,* VCH: Weinheim, 1995; (b) Conwell, E. M. in *Handbook of Organic Conductive Molecules and Polymers,* Nalwa, H. S. (Ed.) *Vol. 4,p.l,* John Wiley: Chichester, 1997.

160. Kaufmann, F. B.; Schroeder, A H; Engler, E, M; Kramer, S. R.; Chambers, J. Q. *J. Am. Chem. Soc.* **1990,** *102,* 483.

161. (a) Genies, E. M.; Boyle, A.; Lapkowski,, M.; Tsintavis, C. *Synth. Met.* **1990,** *36,* 139; (b) Green, A. J.; Woodhead, A. E. *J. Chem. Soc. Trans.* **1910,** *97,* 2388.

162. Goffe, A. H. L. in *Handbook of Organic Conductive and Polymeric Materials,* Nalwa, H. S. (Ed.) *Vol. 3,* p.745, John Wiley: Chichester, 1997.

163. Lu, F.-L.; Wudl, F.; Nowak, M.; Heeger, A. J. *J. Am. Chem. Soc.* **1986,***108,* 8311.

164. Sadhigi, J. P.; Singer, R. A.; Buchwald, S. L. *J. Am. Chem. Soc.* **1998**, *120*, 4960.

165. Yue, J.; Epstein, A. J. *J. Am. Chem. Soc.* **1990**, *112*, 2800.

166. Wang, L. X.; Soczka-Guth, T.; Havinga, E.; Mullen, K. *Angew. Chem. Int. Ed. Engl.* 1996,55, 1495.

167. Sayre, C. N.; Collard, D. M. *J. Mater. Chem.* **1997,** 7, 909.

168. Ogura, K.; Saino, T.; Nakayama, M.; Shiigi, H. *J. Mater. Chem.* **1997,** 7, 2363.

169. Kfivka, I.; Prokes, J.; Tobolkova, E.; Stejskal, J. *J. Mater. Chem.* **1999,** *9,* 2425.

170. (a) Posudievsky, O. Y.; Biskulova, S. A.; Pokhodenko, V. D. *J. Mater. Chem.* **2002,** *12*, 1446; (b) Guey, W. C; Yih, H. J.; Sheng, H. S. *J. Mater. Chem.* **2001,** *11*, 2061.

171. Yan, F.; Xue, G. *J. Mater. Chem.* **1999,** *9,* 3035.

172. Cao, H.; Xu, Z.; Sheng, D. Hong, J.; Sang, H.; Du, Y. *J. Mater. Chem.* **2001,** 77, 958.

173. Huang, L.; Wang, Z.; Wang, H.; Cheng, X.; Mitra, A.; Yan, Y. *J. Mater. Chem.* **2002**, *12*, 388.

174. Yang, Y.; Wan, M. *J. Mater. Chem.* **2002**, *12*, 897.

175. Matsuo, Y.; Higashika, S.; Kimura, K.; Miyamoto, Y.; Fukutsuka, T.; Sugie, Y. *J. Mater. Chem.* **2002**, *12*, 1592.

CHAPTER 2

Optical Materials Based on Diammodicyanoquinodimethanes

Papers published

- Jayanty, S.; Radhakrishnan, T. P. *Chem. Mater.* 2001,*13,* 2460.
  Modeling Molecule-in-a-Crystal : The Case of Push-pull Quinonoids.

- Jayanty, S.; Radhakrishnan, T. P. *Chem. Mater.* 2001,*13,* 2072.
  Solid State Charge Transfer Promoted by an Anchoring Agent : A 2-component Analogue
  of Kofler's Ternary Complex.

- Jayantv. S.: Radhakrishnan, T. P. *Chem. Eur. J.* (*in press*).
  Enhanced Fluorescence of Remote Functionalized Diaminodicyanoquinodimethanes in
  the Solid State and Fluorescence Switching in a Doped Polymer by Solvent Vapors.

2.1   INTRODUCTION

Over the past few decades, a wide range of molecular crystals[1,2] have been developed for optical and nonlinear optical applications. Molecules with delocalized *n*-electron systems, often with donor-acceptor (push-pull) structure possess interesting optical and nonlinear characteristics. A brief account of various classes of optical materials and their properties has been presented in Sec. 1.2. We have investigated several new molecular crystals which exhibit interesting optical properties in the solid state. We have also developed simple computational approaches to model these molecules as they exist in the bulk materials providing useful insight into structure/property relationships and materials attributes. We find that the computations incorporating standard solvation models provide an understanding of the role of the crystal lattice in the structural modifications that some molecules undergo when they form the crystal.

Previous studies on diaminodicyanoquinodimethanes (DADQ's) in our laboratory[3,7] have revealed that these molecules can exhibit strong second order nonlinear optical responses.[4,8] This has encouraged us to carry out further investigations on these and related systems. DADQ's are strongly zwitterionic molecules exhibiting large ground state molecular twist between the diaminomethylene unit and the benzenoid ring plane. The molecular twist has significant impact on the linear and nonlinear optical properties of these molecules and hence on the materials based on them. A prominent difference in the molecular twist was observed between the structure of these molecules in the crystalline state and their computed geometry which describes the isolated molecule. We have addressed the problem of modeling this critical molecular feature, through the general concept of a 'molecule-in-a-crystal'. This investigation is discussed in Sec. 2.2. We have modeled these push-pull quinonoid structures, using semiempirical quantum chemical computations including solvation effects. Such computations are found to reproduce the structural feature in the crystal accurately and thus provide a simple description of the molecular environment within the crystal. We have further tested this modeling approach by examining the crystal structure of a new member of the series, namely, bis(*p*-toluenesulfonate) salt of 7,7-bis(piperazino)-8,8-dicyanoquino-dimethane, a system with a highly ionic structure. The ionic structure could be

incorporated without affecting the π-conjugated chromophore part, using the amino group which is a nonconjugated part of the molecule. We refer to such functionalities as 'remote' since they do not disturb the low lying exciting states of the chromophore and at the same time facilitates new intermolecular interactions leading to specific molecular assemblies.

Sec. 2.3 deals with a novel situation involving charge transfer complex formation exclusively in the solid state between BPDQ and picric acid. The critical role of proton transfer and intermolecular H-bonding in the charge transfer interaction was demonstrated through control experiments and single crystal x-ray investigations. The secondary amine moiety of piperazine units in BPDQ play the role of anchoring agents facilitating the charge transfer. Computational studies provided insight into the origin of the charge transfer interaction.

In Sec. 2.4 we discuss in detail a new class of zwitterionic molecules possessing remote functionalities. These systems exhibit a dramatic enhancement of light emission in the solid state and when doped in polymer films, when compared to the solution state. Crystal structure analysis of prototypical molecules reveals the role of the remote functionality in the solid state organization. Semiempirical quantum chemical computations suggest a model to explain the fluorescence enhancement as arising due to the inhibition of the vertical excited state relaxation to a nonemitting state. The potential sensor/switch response of a doped polymer film triggered by solvent vapors is also demonstrated. Sec. 2.5 provides a summary of the work presented in this chapter.

2.2   MODELING MOLECULE-IN-A-CRYSTAL' : THE CASE OF PUSH-PULL QUINONOIDS

Structural modifications that molecules exhibit in the crystalline state when compared to their isolated state provide important insight into the microenvironment in the molecular crystal. Modeling molecule-in-a-crystal is critical in drawing correlations between molecular structure/property and materials attributes, an important prerequisite

for the design of molecular materials. A pertinent case would be the evaluation of local field factors for the computation of nonlinear optical (NLO) susceptibilities of crystals from molecular hyperpolarizabilities.[8] Molecule-in-a-crystal can be described by modeling its structure, molecular as well as electronic; special attention should be paid to features which dominate the molecular contribution to the materials properties. Such computations are usually complicated since a variety of intermolecular interactions[9] coexist. A popular approach is to use embedding models[10] wherein the effect of the lattice around a molecule is assessed using crystal structure information and computed interaction energies. Conformational changes of molecules in solutions and enzyme active sites are commonly modeled using implicit solvation models.[11] The medium effects on large geometry changes of donor-acceptor complexes[12] and crystal structure geometry of a transition state analog[13] have been replicated using computations including solvation effects. Unlike the embedding models, the latter approach does not require the crystal packing information. The modification of molecular structure by the crystal forces are often subtle rendering the computational description difficult. Therefore molecules which undergo large structural changes between the isolated state and the crystal environment are of special interest.

The push-pull molecules, diaminodicyanoquinodimethanes (DADQ's) provide an ideal test case, since they exhibit large structural changes between their computed geometries (reflecting the isolated state) and the molecular geometries in crystals. We have considered several systems developed in our laboratory during earlier studies and a new member of the family (Fig. 2.1). They are 7,7-bis(pyrrolidino)-8,8-dicyanoquinodimethane (1), 7,7-bis(2(R)-methoxymethylpyrrolidino)-8,8-dicyanoquino-dimethane (2), 7,7-bis(piperidino)-8,8-dicyanoquinodimethane (3), 7,7-bis(piperazino)-8,8-dicyanoquinodimethane (4), 7,7-bis(morpholino)-8,8-dicyanoquinodimethane (5), 7,7-bis(propylamino)-8,8-dicyanoquinodimethane (6), 7,7-bis(pentylamino)-8,8-dicyano-quinodimethane (7), 7,7-bis(3(R)-hydroxypyrrolidino)-8,8-dicyanoquinodimethane (8) and 7,7-bis(piperazinium)-8,8-dicyanoquinodimethane (9) bis(p-toluenesulfonate); it may be noted that 4 is BPDQ referred to earlier and 9, its diprotonated state. Developing the concept of modeling molecule-in-a-crystal,[14] we are able to demonstrate that the role of crystal lattice in structural modification can be mimicked satisfactorily using standard solvation modeling subroutines in semiempirical quantum chemical calculations.
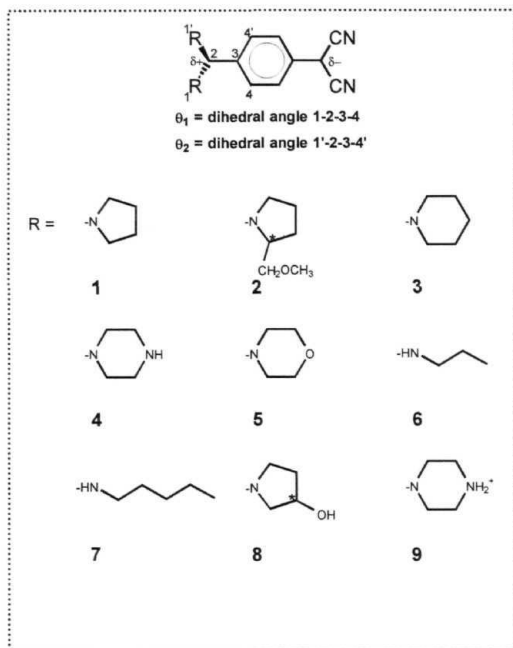
Figure 2.1 *The DADQ molecules considered in our study, the angle 9 in the text is the average of θ₁ and θ₂ indicated in the figure.*

<u>Modeling the molecular structures in crystals</u>

The large dihedral twist between the diaminomethylene group and the six member aromatic ring in the zwitterionic DADQ molecules arises as a result of the steric interaction between the amino group substituents and the *ortho* H atoms of the ring. The twist is facilitated by the zwitterionic nature and the nearly single bond connecting the diaminomethylene group and the ring (Fig. 2.2). The highly zwitterionic nature is reflected in the large dipole moment of these molecules.[15] Computational studies[516] have shown that the excitation energy and hyperpolarizability of these molecules and hence their solid state NLO properties are very sensitive to the dihedral twist 0 (Fig. 2.1). The

twist angle, θ_{cryst} from single crystal x-ray studies are collected in Table 2.1. The twist angle, θ_0 from the geometry optimization using the **AM1**[17] **semiempirical** method shows good agreement with θ_{cryst} only in the case of molecules 1 and 2; in 3 - 8, the θ_{cryst} are considerably higher. The enhanced θ_{cryst} of 8 compared to 1 and 2 has been attributed to extensive **intermolecular** H-bonding present in the crystal.[7] 9 is the ionic system we have studied[14] which shows very large discrepancy between the θ_{cryst} and θ_0.
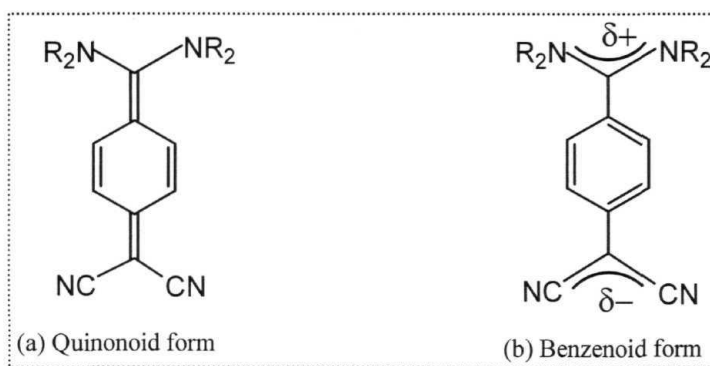
Figure 2.2 *Molecular structure of DADQ's : (a) quinonoid and (b) benzenoid forms.*

The discrepancy between the computed and experimental values of 9 in most of the cases points to the role of the polar microenvironment in the crystal lattice *(cf.* Ref. 12) which stabilizes the zwitterionic form. Modeling of the solvent selection of polymorphs in a molecular crystal using AMI/COSMO calculations on supramolecular **clusters**[18] was demonstrated in our laboratory recently. We hypothesized that the influence of the crystalline environment can be mimicked using the dielectric continuum model used in the solvation routine, COSMO.[19] Full geometry optimization of 1 - 8 starting with the AM1 optimized geometries mentioned above and invoking different dielectric constants, e within the solvation model[20] showed that even at low 8, θ_ε is higher than the θ_0. Generally θ_ε is found to increase with e and saturate at higher values; Fig. 2.3 demonstrates this for 1 - 8. The θ_ε which agree best with θ_{cryst} and the corresponding e are collected in Table 2.1; we **find** that the rest of the computed molecular geometry at

this e also agrees well with the experimental geometry. As noted earlier, 1 and 2 require no solvation modeling, implying that the molecular dihedral twist observed in the crystal is essentially a feature of the isolated molecule. The low values of e required for **3** - **7** are

Table 2.1 *Twist angles of molecules in Fig. 2.1 from single crystal x-ray* **analysis,**[a] θ_{cryst}, *the AM1 computed values,* θ_0 *and the AM1/COSMO computed values,* θ_ε *which show the best agreement with* θ_{cryst} *and the corresponding s.*

Molecule	θ_{cryst} (°) [Ref.]	θ_0 (°)	θ_ε (°)	8
1	55.2 [4]	58.2		–
2	54.1 [5]	57.5		
3[b]	46.6 [211	30.2	45.7	2
4[b]	42.9 [211	28.3	44.8	2
5	48.3 [21]	24.5	48.8	3
6	47.0 [6]	28.0	45.7	3
7	47.1 [61	29.3	47.1	3
8	73.8 [71	58.7	73.9	8
9	52.4 [141	**14**	54.5	20

[a] The θ values shown are the average of the two dihedral angles (Fig 2.1) in these bis-substituted systems. [b]There are two molecules in the crystallographic asymmetric unit with very similar θ values; average is provided.

suggestive of a weakly polarizable molecular environment arising from nominal intermolecular interactions. Intermolecular H-bonding has been observed in 6[6] and 7.[6] e = 4 also reproduces the correct twist angle in these crystals. The higher value of ε required in the case of 8 appears to reflect the impact of the extensive H-bonding interactions.[7] The e required in the case of 9 is even higher and we discuss this system in detail below.
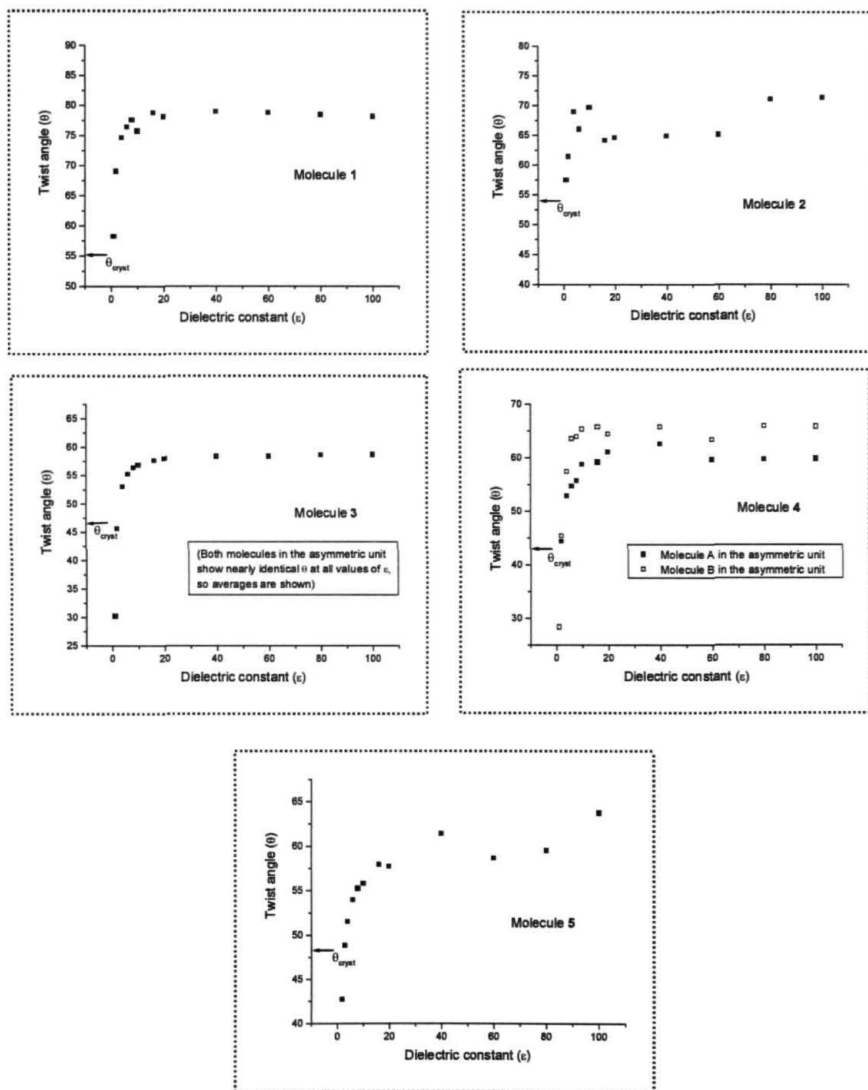
Figure 2.3 *(contd.)*
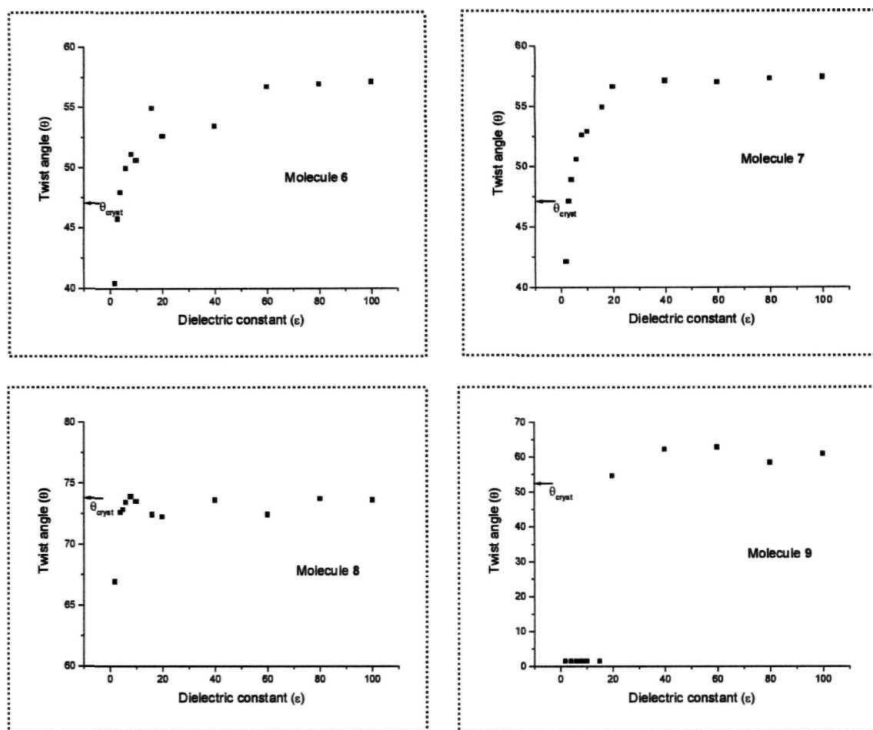
Figure *23* *(contd.)* *AM1/COSMO calculated twist angle as a function of the dielectric constant employed in the calculation for molecules 1-9 in Fig. 2.1. The twist angle obtained from crystal structure analysis, θ_{cryst} are indicated.*

<u>*Bis(p-toluenesulfonate)* salt of *7,7-bis(piperazinium)-8,8-dicyanoquinodimethane*, *9(Tos)₂*</u>

The new system **9(Tos)2** synthesized and structurally characterized is a stringent test case for the modeling approach discussed above, since the **AM1** computed 6 was very much different from the experimental value (Table 2.1). 9(Tos)2 was synthesized by

the addition of *p*-toluenesulfonic acid to 4. The remote amino functionality plays the crucial role of facilitating the formation of an ionic complex without interfering with the π-conjugated push-pull chromophore system.

4 was synthesized as reported earlier.[21,22] To a warm solution of 0.10 g (0.31 mmol) of 4 in 25 ml of acetonitrile was added a solution of 0.118 g (0.62 mmol) *of p*-toluenesulfonic acid in acetonitrile. Yellow colored microcrystalline compound precipitated out. This was filtered and recrystallized from water to produce 0.175 g (80%) of **9(Tos)₂**. M.P. = 310 - 315°C (dec); FT-IR (KBr) : v/cm^{-1} = 2982, 2760, 2175, 2139, 1165; UV-Vis (ethanol) : λ_{max}/nm= 240, $\lambda_{cut-off}$/nm = 449; ^{1}H-NMR (d_6-DMSO) : 5/ppm = 2.2-2.3 (s, 6H), 3.6-3.9 (m, 16H), 6.8-6.9 (d, 2H), 7.1-7.2 (d, 4H), 7.3-7.4 (d, 4H), 8.7-9.2 (s, 4H), (H-bonded protons on N not observed).

Crystals of **9(Tos)2** grown from water belong to P2/c space group with half the molecule and 2.5 water molecules in the asymmetric unit. Crystallographic data are given in Table 2.2. The molecular structure of 9 is shown in Fig. 2.4. A large dihedral twist, of 52.4° between the diaminomethylene unit and the aromatic ring plane is observed. Extended H-bonding involving the piperazinium, cyano and sulfonate groups and water molecules produces supramolecular squares and rectangles in this crystal. The view of the crystal packing along the b axis (Fig. 2.5) shows the distribution of tosylate ions and water molecules around the push-pull quinonoid moiety that leads to a highly polar environment; the molecular twist also can be seen clearly. Interestingly, AM1 calculations on 9 showed a negligible θ_0 of 1.4°. This planarization possibly results from the destabilization of the positive charge at the diaminomethylene end of the zwitterionic form due to the protonation on the piperazine moieties. In the AM1/COSMO optimization, the θ remains 1.4° till e = 15 and suddenly increases thereafter (Fig. 2.2). The experimental angle is recovered at s = 20 (Table 2.1). The large enhancement of θ and its modeling using a high ε reflects the strongly ionic microenvironment and the abundance of H-bonded water molecules in **9(Tos)2**.

Table 2.2 *Crystallographic data for 9(Tos)2*

Compound	9(Tos)₂. 5H₂O
Molecular formula	$C_{16}H_{24}N_3O_{5.5}S$
Formula weight	378.44
Crystal system	Monoclinic
Space group	P2/c
a/A	9.659(3)
b/A	12.798(4)
c/A	16.185(2)
a / deg.	90
P / deg.	104.054(18)
y / deg.	90
Z	4
ρ_{calc} / g cm⁻³	1.295
u / cm"¹	2.00
Number of reflections	4453
Number of reflections with $I > 2\sigma_I$	3073
Number of parameters	260
GOF	1.016
R (for I > 2a,)	0.0496
wR²	0.1324

Overview of the **'molecule-in-a** *crystal' model*

The present study demonstrates that the molecular structure modification occurring in a crystal environment can be conveniently modeled using solvation-included geometry optimization at the semiempirical level. Such an analysis also provides useful insight into the dielectric constant experienced by the molecule in its microenvironment and should be of utility in evaluating accurately the molecular contribution to crystal properties. Assuming a typical refractive index of 1.5 - 2.0, the dielectric constant of organic crystals at optical frequencies will be of the order of 2 - 4. The e needed in the semiempirical solvation calculations are in this range for most of the systems. The larger
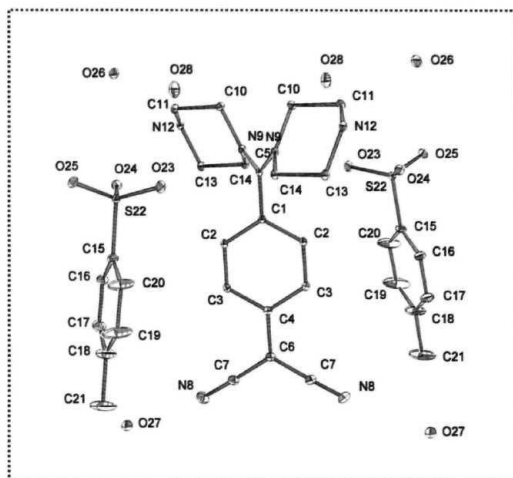
Figure 2.4 *Molecular structure of* **9(Tos)₂.5H₂O** *from single crystal x-ray analysis showing* **10%** *probability thermal ellipsoids (the repeat of labels is due to the fact that the asymmetric unit is half of the formula unit shown).*
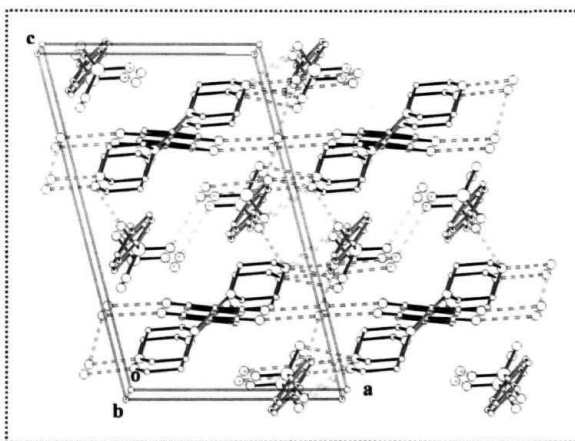
Figure 2.5 *Crystal structure of 9(Tos)2 from single crystal x-ray diffraction analysis showing two molecular arrays parallel to the ac plane.* **H** *atoms are omitted for clarity.*

e required for 8 is compatible with the fact that the dielectric constant of compounds with extensive H-bonding are generally higher.[23] The still larger e in the case of 9 reflects the highly polarizable molecular environment made up of several H-bonded water molecules.

A basic question arises at this point : does the observed structure modification occur when the molecule is in a solvated state in solution or when it associates with others initiating the crystal assembly, and which of these states is the solvation calculation really modeling ? In the case of the push-pull quinonoid systems a tentative answer can be offered. Computational studies noted earlier[5,16] have shown that the excitation energy decreases monotonically with increasing 9. However the electronic absorption data of 1 - 9 in solution do not indicate any clear correlation between the absorption maxima and the θ_{cryst} (Table 2.3). This suggests that the structural modification observed in the crystalline state is not initiated when the isolated molecule is in solution, but occurs when the supramolecular assembly leading to the crystal is formed. It also indicates that the current solvation calculations actually model the

Table 2.3 *Twist angles, θ_{cryst} of molecules in Fig. 2.1 and the peak position in the absorption spectra of their solutions in methanol, acetonitrile and tetrahydrofuran. The entries are ordered according to increasing θ_{cryst} •*

Molecule	θ_{cryst} 0	λ_{max} (nm)		
		methanol	acetonitrile	THF
4	42.9	414	415	461
3	46.6	405	414	460
6	47.0	362	380	414
7	47.1	363	378	414
5	48.3	423	420	462
9	52.4	422	450	459
2	54.1	398	406	449
1	55.2	366	375	431
8	73.8	372	388	434

microenvironment in crystals. Logical extension of this study would be the modeling of electronic structure and properties of molecules in the crystal; preliminary explorations suggest that this is a promising approach. In Sec. 2.4 we use the AM1 /COSMO computations to assesss the spectroscopic states of molecules in solution as well as in the solid state and in Sec. 3.2 we consider detailed analysis of solid state molecular structure and charge distribution. Solvation-included quantum chemical computations should prove to be a powerful and convenient tool to study different aspects of the 'molecule-in-a-crystal'.

2.3 EXCLUSIVE SOLID STATE CHARGE TRANSFER PROMOTED BY AN ANCHORING AGENT : A TWO COMPONENT ANALOG OF KOFLER'S TERNARY COMPLEX

Picric acid is a classic example of a versatile electron acceptor molecule for charge transfer (CT) complexes. It is known to form colored charge transfer complexes with a wide variety of donor molecules and has proved useful in qualitative and quantitative analysis protocols.[24] A large number of picric acid complexes have been characterized crystallographically; a survey of the Cambridge Crystallographic Database[25] shows 282 hits for purely organic complexes alone. While the majority of charge transfer complexes of picric acid are yellow, several complexes are known to be red to deep red indicating a lower CT energy. A cursory examination of the red charge transfer complexes reveals an interesting phenomenon; picric acid exists in the neutral form in some systems and the lower CT energy in these usually arises due to the strong donor molecules present;[26"30] whereas in the others, it is deprotonated to form the picrate ion. However, an early example of a red complex, the Kofler's ternary complex consisting of naphthylamine, pyridine and picric acid[31,32] is a curious case. Spectroscopic and crystallographic studies suggest that the color is due to charge transfer from naphthylamine to the picrate ion.[32"34] Though counterintuitive, based on spectroscopic experiments[32"33] it has been suggested that the picrate ion is as good an acceptor as picric acid. Further it appears that the proton transfer between picric acid and pyridine is crucial for the formation of the red complex; we believe that pyridine plays the role of *an*

anchoring agent in facilitating the charge transfer between the weak donor and the picrate ion. Such a phenomenon may have wider generality. The 'picrate effect' demonstrated in the extraction selectivities of aromatic group-containing crown ethers for alkali metal cations[35] is a consequence of the π-π interaction between the aromatic moiety and the picrate ion and its influence on the binding of the metal ion by the crown ether. This can be visualized as the inverse phenomenon to the anchoring of the picrate by the alkali metal ions. Picrate ion is also considered as an interesting ligand in the preparation of luminescent plastics.[36]

As noted earlier, DADQ's [5-7,37] exist in strongly zwitterionic benzenoid form. We observed an unexpected red complex formation between the zwitterionic push-pull molecule, 7,7-bis(piperazino)-8,8-dicyanoquinodimethane (4) and picric acid; exclusively in the solid state.[38] We have carried out detailed crystallographic characterization of this material and several control experiments which show that the complex formed between 4 and picric acid is a 2-component analog of the Kofler's ternary complex. The secondary amine moiety of the piperazine units in 4 play the role of anchoring agents and the electron rich dicyanomethylene end of the zwitterions participate in the charge transfer with the picrate ions. Computational studies support the earlier suggestions regarding the electron accepting capability of the picrate ion and provide insight into the nature of the charge transfer interaction.

The complex of 4 with picric acid presents a graphic case of intermolecular charge transfer facilitated by molecular anchoring The remote amine end of 4 carries out the function of a trigger by helping set up the suitable juxtapositioning of the molecules to facilitate the charge transfer. 9, the diprotonated form of 4 (Fig 2.1) formed by proton transfer from picric acid, engages in a charge transfer process with the picrate ion which can be visualized as a response. Thus 4 operates as a novel molecular device wherein the charge transfer is triggered by remote intermolecular interactions.

Synthesis and computational details

      4 was synthesized following the procedure reported earlier.[21,22] Crystal structure of 4 has also been reported in Ref. 21. The complex with picric acid was prepared by mixing saturated acetonitrile solutions of 0.10 g (0.31 mmol) of 4 and 0.14 g (0.62 mmol) of picric acid. The complex precipitated out as a reddish brown microcrystalline powder. Single crystals were grown by a diffusion process. 4 and picric acid were taken as acetonitrile solutions in the two limbs of an inverted Y-tube and contact between the solutions was established by careful addition of the solvent. Deep red crystals appeared at the confluence of the two limbs in 3 - 4 days.

      Charge densities on the bisprotonated 4 *ie.* 9, and picrate ion (Pic) were estimated using *ab initio* calculations at the B3LYP/6-31G* level.[39] The calculations employed molecular geometries from the crystal structure analysis; H atom positions alone were optimized. Polar environment around molecules in crystals can be mimicked satisfactorily using solvation models built into quantum chemical programs. The study of DADQ's[14] discussed in the previous section as well as earlier computations by Jiao and Schleyer on donor-acceptor complexes[12] have shown that critical geometric parameters in the crystalline state can be reproduced satisfactorily by incorporating an e ~ 2 - 20. In the present case, we have used the polarized continuum model[40,41] for solvation with ε = 36.64 (dielectric constant of acetonitrile) to mimic the crystalline environment and obtain a realistic picture of the charge polarization in the ions.

Charge transfer phenomenon and spectroscopic studies

      4 is a yellow solid and forms yellow solution in acetonitrile. When this solution is mixed with a solution of picric acid in acetonitrile in 1:2 mol ratio, a reddish brown microcrystalline precipitate forms immediately. The complex can be prepared by grinding together 4 and picric acid in the solid state as well. The diffuse reflectance spectrum of the product is presented in Fig. 2.6. The figure shows also the spectrum of the well-known yellow naphthalene picrate for comparison. The red color of the complex of 4 with picric acid **(9(Pic)₂** as shown below) is indicative of a low energy charge
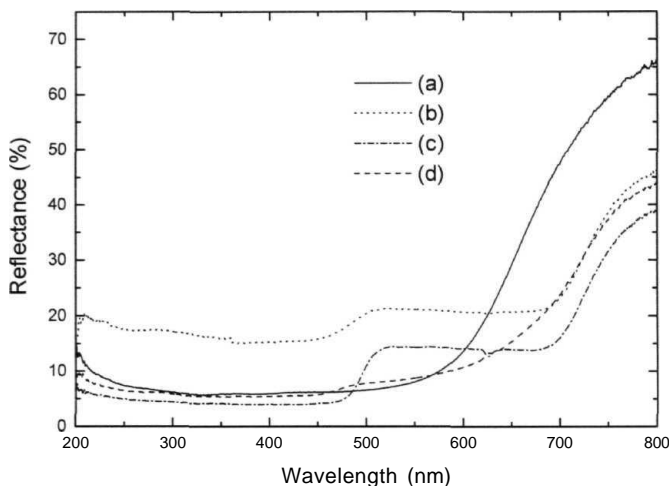
Figure 2.6 *Diffuse reflectance spectra of* **(a)** *9(Pic)₂,* **(b)** *naphthalene-picric acid (c) piperazinium picrate and (d) 11 (Pic) ₂.*

transfer. When the complex is dissolved in excess acetonitrile as well as other polar solvents like water, methanol and dimethylsulfoxide, a yellow solution is obtained. However, the red complex can be retrieved by slow evaporation of the solution.

Electronic absorption spectra of acetonitrile solutions of 4, picric acid and the complex are shown in Fig. 2.7. The peaks at 246 nm and 379 nm in the spectrum of the complex are signatures of the picrate ion (acetonitrile solution of sodium picrate shows peaks at 248 nm and 376 nm) and the peak at 432 nm is similar to that seen for **9(Tos)₂** and hence can be assigned to the dication 9. No CT band is visible and this spectrum shows that the complex exists as 9 and picrate ions in solution. From the solution study and the reflectance spectrum of the solid, we conclude that the dark red colored complex exists only in the solid state. Since 4 is known to be in a strongly zwitterionic state[21] the formation of a CT complex with picric acid, especially in the picrate form, is surprising. To gain insight into the phenomenon, we have investigated several control systems, some of which are shown in Fig. 2.8. Piperazine forms a yellow-colored salt with picric acid.
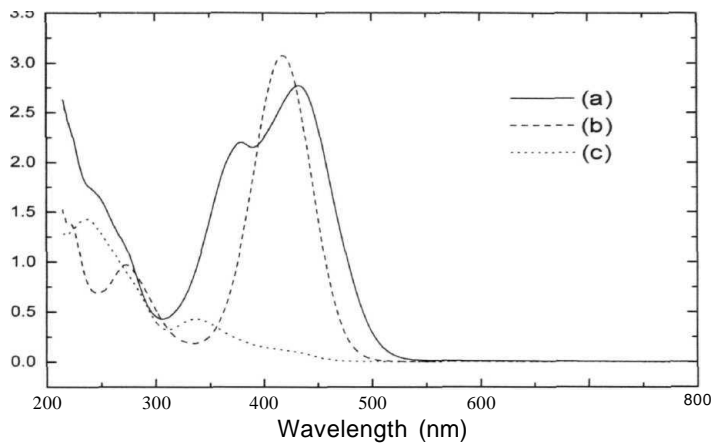
Figure 2.7 *Electronic absorption spectra in acetonitrile solution of (**a**) **9(Pic)2**, (**b**) **4** and (**c**) Picric acid.*
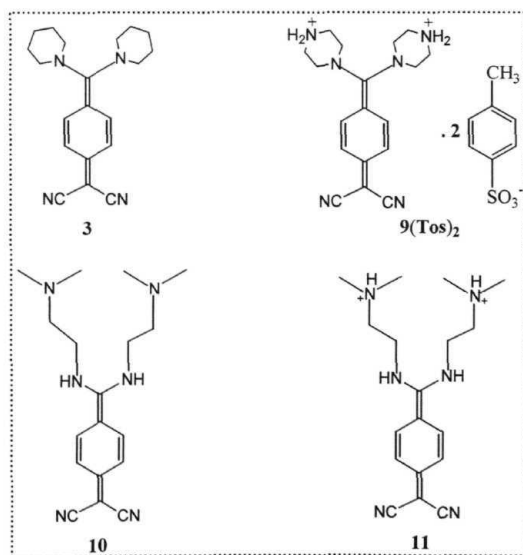
Figure 2.8 *Molecular structures of 3, **9(Tos)₂, 10** and 11.*

In spite of several attempts we found that 7,7-bis(piperidino)-8,8-dicyanoquinodi-methane, 3 does not form a complex with picric acid. Similar was the observation when the *p*-toluenesulfonate salt of **4** *ie.* **9(Tos)2** was mixed with picric acid. However, dark reddish brown precipitate was obtained when 7,7-bis(N,N-dimethylethylenediamine)-8,8-dicyanoquinodimethane, 10 was mixed with picric acid. Diffuse reflectance spectra of piperazinium picrate and the complex of 10 with picric acid (most likely **11(Pic)₂**) are also shown in Fig. 2.6. These studies clearly indicate that the free amine moieties (which are not in conjugation with the zwitterionic system, hence are strongly basic) as well as the delocalized π-electron system in 4, both play a significant roles in the formation of the dark colored complex with picric acid; similar functionalities are present in 10.

The fact that neither functionality alone is sufficient is proved by the color of the piperazinium picrate and the failure of 3 to complex picric acid. It is also observed that 9 which is already engaged by a counterion such as the *p*-toluenesulfonate cannot produce the colored CT complex with picric acid. We conclude tentatively that the secondary amine moiety in 4 helps to anchor the picric acid through proton transfer and/or H-bonding, facilitating CT interaction with the zwitterionic π-system. In an effort to understand the role of the zwitterionic π-system, we have explored some further complexation reactions. 4 forms dark green/brown complexes with well known electron acceptors like TCNQ, TCNE and DDQ and even with weaker acceptors like chloranil. It however, does not produce any characteristic color of CT complexes when mixed with electron donors such as TTF and TMPD. Therefore the zwitterionic π-system appears to be effective only as an electron donor implying that the negative end alone participates in any charge transfer process. We have carried out single crystal x-ray analysis to gain insight into the solid state interaction in the complex of 4 with picric acid.

Crystal structure investigation

Single crystals were grown as deep red rhombus-shaped plates by the diffusion process in acetonitrile; they are found to belong to the triclinic space group, P 1 . The crystallographic data are presented in Table 2.4. The asymmetric unit consists of one bisprotonated ion, 9, two picrate ions and one molecule of acetonitrile (Fig. 2.9). **The** C-

O bond length in the picric acid molecules, 1.241 A and 1.244A (compare with the average value of 1.236 A for picrate ion[42,43] and 1.324 A for picric acid[43,44]) as well as the C-N bond lengths around the secondary amine moiety in the piperazine units of 4, 1.476A, 1.480A, 1.486A and 1.489A (compare with the average value of 1.483 A in **9(Tos)$_2$**[14] and 1.451 A in **4**[21]) clearly indicate the proton transfer from picric acid to 4 in the solid complex leading to the formation of **9(Pic)2.** Further, a careful search of the difference Fourier map did not reveal any H atom bonded to the phenolate oxygen on the picric acid molecules. The bond lengths in 9 indicate clearly the benzenoid structure of

Table 2.4 *Crystallographic data for **9(Pic)$_2$**.CH$_3$CN*

Compound	9(Pic)$_2$
Molecular formula	C$_{32}$H$_{31}$N$_{13}$O$_{14}$
Formula weight	821.70
Crystal system	Monoclinic
Space group	P $\bar{1}$
a/A	10.198(5)
b/A	12.177(3)
c/A	16.041(9)
a / deg.	89.12(3)
P / deg.	72.99(3)
γ / deg.	75.40(3)
Z	2
ρ_{calc} / g cm^{-3}	1.483
μ / cm^{-1}	1.19
Number of reflections	7191
Number of reflections with I > σ$_1$	4759
Number of parameters	533
GOF	1.062
R (for I > 2σ$_1$)	0.0669
wR^2	0.1931
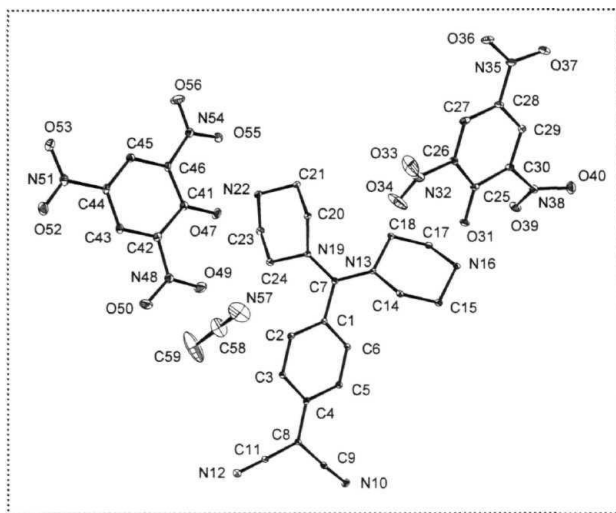
Figure 2.9   *Molecular structure of* **9(Pic)₂**.*CH₃CN from single crystal x-ray diffraction analysis; 5% probability thermal ellipsoids are shown.*

the zwitterionic system.   Examination of the crystal packing revealed four well-defined intermolecular H-bond contacts around the ion, 9.   The piperazinium moieties form H-bonds with the picrate ions: N16···O31 (H16B···O31 = 1.821A, N16-H16B···O31 = 163.9°) and N22···O47 (H22A···O47 = 1.913A, N22-H22A···O47 = 152.8°).   The second piperazinium unit forms an additional H-bond with one of the O atoms of an *ortho* nitro group of the picric acid : N22···O55 (H22B···O55 = 2.132A, N22-H22B···O55 = 160.9°).   The fourth H-bond is found between the first piperazinium moiety and one of the cyano N atoms of another 9: N16···N10 (H16A· ·N10 = 1.920A, N16-H16A···N10 = 168.1°).   Detailed crystallographic data are provided in Appendix B. The H-bonds, especially the first three appear to play a critical role in sequestering the picrate ions into appropriate positions which enables CT interactions with 9.   Fig. 2.10a shows the molecular packing in the unit cell of **9(Pic)₂**.   It is seen that the dicyanomethylene unit of one dication, 9 has close *n-n* contact with the picrate ion anchored by another dication.   View along the *b* axis (Fig. 2.10b) shows in addition, the
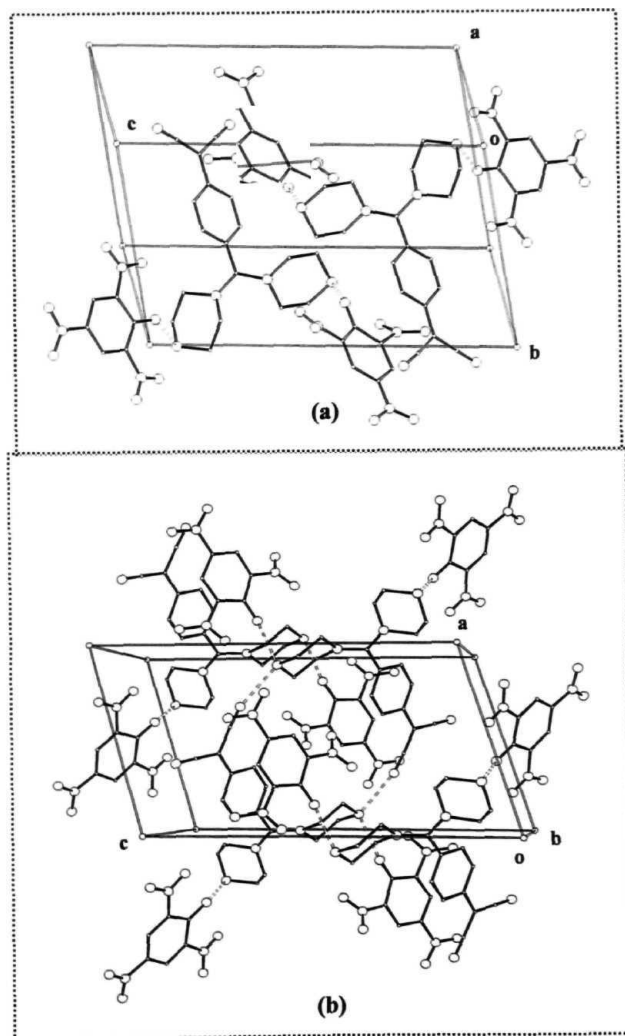
Figure 2.10 (a) *Molecules in the unit cell and (b) unit cell packing along the b axis of* **9(Pic)₂**. *H-bonds* **(= = =)** *are indicated; all H atoms and the solvent molecule of acetonitrile are omitted for clarity.*
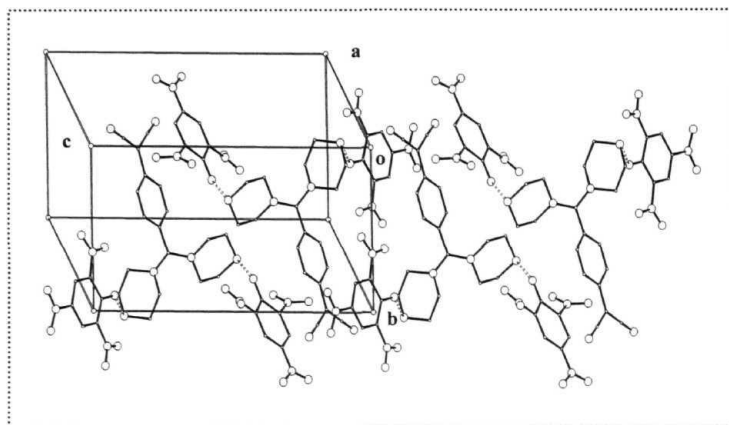
Figure 2.11 *Crystal packing along the c axis of **9(Pic)₂**. H-bonds (= = =) are indicated; all H atoms and the solvent molecule of acetonitrile are omitted for clarity.*

H-bond between the piperazinium unit and the cyano group of neighboring 9 leading to a dimer motif. The packing along the *c* axis shown in Fig. 2.11 reveals the close π-π contact of a second picrate ion to the dicyanomethylene unit of 9. It is thus seen that each 9 has close interaction with two picrate ions on either side and at the same time anchors two other picrate ions through H-bonding interactions, facilitating in turn, their π-π interaction with another dication. The stacking of the dicyanomethyleneunit of 9 and the two picrate ions is shown clearly in Fig. 2.12. We define the least square planes A, B and C based on the dicyanomethylene unit (C8, C9, N10, C11, N12), ring atoms of the first picrate ion (C25 - C30) and ring atoms of the second picrate ion (C41 - C46) respectively. The angle between the planes A and B is 16.9^o and the average distance of the atoms in plane A from the mean plane B is 3.090 A. Similarly the angle between planes A and C is 6.3° and the average distance of the atoms in plane A from the mean plane C is 3.220 A. This is highly suggestive of the existence of strong *n-n* interaction between the dicyanomethylene unit and the picrate ion rings which should facilitate charge transfer.
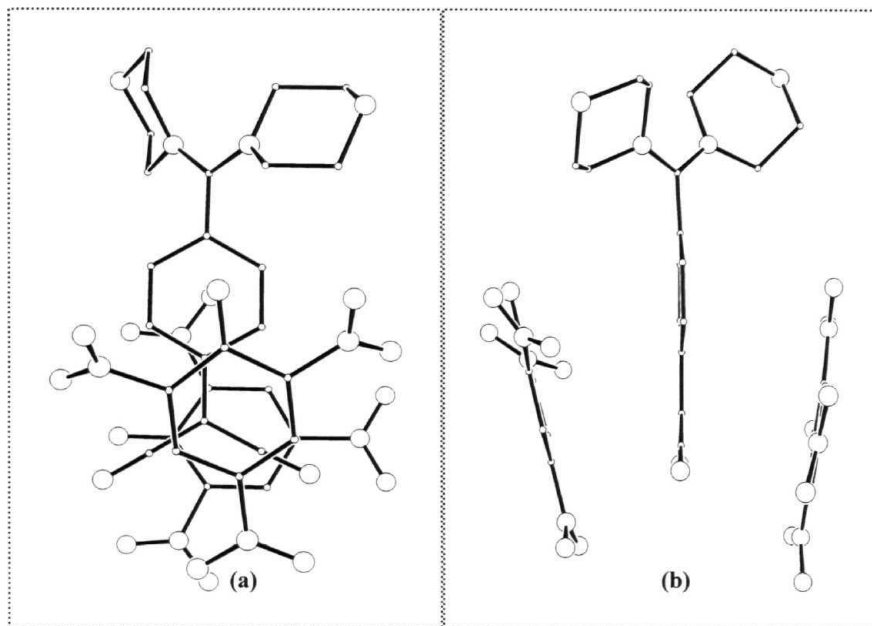
Figure 2.12 *View of the overlap of the dication, 9 with the adjacent picrate ions approximately (a) perpendicular and (b) parallel to the mean molecular planes.*

Computational studies supporting charge transfer

We have examined the possibility of charge transfer by calculating the atomic charges on 9 and the picrate ions using the molecular geometry from crystal structure analysis as noted earlier. The net charges possessed by different parts of these ions revealed through *ab initio* calculations are shown in Fig. 2.13. The dicyanomethylene unit in 9 possesses considerable negative charge and is a potential π-electron donor moiety; it is also obvious that this ion cannot act as a π-electron acceptor because of the steric bulk and nonplanar structure at the positive end. The picrate ions, interestingly
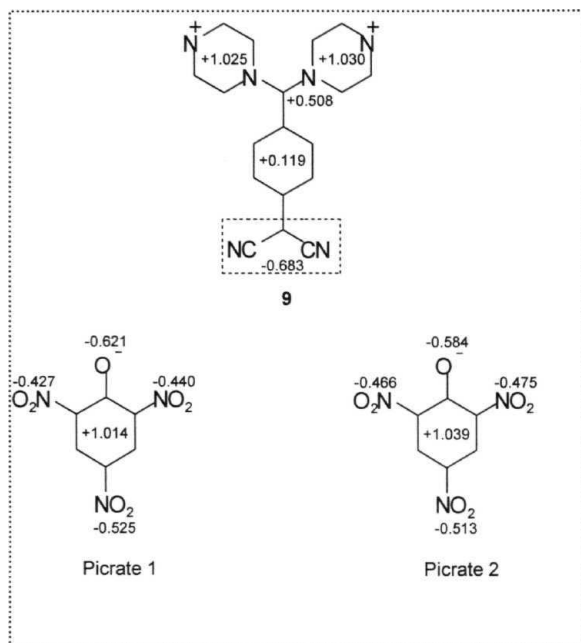
Figure 2.13 *Ab initio computed group atomic charges on different parts of 9 and the picrate ions in* **9(pic)₂***.*

reveal a full-fledged positive charge in the ring surrounded by approximately —2 charge accommodated in the phenolate and nitro groups. This is strongly suggestive of the π-electron accepting nature of the picrate ion proposed earlier.[32] The distribution of the calculated charges also supports the possibility of *n-n* CT interaction in the configuration shown in Fig. 2.12.

The crystallographic investigation together with the computational studies on **9(pic)₂** show that remote **amino** functionality in 9 helps to organize the DADQ moiety and the picrate ions so as to facilitate the charge transfer interaction.   Since the organisation is a solid state phenomenon the CT occurs only in the solid state.

2.4 ENHANCED FLUORESCENCE OF REMOTE FUNCTIONALIZED DIAMINODICYANOQUINODIMETHANES IN THE SOLID STATE AND FLUORESCENCE SWITCHING IN A DOPED POLYMER BY SOLVENT VAPORS

The strong fluorescence exhibited by most organic dye molecules in the monomeric state is quenched in the aggregated state. The current focus on the photoluminescence and electroluminescence of molecular materials provides impetus to explore novel chromophores which not only do not suffer fluorescence quenching in the aggregated state, but display enhanced light emission in the solid state and in polymer films. There are only few reports of such cases. The superradiance observed in some thiacarbocyanine molecules has been attributed to dynamic energy transfer from the monomeric species to aggregate structures.   The highly emissive phase of a poly(*p*-phenyleneethynylene) was proposed to either arise from the metastable skewed chain alignments that allowed efficient interchain interactions or result from planarization effects.[46,47]   Nano-sized aggregates of a sterically crowded silole[48] and a biphenyl substituted ethylene[49] have been reported to show strong light emission, presumably due to significant ground state conformational changes accompanying the aggregate formation. These reports suggest interesting and useful application potential in areas such as electroluminescence and sensors. However detailed pictures of the physical origin of many of these observations are yet to emerge.

During the investigations of the zwitterionic diaminodicyanoquinodimethanes (DADQ)[5-7,14,38,50] in our laboratory, we have found that several molecules, especially the ones bearing remote functionalities[14,38,50] show enhanced fluorescence in the solid state compared to the solutions; similar effect was observed with these molecules doped in polymer films. The role of viscous solvents and polymer matrices in enhancing the light emission of two related molecules have been investigated by Bloor *et al.*[51] Even though similar effects in solids were briefly noted, no detailed studies were presented or the impact of the molecular assembly in crystals analyzed. Further, these molecules do not possess remote functionalities involved in intermolecular noncovalent interactions, which as we show below is a crucial feature in our systems. Our detailed investigation of the solution and solid state of a family of molecules and doped polymer films, establishes the

generality of this interesting phenomenon and the molecular design principle involved. Zwitterionic DADQ's are prone to aggregation and the remote functionalities such as amino groups facilitate specific and directed intermolecular interactions promoting extended assembly. The remote groups appear to contribute positively to the fluorescence enhancement since all the remote functionalized DADQ's we have examined exhibit this effect whereas many of the DADQ's without such functionality do not. More significantly, the presence of the remote groups imparts appreciable solubility to these molecules in water in addition to organic solvents. This is an important advantage since it facilitates convenient doping of these molecules in polymers which are soluble only in water, allowing their application in instances such as organic vapor sensing.

Our systematic investigation of a family of DADQ molecules possessing remote amino functionality including some in the form of salts (Fig. 2.14) are presented in this
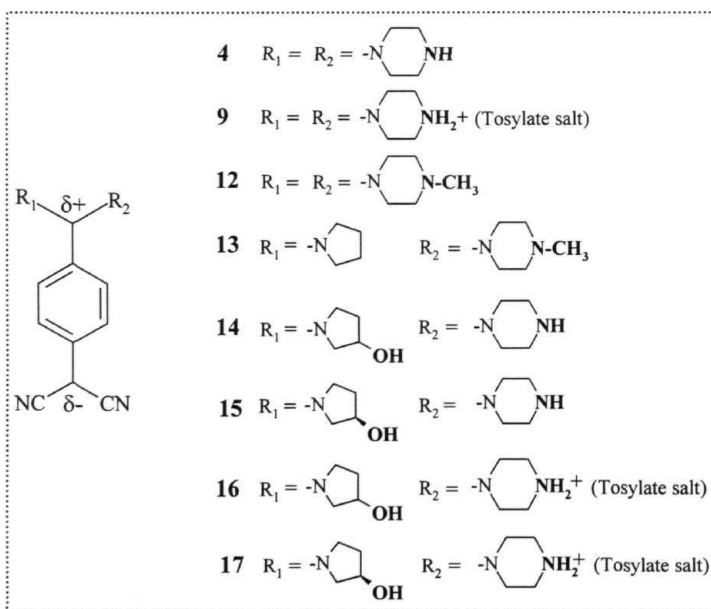
Figure 2.14 *Molecules considered in this study; the remote functionalities are shown in bold.*

section. Our studies establish their enhanced fluorescence in the solid state and in polymer films.[52] We present also crystal structures of prototypical systems and semiempirical computational analysis of the molecular structure and energy in the ground and excited states leading to a simple model to explain this interesting phenomenon. A novel application potential of these materials is demonstrated through experiments on a **chromophore** doped in polymer film, showing reversible cycles of solvent vapor triggered fluorescence switching.

*Synthesis **and** characterization*

4 has been synthesized in our laboratory earlier.[21] Synthesis of **9(Tos)2** has been described in Sec. 2.2. 12 - 17 were prepared using minor modifications of procedures reported[5-7,21,22] for similar molecules (Schemes 2.1, 2.2, 2.3). Three typical cases in the new series are described below.

7,7-bis(N-methylpiperazino)-8,8-dicyanoquinodimethane, 12 : 0.34 g (3.4 mmol) of N-methylpiperazine was added to a warm solution of 0.30 g (1.47 mmol) of TCNQ in 30 ml of acetonitrile (CAUTION : HCN is the byproduct). The solution turned dark green immediately and changed to yellow subsequently. Yellow crystalline product, 12 formed in about 2 h. The reaction mixture was stirred for 2.5 h more at 75°C. The precipitate was filtered and dried (0.39 g, 82% yield). This synthesis follows Scheme 2.1.

7-(N-methylpiperazino)-7-pyrrolidino-8,8-dicyanoquinodimethane, 13 : 0.094 g (1.32 mmol) of pyrrolidine was added to a warm solution of 0.30 g (1.47 mmol) of TCNQ in acetonitrile. The solution turned purple immediately and a purple crystalline compound precipitated in 2 h. The reaction mixture was stirred for 2.5 h more at 75°C. The precipitate of 7-pyrrolidino-7,8,8-tricyanoquinodimethane, PTCNQ was filtered and dried (0.305 g, 83% yield). 0.12 g (1.2 mmol) of N-methylpiperazine was added to a warm solution of 0.20 g (0.98 mmol) of PTCNQ in 20 ml of acetonitrile and the solution was stirred at 70°C for 30 min and then at 30°C for 1 h. Yellowish green fluorescent precipitate of 13 which separated out was filtered and dried (0.21 g, 81% yield). This synthesis follows Scheme 2.2.
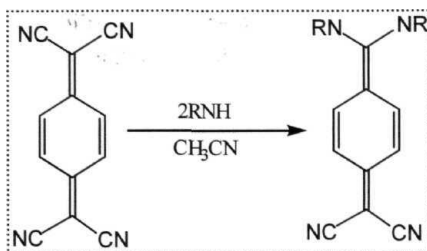
Scheme 2.1
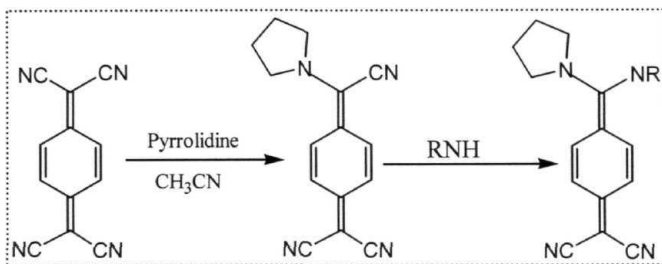
Scheme 2.2
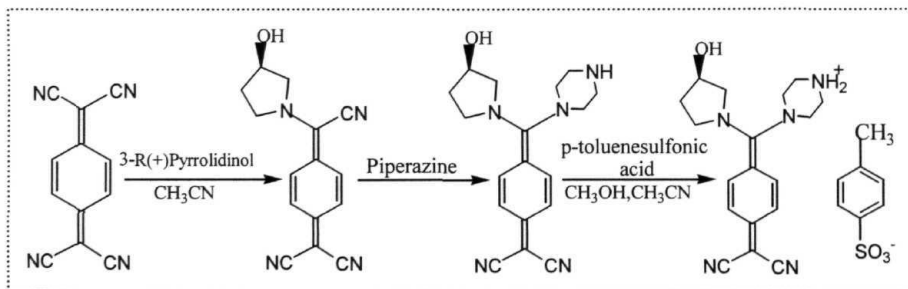
Scheme 2.3

7-(3-R(+)-hydroxypyrrolidino)-7-(piperazinium-8.8-dicyanoquinodimethane **p-toluenesulfonate, 17(Tos)** : **15** was synthezied allowing similar procedure as for **13**. Acetonitrile solution of 0.175 g (1 mmol) of *p*-toluenesulfonic acid was added to an acetonitrile solution of 0.25 g (0.73 mmol) of 15. The yellow microcrystalline powder of the tosylate salt, **17(Tos)** which precipitated out immediately was filtered and dried (0.307 g, **77%** yield). This synthesis follows Scheme 2.3.

Characterization including single crystal structure of 4[21] and **9(Tos)2**[14] have been reported earlier. The detailed characterization of the new compounds are provided below.

7,7-bis(N-methylpiperazino)-8,8-dicyanoquinodimethane, 12 : Yield = 82%. Recrystallized from acetonitrile. M.P. = 278-280°C (dec); FT-IR (KBr) : v/cm^{-1} = 2172.0, 2135.4, 1595.3, UV-Vis (acetonitrile) : λ_{max}/nm 269, 420; ^{1}H-NMR (CDCl$_3$) : δ/ppm = 1.7 (s, 6H), 2.6-2.7 (m, 8H), 3.5-3.6 (m, 8H), 7.1 (s, 4H); ^{13}C-NMR (d$_6$-DMSO) : δ/ppm = 34.5, 45.5, 50.9, 54.6, 114.1, 118.1, 123.2, 131.8, 149.8, 168.8; elemental analysis (calculated for C$_{20}$H$_{26}$N$_6$) : %C = 68.31 (68.57), %H = 7.11 (7.43), %N = 24.61 (24.00).

7-(N-methylpiperazino)-7-pyrrolidino-8,8-dicyanoquinodimethane, 13 : Yield = 75%. Recrystallized from acetonitrile. M.P. = 260-262°C (dec); FT-IR (KBr) : v/cm^{-1} = 2941.7, 2170.1, 2133.5, 1595.3, UV-Vis (acetonitrile) : λ_{max}/nm= 267, 407; ^{1}H-NMR (CDCl$_3$) : δ/ppm = 1.6 (s, 3H), 2.0-2.1 (t, 4H), 2.15-2.25 (t, 4H), 3.5-3.6 (t, 4H), 3.60-3.75 (t, 4H), 7.0 (s, 4H); ^{13}C-NMR (d$_6$-DMSO) : δ/ppm = 24.1, 25.7, 33.1, 45.5, 50.1, 52.7, 54.6, 115.2, 118.1, 123.7, 130.5, 148.3, 165.9; elemental analysis (calculated for C$_{19}$H$_{23}$N$_5$) : %C = 70.93 (71.03), %H = 7.22 (7.17), %N = 21.72 (21.80).

7-(3-hydroxypyrrolidino)-7-piperazino-8,8-dicyanoquinodimethane, 14 : Yield = 75%. Recrystallized from acetonitrile-methanol. M.P. = 245-246°C (dec); FT-IR (KBr) : v/cm^{-1} = 3390.0, 2170.1, 2131.5, 1597.2; UV-Vis (acetonitrile) : λ_{max}/nm= 273, 407; ^{1}H-NMR (d$_6$-DMSO) : δ/ppm = 1.9-2.1 (m, 3H), 2.75-2.90 (m, 4H), 3.7-3.8 (m, 4H), 4.3-4.4 (m, 4H), 5.3 (s, 1H), 6.8-6.9 (d, 2H), 7.15-7.20 (d, 2H), hydroxy proton was not observed; ^{13}C-NMR (d$_6$-DMSO) : δ/ppm = 32.5, 33.1, 34.2, 46.1, 50.6, 51.8, 60.3, 67.6,

69.1, 115.1, 118.1, 123.8, 130.6, 148.3, 166.5; elemental analysis (calculated for $C_{18}H_{21}N_5O$) : %C = 66.86 (66.87), %H = 6.49 (6.50), %N = 21.68 (21.67).

7-(3-*R*(+)-hydroxypyrrolidino)-7-piperazino-8,8-dicyanoquinodimethane, 15 : Yield = 77%. Recrystallized from acetonitrile-methanol. M.P. = 213-215°C (dec); FT-IR (KBr) : ν/cm^{-1} = 3308.0, 2170.0, 2131.0, 1597.0; UV-Vis (acetonitrile) : λ_{max}/nm = 270, 408; ^{1}H-NMR (d$_6$-DMSO) : 5/ppm = 1.8-2.1 (m, 3H), 2.7-2.9 (m, 4H), 3.6-3.9 (m, 4H), 4.2-4.5 (t, 4H), 5.3 (s, 1H), 6.8-6.9 (d, 2H), 7.2-7.35 (d, 2H), hydroxy proton was not observed; ^{13}C-NMR (d$_6$-DMSO) : S/ppm = 32.2, 33.0, 34.3, 46.0, 50.6, 51.7, 60.3, 68.0, 69.1, 115.1, 118.1, 123.8, 130.6, 148.3, 166.5; elemental analysis (calculated for $C_{18}H_{21}N_5O$) : %C = 66.22 (66.87), %H = 6.85 (6.50), %N = 21.68 (21.67).

7-(hydroxypyrrolidino)-7-piperazinium-8,8-dicyanoquinodimethane *p*-**toluene-sulfonate, 16(Tos)** : Yield = 75%. Recrystallized from acetonitrile-methanol. M.P. = 250-255°C (dec); FT-IR (KBr) : ν/cm^1 = 3398.2, 3022.8, 2177.8, 2137.0, 1597.0, 1005.0, 887.0, 814.0; UV-Vis (acetonitrile) : λ_{max}/nm = 267, 422; ^{1}H-NMR (d$_6$-DMSO) : 5/ppm = 1.9-2.0 (m, 3H), 2.1-2.2 (m, 4H), 2.3 (s, 3H), 3.8-4.0 (m, 4H), 4.30-4.45 (t, 2H), 5.25-5.40 (m, 2H), 6.8-6.9 (m, 2H), 7.1-7.2 (d, 2H), 7.3-7.4 (m, 2H), 7.5-7.6 (d, 2H), 8.85-9.15 (s, 2H), hydroxy proton was not observed; ^{13}C-NMR (d$_6$-DMSO) : 8/ppm = 21.0, 32.5, 33.3, 34.0, 43.1, 44.7, 49.7, 50.8, 60.1, 60.6, 67.5, 69.1, 114.7, 118.1, 123.7, 125.7, 128.4, 130.7, 138.2, 145.5, 148.5, 167.0, the extra peaks additional to the number of symmetry inequivalent atoms appears to result from clustering of these zwitterionic molecules, since we have verified their reproducibility and by repeated purification ensured that they are not due to any impurities which is further confirmed by the satisfactory elemental analysis; elemental analysis (calculated for $C_{25}H_{29}N_5SO_4$) : %C = 60.62 (60.61), %H = 5.89 (5.86), %N = 14.24 (14.14).

7-(3-*R*(+)-hydroxypyrrolidino)-7-(piperazinium)-8,8-dicyanoquinodimethane *p*-**toluenesulfonate, 17(Tos)** : Yield = 77%. Recrystallized from acetonitrile-methanol. M.P. = 239-244°C (dec); FT-IR (KBr) : ν/cm^1 - 3362.2, 3015.0, 2177.8, 2137.3, 1597.2, 1005.0, 887.3, 814.0; UV-Vis (acetonitrile) : λ_{max}/nm= 265, 408; ^{1}H-NMR (d$_6$-DMSO) : 5/ppm = 1.9-2.0 (m, 3H), 2.1-2.2 (m, 4H), 2.3 (s, 3H), 3.6-3.9 (m, 4H), 4.25-4.45 (m, 2H), 5.25-5.40 (m, 2H), 6.8-6.9 (m, 2H), 7.1-7.2 (d, 2H), 7.25-7.4 (m, 2H), 7.5-

2H), 8.8-9.2 (s, 2H), hydroxy proton was not observed; ^{13}C-NMR (d_6-DMSO) : 8/ppm = 21.0, 32.6, 33.7, 34.1, 43.0, 47.1, 50.7, 51.3, 60.0, 61.0, 67.6, 69.3, 114.5, 118.1, 123.6, 125.7, 128.4, 130.9, 138.4, 145.2, 148.8, 166.7, the extra peaks additional to the number of symmetry inequivalent atoms appears to result from clustering of these zwitterionic molecules, since we have verified their reproducibility and by repeated purification ensured that they are not due to any impurities, which is further confirmed by the satisfactory elemental analysis; elemental analysis (calculated for $C_{25}H_{29}N_5SO_4$) : %C = 60.55 (60.61), %H = 5.93 (5.86), %N = 14.21 (14.14).

Fabrication of doped polymer films

We have considered only water soluble polymers, PVA (MW = 150,000) and PSS (MW = 70,000), since we are interested in exploring the fluorescence response of the doped polymer films in presence of organic solvent vapors; however these compounds can be incorporated in other polymers as well. Equal volumes of aqueous solutions of the compound (5 mM) and the polymer (~ 0.2 g/ml) were mixed and subjected to ultrasonication for 5 min. The films were prepared by spin casting on glass plates followed by drying in a vacuum desiccator and hot air oven at 80°C for 1 h each. Instrumentation details are provided in Appendix A.

Enhanced fluorescence in solids and doped polymer films

The electronic absorption spectra of solutions and doped polymer films and the specular reflectance of solids in the form of KBr pellets were investigated. The instrumentation is described in Appendix A. The concentrations were adjusted to achieve an optical density of ~ 0.3 in all cases. The reflectance spectra were converted to absorption profiles using the Kubelka-Munk function. The weight content of the solid compound in KBr was adjusted in each case to achieve a final optical density of ~ 0.3. The emission spectra were recorded by exciting approximately 10 nm below the absorption λ_{max}. The spectra are normalized by dividing by the optical density at λ_{max} of

the same sample, so that a fair comparison can be made between the intensity of emission from solution, solid and polymer films.

The whole family of molecules (Fig. 2.14) exhibited fluorescence enhancement to varying extents in the crystalline state and in polymer films, compared to the solutions. We present the detailed results for 13 as an illustrative case and subsequently provide a summary of the observations for the whole family. The absorption and emission spectra of 13 in solvents of different polarity are shown in Fig. 2.15. The negative solvatochromism of the absorption spectra indicates the highly polar nature of the ground state of the molecule consistent with dipole moment measurements on similar molecules reported earlier.[15,53,54] The fluorescence quantum yield of 13 in acetonitrile solution estimated by comparison with quinine sulfate is only about 0.11%; this is typical of such molecules.[51] However, the solid sample as well as 13 doped in polymer films, polyvinyl alcohol (PVA) and poly(sodium 4-styrenesulfonate) (PSS) show bright green light emission when excited near their absorption peaks. The bright emission of crystals of 13 placed in its solution is shown in Fig. 2.16. The polymer films show clearly visible fluorescence even under ambient lighting. The spectra of 13 in the solid state and in
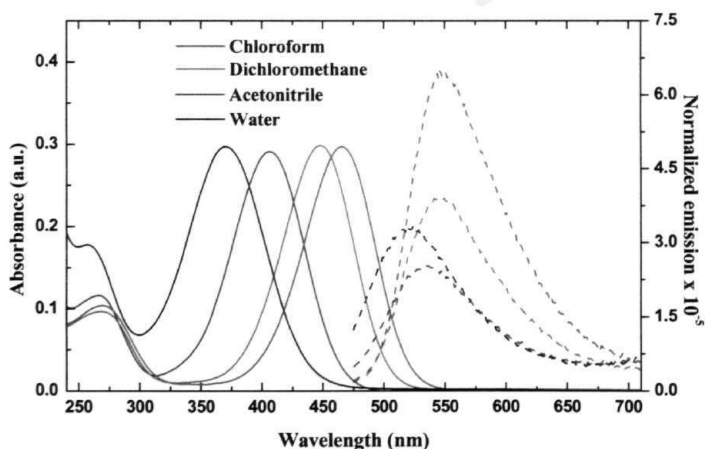
Figure 2.15 *Absorption (full line) and emission (broken line) spectra of 13 in different solvents. The emission spectra are normalized by dividing by the optical density at λ_{max}*

polymer films are presented in Fig. 2.17. The strong enhancement of the emission compared to the solutions is evident from the normalized intensities. The absorption spectra in the solid state and in polymer films show similar linewidth and shape as the solution spectra, indicating that the electronic states involved are molecular; unlike the systems reported earlier[46,47,49] the molecular aggregation appears to have little impact on the electronic absorption spectra.
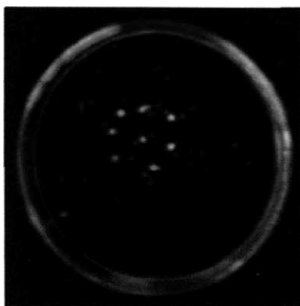
Figure 2.16 *Crystals of 13 placed in its solution and irradiated with UV light (365 nm).*
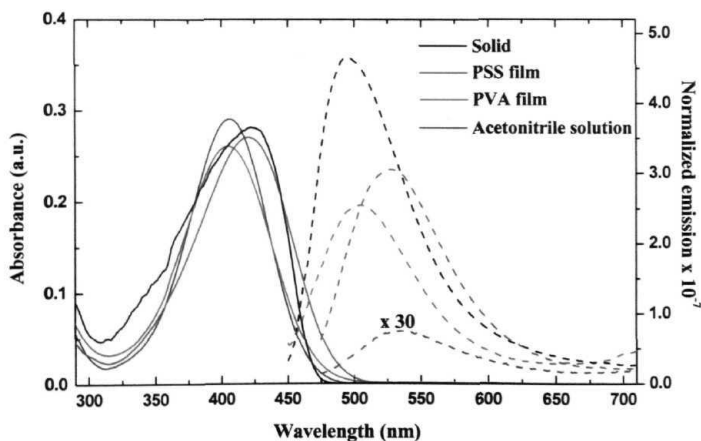
Figure 2.17 *Absorption (full line) and emission (broken line) spectra of 13 in solid state, polymer films and acetonitrile solution (λ_{max} for absorption are similar). The emission spectra are normalized by dividing by the optical density at $\lambda_{max.}$.*

The excitation spectra of the various cases, solution, solid and polymer films, show close resemblance to the absorption spectra suggesting that the emission is from the vertically excited state. The Stokes shifts observed are also within the range expected for vibrational relaxation alone of the excited state. The absorption and emission maxima of the full set of compounds in low polar solvents like chloroform and dichloromethane and high polar solvents like acetonitrile and water are given in Table 2.5. The emission intensity of the various molecules in different solvents are of the same order of magnitude, but as in the case of 13 (Fig. 2.15) the emission from low polar solvents are found to be slightly stronger than that from more polar solvents. Table 2.6 presents the absorption and emission maxima in acetonitrile solution, solid state and doped polymer films; the absorption λ_{max} of solids and doped polymer films are closest to that in acetonitrile than in other solvents. The large enhancement of the normalized emission intensity in the solid state and in polymer films over the acetonitrile solution for the various compounds are also listed in Table 2.6; the enhancement factor, R ranges from 10 to 227. It is important to note that, the measured fluorescence intensities of the solids and doped polymer films may be less than the actual values due to factors such as self-absorption and wave guiding. The latter is particularly relevant for polymer films where the light emission from the edges is not fully accounted for in the normal sample

Table 2.5 *Absorption and emission maxima for the different molecules in solvents of low and high polarity.*

| Molecule | $\lambda_{max}^{a\ s}$ $[\lambda_{max}^{em}]$ /nm | | | |
	Chloroform	Dichloromethane	Acetonitrile	Water
4	467 [5521		418 [5391	400 [535]
9(Tos)₂	*	*	449 [5491	406 [540]
12	472 [5461	456 [5471	420 [543]	390 [5281
13	460 [5461	448 [5411	407 [538]	369 [520]
14	461 [5421	444 [5421	407 [5331	380 [530]
15	461 [5481	445 [5471	408 [539]	379 [5331
16(Tos)	*		422 [540]	379 [5311
17(Tos)	•		408 [536]	378 [5311

* compound insoluble

geometry employed.   While these effects are difficult to quantify, the qualitative considerations indicate that the fluorescence enhancements we report for these materials are really their lower limits. Deactivation of the chromophore excited state due to collisions with solvent molecules may contribute to the lower fluorescence observed in solutions.   However, in view of the fact that in spite of such effects, most organic dye molecules exhibit stronger fluorescence in solution than in the solid state, one has to seek an explanation for the enhanced fluorescence of the aggregated states observed in the present materials.

Table 2.6 *Visible absorption (λ_{max}^{abs})   and emission (λ_{max}^{em}) peaks of the full family of compounds in acetonitrile solution, solid state and in PVA and PSS films and the ratio, R of the maximum intensity of the normalized emission in the solid and polymer films to that in acetonitrile solution.*

	Solid		PVA film		PSS film	
Molecule	[λ_{max}^{em}] / nm	**R**	λ_{max}^{abs} [$\wedge_{max~J}$] / **nm**	**R**	λ_{max}^{abs} [$\wedge_{max~J}$] / **nm**	R
4	418 [525]	**13**	408 [526]	18	431 [5431	29
9(Tos)₂	423 [526]	227	411 [509]	60	447 [5471	34
12	422 [4921	171	414 [5141	38	431 [5361	27
13	422 [495]	216	405 [505]	100	420 [5271	132
14	419 [534]	63	391 [5141	14	415 [5261	69
15	410 [5531	27	390 [5101	218	413 [5241	31
16(Tos)	418 [5181	23	398 [5181	25	422 [5281	36
17(Tos)	403 [5311	30	399 [5231	33	421 [5251	35

Crystal structure investigations

Before embarking on an investigation of the origin of the fluorescence enhancement we have carried out single crystal x-ray structure analysis of 12 and 13 to gain insight into the molecular structure of these compounds and to explore the role of the remote functionality. 12 is found to belong to the monoclinic space group, $P2_1/n$[55] and 13 to the orthorhombic space group, Pbca respectively. The basic crystallographic data are presented in Table 2.7 and the molecular structures are shown in Fig. 2.18. Both molecules show the strong twist between the diaminomethylene unit and the benzenoid ring plane, a feature common among these molecules as discussed in Sec. 2.2.;[3,7,14,38,50] the dihedral angles, C2-C1-C7-N9 and C6-C1-C7-N10 are 52.6 and 53.5 in 12 and 50.6 and 53.0 in 13 respectively. It should be noted that the situation is quite different from that in the case of the phenyleneethynylenes,[46,47] silole[48] and cyanobiphenylethylene[49] where the planar ground state conformation in the aggregates is considered to be an important factor contributing to the strong fluorescence. The bond lengths in the

Table 2.7 *Crystallographic data for 12 and 13.*

Compound	12	13
Molecular formula	$C_{20}H_{26}N_6$	$C_{19}H_{23}N_5$
Formula weight	350.47	321.42
Crystal system	Monoclinic	Orthorhombic
Space group	$P2_1/n$ (No. 14)	Pbca (No. 61)
a/A	8.581(3)	16.32(7)
b/A	20.157(3)	12.400(17)
c/A	11.4040(13)	18.13(2)
P/deg.	90.085(18)	90.0
Z	4	8
μ / cm"^{1}	0.74	0.72
No. of reflections with	$I > 2\sigma_I = 3080$	$I > a, = 4597$
No. of parameters	235	217
GOF	0.992	0.983
R [for $I > 2\sigma_I$]	0.0429	0.0550

aromatic ring of **12** and 13 are typical of benzenoid structures and point to the zwitterionic nature of the molecules.[3] Examination of intermolecular contacts in these crystals reveals moderately close ones between the carbon atoms connected to the remote N atom of the piperazine units and the negatively polarized dicyanomethylene end of the zwitterionic diaminodicyanoquinodimethane moiety. The extended structure which results from such contacts in **12** and 13 are shown in Fig. 2.19. Even though these noncovalent interactions are likely to be weak, their cooperative influence would steer the organization of the zwitterionic DADQ molecules and contribute to the enhanced tendency of these remote functionalized molecules towards aggregate formation. Strong intermolecular H-bond interactions mediated by the remote groups have been observed in 9(Tos)2[14] and a derivative of 14 and 15[7] in earlier studies. All these molecular associations are likely to play a significant role in obstructing the excited state conformational relaxation discussed below.
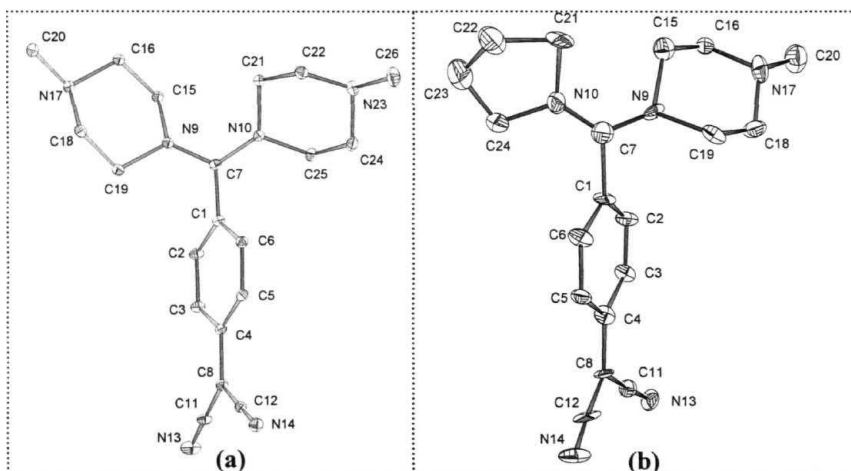
Figure 2.18 *Molecular structure of (a)* **12** *and (b) 13 from single crystal x-ray analysis. 10% probability thermal ellipsoids are indicated and hydrogen atoms are omitted for clarity.*
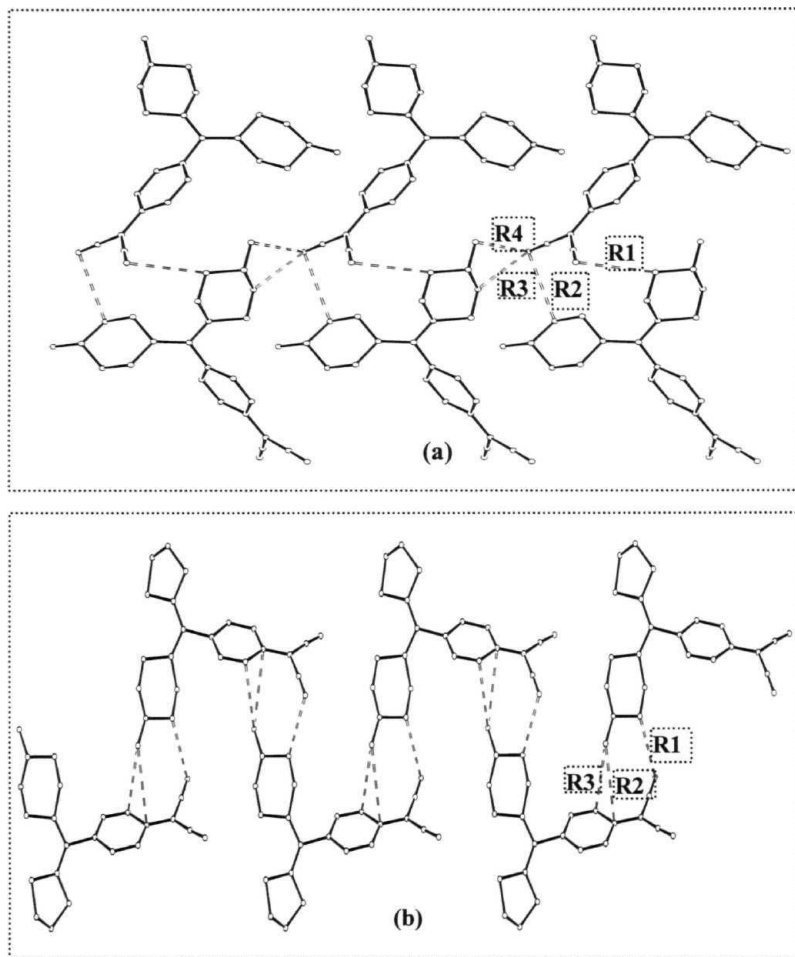
Figure 2.19 *Intermolecular contacts (broken lines) leading to tape structures in (a) 12 (extending along the crystallographic a axis; Rl = 3.399, R2 = 3.564, R3 = 3.711, R4 = 3.787 A) and (b) 13 (extending along the crystallographic b axis; Rl = 3.698, R2 = 3.760, R3 = 3.897 Å).*

A model for   the fluorescence enhancement phenomenon

In order to investigate the likely molecular structure in solution, we have optimized the geometry of 13 using the AM1 method. The molecular structure from crystal analysis served as a convenient starting point for the optimization and the solvent environment was modeled by invoking the COSMO subroutine[19] employing various dielectric constants in the range 1 to 80. Enthalpies of formation were computed following full configuration interaction (CI) calculation within the 6 molecular orbitals bracketing the HOMO/LUMO, involving the 400 singlet microstates. As demonstrated in Sec. 2.2,[14] the same approach can be used to model the impact of the molecular environment in the solid state as well. Similar to our earlier observation on related molecules, the molecular twist, 6 of the optimized ground state geometry of 13 is found to increase with the dielectric constant, s employed in the computation; it increases from 39.8° at e = 1 and saturates at a value of about 66° at e > 40. The θ observed in the crystal is obtained when ε is in the range 2 - 4 . CI calculations on the optimized ground state geometry provided the excitation energies. The enthalpy of formation of the ground state and the lowest vertical excited state at different s are plotted in Fig. 2.20. The computed λ_{max} at the appropriate e values agree very well with those observed for low polar solvents like dichloromethane and chloroform as well as the highly polar solvent, water (Table 2.5). The λ_{max} at E = 4 is in good agreement with the experimental value in the solid state. As noted earlier, the observed emission is likely to be from the vertical excited state alone. Even though geometry relaxation of the excited state is unlikely in the rigid solid state or polymer matrix, it is quite feasible in the solution state. In order to investigate the likely geometry relaxation, we have optimized the excited state structure under different ε values. The conspicuous change is the increase of 9 to ~ 90° in all cases. The enthalpy of formation of these optimized geometries are also plotted in Fig. 2.20. The figure also shows the enthalpy of formation of the ground states of these geometries from which we can estimate the upper bound for the emission energies of these relaxed geometries. The values are found to be in the range, 1588 - 673 nm (for s ranging from 1 - 80), very much smaller than the observed emission energies suggesting that no visible light emission from the relaxed excited state geometries is observed in the solution, solid or polymer film. These computational results combined with the experimental facts noted earlier lead us to the conclusion that the enhancement of the
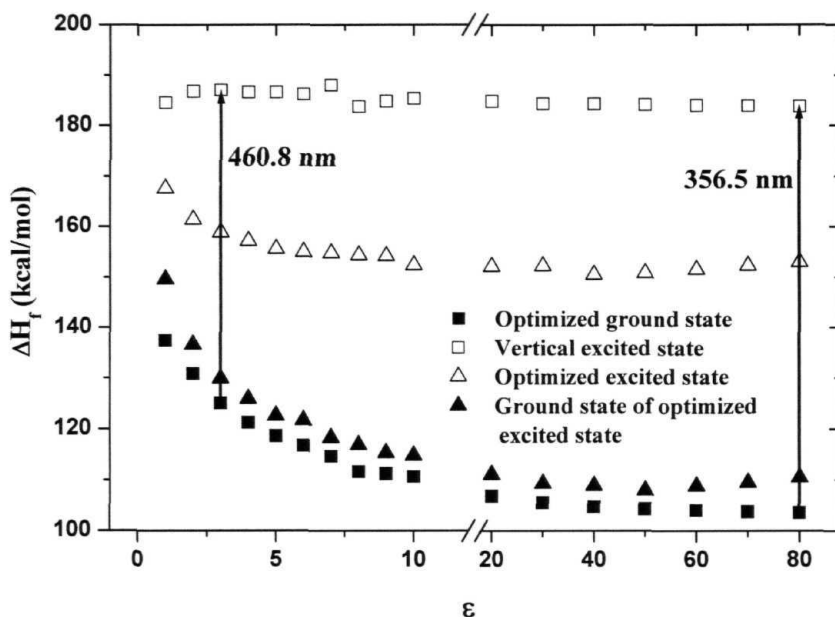
Figure 2.20 *AM1/COSMO/CI calculated enthalpy of formation at different ε, of 13 in the optimized ground state, the lowest vertical excited state, the optimized excited state and the ground state of the optimized excited state.*

fluorescence in the solid state and polymer films arise as a result of arresting the geometry relaxation of the excited fluorescent state to a nonfluorescent state. Conversely, geometry relaxation of the excited state leads to diminished fluorescence in solutions (Fig. 2.21). The situation is reminiscent of the TICT model[56] wherein planar and twisted excited state geometries are considered; however in our systems, both excited state geometries are twisted and the difference is in the extent of twisting. The current model is consistent with the qualitative picture proposed earlier for the matrix dependence of light emission from similar **molecules.**[51] It is important to note that in the picture we develop for the DADQ's, the role of molecular aggregation is to facilitate
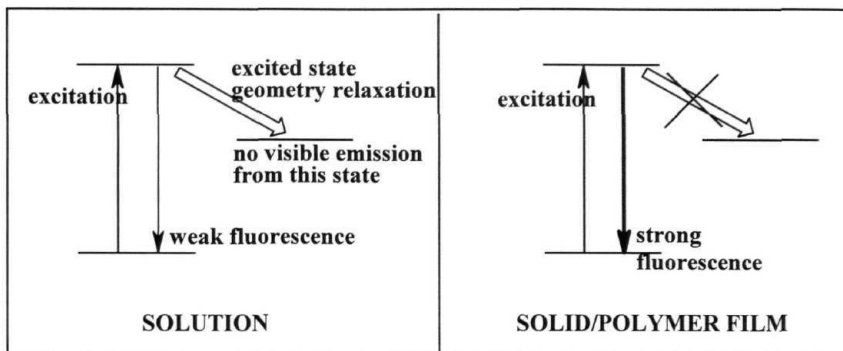
Figure 2.21 *Schematic diagram illustrating the mechanism of fluorescence enhancement of diaminodicyanoquinodimethanes in the solid state and doped polymer films.*

further, the inhibition of excited state structure relaxation, rather than to force any kind of ground state geometry changes as implied in the models put forward in the case of the systems reported **earlier**.[47- '] The energy gap between the vertical and relaxed excited states increases with e (Fig. 2.20) suggesting that, as the polarity of the solvent environment increases, the relative population of molecules in the vertical excited state would diminish progressively leading to reduction of fluorescence intensity; this is in agreement with the emission spectra observed in solution (Fig. 2.15).

Switching of fluorescence in a doped polymer film triggered by solvent vapors

In order to examine the application potential of the fluorescence enhancement phenomenon, we have carried out an experiment on PVA films containing 13, by alternately exposing it to chloroform vapors and drying. The fluorescence intensity of the film showed a clear reduction when it was enveloped by chloroform vapors emanating from the solvent placed at the bottom of the spectrometer cuvette. When the chloroform
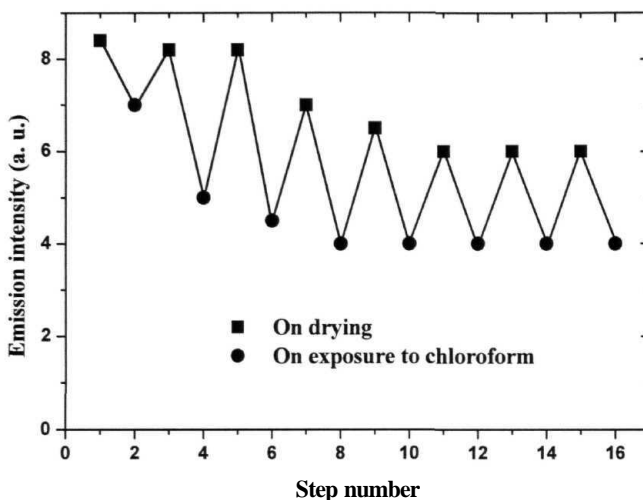
Figure 2.22 *The variation of emission maximum (at 505 nm) of 13 in PVA film on exposure to chloroform vapors and subsequent drying, through consecutive steps.*

was removed and the film dried free of the vapors, the original fluorescence intensity was nearly regained (Fig. 2.22). Two subsequent cycles showed stronger reduction of the fluorescence in presence of the vapors and return to higher fluorescence in the dry state. Some change in the dry state fluorescence was observed during the initial cycles. The values stabilized subsequently and good reversibility was attained. At this stage, the reduction of fluorescence due to the vapors is quite substantial (~ 33%). Since the PVA matrix does not dissolve in chloroform and absolutely no leaching of the compound is observed throughout, we believe that the solvent vapors diffuse into the film and possibly cause local dissolution of part of the compound leading to fluorescence reduction. On drying, solid microaggregates may be formed again, recovering the enhanced fluorescence. Alternately, a mild softening of the PVA matrix induced by the solvent vapor may facilitate structure relaxation and fluorescence quenching, which is reversed on drying. The present study provides a quantitative demonstration of the reversibility and repeatability of solvent vapor induced switching of the enhanced fluorescence in a chromophore doped polymer film.

2.5 SUMMARY

Investigations presented in Sec. **2.2** show that the molecular structure modification occurring in a crystal environment can be conveniently modeled using solvation-included geometry optimization at the semiempirical level. Such an analysis also provides useful insight into the microscopic dielectric constant experienced by the molecule and should be of utility in evaluating accurately the molecular contribution to crystal properties. Assuming a typical refractive index of 1.5 - 2.0, the dielectric constant of organic crystals at optical frequencies will be of the order of 2 - 4. The e needed in the semiempirical solvation calculations are in this range for most of the systems. The larger ε required for 8 is compatible with the fact that the dielectric constant of compounds with extensive H-bonding are generally higher.[23] The still larger E in the case of **9(Tos)2** reflects the highly polarizable molecular environment made up of several H-bonded water molecules. Our preliminary explorations suggest that quantum chemical computations incorporating standard solvation model should prove to be a convenient tool to study different aspects of the 'molecule-in-a-crystal'. The generality of this approach needs to be explored using further computational studies at different levels, in close parallel with structural investigation of molecular crystals.

The mode of CT complexation between push-pull zwitterionic molecules and picric acid was explored in Sec 2.3. The CT occurs only in the solid state and requires the anchoring of the picric acid in the form of picrate ion by the remote amine functionality in the push-pull molecule. This picture is elaborated using the crystal structure analysis of **9(Pic)$_2$**. The π-π interaction between the dicyanomethylene moiety of 9 and the picrate ion and its facilitation by the H-bonding of the picrate ion to the piperazinium moiety are revealed. The mode of CT interaction is demonstrated using computed atomic charges on the respective ions. The mechanism of induction of charge transfer presented in this study also provides insight into the role of pyridine as an anchoring agent in the Kofler's ternary complex and other amine picrates. The 'picrate effect'[35] is in a general sense a similar phenomenon and is of interest in analytical applications. The utility of anchoring agent mediated charge transfer materials would be an important subject for further studies in this area.

We have presented a new family of remote functionalized zwitterionic diaminodicyanoquinodimethanes in Sec. 2.4 and demonstrated enhanced light emission from their aggregated state in the solid state and in polymer films. The utility of the remote functionality in promoting molecular assembly is revealed by the detailed crystallographic analysis of two of the molecules. A viable mechanism for the fluorescence enhancement is proposed through semiempirical computational analysis of the ground and excited state geometries and energies. We believe that such analysis may prove useful in understanding the basis for similar observations in other molecules reported previously. Excited state dynamics in solution, solid and doped polymer films as well as their temperature dependence need to be investigated to gain further insight into the mechanism of fluorescence enhancement operating in these materials. We have demonstrated reversible fluorescence switching in doped polymer films triggered by solvent vapors. These materials provide an ideal testing ground for the fascinating and relatively rare phenomenon of light emission enhancement in aggregates and are potential candidates for the development of novel photonic devices based on such phenomena.

REFERENCES

1. (a) Wright, J. D. *Molecular Crystals.* Cambridge University Press, Cambridge, 1995, 2nd Edn.; (b) Pierrot, M. *Structure and Properties of Molecular Crystals.* Elsevier Science, Amsterdam, 1990.

2. (a) Bernstein, J. in *Organic Solid State Chemistry,* Desiraju, G. R. (Ed.) p.471, Elsevier Science, London, 1987; (b) Bernstein, J.; Davey, R. J.; Henck, J. - 0 . *Angew. Chem. Int. Ed.* **1999,** *38,* 3440.

3. Ravi, M.; Radhakrishnan, T. P. *J. Phys. Chem.* **1995,** *99,* 17624.

4. Ravi, M; Rao, D. N.; Cohen, S.; Agranat, I.; Radhakrishnan, T. P. *J. Mater. Chem.* 1996,6, 1853.

5. Ravi, M.; Rao, D. N.; Cohen, S.; Agranat, I.; Radhakrishnan, T. P. *Chem. Mater.* **1997,** *9,* 830.

6. (a) Gangopadhyay, P.; Sharma, S.; Rao, A. J.; Rao, D. N.; Cohen, S.; Agranat, I.; Radhakrishnan, T. P. *Chem. Mater.* **1999**, *11*, 466; (b) Sharma, S.; Radhakrishnan, T. P. *Mol. Cryst. Liq. Cryst.* **2000,** *338,* 257.

7. Ravi, M.; Gangopadhyay, P.; Rao, D. N.; Cohen, S.; Agranat, I.; Radhakrishnan, T. P. *Chem. Mater.* **1998**, *10*, 2371.

8. Zyss, J.; Chemla, D. S. in *Nonlinear Optical Properties of Organic Molecules and Crystals,* Chemla, D. S.; Zyss, J. (Eds.) *Vol. 1,* p.23, Academic Press, New York, 1987.

9. (a) Gavezzotti, A.; Simonetta, M. *Chem. Rev.* **1982,** *82,* 1; (b) Desiraju, G. R. *Crystal Engineering, The Design of Organic Solids,* Elsevier, Amsterdam, 1989; (c) Gavezzotti, A. *Acc. Chem. Res.* **1994,** *27,* 309; (d) Gavezzotti, A. *Crystallogr. Rev.* **1998,** 7, 5.

10. (a) Braga, D.; Grepioni, F. *Organometallics*, **1991**, *10*, 1254; (b) Stockton, G. W.; Godfrey, R.; Hitchcock, P.; Mendelsohn, R.; Mowery, P. C; Rajan, S.; Walker, A. F. *J. Chem. Soc. Perkin Trans. 2* **1998,** 2061; (c) Craw, J. S.; Greatbanks, S. P.; Hillier, I. H.; Harrison, M. J.; Burton, N. A. *J. Chem. Phys.* **1997**, *106*, 6612.

11. Cremer, C. J.; Truhlar, D. J. *Chem. Rev.* **1999,** *99,* 2161.

12. Jiao, H.; Schleyer, P. v. R. *J. Am. Chem. Soc.* **1994,** *116,* 7429; see also Ref. 9 - 12 therein.

13.   Sherer, E. C; Yang, G.; Turner, G. M.; Shields, G. C; Landry, D. W. *J. Phys. Chem. A* **1997,** *101,* 8526.

14.   Jayanty, S.; Radhakrishnan, T. P. *Chem. Mater.* **2001,** *13*, 2460.

15.   Kagawa, Y.; Szablewski, M.; Ravi, M.; Ann Lackman, N.; Cross, G. H.; Bloor, D.; Batsnor, A. S.; Howard, J. A. K. *Nonlinear Optics,* **1999,** *22,* 235.

16.   Gangopadhyay, P.; Ravi, M.; Radhakrishnan, T. P. *Ind. J. Chem.* **2000,** *A39,* 106.

17.   Dewar, M. J. S.; Zoebisch, E. G.; Healy, E. F.; Stewart, J. J. P. *J. Am. Chem. Soc.* **1985,** 707, 3902. MOPAC93 (Fujitsu Inc.) program was used; starting with the molecular structure from crystal structure analysis, geometries were fully optimized using the EF and PRECISE keywords; calculation of the full potential energy surface for θ = 0 - 90° gave minima identical to these optimized geometries. Test calculation at the *ab initio* B3LYP/6-31G* level on 6 gave θ = 29.0° in good agreement with the AM1 results.

18.   Sharma, S.; Radhakrishnan, T. P. *J. Phys. Chem. B* **2000,** *104*, 10191.

19.   Klamt, A.; Shuurmann, G. *Perkin Trans.* **1993,** 799.

20.   Full geometry optimization invoking EF, PRECISE, NSPA=60 and values of EPS mentioned in the text. Test calculations on 6 at the B3LYP/6-31G* level including solvation correction (CPCM) with ether (e = 4.3) gave 0 = 35.4°. $\theta_\varepsilon > \theta_0$ as in the AM1 calculations; however, higher e appears to be necessary to reproduce θ_{cryst}.

21.   Ravi, M.; Cohen, S.; Agranat, I.; Radhakrishnan, T. P. *Struct. Chem.* **1996,** 7, 225.

22.   Hertler, L. R.; Hartzler, H. D.; Acker, D. S.; Benson, R. E. *J. Am. Chem. Soc.* **1962,** *84,* 3387.

23.   Schweitzer, R. C; Morris, J. B. *Anal. Chim. Acta* **1999,** *384,* 285.

24.   (a) Furniss, B. S.; Hannaford, A. J.; Smith, P. W. G.; Tatchell, A. R. *Vogel's Textbook of Practical Organic Chemistry,* p.1 196, ELBS with Longman, Singapore, 1996; (b) Koenig, K. E.; Lein, G. M.; Stuckler, P.; Kaneda, T.; Cram, D. J. *J. Am. Chem. Soc.* **1979,** *101*, 3556.

25.   *3D Search and Research using the Cambridge Structural Database,* Allen, F. H.; Kennard, O. *Chem. Design Autom. News* **1993,** *8,* 131; Cambridge Structural Database Version 5.24.

26. Colquhoun, H. M.; Doughty, S. M; Stoddart, J. F.; Slawin, A. M. Z.; Williams, D. J. *J. Chem. Soc. Perkin Trans. 2* **1986,** 253.

27. Nagata, H.; In, Y.; Doi, M.; Ishida, T.; Wakahara, A. *Ada Crystallogr. B* **1995,** *51,* 1051.

28. Beer, P. D.; Drew, M. G. B.; Grieve, A.; Ogden, M. I. *J. Chem. Soc. Dalton Trans.* **1995,** 3455.

29. Nather, C; Arad, C; Bock, H. *Ada Crystallogr. C* **1997,** *53,* 76.

30. In, Y.; Nagata, H.; Doi, M.; Ishida, T.; Wakahara, A. *Ada Crystallogr. C* **1997,** *53,* 646.

31. Kofler, A. *Z. Elektrochem.* **1944,** 50, 200.

32. Matsunaga,Y.; Saito, G. *Bull. Chem. Soc. Jpn.* **1972,** *45,* 963.

33. Matsunaga,Y.; Saito, G. *Bull. Chem. Soc. Jpn.* **1972,** *45,* 2214.

34. Bernstein, J.; Regev, H. *Ada Crystallogr. B* **1980,** *36,* 1170.

35. Talanova, G. G.; Elkarim, N. S. A.; Talanov, V. S.; Hanes, R. E.; Hwang, H.; Bartsch, R. A.; Rogers, R. D. *J. Am. Chem. Soc.* **1999**, *121*, 11281.

36. Bermudez, V. D. Z.; Carlos, L. D.; Silva, M. M; Smith, M. L. *J. Chem. Phys.* **2000**, *112*, 3293.

37. Ravi, M.; Rao, D. N.; Cohen, S.; Agranat, I.; Radhakrishnan, T. P. *J. Mater. Chem.* 1996,6, 1119.

38. Jayanty, S.; Radhakrishnan, T. P. *Chem. Mater.* **2001**, *13*, 2072.

39. *Gaussian94,* Revision D.2, Frisch, M. J.; Trucks, G. W.; Schlegel, H. B.; Gill, P. M. W.; Johnson, B. G.; Robb, M. A.; Cheeseman, J. R.; Keith, T.; Petersson, G. A.; Montgomery, J. A.; Raghavachari, K.; Al-Laham, M. A.; Zakrzewski, V. G.; Ortiz, J. V.; Foresman, J. B.; Cioslowski, J.; Stefanov, B. B.; Nanayakkara, A.; Challacombe, M.; Peng, C. Y.; Ayala, P. Y.; Chen, W.; Wong, M. W.; Andres, J. L.; Replogle, E. S.; Gomperts, R.; Martin, R. L.; Fox, D. J.; Binkley, J. S.; Defrees, D. J.; Baker, J.; Stewart, J. P.; Head-Gordon, M.; Gonzalez, C ; Pople, J. A.; Gaussian, Inc., Pittsburgh PA; 1995.

40. Miertus, S.; Scrocco, E.; Tomasi, J. *Chem. Phys.* **1981,** *55,* 117.

41. Miertus, S.; Tomasi, J. *Chem. Phys.* **1982,** *65,* 239.

42. Jensen, B. *Ada Chem. Scand. Ser. B* **1975,** *29,* 115.

43. Jensen, B. *Ada Chem. Scand. Ser. B* **1975,** *29,* 891.

44. Herbstein, F. H.; Kaftory, M. *Ada Crystallogr. B* **1976,** *32,* 387.

45.   Ozcelik, S.; Akins, D. L. *J. Phys. Chem.* **1999,***103,* 8926.

46.   Deans, R.; Kim, J.; Machacek, M. R.; Swager, T. M. *J. Am. Chem. Soc.* **2000,** *122,* 8565.

47.   Levitus, M.; Schmieder, K.; Ricks, H.; Shimizu, K. D.; Bunz, U. H. F.; Garcia-Garibay, M. A. *J. Am. Chem. Soc.* **2001**, *123*, 4259.

48.   Luo, J.; Xie, Z.; Lam, J. W. Y.; Cheng, L.; Chen, H.; Qiu, C; Kwok, H. S.; Zhan, X.; Liu, Y.; Zhu, D.; Tang, B. Z. *Chem. Commun.* **2001,** 1740.

49.   An, B.; Kwon, S.; Jung, S.; Park, S. Y. *J. Am. Chem. Soc.* **2002**, *124*, 14410.

50.   Jayanty, S.; Gangopadhyay, P.; Radhakrishnan, T. P. *J. Mater. Chem.* **2002**, *12*, 2792.

51.   Bloor, D.; Kagawa, Y.; Szablewski, M.; Ravi, M.; Clark, S. J.; Cross, G. H.; Pålsson, L.; Beeby, A.; Parmer, C; Rumbles, G. *J. Mater. Chem.* **2001**, *11*, 3053.

52.   Jayanty, S.; Radhakrishnan, T. P. *Chem. Eur. J.* (in press).

53.   Gopalan, R. S.; Kulkarni, G. V.; Ravi, M.;Rao, C. N. R. *New. J. Chem.* **2001,** *25,* 1108.

54.   Cole, J. M.; Copley, R. C. B.; McIntyre, G. J.; Howard, J. A. K.; Szablewski, M.; Cross, G. H. *Phys. Rev. B* **2002,** *65,* 125107.

55.   The data were collected and structure solved under monoclinic P lattice; however the β angle deviates from 90° by only 0.085 (18). Therefore we have examined the lattice transformation to orthorhombic P; however the set of systematic absences found in the transformed reflection data is not compatible with any of the space groups in this Bravais lattice. Further, we have checked the symmetry of the Friedel pairs of several reflections; out of the four pairs in an (hkl) set, the intensity of reflection of two are distinctly different from (ranging from 2 - 50% of) the other two, indicating the monoclinic symmetry of the lattice.

56.   (a) Rettig, W. *Angew. Chem. Int. Ed. Engl.* 1986, *25,* 971; (b) Bhattacharya, K.; Chowdhury, M. *Chem. Rev.* **1993,** *93,* 507.

CHAPTER 3

Nonlinear Optical Materials Based on Diaminodicyanoquinodimethane

Papers published

- <u>Jayanty, S.</u>; Gangopadhyay, P.; Radhakrishnan, T. P. *J. Mater. Chem.* **2002**, *12*, 2792. Steering Molecular Dipoles from **Centrosymmetric** to **Noncentrosymmetric** and SHG Active Assembly Using Remote Functionality and Complexation.

- <u>Jayanty, S.</u>: Radhakrishnan, T. P. *(submitted).* Spontaneous Resolution through Helical Assembly of a **Conformationally** Chiral Molecule With an Unusual Zwitterionic Structure.

3.1　INTRODUCTION

Design of functional molecules and their tailored assembly into materials with specific attributes is an area of continuing interest at the interface of synthetic chemistry and condensed matter science. Fabrication of nonlinear optical (NLO) materials pose significant challenges at the level of molecular synthesis as well as materials fabrication. For instance, the development of efficient molecular NLO materials for quadratic effects[1] such as optical second harmonic generation (SHG) comprises of the synthesis of molecular units possessing large hyperpolarizability (P) and their assembly into a noncentrosymmetric bulk structure so as to achieve suitable orientation of the β tensor components.[2] However the organization of these building blocks into optimal lattice structures with the desired molecular orientations is a difficult problem. Centrosymmetric arrangements are statistically favored in most of the organic crystals. Hence the development of molecular and crystal design techniques for the assembly of desired noncentric lattices is of great importance. In Sec. 1.3 we have discussed several techniques which include physical and chemical methods for the fabrication of the noncentric assemblies. Well known methods such as incorporation of stereogenic centres have been employed in our laboratory to synthesize SHG materials based on diaminodicyanoquinodimethanes (DADQ's).[3] New approaches have been developed during these investigations for the creation of noncentrosymmetric bulk crystal lattices for SHG. Attachment of optimally long alkyl chains to dipolar NLO chromophores like DADQ[4] and *p*-nitroaniline[5] relies on a subtle interplay of dipolar energies and dispersion interactions, the latter influenced primarily by the alkyl chain length.[5] Helical superstructures of axially chiral push-pull *p*-nitroaniline based molecules formed through dipolar nitro group interactions[6] have been shown to be capable of enhanced SHG. In the present work, we have explored new systems which form noncentric lattices through cocrystallization and spontaneous resolution processes.

Cocrystallization and salt formation of NLO-phores with partner molecules and molecular ions are known to be efficient methods to generate quadratic NLO materials.[7] In Sec. 3.2 we explore the utilization of flexible pendant groups bearing a remote functionality and their complexation with an appropriate partner leading to the fabrication of a DADQ based noncentrosymmetric molecular crystal lattice capable of SHG.[8] N,N-

dimethylaminoethylene groups attached to the **amino** groups of the diaminodicyanoquinodimethane serve as the pendant groups and terephthalic acid as the complexing partner. We have also carried out investigation of the crystal structures of the chromophore alone as well as its complex which allowed us to demonstrate the crucial role of the pendant group and the complexing partner in the formation of the **noncentrosymmetric** lattice of the complex with concomitant induction of optical second harmonic generation capability.

Sec. 3.3 presents the formation of orthogonal helical superstructures in the crystals of a conformationally chiral zwitterionic molecule derived from a DADQ molecule.[9] With a molecule of water included in the lattice, the helical structures are formed through a network of H-bond pathways and electrostatic interactions and when no water is included, through electrostatic interactions alone. Following the methodology developed in Sec. 2.2 for modeling structural features, a systematic protocol for the computation of charge distribution on the 'molecule-in-the-crystal' is presented; the computed charges provide insight into the origin of the **intermolecular** electrostatic interactions. H-bonding is one of the most common interactions exploited in the fabrication of helical **supramolecular** assemblies.[10] In our system, the low symmetry of the twisted molecule coupled with the extended H-bond as well as electrostatic interactions lead to the formation of helical superstructures along orthogonal crystallographic directions. The homochirality associated with the orthogonal helical assemblies leads to spontaneous resolution in the crystals. Once again, the appreciable hyperpolarizability of the molecule coupled with the noncentric lattice structure lead to the observation of moderate SHG in this material. This novel system we have investigated has facilitated a systematic analysis of a complex set of molecular level interactions that form the basis for the persistent spontaneous resolution of a conformationally chiral molecule in the solid state. Sec. 3.4 provides a summary of **the** work presented in the chapter.

3.2 STEERING MOLECULAR DIPOLES FROM CENTROSYMMETRIC TO NONCENTROSYMMETRIC AND SHG ACTIVE ASSEMBLY USING REMOTE FUNCTIONALITY AND COMPLEXATION

As noted earlier, 7,7-diamino-8,8-dicyanoquinodimethane (DADQ) is a versatile push-pull chromophore structure amenable to a wide variety of substitutions at the amino end, providing chromophores possessing large[11] and tunable hyperpolarizability.[12,13] Ashwell and coworkers have investigated the NLO properties of related TCNQ derivatives as LB films.[14] There has been considerable interest in the exploitation of similar systems as prototypes for molecular rectifiers.[15] We have explored the introduction of a variety of conformationally rigid as well as flexible pendant groups with remote Lewis base functionality, which can be used to induce specific interactions between the molecule and its neighbors. As discussed in Sec. 2.2, the pendant groups could be used in salt formation and creation of a polar environment to model the impact of such an environment on the molecular structure.[16] We have shown in Sec. 2.3 that charge transfer complexation phenomena could be triggered by such 'anchoring groups'.[17] We have subsequently seen that 7,7-bis(N,N-dimethylethylenediamino)-8,8-dicyano-quinodimethane (10) (Figs. 2.8, 3.1) discussed in connection with the solid state CT complex formation in Sec. 2.3, forms a centrosymmetric crystal lattice. This is a commonly observed phenomenon with several DADQ molecules.[18] The situation arising due to the disengagement of one of the pendant groups from intermolecular interactions through the formation of an intramolecular H-bond is highlighted in the structure of 10. We have explored the complexation of 10 with a variety of partner molecules in an attempt to fabricate noncentric SHG active lattice following the salt formation model (Sec. 1.3) or other possible avenues. Though the former was not realized, experimentation with a variety of aliphatic and aromatic diacids and diols, led to the choice of terephthalic acid (TPA) from which proton transfer occurs to the remote base functionality leading to a desirable engagement of the pendant groups in intermolecular H-bonds in the **11** (TPA) complex. This facilitates a set of noncovalent interactions which drive the dipolar molecules into an unusual orthogonal orientation leading to a noncentrosymmetric lattice exhibiting moderate solid state SHG. The role of the pendant groups and the complexation in the formation of noncentric lattice are conspicuous in view of the dominant tendency of DADQ's to form centrosymmetric lattices.[18]
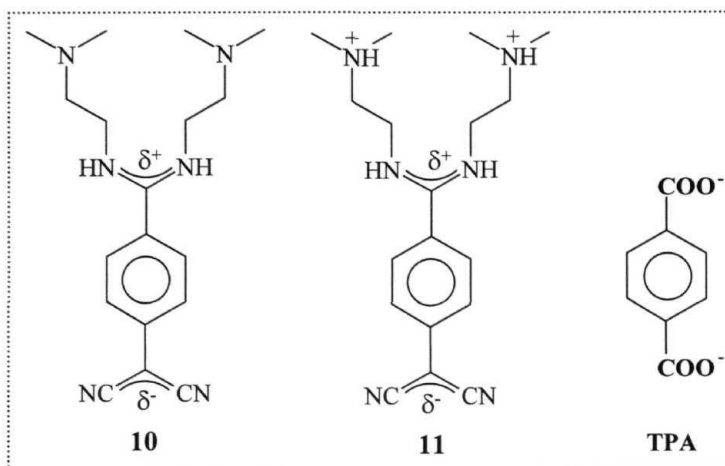
Figure 3.1 *Molecular structures of **10, 11** and terephthalate (TPA).*

Synthesis and characterization

7,7-bis(N,N-dimethylethylenediamino)-8,8-dicyanoquinodimethane, 10 : 10 was synthesized following the protocols reported earlier.[19,20] To a warm solution of 0.10 g (0.49 mmol) of tetracyanoquinodimethane in 30 ml of acetonitrile was added 0.108 g (1.22 mmol) of N,N-dimethylethylenediamine. The solution turned green immediately and a light yellow precipitate appeared. The reaction mixture was stirred at 65°C for 2.5 h, cooled to 30°C and filtered to produce 0.14 g (87% yield) of pale yellow 10. It was purified by recrystallization from acetonitrile. Crystals were grown from methanol-acetonitrile. 10 was characterized as follows : M.P. = 246 - 248°C (dec); FT-IR (KBr) : ν/cm^{-1} = 3234, 2179, 2137, 1601; UV-Vis (ethanol) : λ_{max}/nm= 374, = 450; ^{1}H-NMR (CDCl$_3$) : 5/ppm = 2.25 (s, 6H), 2.40 (s, 6H), 2.50 (t, 2H), 2.65 (t, 2H), 3.52 (m, 4H), 6.95 (d, 2H), 7.25 (d, 2H) (H-bonded protons on N were not observed); ^{13}C NMR (d$_6$-DMSO) : 5/ppm = 32.3, 44.9, 58.2, 114.6, 117.4, 123.9, 129.7, 148.0, 165.1; elemental analysis (calculated for C$_{18}$H$_{26}$N$_6$) : %C = 66.18 (66.26), % H = 8.10 (7.98), % N = 25.65 (25.76).

7,7-bis(N,N-dimethylethylenediammonium)-8,8-dicyanoquinodimethane terephth-alate, ll(TPA) : Ethanol solutions of equivalent amounts of 10 and terephthalic acid were mixed at room temperature. On slow evaporation over 12 h pale yellow crystals of the 1:1 complex appeared. The complex was characterized as follows : M.P. = 238 - 242°C (dec); FT-IR (KBr) : ν/cm^{-1} = 3238, 2166, 2129, 1637, 1597; UV-Vis (ethanol) : λ_{max}/nm = 374, 241, $\lambda_{cut\text{-}off}$/nm = 450; ^{1}H-NMR (d$_6$-DMSO) : 5/ppm = 2.15 (s, 6H), 2.31 (s, 6H), 2.48 (m, 2H), 2.62 (m, 2H), 3.43 (m, 4H), 6.83 (d, 2H), 7.28 (d, 2H), 8.01 (s, 4H) (H-bonded protons on N's were not observed); ^{13}C NMR (d$_6$-DMSO): 5/ppm = 32.3, 44.4, 57.2, 114.6, 117.4, 123.9, 129.3, 129.6, 135.6, 147.9, 165.0, 167.6; elemental analysis (calculated for C$_{26}$H$_{32}$N$_6$O$_4$) : % C = 63.76 (63.41), % H = 6.77 (6.50), % N = 17.13(17.07).

Role of the pendant group in the formation of noncentric lattice : Crystal structure investigations

Substituted diaminodicyanoquinodimethanes possess large ground state dipole moment in solution[21] and even larger dipole moment in the solid state[22] as a result of the strongly zwitterionic structure resulting from their push-pull nature. The zwitterionic character is clearly revealed by the benzenoid ring structure observed in their crystals.[18,19] These molecules possess large hyperpolarizability, which is extremely sensitive to the molecular twist between the diaminomethylene moiety and the benzenoid ring plane.[12,13] The crystals however show a strong predilection towards centrosymmetric organization,[18] possibly promoted by the large ground state dipole moment. Crystallographic studies that we describe below reveal the role of the remote functionality and complexation in the generation of a noncentrosymmetric lattice.

Crystals of 10 belong to the P2$_1$/c space group. The crystallographic data are collected in Table 3.1 and the asymmetric unit is shown in Fig. 3.2. The chromophore part of 10 shows a structure similar to those of other DADQ's. The twist angle (average of the dihedral angles, N1-C13-C7-C8 and N2-C13-C7-C12) is 39.7°. The N,N-dimethylaminoethylene chain attached to one of the amino groups (N1) adopts

multiple *gauche* conformations so as to fold back and enter into an intramolecular H-bond with the other amino group (N2); the appreciable positive charge of the zwitterionic motif residing on the amino groups makes them good proton donors. The H-bond parameters are collected in Table 3.2. The intramolecular H-bond effectively disengages the remote base functionality of one of the pendant groups as well as one amino group (N2) from entering into any effective intermolecular interactions. The amino group (N1) however forms an intermolecular H-bond with the cyano nitrogen of a neighboring molecule (Table 3.2) leading to a chain structure along the *b* axis (Fig. 3.3). Adjacent chains oriented in opposite directions are related by an inversion center. Significantly, no H-bonding or other noncovalent interactions are observed between the chains.

Table 3.1 *Crystallographicdata for 10 and **11(TPA)***

Compound	10	11(TPA)
Molecular formula	$C_{18}H_{26}N_6$	$C_{26}H_{32}N_6O_4$
Formula weight	326.45	492.58
Crystal system	Monoclinic	Monoclinic
Space group	$P2_1/c$ (No.14)	Cc (No.9)
a/A	13.121(3)	13.2413(11)
b'A	10.192(4)	12.5696(8)
c/A	15.463(2)	15.3847(11)
P /deg.	111.94(2)	95.004(6)
Z	4	4
$\rho_{calc.}$ / g cm^{-3}	1.130	1.283
MA)	0.71703	0.71703
μ / cm^{-1}	0.71	0.89
Number of unique reflections	4384	3068
Number of reflections with $I \geq \sigma_I$	1846	2914
Number of parameters	223	335
GOF	0.946	0.951
R (for I > 2a,)	0.0483	0.0502
wR^2	0.1298	0.1171
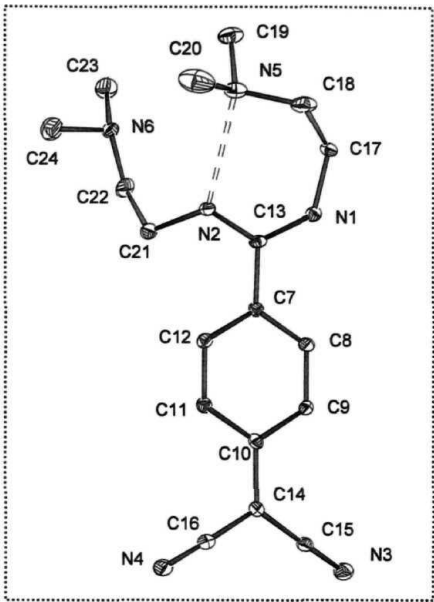
Figure 3.2 *Molecular structure of 10 from single crystal x-ray structure analysis. **10%** probability thermal ellipsoids are shown; the dashed line indicates **H-bonding;** H atoms are omitted for clarity.*

Table 3.2 *Significant intramolecular (symmetry : x, y, z) and **intermolecular** H-bonds in crystals of 10. D and A are the H-bond donor and acceptor atoms respectively in the D-H...A bond; r and θ **are** the relevant distance and angle.*

D-H	A [Symmetry]	$r_{D...A}$ (Å)	$\theta_{D-H...A}$ (°)
N2-H2	N5 [x, y, z]	2.839	155.4
N1-H1	N4 [-x+1, y-0.5, -z+0.5]	2.879	156.4
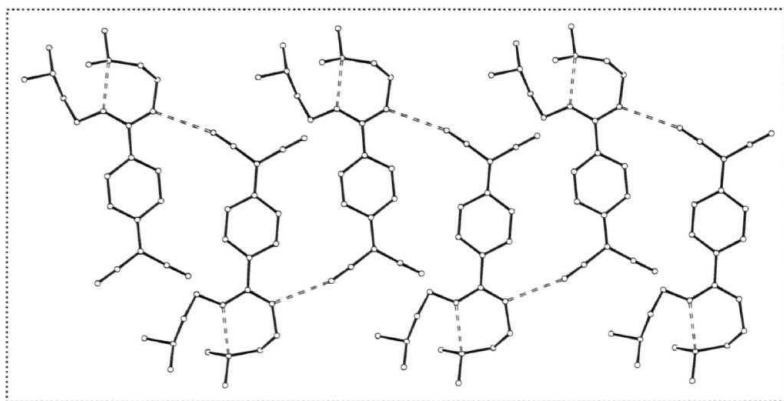
Figure 3.3 *Molecular chains propagating along the b axis in 10. The dashed lines indicate H-bonds; H atoms are omitted for clarity.*

Interestingly, crystals of **ll(TPA)** complex are found to belong to the **noncentrosymmetric** space group, Cc. The crystallographic data are collected in Table 3.1 and the asymmetric unit is shown in Fig. 3.4. The molecular structure of the diprotonated moiety, **11,** in the complex shows important differences from that of the unprotonated molecule in the crystal of 10. In the NLO-phore unit, namely the diaminodicyanoquinodimethane part, the main deviation is in terms of the twist angle. The angle is now enhanced to 48.4° (mean of the dihedral angles as noted earlier), possibly a consequence of the large number of intermolecular H-bonds that arise in this crystal as shown below. The more significant structural variation occurs in the pendant chains. Both N,N-dimethylaminoethylene groups in **11** are spread outwards so that they are able to enter into intermolecular interactions. One of these groups is connected to the TPA partner through multiple and bifurcated H-bonds (Fig. 3.4). The other group engages the TPA from a neighboring complex unit so that an extended chain structure propagating along the *b* axis emerges (Fig. 3.5). The C-0 bond lengths in TPA (C35-025 = 1.274 A, **C35-O26** = 1.227 A) clearly indicate deprotonated carboxylic acid groups; hence the protons were added to the tertiary amine nitrogen atoms during the structure refinement. This also verifies the formation of 11. The significant H-bond parameters in **ll(TPA)** are collected in Table 3.3.
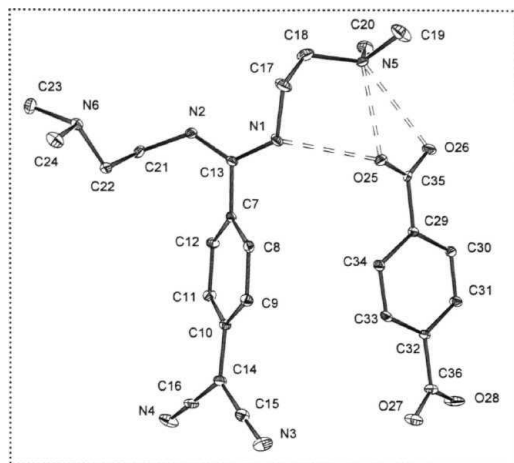
Figure 3.4 *Molecular structure of **ll(TPA)** from single crystal x-ray structure analysis. 10% probability thermal ellipsoids are shown; the dashed line indicates H-bond; H atoms are omitted for clarity.*
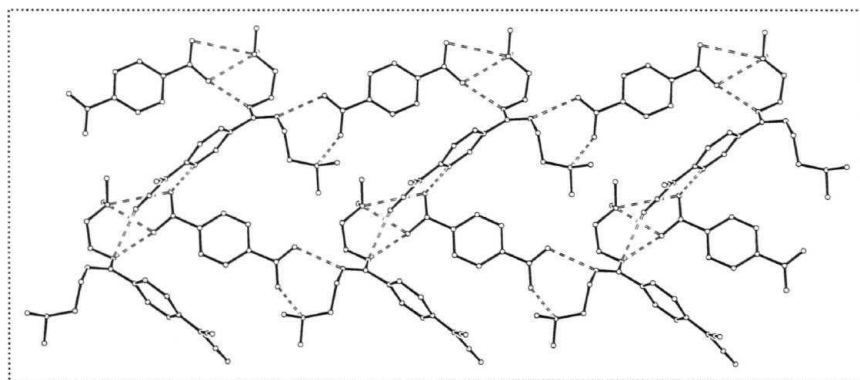
Figure 3.5 *Molecular chains propagating along the b axis in **ll(TPA)**. The dashed lines indicate H-bonds and close electrostatic interactions; an additional short contact C13...N3' in **ll(TPA)** is not indicated and all H atoms are omitted for clarity.*

Table 3.3 *Significant intramolecular (symmetry : x, y, z) and intermolecular H-bonds in*
11(TPA) *complex. D and A are the H-bond donor and acceptor atoms respectively in the*
D-H...A bond; r and θ are the relevant distance and angle.

D-H	A [Symmetry]	$r_{D...A\,(A)}$	$\theta_{D-H...A}$ $(°)$
N1-H1	O25 [x, y, z]	2.722	140.2
N5-H5	O25 [x, y, z]	2.669	166.5
N5-H5	O26 [x, y, z]	3.190	132.5
N2-H2	O28 [x, y+1.0, z]	2.746	157.4
N6-H6	O27 [x, y+1.0, z]	2.606	159.4
C9-H9	O26 [x, -y, z+0.5]	3.497	150.5

Unlike the chains in 10, the H-bonded chain in **ll(TPA)** constituted of alternating
11 and TPA, enters into several noncovalent interactions with the adjacent chain which is
related by the glide reflection operation.   The significant noncovalent interactions
between these chains are (i) the electrostatic interactions between the amino and cyano
ends carrying partial positive and negative charges respectively, resulting in the short
contacts N1...N3' (3.475 A) and C13...N3' (3.404 A) and (ii) the weak H-bond, C9-
H9...O26' (Table 3.3, Fig. 3.5).   As a result of these interactions the dications **11** of
adjacent chains adopt an interesting orientation wherein the molecular dipole vectors are
oriented nearly orthogonal to each other; the angle between the C13-C14 vectors is 99.0°.
Further, the mean planes of their benzenoid rings are also nearly orthogonal to each other,
the angle being 80.6°.   A view of the electrostatically bound **11**'s with orthogonal dipole
vectors and ring planes propagating along the c axis is shown in Fig. 3.6.

A comparison of the unit cell dimensions of 10 and **11 (TPA)** (Table 3.1) is
instructive; the cell dimension ***a*** shows a very small increase on complexation whereas *c*
shows a small decrease.   The presence of the TPA counterions in the H-bonded chains
propagating along *b,* causes this dimension to increase by ~ 2.4 A.   The calculated
density shows a clear and significant increase (~ **13.5%)** from **10** to **11(TPA)**.   This
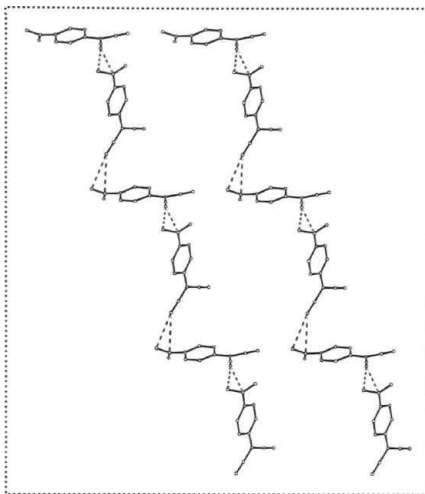
Figure 3.6 *Chains of 11, formed through electrostatic interactions, propagating along the c axis in **ll(TPA)**. Dashed lines indicate the close electrostatic interactions; the N,N-dimethylaminoethylene chains and all H-atoms are omitted for clarity.*

implies that the large number of **intrachain** H-bonds (along *b)* and interchain noncovalent interactions in **ll(TPA)** lead to a tighter packing of the crystal lattice. The values of the unit cell dimensions suggest that there is a gross similarity in the lattice structures of **10** and **ll(TPA);** the emergence of new noncovalent **intermolecular** interactions influence the breaking of the center of inversion symmetry and formation of the orthogonal orientation of the **11** moieties in the latter.

Second harmonic generation in ll(TPA)

Semiempirical AM1/TDHF[23] computations on 10, using the molecular structure from single crystal analysis with the H atom positions alone optimized, shows that it possesses a significant ground state dipole moment of 23.2 D and a large static β of -85.2 x 10^{-30} esu. However, the centrosymmetric structure adopted by this compound rules out

all quadratic NLO properties. The static β computed for 11 without taking into account the protonation at the tertiary amine ends of the pendant groups is -96.5 x 10" esu. The enhancement of β is a consequence of the increased twist angle.[12] Interestingly, **11** in the diprotonated state shows a calculated static β of -70.7 x 10^{-30} esu. The reduction is a consequence of the destabilization of the partial zwitterionic structure as a result of the positive charge accumulation on the remote functionality. The computations also show that 10 as well as 11 follow the one-dimensional model with the major β tensor component coincident with the dipole axis along C13-C14. The nearly orthogonal orientation of NLO-phore units in the crystal of **11(TPA)** leads to an angle of 40.5° and 139.5° respectively between the crystallographic *b* axis and the molecular dipole axes of the two molecules related by the glide plane. In the context of the oriented gas model,[24] these considerations suggest a moderate SHG in the complex.

11(TPA) is found to have good thermal stability (M.P. = 240°C) and stability towards laser radiation (at a power of ~ 1 GW cm"[2]). SHG from microcrystalline powders was examined using the Kurtz-Perry[25] method. Details of the experiment are provided in Appendix C. Table 3.4 presents the SHG of **ll(TPA)** at various particle sizes. The particle size dependence of the SHG indicates phase-matchable behavior. The moderate SHG of ~ 9 U observed at saturation is in agreement with the expectation based on the oriented gas model noted above.

Table 3.4 *SHG of microcrystalline powder of ll(TPA) at various particle sizes. 1 U SHG of urea having particle size > 150 μm.*

Particle size (urn)	SHG/U
< 100	7.4
100-150	8.7
150-200	8.7
200 - 250	8.7
250 - 300	8.2
>300	9.3

3.3 SPONTANEOUS RESOLUTION THROUGH HELICAL ASSEMBLY OF A CONFORMATIONALLY CHIRAL MOLECULE WITH AN UNUSUAL ZWITTERIONIC STRUCTURE

Molecular assembly in crystals is directed by the concomitant influence of a variety of intermolecular interactions. The resulting organization in the crystal along with the molecular characteristics determine the attributes of the materials. Among the various molecular superstructures that exert critical control on the materials properties, helical organization is one of the most fascinating, for reasons of symmetry as well as the cooperativity of extended interactions associated with such structures. The inherent chirality of helical structures is of considerable interest in the design of liquid crystals[26] and quadratic nonlinear optical materials for applications such as second harmonic generation.[6,27] A wide variety of intermolecular interactions have been harnessed to build helical molecular assemblies. H-bonding is the method of choice in many cases.[10] There are a number of helical coordination polymers where the metal-ligand interactions and the chirality of the ligand or the coordination geometry are effectively exploited.[28] Formation of helical superstructures of axially chiral push-pull molecules achieved through dipolar nitro group interactions has been reported from our laboratory.[6] The helicity of the extended structures in most of these cases stems directly from the chirality, often axial C_2 symmetry, of the building blocks. Polyisocyanides and polyheteroarenes are interesting cases where steric factors drive the formation of the helical structure of the polymer backbone.[29]

Another context in which helical assembly assumes fundamental significance is when it is accompanied by spontaneous resolution in crystals. Spontaneous resolution has important implications for areas such as chirality in nature,[30] enantioselective synthesis[31] and advanced materials design.[32] Fundamental thermodynamic aspects of spontaneous generation of optical activity have been discussed early on.[33] The intimate relation between chirality and crystals[34] as well as spontaneous resolution in supramolecular architectures[35] have been reviewed recently. Since little is known about the factors that govern conglomerate formation, it is of great interest to examine the formation of helical assemblies that trigger such events and the molecular level structure and interactions that lead to such chiral supramolecular associations. Molecules which

are chiral, not due to the presence of a stereogenic atom but because of a specific **conformational** structure that lacks all improper rotation symmetries, and the enantiomeric forms of which can be interconverted through rotation about a single bond, could be called **conformationally** chiral.[36]   Conformationally chiral compounds which resolve spontaneously in the crystalline state (l,l'-binaphthyl is a classic example[37]) are particularly significant since the barriers to racemization in such molecules are relatively low and therefore the conglomerate formation through **supramolecular** assembly is a particularly subtle phenomenon.

In Chapter 2 we have described a number of interesting phenomena associated with remote functionalized DADQ's. One of the systems which showed enhanced solid state fluorescence (Sec. 2.4)[38] is **12.** During our investigations of a salt of **12,** namely **18(Iod)2,** we have discovered a rather unexpected, but simple reaction leading to a novel derivative,   7-(N,N-dimethylpiperazinium)-7-oxo-8,8-dicyanoquinodimethane,   **19** (Scheme 3.1), which possesses cyano groups, an amide group and a quarternary ammonium functionality capable of participating in **intermolecular** H-bonds and electrostatic interactions.   19 is found to exhibit spontaneous resolution through helical organization in crystals, utilizing a variety of electrostatic and **H-bond** interactions.[9] Charge distribution estimated using a systematic protocol based on semiempirical computations suggests an unusual zwitterionic structure with the negative charge residing on the dicyanomethylene end of the conjugated π-**electron** system and a compensating positive charge on the nonconjugated **remote**[8,17,38] ammonium functionality.   The molecule is conformationally chiral owing to the strong molecular twist between the amide group and the benzenoid ring plane, a feature similar to that found in the precursor DADQ molecules as well;[4,8,17,19,38] there are no stereogenic atoms on the molecule. We found that the crystals of 19 formed with and without water of crystallization reveal helical supramolecular organization along the three crystallographic directions, the former through a combination of electrostatic interactions and H-bonds and the latter through electrostatic interactions alone. The concomitant formation of the helical motifs expresses the **homochirality** of the molecular assembly leading to the spontaneous resolution in these crystals.

Synthesis and characterization

The diiodide salt of 7,7-bis(N,N-dimethylpiperazinium)-8,8-dicyanoquinodi-methane (12), namely **18(Iod)2** and 7-(N,N-dimethylpiperazinium)-7-oxo-8,8-dicyanoquinodimethanide (19) were synthesized and characterized as described below. It may be noted that, we denote the iodide ion by the non-standard notation Iod, to be consistent with the notations we have used for tosylate (Tos) and picrate (Pic).

7,7-bis(N,N-dimethylpiperazinium)-8,8-dicyanoquinodimethanediiodide (18(Iod₂)) :
Synthesis of 7,7-bis(N-methylpiperazino)-8,8-dicyanoquinodimethane (12) has been described in Sec. 2.4.[38] 1.03 g (7.22 mmol) of freshly distilled methyl iodide was added to 0.25 g (0.71 mmol) of 12 dissolved in 30 ml of acetonitrile (Scheme 3.1). The solution changed from yellow to deep orange. It was stirred at 25°C for 30 min when a yellow microcrystalline product separated out. Stirring was continued for 7 h more to ensure the completion of the reaction. The precipitate was filtered, washed and dried to give 0.37 g (82% yield) of yellow **18(Iod)₂**. It was recrystallized from water. M.P. = 270-275°C (dec); FT-IR (KBr) : ν/cm^{-1} = 2993.0, 2173.9, 2135.4, 1597.2, 1460.2; UV-Vis (acetonitrile) : λ_{max}/nm = 462.5, 355.0, 247.5; elemental analysis (calculated for $C_{22}H_{32}N_6I_2$) : %C = 41.54 (41.77), %H = 5.01 (5.06), %N = 13.35 (13.30).
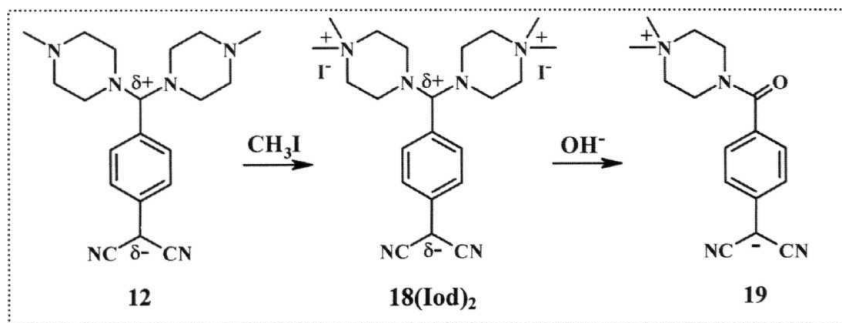
Scheme 3.1
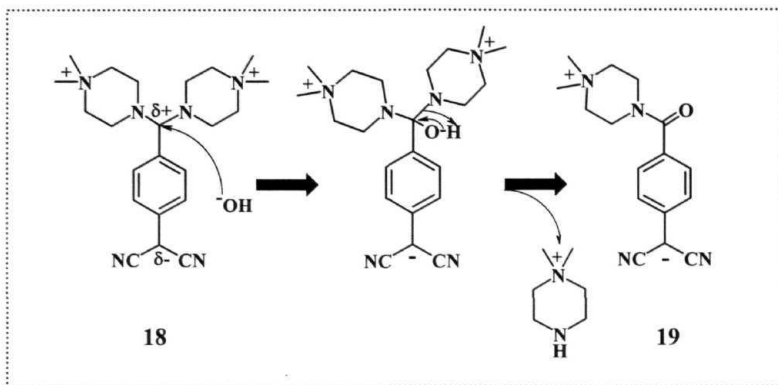
Scheme 3.2

When we attempted the substitution of the iodide ions in **18(Iod)₂** by organic ions such as Tos or TPA, through reactions with the corresponding salts in aqueous medium, it was found that instead of anion substitution, one of the piperazinium unit was displaced and replaced by an oxygen atom. This rather unexpected reaction can be easily rationalized and achieved by a directed approach by simply dissolving **18(Iod)₂** in aqueous solution of KOH. The formation of **19** is likely to involve the attack of OH" on the diaminomethylene carbon followed by the expulsion of a piperazine (Scheme 3.2).

7-(N,N-dimethylpiperazinium)-7-oxo-8,8-dicyanoquinodimethanide (19) and its hydrate (19.H₂O) : Solutions of 0.30 g (0.47 mmol) of **18(Iod)₂** in 30 ml of water and 0.04 g (0.71 mmol) of KOH in 2 ml of water were mixed. Pale yellow microcrystalline product formed immediately was filtered, washed and dried to give 0.102 g (77% yield) of **19.H₂O** (Scheme 3.1). It was recrystallized from water-methanol (1:1). M.P. = 295-300°C (dec); FT-IR (KBr) : v/cm⁻¹ = 3476.0, 3034.3, 2166.3, 2123.8, 1628.1 (C=O stretch), 1599.1, 1419.7; UV-Vis (acetonitrile) : λ_{max}/nm= 355.0, 224.0; ¹H-NMR (d₆-DMSO): δ/ppm = 3.3-3.4 (s, 6H), 3.4-3.5 (t, 4H), 3.8-3.9 (t, 4H), 6.7-6.8 (d, 2H), 7.2-7.3 (d, 2H); ¹³C-NMR (d₆-DMSO) : δ/ppm = 7.3, 30.2, 50.8, 60.5, 117.4, 121.6, 125.1, 128.8, 145.3, 170.4; elemental analysis (calculated for C₁₆H₁₈N₄O.H₂O) : %C = 63.75 (64.00), %H = 6.68 (6.66), %N = 18.85 (18.66).

When concentrated solution of **18(Iod)₂** and ~ 0.02 M KOH were mixed and kept for 6 h, crystals of 19 without water molecule (M.P. = 285-290°C) were obtained. However, slow recrystallization (~ 24 h) of 19 in methanol-water yielded **19.H₂O**.

<u>*Molecular and Crystal structure of 18(Iod)₂*</u>

The diiodide salt, 18(Iod)2 shows the unusual enhancement of fluorescence in the solid state, similar to its precursor molecule, 12 (Sec. 2.4).[38] Crystal structure analysis showed that 18(Iod)2 possesses a centrosymmetric lattice belonging to the monoclinic P2₁/c space group with one molecule in the asymmetric unit. The crystallographic details are given in Table 3.5. The molecular structure and crystal packing are shown in Figs.

able 3.5 *Crystallographic data for **18(Iod)₂, 19.H₂O** and **19***

Compound	18(Iod)₂	19.H₂O	19
Molecular formula	$C_{22}H_{32}N_6I_2$	$C_{16}H_{20}N_4O_2$	$C_{16}H_{18}N_4O$
Formula weight	634.34	300.36	282.34
Crystal system	Monoclinic	Orthorhombic	Orthorhombic
Space group	P2₁/c (No. 14)	P2₁2₁2₁ (No. 19)	P2₁2₁2₁ (No. 19)
a/A	13.0471(14)	10.064(4)	10.5556(17)
b / A	16.2113(18)	11.40(2)	10.645(6)
c/A	13.0823(16)	14.047(9)	13.0717(15)
P / deg.	111.207(9)	90	90
v/A³	2579.7(5)	1612(4)	1468.8(9)
Z	4	4	4
ρ_{calc} / g cm⁻	1.633	1.237	1.277
μ/ cm⁻¹	24.58	0.84	0.83
No. of reflections with	I > 2σ₁ = 3486	I > a, = 1582	I > a, = 1927
No. of parameters	271	211	196
GOF	0.806	0.937	1.054
R [for I > 2σ₁]	0.0282	0.0583	0.0472
wR²[for I > 2σ₁]	0.0905	0.1736	0.1063

3.7. and 3.8 respectively. Like other DADQ's, **18(Iod)₂** exhibits a zwitterionic structure, which is reflected in the nearly benzenoid geometry of the aromatic ring. We have previously defined the quinonoid-benzenoid character (QBC) in terms of the deviations of the bond lengths in the six member ring from an ideal value of 1.400 A, such that the latter has a QBC value of 1.000.[12] Based on the bond lengths from crystal structure, the QBC value of **18** is found to be 0.724. The zwitterionic structure is promoted by the strong molecular twist of 49.3° (average of the dihedral angles $N9\text{-}C7\text{-}C1\text{-}C2 = 49.0°$ and $N10\text{-}C7\text{-}C1\text{-}C6 = 49.6°$). As noted earlier, this twist arising due to steric factors is a common feature among the DADQ's.[16]
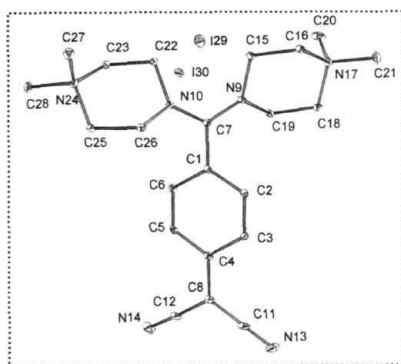
Figure 3.7   *Molecular structure of 18(Iod)2 from single crystal x-ray analysis; 10% probability thermal ellipsoids are shown; H atoms are omitted for clarity.*
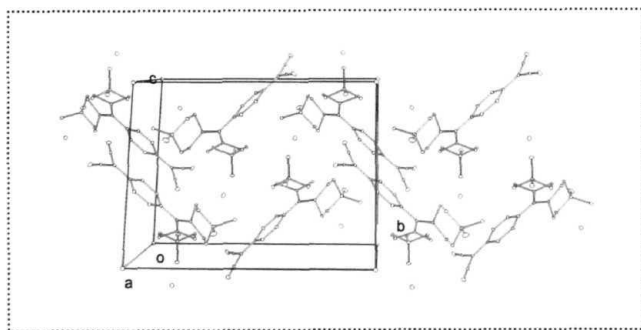
Figure 3.8 *Packing of molecules in* **18(Iod)₂**; *H atoms are omitted for clarity.*

Molecular structure of 19

Crystals of **19.H₂O** are found to belong to the chiral space group, $P2_12_12_1$ with one molecule in the asymmetric unit (Fig. 3.9). The crystallographic details are given in Table 3.5. The Flack parameter could be refined in the case of this crystal and gave a value of 0.085(0.007). The molecular structure again shows a strong twist of 49.5° (average of the dihedral angles N9-C7-C1-C2 = 50.6° and O10-C7-C1-C6 = 48.4°). The benzenoid ring bond lengths are more symmetric than in **18(Iod)2;** this is reflected in the higher QBC value of 0.844. Chemical characterization and crystal structure analysis showed that no counterion is present, hence **19** is overall a neutral molecule. **19** without water molecule also crystallizes in $P2_12_12_1$ space group (Table 3.5). The molecular structures are found to be nearly identical in crystals of **19.H₂O** as well as **19.**
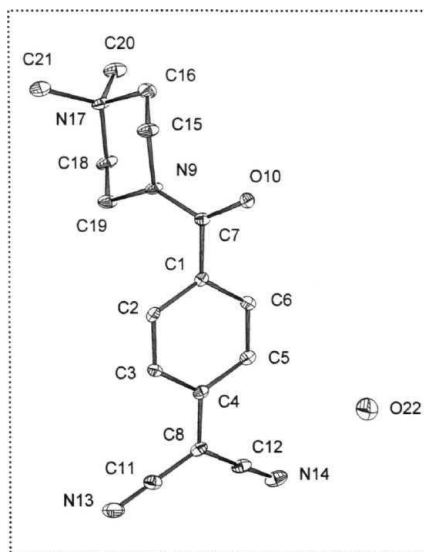
Figure 3.9 *Molecular structure of* **19**.*H₂O from single crystal x-ray analysis; 10% probability thermal ellipsoids are shown; H atoms are omitted for clarity.*

*Modeling the molecular structure **and** charge distribution in 18 **and** 19*

      The molecular structure of 19 appears to be quite unusual since it would have a localized positive charge on the nonconjugated ammonium ion and the compensating negative charge has to be accommodated on the delocalized π-system. The charge distribution would be a significant factor controlling its molecular assembly. Therefore we first attempted to model the charge distribution on 19; 18 was also analyzed as a control system. A realistic modeling of the molecular electronic structure in the solid state needs to take into account the influence of the environment. In Sec. 2.2 we have seen that **semiempirical AM1**[23] calculations incorporating the solvation subroutine COSMO[39] are quite successful in modeling the twisted structure of DADQ's as they exist in the crystal lattice, the so called 'molecule-in-a-crystal'.[16] Therefore we have first explored the dielectric constant, ε required in AM1 /COSMO to model the molecular structures satisfactorily and then estimated the charge distribution at similar e.

      AM1/COSMO computations involving full geometry optimization with an imposed e of 20 or higher are found to reproduce quite well, the molecular structure of the dication 18 as well as 19 in the solid state. In fact these computations provided helpful support for deciding on the atom O10 in 19 during x-ray structure refinement. Table 3.6 lists significant geometry parameters computed at e = 20. The inadequacy of using **AM1** alone is also demonstrated in the table.

      As noted above, the geometry optimization provided an estimate of the e that may be employed to mimic the molecular environment in the crystal. We have computed the atomic charge distribution on 18 (Fig 3.10, Table 3.7) and 19 (Fig 3.11, Table 3.8) by the **AM1/COSMO** method employing a range of e values; the molecular structure from the crystal analysis was used with H atom positions alone optimized. When the ε values employed in the computation are low, the computed charge distribution varies strongly with the ε. However, a consistent charge distribution is obtained at higher values of ε, typically at > 20. In the case of 19, this is graphically illustrated in Fig. 3.12. Based on the geometry optimization experience above, the charge distribution computed at $\varepsilon = 20$ is expected to be realistic estimates for the crystal state; Fig. 3.13 provides a schematic

Table 3.6 *Significant bond lengths (A : C1-C7; B : average of C1-C2 and C1-C6, C : average of C2-C3 and C5-C6, D : average of C3-C4 and C4-C5, E : C4-C8, F = average of C7-N9 and C7-N10 for 18 and C7-N9 for 19, G = C7-O10 for 19) in A and twist angle 0 in degrees, in the dication, 18 in 18(Iod)2 and 19 in 19.H₂O from x-ray structure analysis and from AMl and AM1/COSMO (ε = 20) computations (see Figs. 3.7 & 3.9 for atom labeling).*

Parameter	18 (A / degree)			19 (A / degree)		
	X-ray	AM1	AM1/ COSMO	X-ray	AM1	AM1/ COSMO
A	1.477	1.381	1.474	1.489	1.438	1.479
B	1.396	1.456	1.408	1.395	1.418	1.402
C	1.372	1.349	1.380	1.382	1.369	1.387
D	1.414	1.454	1.419	1.391	1.434	1.414
E	1.450	1.365	1.416	1.489	1.392	1.425
F	1.338	1.431	1.369	1.337	1.461	1.392
G		-	-	1.241	1.253	1.260
e	49.3	1.6	50.4	49.5	15.8	45.4
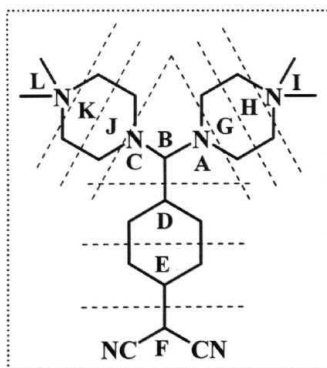
Figure 3.10 *Definition of atom groups for representing charge distribution on 18.*

Table 3.7 *AM1 and AM1/COSMO computed group charge distribution in the dication,*
18 imposing different ε. The definition of the groups are indicated in Fig. 3.10.

Group	AM1	AMI/COSMO (E = 20)	AMI/COSMO (E = 30)	AMI/COSMO (ε = 40)	AMI/COSMO (E = 50)	AMI/COSMO (E = 80)
A	-.31	-.28	-.28	-.28	-.28	-.28
B	.26	.40	.40	.40	.40	.40
C	-.30	-.25	-.25	-.25	-.25	-.25
D	-.24	-.01	.00	.00	.01	.01
E	.10	-.01	-.01	-.01	-.01	-.02
F	-.19	-.80	-.82	-.82	-.83	-.83
G	.45	.52	.52	.52	.52	.52
H	.36	.41	.41	.41	.41	.41
I	.53	.54	.54	.54	.54	.54
J	.44	.51	.51	.51	.51	.51
K	.37	.43	.43	.43	.43	.43
L	.53	.54	.54	.54	.54	.54
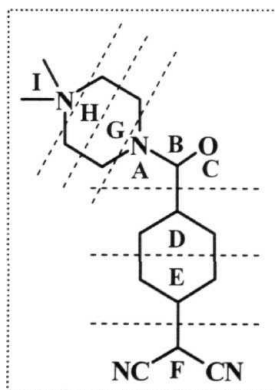
Figure 3.11 *Definition of atom groups for representing charge distribution on 19.*

Table 3.8 *AM1 and AM1/COSMO computed group charge distribution in 19 imposing different ε. Definition of the groups are indicated in Fig. 3.11.*

Group	AM1	AM1/COSMO (E = 20)	AM1/COSMO (E = 30)	AMI/COSMO (E = 40)	AMI/COSMO (E = 50)	AM1/COSMO (ε = 80)
A	-.35	-.33	-.33	-.33	-.33	-.33
B	.38	.42	.42	.42	.42	.42
C	-.36	-.50	-.50	-.50	-.51	-.51
D	-.19	-.03	-.03	-.02	-.02	-.02
E	.02	-.05	-.05	-.05	-.05	-.05
F	-.70	-.89	-.89	-.90	-.90	-.90
G	.43	.47	.47	.47	.47	.47
H	.34	.40	.40	.40	.40	.40
I	.44	.51	.51	.51	.51	.51
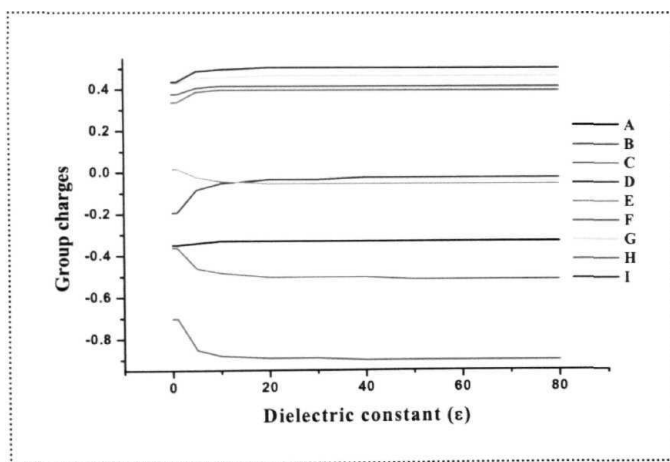
Figure 3.12 *Variation of the AM1/COSMO computed group charges on 19 with the dielectric constant imposed; see Fig. 3.11 for definition of the groups.*
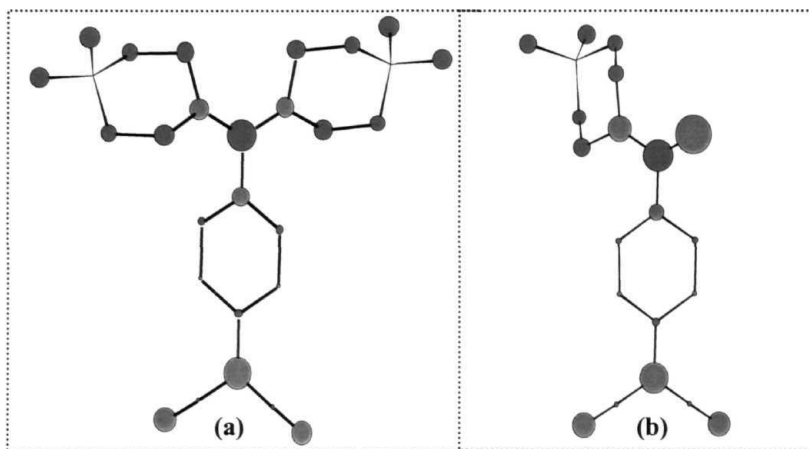
Figure 3.13 *AMI/COSMO (s = 20) computed charge distribution in (a) the **dication**, 18 and (b) 19; purple and cyan indicate positive and negative charges respectively and the radius of the circle is proportional to the net charge on an atom and any H atoms connected to it.*

representation of these values for 18 and 19. The zwitterionic nature of the π-electron system in 18 is revealed by the negative charge on the dicyanomethylene group (the group charge is -0.80) and the positive charge at the diaminomethylene end (the group charge including the carbons connected to the N atoms is +0.90). Nearly a full positive charge each is seen on the **quarternary** ammonium moieties. The charge distribution computed at e = 20 for 19 suggests an unusual zwitterionic structure consisting of a net negative charge on the dicyanomethylene moiety (the group charge is -0.89) and a positive charge on the **quarternary** ammonium group (the group charge is +0.91); further the amide moiety shows strong charge polarization. The charge distribution is thus strongly asymmetric and different from that in 18. This appears to play a key role in evolving the very different molecular assembly observed in 19, described below.

Helical superstructures in crystals of 19.H₂O and 19

DADQ's with their ground state molecular twist are chiral structures, C_2 symmetric when the amino functionalities are identical. However, like **18(Iod)2,** so far none of them have formed chiral crystal lattices, except those in which stereogenic centers **were** incorporated.[4,40] **19** presents a new situation with lower molecular symmetry (C_1) and the consequent asymmetric charge distribution as described above. Further, the molecule possesses well exposed charge localized centers which can enter into strong intermolecular electrostatic interactions. The crystal structure of **19.H₂O** reveals short intermolecular contacts (shorter than the sum of the van der Waal radii of the atoms involved) between the amide oxygen atom and the quarternary ammonium group; the closest C...0 distances are 3.231 (C20...O10) and 3.390 A (C21...O10); the resulting N17...O10 distance is 3.580 A. These intermolecular contacts indicate appreciable electrostatic interactions which in turn lead to the formation of an *M*-helix motif along the crystallographic *b* axis (Fig. 3.14); two piperazinium-carbonyl moieties, (N17[C15,C16,C18,C19]N9-C7-O10) connected in succession make up one turn of the helix. In this as well as the later figures, the view along the packing axis helps to clarify the helicity of the superstructures. **19.H₂O** exhibits also extended H-bond interactions between the cyano groups and the water molecule of crystallization; the relevant distances (angles) are, $r_{O22.. N13}$ = 3.017 A ($\theta_{O22-H22B.. N13}$ = 149.16°) and $r_{O22 ..N14}$ = 3.038 A ($\theta_{O22-H22A}$ ...NU =157.31°). These lead to the formation of a *P*-helix structure along the crystallographic *c* axis (Fig. 3.15). The combination of the two *2* symmetric helical superstructures along the orthogonal crystallographic directions generates *2* symmetry along the third direction. The assembly of the two supramolecular helices along the orthogonal axes can therefore be identified as the genesis of the 222 symmetry of **the** crystal space group (Table 3.5). The *M*-helix formed along the *a* axis can be visualized as arising from a combination of the electrostatic interactions and H-bonds (Fig. 3.16).

Interestingly, crystals of **19** grown from concentrated solutions showed a slightly different unit cell. As mentioned earlier, structure investigation showed that this crystal does not contain the water molecule; however, it belongs to $P2_12_12_1$ space group (Table 3.5) with one molecule in the asymmetric unit having nearly identical molecular structure
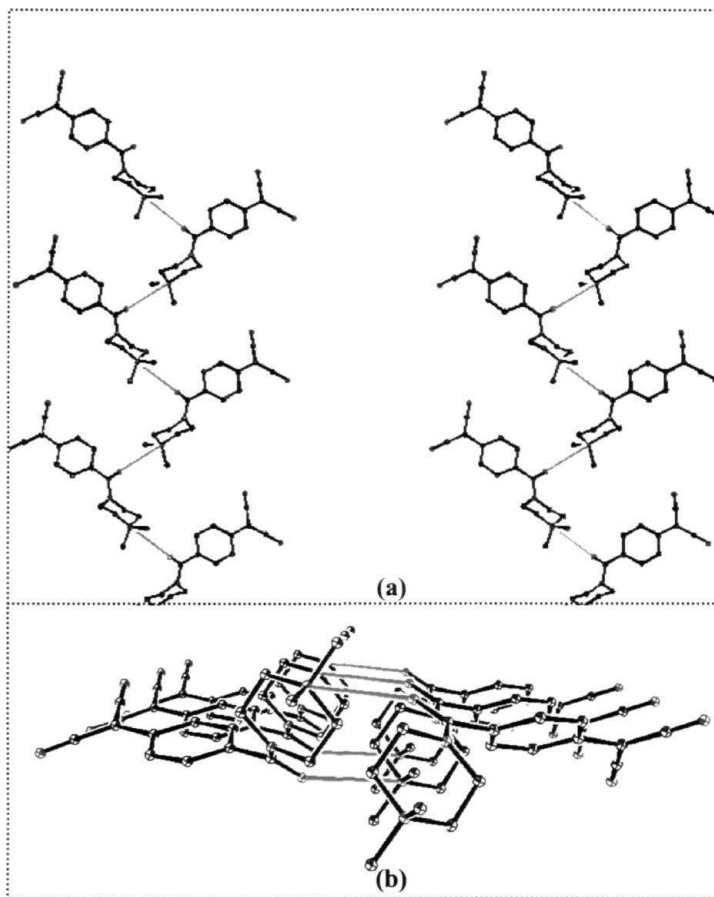
Figure 3.14 *M-helical assembly in 19.H₂O crystal along the b axis; the electrostatic interactions (cyan) are indicated between O10 and N17 for easier viewing : (a) stereo view perpendicular to the helical axis and (b) view along the helical axis. C (black), N (blue) and O (red) atoms are shown.*
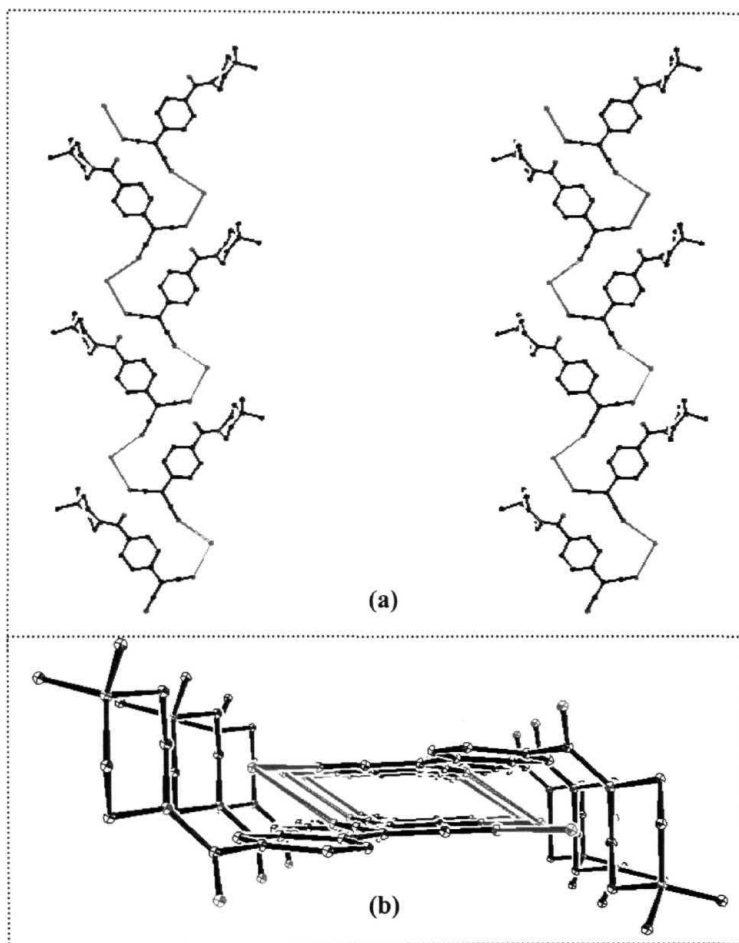
Figure 3.15 *P-helical assembly in* **19.H₂O** *crystal along the c axis; the H-bonds (green) are indicated : (a) stereo view perpendicular to the helical axis and (b) view along the helical axis. C (black), N (blue) and O (red) atoms are shown.*
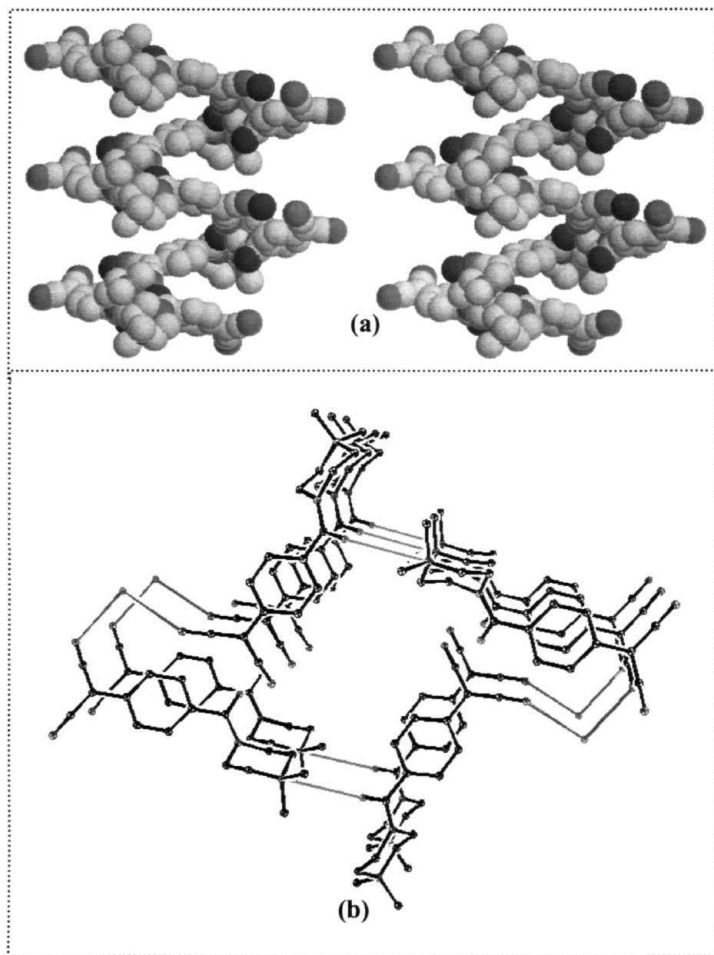
Figure 3.16 *M-helical* assembly in *19.H₂O* *crystal along the a axis formed through electrostatic and H-bond interactions : (a) stereo view perpendicular to the helical axis; space filling model with C (grey), N (blue) and O (red) atoms are shown; (b) view along the helical axis, the cyan and green lines indicate the electrostatic interactions and H-bonds respectively.*

as before. The significant observation in this crystal is that, once again helical supramolecular assemblies are formed along each of the crystallographic directions. Since H-bonding option does not exist now, all intermolecular contacts are based on electrostatic interactions and the considerably short distances indicate that these are likely to be strong. The supramolecular assemblies along the crystallographic *a, b* and *c* axes are formed through the C20...O10 (3.279 A), C18...O10 (3.069 A) and C7...N14 (3.261 A) contacts respectively (Figs. 3.17-3.19). The crystal structures of 19 with and without water molecule of crystallization demonstrate the persistent tendency of this molecule towards helical supramolecular organization. The extended lattice structure built through multiple noncovalent interactions including the strong electrostatic ones also appear to lead to the high melting point (~300°C) of crystals of 19.

Spontaneous resolution in the solid state of 19 and second harmonic generation study

Several cases of spontaneous resolution of achiral molecules through H-bonded assemblies are known.[3541] Spontaneous resolution has also been achieved through cocrystallization. In the crystals of 19, single component helical superstructures are formed from conformationally chiral zwitterionic molecules through electrostatic and H-bond interactions. The inherent homochirality of the orthogonal helical assemblies lays the basis for the spontaneous resolution.

Reflectance spectra of 19 were recorded in the form of KBr pellets (~ 0.1-0.2 mg microcrystals ground with 80-100 mg of KBr were pressed into pellets) and converted to the absorption profile using the Kubelka-Munk function. Since large single crystals were difficult to grow, we have attempted to measure the CD of small single crystals by grinding with KBr and forming solid pellets. As reported earlier,[43] considerable optimization of conditions was required. A single crystal weighing ~ 0.5 - 1.5 mg was ground with 80 - 100 mg of KBr in an agate mortar and pressed into pellets using a pressure of ~10 ton in a standard press. The pellets were typically 0.5 - 0.6 mm thick. The circular dichroism (CD) spectra were recorded (instrumentation details are provided in Appendix A) by employing a band width of 2 nm and were smoothed using standard smoothing functions. After several attempts with many crystals we were able to obtain
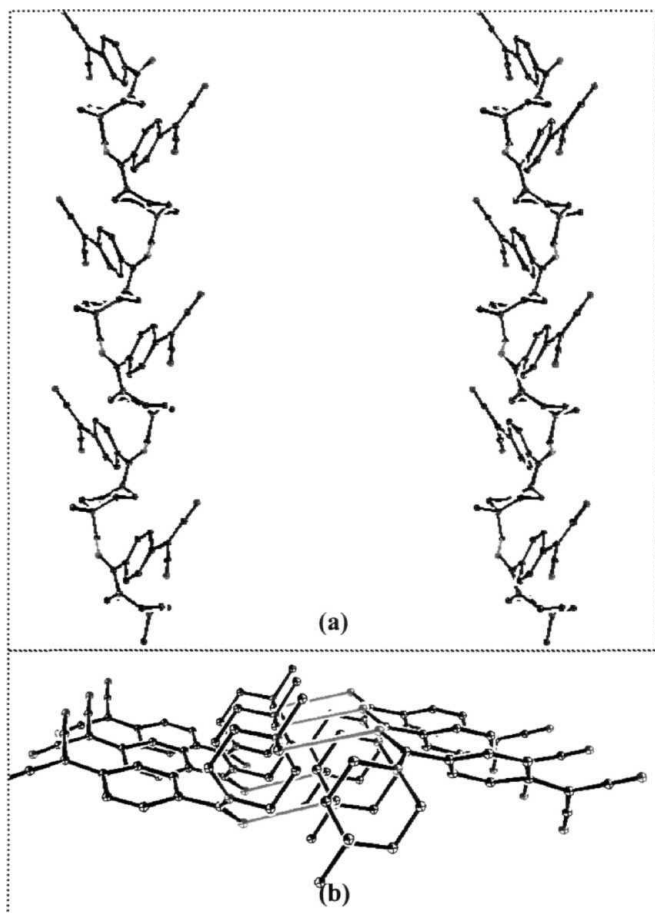
Figure 3.17 *M-helical assembly in 19 crystal along the a axis; the electrostatic interactions (cyan) are indicated : (a) stereo view perpendicular to the helical axis; (b) view along the helical axis. C (black), N (blue) and O (red) atoms are shown.*
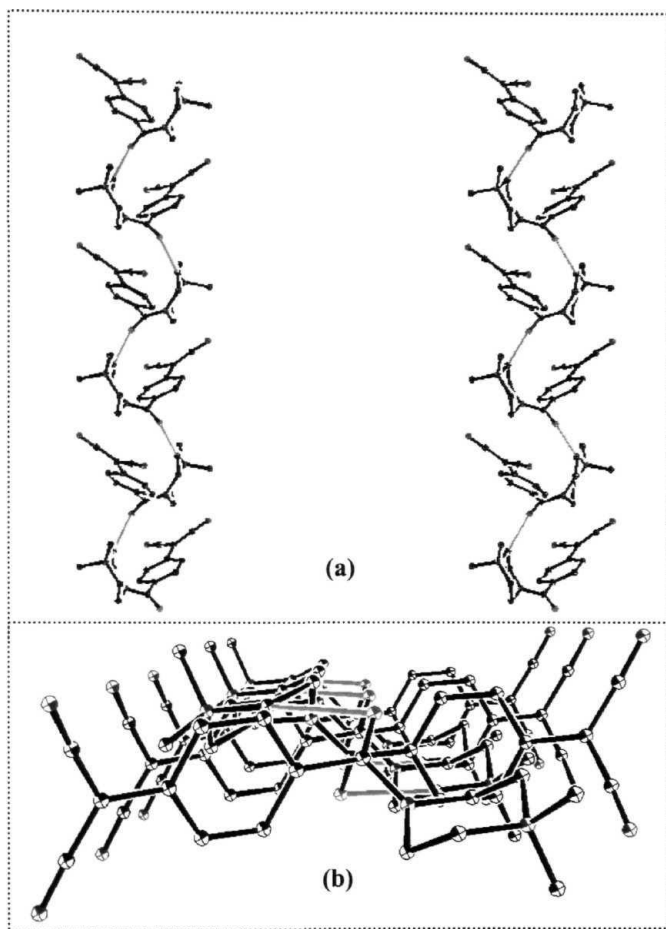
Figure 3.18 *M-helical* assembly in 19 crystal along the b axis; the electrostatic interactions (cyan) are indicated : (a) stereo view perpendicular to the helical axis; (b) view along the helical axis. C (black), N (blue) and O (red) atoms are shown.
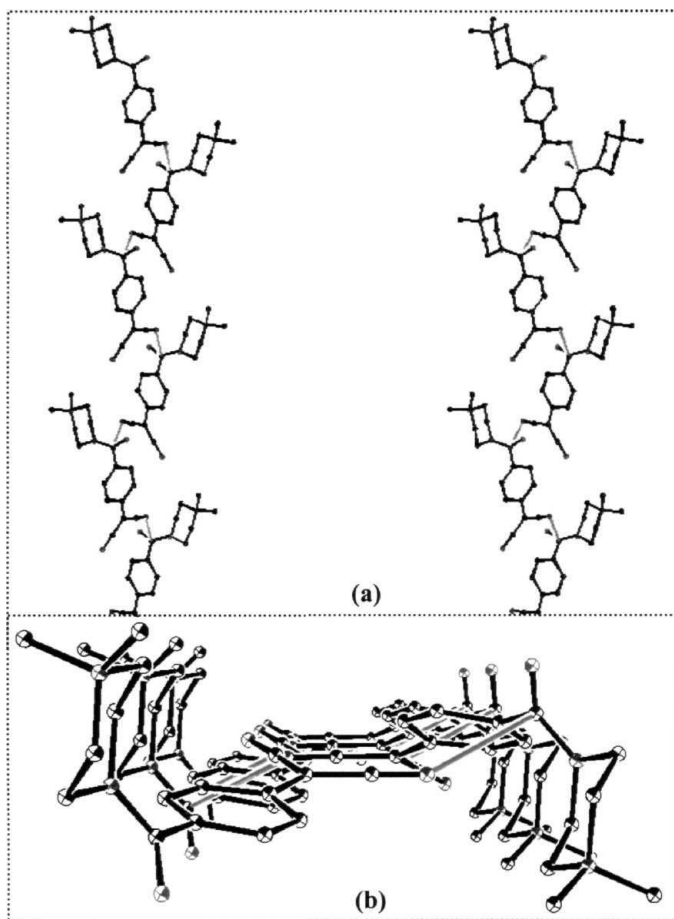
Figure 3.19   *M-helical assembly in **19** crystal along the c axis; **the** electrostatic interactions (cyan) are indicated : (a) stereo view perpendicular to the helical axis; (b) view along the helical axis. C (black), N (blue) and O (red) atoms are shown.*

spectra showing a negative CD. Fig. 3.20 shows the CD spectrum along with the absorption profile; the molar ellipticity is calculated as reported in Ref. 43. In spite of extensive efforts, the spectrum of the enantiomorphous crystal showing positive CD has proved elusive so far. We have also carried out CD spectral measurements on solutions made from single crystals of **19.H$_2$O** in DMSO; each sample was prepared from one single crystal. The spectra recorded at room temperature were very noisy, however a negative CD could be clearly discerned, suggesting that the chiral structure is at least partially preserved in solution. When the solution was heated and maintained at 105°C for 24 h, and then cooled back to room temperature the CD disappears completely, indicating the racemization of **19.**
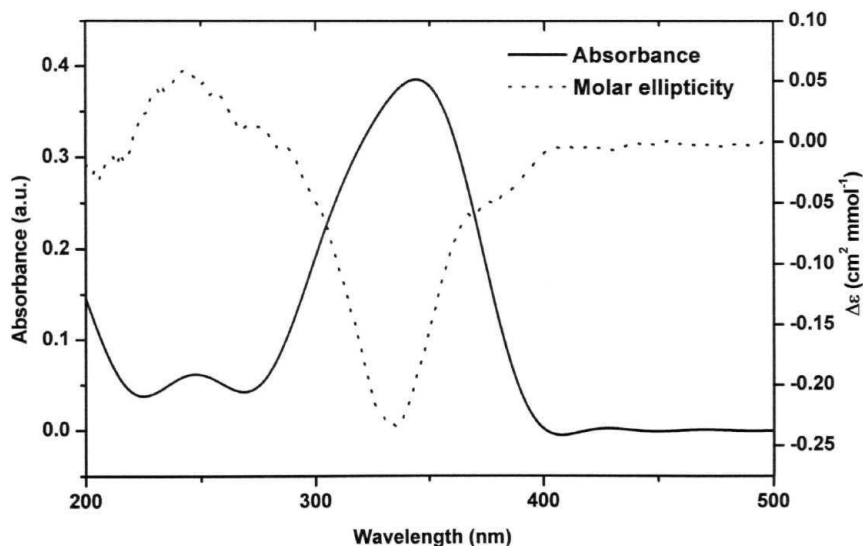
Figure 3.20 *The electronic absorption and circular dichroism spectra of* **19.H$_2$O** *single crystal ground with KBr and fabricated in* **the** *form of pellet.*

AM1/TDHF computation indicates that 19 has an appreciable first order hyperpolarizability; the static β is calculated to be 51.9 esu. Therefore the **noncentrosymmetric** material is expected to show **SHG** in the solid state. Kurtz-Perry[25] measurements (details are provided in Appendix C) on microcrystalline samples show a moderate value, 2 - 3 times that of urea (Table 3.9). The particle size dependence of the SHG indicates **phase-matchable** behavior.

Table 3.9 *SHG of microcrystalline powder of* **19.H₂O** *at various particle sizes. 1 U = SHG of urea having particle size > 150 μm.*

Particle size (urn)	SHG/U
< 100	2.1
100-150	2.0
150-200	2.5
200-250	2.4
250-300	2.0
>300	2.0

3.4   SUMMARY

In this chapter, we have presented the investigations of novel nonlinear optical molecular materials based on DADQ's fabricated through simple synthetic strategies. In Sec. 3.2 we have presented the structural characterization and solid state SHG of the complex of a remote functionalized DADQ molecule. The critical role of (i) the flexible pendant groups with 'sticky ends' and (ii) the **complexation** partner, in directing the assembly of the NLO chromophore is brought out by the parallel solid state structural investigations of the DADQ molecule and its complex. This exercise demonstrates a simple chemical synthetic approach to the modification of crystal architecture using remote functionalities. This approach can be extended to the use of these remote

functionalities to attach the NLO chromophore to a variety of template structures to design desired chromophore orientations and assemblies.

In Sec. 3.3 we have described the discovery of a new derivative from a DADQ molecule. The new molecule is conformationally chiral, and possesses an unusual zwitterionic structure. Semiempirical computational modeling of the 'molecule-in-the-crystal' reveals the presence of enhanced charges on several atoms which together with the H-bond functionalities present on the molecule lead to multiple and relatively strong intermolecular interactions. The low symmetry of the twisted molecule coupled with the extended noncovalent interactions lead to the formation of helical superstructures along orthogonal crystallographic directions. The homochirality associated with the orthogonal helical assemblies leads to the spontaneous resolution in the crystalline state as well as moderate SHG capability. This molecule should serve as a prototype to guide novel strategies that exploit a wide spectrum of molecular level interactions to achieve chiral supramolecular assemblies.

REFERENCES

1. (a) Günter, P. *Nonlinear Optical Effects and Materials, Springer Series in Optical Sciences, Vol. 72,* Springer-Verlag, Heidelberg, 2000; (b) Wolff, J. J.; Wortmann, R. *Adv. Phys. Org. Chem.* **1999,** *32,* 121; (c) Prasad, P. N.; Williams, D. J. *Introduction to Nonlinear Optical Effects in Molecules and Polymers,* John Wiley: New York, 1991.

2. (a) *Nonlinear Optical Properties of Organic Molecules and Crystals,* D. S. Chemla and J. Zyss, (Eds.) *Vol. 1,* Academic Press: New York, 1987; (b) Nie, W. *Adv. Mater.* **1993,** J, 520; (c) Kanis, D. R.; Ratner , M. A.; Marks, T. J. *Chem. Rev.* **1994,** *94,* 195; (d) Marks ,T. J.; Ratner, M. A. *Angew. Chem. Int. Ed. Engl.* **1995,** *34,* 155; (e) Zyss, J.; Nicoud, J. F. *Curr. Opin. Solid State Mater. Sci.* **1996,** 7,533.

3. (a) Ravi, M. *Ph. D. Thesis,* University of Hyderabad, 1997; (b) Gangopadhyay, P. *Ph. D. Thesis,* University of Hyderabad, 2002.

4. (a) Gangopadhyay, P.; Sharma, S.; Rao, A. J; Rao, D. N.; Cohen, S.; Agranat, I. Radhakrishnan, T. P. *Chem. Mater.* **1999**, *11*, 466; (b) Gangopadhyay, P.; Rao, S. V.; Rao, D. N.; Radhakrishnan, T. P. *J. Mater. Chem.* **1999,** *9,* 1699; (c) Sharma, S.; Radhakrishnan, T. P. *Mol.Cryst. Liq. Cryst.* **2000,** *338,* 257.

5. Gangopadhyay, P.; Radhakrishnan, T. P. *Chem. Mater.* **2000**, *12*, 3362.

6. Gangopadhyay, P.; Radhakrishnan, T. P. *Angew. Chem. Int. Ed.* **2001,** *40,* 2451.

7. (a) Wong, M. S.; Pan, F.; Bosch, M.; Spreiter, R.; Bosshard, C; Gunter, P.; Gramlich, V. *J. Opt. Soc. Am. B* **1998**, *15*, 426; (b) Marder, S. R.; Perry, J. W. Schaefer, W. P. *Science* **1989,** *245,* 626.

8. Jayanty, S.; Radhakrishnan, T. P. *J. Mater. Chem.* **2002**, *12*, 2792.

9. Jayanty, S.; Radhakrishnan, T. P. *{Submitted).*

10. (a) Geib. S. J.; Vicent C; Fan, E.; Hamilton, A. D. *Angew. Chem. Int. Ed. Engl.* **1993,** *32,* 119; (b) Harris, K. D. M. *Chem. Soc. Rev.* **1997,** *26,* 279; (c) Norsten, T. B.; McDonald, R.; Branda, N. R. *Chem. Commun.* **1999,** 719; (d) Koe, J. R.; Fujiki, M.; Motonaga, M.; Nakashima, H. *Chem. Commun.* **2000,** 389; (e) Hirschberg, J. H. K. K.; Brunsveld, L.; Ramzi, A.; Vekemans, J. A. J. M.; Sijbesma, R. P.; Meijer, E. W. *Nature* **2000,** *407,* 167.

11. (a) Lalama, S. J.; Singer, K. D.; Garito, A. F.; Desai, K. N. *Appl. Phys. Lett.* **1981,** *39,* 940; (b) Szablewski, M.; Thomas, P. R.; Thornton, A.; Bloor, D.; Cross, G. H.; Cole, J. M.; Howard, J. A. K.; Malagoli, M.; Meyers, F.; Bredas, J.; Wenseleers, W.; Goovaerts, E. *J. Am. Chem. Soc.* **1997,** *119,* 3144; (c) Hackman, N. A.; Bloor, D.; Cross, G. H.; Ravi, M.; Szablewski, M; Ledoux, I.; Deveau, S.; Zyss, J. *SPIE Proc.* **2000,** *4106,* 154.

12. Ravi, M.; Radhakrishnan, T. P. *J. Phys. Chem.* **1995,** *99,* 17624.

13. Gangopadhyay, P.; Ravi, M.; Radhakrishnan, T. P. *Ind. J. Chem.* **2000,** *A39,* 106.

14. (a) Ashwell, G. J.; Dawnay, E. J. C; Kuczynski, A. P.; Szablewski, M.; Bryce, M. R.; Grainger, A. M.; Hasan, M. *J. Chem. Soc. Farad. Trans.* **1990,** *86,* 1117; (b) Ashwell, G. J.; Dawnay, E. J. C; Kuczynski, A. P.; Lynch, D. E.; Yu, G.; Bucknall, D. G. *J. Mater. Chem.* **1995,** *5,* 975.

15. (a) Martin, A. S.; Sambles, J. R.; Ashwell, G. J. *Phys. Rev. Lett.* **1993,** *70,* 218; (b) Metzger, R. M. *Acc. Chem. Res.* **1999,** *32,* 950.

16. Jayanty, S.; Radhakrishnan, T. P. *Chem. Mater.* **2001,** *13,* 2460.

17. Jayanty, S.; Radhakrishnan, T. P. *Chem. Mater.* **2001,** *13,* 2072.

18. (a) Ravi, M.; Rao, D. N.; Cohen, S.; Agranat, I.; Radhakrishnan, T. P. *J. Mater. Chem.* **1996,** *6,* 1853; (b) Ravi, M.; Rao, D. N.; Cohen, S.; Agranat, I.; Radhakrishnan, T. P. *Struct. Chem.* **1996,** 7, 225.

19. (a) Ravi, M.; Rao, D. N.; Cohen, S.; Agranat, I.; Radhakrishnan, T. P. *J. Mater. Chem.* **1996,** *6,* 1119; (b) Ravi, M.; Rao, D. N.; Cohen, S.; Agranat, I.; Radhakrishnan, T. P. *Chem. Mater.* **1997,** *9,* 830; (c) Ravi, M.; Gangopadhyay, P.; Rao, D. N.; Cohen, S.; Agranat, I.; Radhakrishnan, T. P. *Chem. Mater.* **1998,** *10,* 2371.

20. Hertler, L. R.; Hartzler, H. D.; Acker and, D. S.; Benson, R. E. *J. Am. Chem. Soc.* **1962,** *84,* 3387.

21. Kagawa, Y.; Szablewski, M.; Ravi, M.; Hackman, N.; Cross, G. H.; Bloor, D.; Batsanov, A. S.; Howard, J. A. K. *Nonlin. Optics.* **1999,** *22,* 235.

22. (a) Gopalan, R. S.; Kulkarni, G. V.; Ravi, M.; Rao, C. N. R. *New. J. Chem.* **2001,** *25,* 1108; (b) Cole, J. M.; Copley, R. C. B.; McIntyre, G. J.; Howard, J. A. K.; Szablewski, M.; Cross, G. H. *Phys. Rev. B* **2002,** *65,* 125107.

23. (a) Dewar, M. J. S.; Zoebisch, E. G.; Healy, E. F.; Stewart, J. J. P. *J. Am. Chem. Soc.* **1985,** 707, 3902; (b) Dupuis, M.; Karna, S. *J. Comput. Chem.* **1991,** *12,* 487; (c) MOPAC93 © Fujitsu Inc.

24. Zyss, J.; Oudar, J. L. *Phys. Rev. A* **1982,** *26,* 2028.

25. Kurtz, S. K.; Perry, T. T. *J. Appl. Phys.* **1968,** *39,* 3798.

26. (a) Collins, S. K.; Yap, G. P. A.; Fallis, A. G. *Org. Lett.* **2000,** 2, 3189; (b) Li, C. Y.; Jin, **S.;** Weng, X.; Ge, J. J.; Zhang, D.; Bai, F.; Harris, F. W.; Cheng, S. Z. D.; Yan, D.; He, T.; Lotz, B.; Chien, L.-C. *Macromolecules* **2002,** *35,* 5475; (c) Yoshiba, K.; Teramoto, A.; Nakamura, N.; Sato, T. *Macromolecules* **2003,** *36,* 2108.

27. (a) Kauranen, M; Verbiest, T.; Boutton, C; Teerenstra, M. N.; Clays, K.; Schouten, A. J.; Nolte, R. J. M.; Persoons, A. *Science* **1995,** *270,* 966; (b) Deussen, H. -J.; Hendrickx, E.; Boutton, C; Krog, D.; Clays, K.; Bechgaard, K.; Persoons, A.; Bjørnholm, T. *J. Am. Chem. Soc.* **1996,** *118,* 6841; (c) Clays, K.; Hendrickx, E.; Verbiest, T.; Persoons, A. *Adv. Mater.* **1998,** *10,* 643; (d) Verbiest, T.; Elshocht, S. V.; Kauranen, M.; Hellemans, L.; Snauwaert, J.; Nuckolls, C; Katz, T. J.; Persoons, A. *Science* **1998,** *282,* 913; (e) Panda, M.; Chandrasekhar, J. *J. Am. Chem. Soc.* **1998,** *120,* 13517; (f) Elshocht, S. V.; Verbiest, T.; Kauranen, M.; Ma, L.; Cheng, H.; Musick, K. Y.; Pu, L.; Persoons, A. *Chem. Phys. Lett.* **1999,** *309,* 315.

28. (a) Abrahams, B. F.; Batten, S. R.; Hamit, H.; Hoskins, B. F.; Robson, R. *Chem. Commun.* **1996,** 1313; (b) Piguet, C; Bernardinelli, G.; Hopfgartner, G. *Chem. Rev.* **1997,** *97,* 2005; (c) Aspinall, H. C; Bickley, J. F.; Dwyer, J. L. M.; Greeves, N.; Steiner, A. *Angew. Chem. Int. Ed* **2000,** *39,* 2858.

29. (a) Bassani, D. M; Lehn, J.-M.; Baum, G.; Fenske, D. *Angew. Chem. Int. Ed. Engl.* **1997,** *36,* 1845; (b) Rowan, A. E.; Nolte, R. J. M. *Angew Chem. Int. Ed.* **1998,** *37,* 63.

30. Addadi, L.; Lahav, M. in *Origins of Optical Activity in Nature,* Walker, D. C. (Ed.), Elsevier, Amsterdam, 1979; (b) Gardner, M. *The New Ambidextrous Universe: Symmetry and Asymmetry, from Mirror Reflections to Superstrings,* W.H. Freeman and Company, New York, 1990.

31. (a) Sanders, C. J.; Gillespie, K. M.; Bell, D.; Scott, P. *J. Am. Chem. Soc.* **2000,** *122,* 7132; (b) Berkessel, A.; Gasch, N.; Glaubitz, K.; Koch, C. *Org. Lett.* **2001,**

3, 3839; (c) Huang, Y.; Iwama, T.; Rawal, V. H. *J. Am. Chem. Soc.* **2002,***124,* 5950; (d) Sato, I.; Kadowaki, K.; Urabe, H.; Jung, J. H.; Ono, Y.; Shinkai, S.; Soai, K. *Tetrahedron Lett.* **2003,** *44,* 721; (e) Sakamoto, M; Iwamoto, T.; Nono, N.; Ando, M.; Arai, W.; Mino, T.; Fujita, T. *J. Org. Chem.* **2003,** *68,* 942.

32. (a) Gong, B.; Zheng, C; Zeng, G.; Zhu, J. *J. Am. Chem. Soc.* **1999,***121,* 9766; (b) Gao, E.; Bai, S.; Wang, Z.; Yan, C. *J. Am. Chem. Soc,* **2003,** *125,* 4984.

33. Agranat, I.; Perlmutter-Hayman, B.; Tapuhi, Y. *Nouv. J. Chim.* **1978,** *2,* 183.

34. L. Addadi, M. Geva, *Cryst. Eng. Comm.* **2003,** *5,* 140.

35. Perez-Garcia, L.; Amabilino, D. B. *Chem. Soc. Rev.* **2002,** *31,* 342.

36. The term 'atropisomers' could be used to describe such structures (E. L. Eliel, S. H. Wilen, L. N. Mander, *Stereochemistry of Organic Compounds,* John Wiley, 1994). However, we prefer the term 'conformationally chiral' since it clarifies the chiral nature and its structural origin. Profs. E. L. Eliel and K. Mislow also concur that this terminology is quite appropriate (personal communications).

37. (a) Pincock, R. E.; Perkins, R. R.; Ma, A. S.; Wilson, K. R. *Science* **1971**, *174,* 1018; (b) Wilson, K. R.; Pincock, R. E. *J. Am. Chem. Soc.* **1975,** *97,* 1474.

38. Jayanty, S.; Radhakrishnan, T. P. *Chem. Eur. J.* (in press).

39. Klamt, A.; Shuurmann, G. *Perkin Trans. 2* **1993,** 799.

40. Gangopadhyay, P.; Rao, D. N.; Agranat, I.; Radhakrishnan, T. P. *Enantiomer* **2002,** 7, 119.

41. (a) Kinbara, K.; Hashimoto, Y.; Sukegawa, M.; Nohira, K.; Saigo, K. *J. Am. Chem. Soc.* **1996**, *118,* 3441; (b) K. Kinbara, Y. Tagawa, K. Saigo, *Tetrahedron : Asymm.* **2001**, *12,* 2927.

42. Koshima, H. *J. Mol. Struct.* **2000,** *552,* 111.

43. Minguet, M.; Amabilino, D. B.; Wurst, K.; Veciana, J. *J. Chem. Soc. Perkin 2* **2001**, 670.

CHAPTER 4

Semiconducting Materials Based on
Polyelectrolyte Templated Polyaniline and
Tetrathiafulvalene

Papers published

- Jayanty, S.; Prasad, G. K.; Sreedhar, B.; Radhakrishnan, T. P. *Polymer* (*in press)*. Polyelectrolyte Templated Polyaniline - Film Morphology and Conductivity.

- Jayanty, S.; Radhakrishnan, T. P. *J. Mater. Chem.* 1999, *9,* 1707. 'Core and Sheath' Structure of a TTF Complex Forming a Square Grid.

4.1   INTRODUCTION

Several classes of organic charge transfer complexes, ion-radical salts and conjugated polymers have been investigated which show electrical properties ranging from semiconductivity to superconductivity.[1]   In Sec. 1.4 we have briefly discussed various classes of conducting materials and the properties exhibited by them. Polymer systems[1,2] with special properties constitute a field of increasing scientific and technological interest offering synthetic chemists an opportunity to develop a broad variety of new materials.   In chapters 2 and 3 we have investigated several novel chromophores and NLO-phores with covalently attached but remote functionalities that strongly influence the molecular assembly.   This led to the discovery of a variety of interesting phenomena and the fabrication of novel optical and nonlinear optical materials. We have extended this logic to the control of molecular assembly through the utilization of template structures and the fabrication of semiconducting molecular and polymeric materials providing insight into the correlation of molecular organization and materials attributes. In this chapter we present our explorations in this direction leading to the fabrication of novel semiconducting molecular materials.

In Sec. 4.2 we explore a simple synthetic protocol for the development of stable aqueous colloidal solutions of poly(4-styrenesulfonate) templated polyaniline.   The electrical conductivity and submicro/nano features observed in their spin coated films are shown to be correlated to the polyelectrolyte template molecular weight.   This study demonstrates the utility of the polyelectrolyte template as a new design element for conducting polymer films.[3]

In Sec. 4.3 we present the synthesis and conductivity studies of a new class of molecular materials which incorporate tetrathiafulvalene (TTF) and polyionic polymers such as poly(4-styrenesulfonate), poly(vinylsulfate) and poly(4-styrenesulfonate-*co*-maleic acid). Enhancement of the conductivity by $\sim 10^2$ -10^4 over the starting TTF salt was observed in these new materials. We present also the interesting crystal structure of the pentacarbomethoxycyclopentadienide (PMC) salt of TTF. This complex is found to have an unusual 2-dimensional structure wherein trimerized segregated stacks of TTF run in orthogonal directions forming a square grid. The counterions form a sheath structure

around the core made up of the TTF stacks. Single crystal conductivity studies reveal anisotropic character consistent with the TTF organization.[4]

4.2   POLYELECTROLYTE TEMPLATED POLYANILINE - FILM MORPHOLOGY AND CONDUCTIVITY

Polyaniline (PANI) is one of the most extensively studied materials among the conducting polymers. The reasons for this are manifold. Synthesis of PANI is simple and facile, through chemical as well as electrochemical means,[5"9] and the polymer shows a high degree of chemical stability. It is conveniently doped using protons to achieve a wide range of optical characteristics and conductivities,[6-14] facilitating applications ranging from sensors to smart windows.[6,7] Recently PANI and its composites have been shown to exhibit several submicro and nano architectures[2,3"16] which have significant impact on the materials attributes. The basic problems of solubility and processability of PANI have been addressed through approaches such as self-doping,[10,12,17] choice of different counterions[15,16,18] and templating.[12,19-22] The latter technique employing polyelectrolytes is particularly successful in improving aqueous solubility and hence is significant from the point of view of environmental considerations and processing methodology. It has been suggested that polyelectrolytes serve as nanoreactors during the enzymatic oxidative polymerization of aniline.[21] It is of considerable interest to establish correlations between features of the polyelectrolyte template and the electrical conductivity of the film so that new design strategies can be evolved.

We have developed a simple and convenient protocol for the synthesis of poly(4-styrenesulfonate) (PSS) templated PANI (along similar lines as reported in Ref. 23) and the fabrication of good quality films by adding trace amounts of polyvinyl alcohol (PVA). Interestingly, the electrical conductivity of the films is found to depend on the template molecular weight. Scanning electron microscopic examination of the films reveals submicro and nano level features which depend on the molecular weight of the PSS used and the amount of the PVA additive, providing insight into the morphology dependence of the electrical conductivity. Many of the microscopic characterizations of

soluble PANI in earlier work were on the colloidal state[22,24] or on bulk powders.[15,25] We have focussed attention on the films which would be of direct relevance to most of the practical applications. Our study highlights the role of the template molecular weight as a design element in the fabrication of conducting PANI.

*Synthesis **and** characterization*

PANI-PSS was synthesized in aqueous solution by the oxidative polymerization of aniline using ammonium peroxodisulfate and hydrochloric acid in presence of poly(sodium 4-styrenesulfonate) (NaPSS). NaPSS with average molecular weights, 100 kDa and 70 kDa were used; the resulting polymers will be denoted respectively as PANI-PSS-100 and PANI-PSS-70. The lOOkDa polymer was obtained from Acros Organics and the 70kDa polymer from Aldrich Chemical Co. Aniline was distilled twice under reduced pressure. Millipore Milli-Q water (resistance = 18 MΩ) was used in all preparations. 0.42 ml (4.6 mmol) aniline was added to 15 ml of 3M hydrochloric acid. 2.78 g (13.5 mmol of monomer) of NaPSS dissolved in 13 ml of water was added with continuous stirring over 10-15 min. The entire solution was cooled to 0 - 5°C and 1.02 g (4.4 mmol) of ammonium peroxodisulfate dissolved in 8 ml of water was added dropwise over 20 - 30 min. The solution was stirred for 2.5 h to complete the polymerization. The final solution diluted with water (total weight = 43 g) was subjected to dialysis (dialysis bags with 50 kDa cut-off were boiled with EDTA and NaHCO$_3$ prior to use) with aqueous HC1 (pH = 4) changed every 20 min, three times. The dialyzed colloidal solution (weight = 48 g) was centrifuged for 90 - 120 min with the supernatant water removed and replaced with fresh water three times during this period. 17 g of the colloid was diluted by adding 10 ml of water and sonicated for 15 min. 7 g of the resulting solution was mixed with different weights (0.032, 0.064, 0.096, 0.128 g) of aqueous solutions of PVA (1.13 g PVA dissolved in 10 ml water).

Samples in the form of KBr pellets were made from vacuum dried PANI-PSS for FT-IR spectra. The spectra of PANI-PSS-100 and PANI-PSS-70 are similar. The peaks at 1561 and 1487 cm^{-1} are characteristic of the C=C stretching vibration of the quinonoid and benzenoid rings respectively. The bands at 1294 and 1238 cm^{-1} correspond to C-H

bending vibrations. These peaks are similar to those reported earlier.[12] The PANI produced in our synthesis protocol is in the emeraldine salt form. UV-Vis spectra of the PANI-PSS show, besides the 355 run and 418 run peaks, the polaron absorptions. The polaronic bands of the colloidal solutions and spin coated films of PANI-PSS-70 show peaks at 783 nm and 706 nm respectively. Addition of PVA has no effect on the former, but causes a further blue shift to 693 nm in the latter. The blue shift observed on film formation possibly arises due to the rigidification of the polymer chains restricting polaron delocalization to smaller segments, which is further enhanced in the film containing PVA. PANI-PSS-100 similarly shows the band maxima at 820 nm and 722 nm respectively in the colloidal solution and film. Once again, PVA addition causes a shift in the film alone, with the peak observed at 694 nm. The red shift observed for the solution and film of PANI-PSS-100 (with respect to PANI-PSS-70) signifies relatively longer conjugated segments with less kinks and defects, most likely facilitated by the formation of longer PANI chains. At present we cannot confirm this through the determination of the PANI molecular weight which is complicated due to the coexistence of the strongly bound polyionic chains in PANI-PSS.[19]

X-ray photoelectron spectroscopy

Powder samples of PANI-PSS can be obtained by precipitation on addition of acetone or methanol to the colloidal solution or by removal of the water under dynamic vacuum. The dried powder compactions were characterized by XPS analysis. The instrumentation details are provided in Appendix A and the significant data are presented in Table 4.1. The N(1s) peak is normally deconvoluted into three, with the lowest one at ~ 399.5 eV assigned to neutral amine/imine sites and the higher ones at > 400 eV assigned to protonated N, their exact identities still being a matter of discussion.[10,20] We have deconvoluted the N(1s) peak into two, representing the unprotonated and protonated states (Fig. 4.1); the relative intensities indicate the extent of protonation of PANI in PANI-PSS-100 and PANI-PSS-70 to be respectively 0.64 and 0.54. The relatively high values suggest protonation of the imine as well as amine N sites, promoted possibly by the polymeric sulfonic acid template formed from the PSS in the acid medium; it may be noted that even higher protonation levels have been reported for polyaniline-

Table 4.1 *Selected XPS data for PANI-PSS films.*

Sample	Peak/eV [atom %]				Protonation level of N	Atom % $SO_3^-H^+$
	S	N	NH^+	Na		
PANI-PSS-100	168.37 [8.20]	399.06 [0.93]	401.02 [1.66]	1071.23 [4.70]	0.64	1.84
PANI-PSS-70	168.04 [7.40]	399.43 [1.50]	401.42 [1.72]	1071.04 [3.44]	0.54	2.24

polyelectrolyte complexes.[20] The XPS analysis rules out the presence of Cl but indicates that Na is present in PANI-PSS, implying that SO_3^- groups on the PSS chains are associated with H^+, NH^+ and Na^+. The composition of $SO_3^-H^+$ ($x_{SO_3^-H^+}$) can be inferred from the atomic percentages of sulfur (x_S), all of which exists in the form of SO3", protonated nitrogen (x_{NH}^+) and sodium ions (x_{Na}^+), by imposing the charge balance, $x_S = (x_{SO_3^-H^+} + x_{NH^+} + x_{Na^+})$; the values are presented in Table 4.1. Based on this, the relative amounts of the amine and sulfonate groups in the protonated state *ie.* $x_{NH}^+/x_{SO_3^-H^+}$ can be estimated. Interestingly this ratio appears to be quite similar (~ 0.8 - 0.9) in the two polymer samples indicating that the same equilibrium controls the proton distribution in both.

Thin film fabrication and conductivity

The polymer films were fabricated by spin coating on glass plates or pieces of aluminum foil. The glass plates were cleaned with detergent followed by high purity water and *iso*-propyl alcohol and dried in a hot air oven at 90°C. 1 cm^2 pieces of aluminum foils were cleaned by rubbing with acetone and dried in hot air oven. Typical spinning speeds and times employed for the spin coating were 2000 rpm and 30 sec. Films of PANI-PSS were fabricated using the colloidal solutions directly or after mixing with small amounts of aqueous PVA solution. Four different blends were prepared

(a)

(b)
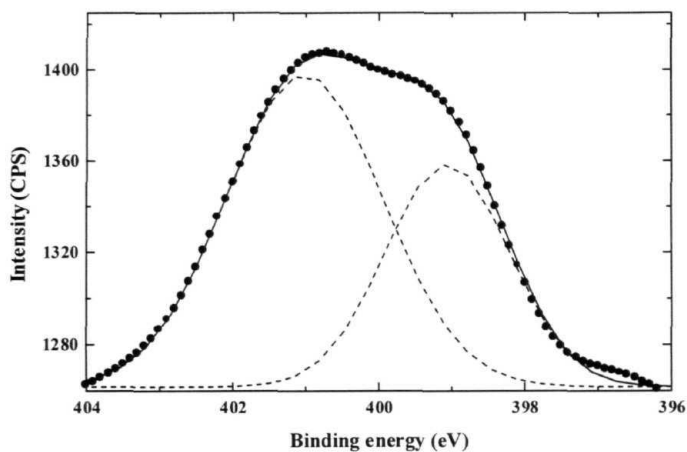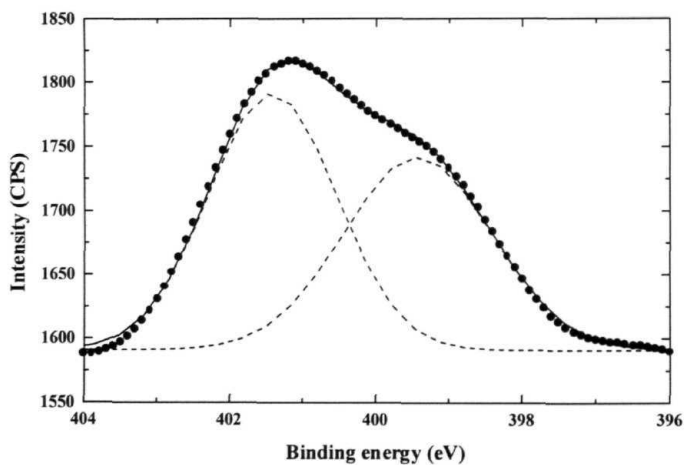
Figure 4.1 *The N(ls) peaks in the XPS spectrum of (a) PANI-PSS-100 and (b) PANI-PSS-70; the smoothed experimental data (•), the fit using multiple Gaussian functions (———) and the deconvolution (-—-) are shown.*

containing 0.046, 0.092, 0.138 and 0.184 weight % of PVA. The PVA addition makes the colloids stable for several months. The colloids are spin coated to form films. PANI-PSS without PVA additive does not coat well beyond a single layer. Interestingly, addition of the trace amount ($\sim$ 0.05 weight %) of PVA vastly improves the film quality and facilitates fabrication of multiple coatings. The coated films were dried under dynamic vacuum for 10 h and then in a hot air oven at 80°C for 1 h before conductivity measurements or SEM study discussed later. The films are quite uniform, as revealed by the smooth scaling of the film thickness (determined by viewing the film cross section in an SEM) with the number of layers coated. We find that the average thickness of a single layer is $\sim$ 270 nm.

PANI-PSS without any PVA additive where only single layers could be coated, showed high resistance; therefore conductivity could not be measured reliably. However, 4-probe conductivity measurements (details are given in Appendix D) could be carried out on thicker films (15 layers on glass) of PANI-PSS containing different amounts of PVA. The conductivity changes very little with the PVA composition in the case of PANI-PSS-100 and even less in PANI-PSS-70 (Table 4.2). This is primarily due to the fact that the quantity of PVA added is very small. It is also consistent with observations

Table 4.2 *4-probe room temperature conductivity of PANI-PSS films containing different amounts of PVA additive.*

Weight % of PVA	a ($10^{'2}$ S cm^{-1})	
	PANI-PSS-100	**PANI-PSS-70**
0.046	**8.3**	**4.5**
0.092	**8.3**	**3.6**
0.138	**9.1**	**3.6**
0.184	12.5	**3.7**

that conducting polymers manifest self-assembly leading to little interference to the conducting pathways from the electrically insulating additive.[921] The more significant observation presented in Table 4.2 is the sensitivity of the film conductivity to the molecular weight of the template polyelectrolyte; the higher molecular weight PSS leads to improved conductivity in the film. Together with the shift of the polaronic band with the molecular weight of the template noted earlier, this observation suggests that the polyelectrolyte acts as a nanoreactor template, controlling the polymerization process;[21] the longer PSS chains promote the formation of more extended and possibly better aligned PANI chains.

Scanning electron microscopy

We have examined the morphology of the films to gain insight into its influence on the conductivity. Though the morphological features are similar for films coated on glass and aluminum foil, the latter provided better clarity in general. Hence the micrographs presented are of films coated on aluminum foil substrates. Fig. 4.2 shows scanning electron micrographs of PANI-PSS-100. The influence of PVA addition is clearly visible. The morphology is nearly circular disc-like in the absence of PVA (Fig. 4.2a); the packing density is low since, as noted earlier, a single layer alone is coated. The shape resembles those observed in similar instances reported earlier[22] and the diameter is approximately 250 - 350 nm. It turns into a distinct rod shape when 0.09 weight % of PVA is added (Fig. 4.2c). At this stage the rods are typically 80 - 100 nm wide and 220 - 400 nm long. As the PVA content is increased the rod length goes up to ~ 1 urn with small increase in the average width (Fig. 4.2d). However the packing density is reduced at higher PVA content. The morphology of the PANI-PSS-70 are shown in Fig. 4.3. The trends with PVA addition are similar to those in the previous set, though less dramatic. More significantly the sizes of the different features are distinctly smaller. For example, the discs in Fig. 4.3a show average diameters in the range 30 - 60 nm and the rods in the case of films with 0.09 weight % of PVA (Fig. 4.3c) are typically 55 - 70 nm wide and 120 - 300 nm long. The former are slightly larger than the sizes reported earlier for PANI-PSS.[23] At the highest PVA content, a mixture of rods and discs are observed.
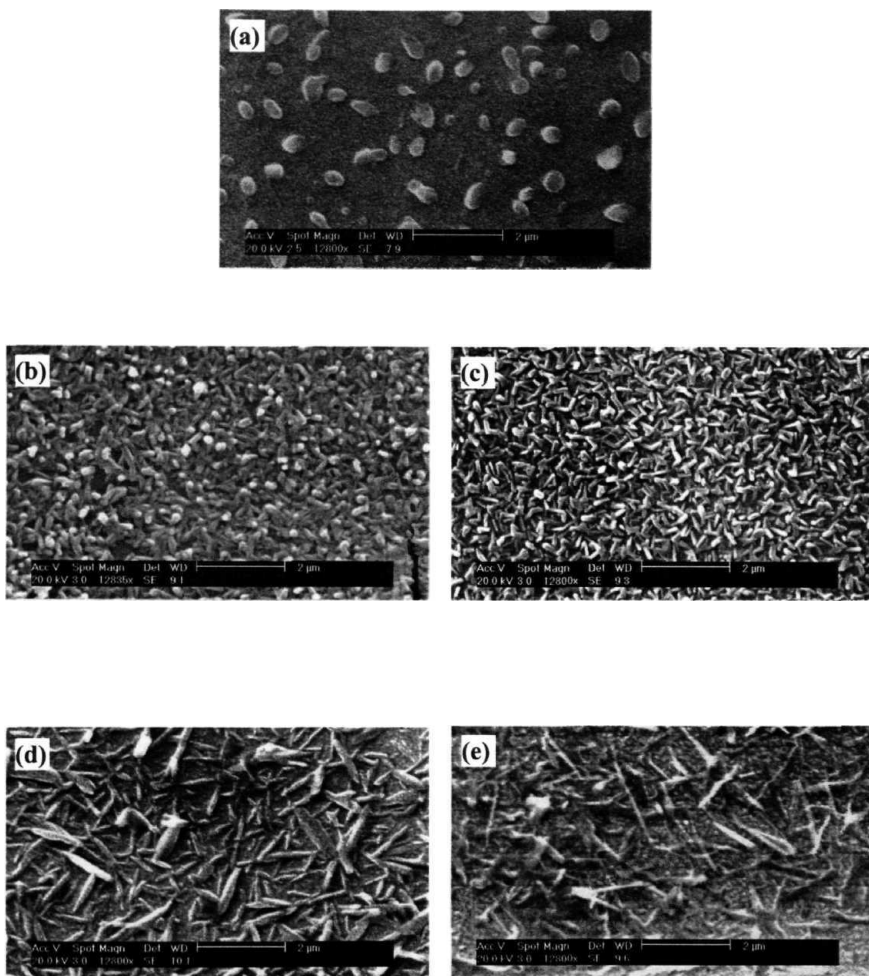
Figure 4.2 *Scanning electron micrographs of PANI-PSS-100 containing (a) 0.000, (b) 0.046, (c) 0.092, (d) 0.138 and (e) 0.184 weight % of PVA additive.*
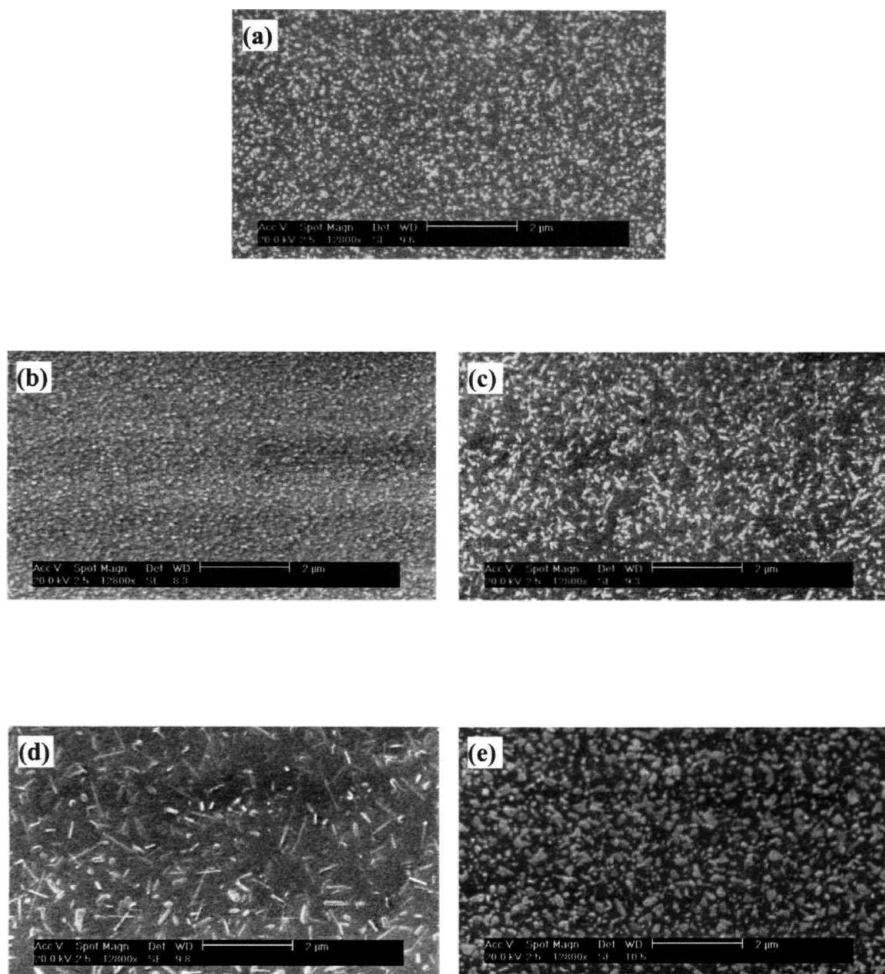
Figure 4.3 *Scanning electron micrographs of PANI-PSS-70 containing (a) 0.000, (b) 0.046, (c) 0.092, (d) 0.138 and (e) 0.184 weight % of PVA additive.*

It is instructive to analyze the possible role of PVA in the morphology changes and its impact on the conductivity of the **PANI-PSS** films. In view of its extremely small **mol** ratio with respect to PANI-PSS, PVA is likely to be engaged only in some surface level molecular interactions with PANI-PSS aggregates. Such a picture is consistent with its stabilizing influence on the PANI-PSS colloid and further suggests that the assembly of the aggregate structures observed in the spin-coated films may be initiated in the colloidal state itself. The H-bond interactions between PVA and PANI/PSS chains at the periphery of the aggregates, possibly promotes an organized assembly leading to the rod-like morphology which becomes more prominent with increasing PVA content. The conductivity does not show any strong dependence on the percentage of PVA, which may be understood in terms of the simultaneous increase in the size of particles and decrease in their packing density. The higher sensitivity of the conductivity in the case of PANI-PSS-100 compared to PANI-PSS-70 is consistent with the larger morphology changes in the former, noted above. Compared to PANI-PSS-70, the extent of protonation in PANI-PSS-100 deviates more from the optimal 0.50. In spite of this, the latter shows higher conductivity which appears to result from the larger size of the features observed in these films. We infer that the longer PSS chains promote the growth of more extended PANI chains, eventually leading to larger features in the spin coated films. The parallel observed between the thin film conductivity and morphological characteristics points to the relevance of the template polymer molecular weight as a design element for the PANI chains.

4.3 POLYELECTROLYTE TEMPLATED TETRATHIAFULVALENE (TTF) AND THE 'CORE AND SHEATH' STRUCTURE OF A TTF COMPLEX

Planar organic molecules possessing delocalized π-electrons with good electron donating or accepting capabilities are important candidates for molecular conducting materials. Several families of organic donors and acceptors have been developed over the last three decades, which form molecular conductors and superconductors. However the single largest family of organic conductors is still based on TTF, one of the earliest *n*-electron donors. Several excellent reviews may be consulted for the extensive work

published on the TTF family of complexes.[26]   The versatility of TTF stems primarily from its unique electronic and structural features such as the electron rich planar *n*-system, the stability of fractional oxidation states and the d-orbital electrons on the S atoms which enable interstack interactions.   One of the significant factors that has contributed to the singular success of the TTF framework in forming crystalline complexes is the strong tendency it shows towards the formation of stacked structures. Neutral TTF itself has a stacked structure and a second polymorph discovered some years ago has been found to have a chain structure.[27]   TTF forms charge transfer and ion-radical complexes with a wide variety of molecules and counterions.   The counterions used include simple inorganic anions such as halides,[28"0] nitrate[31] or thiocyanate,[32] transition metal complexes[33,34] and organometallics.[35,36]   Examination of the crystal structures of the TTF salts and complexes reveals a wide range of packing motifs with a predilection towards π-stacking.   The regular segregated stacked structure found in many systems[32,34,37"39] including the prototypical TTF-TCNQ[40] is most conducive to metallic conduction.   Effects such as Peierl's instability[41] often lead to dimerized[42,43] or trimerized[35,44,45] segregated stack structures; there is even an example with a pentamerized stack of TTF.[46]   Though uninteresting from the point of view of conducting materials, several TTF complexes show mixed stack structure incorporating the counterions in the TTF column.[47]   There exist also TTF complexes where isolated monomeric,[34,48] dimeric[36,49] or trimeric[50] TTF's are present.

A survey of these structural variations manifested by TTF complexes suggests that TTF based systems provide a fertile ground to explore novel stacking patterns. Strongly 1-dimensional structures are prone to low temperature instabilities such as Peierl's distortion that lead to metal-semiconductor transition.   From the point of view of stabilizing the metallic state in molecular conductors 2 and 3-dimensional structural motifs are important.   Several polymeric materials containing TTF have been synthesized and characterized.[51,52]   Among those which show high conductivity,[52,53] some are prepared by doping a polymer containing TTF with electron acceptor molecules and others involve the polymer itself as the electron acceptor.   Exploration of molecular and polymeric materials based on TTF complexes continues to be a fruitful exercise as they provide new approaches to highly conducting molecular materials.

Synthesis and conductivity studies of polyanion salts of tetrathiafulvalene

We have considered the synthesis of polymeric salts of TTF where TTF^+ is combined with polyanions. We envisaged that such systems would simultaneously develop an ordering of the polymer chains and stacking of TTF^+ ions. The inherent tendency of TTF and its ions to stack would encourage the polymer chain to order and the spacing of the charge sites on the polyanion in turn would control the interplanar distances in TTF stacks. Mixed valence systems can form if appropriate amounts of TTF and TTF^+ are incorporated in the stacks. We have utilized poly(4-styrenesulfonate) (PSS) in Secs. 2.4 and 4.2. In the following preliminary studies we have used PSS (with molecular weights 100 kDa and 70 kDa) as well as other polyanions such as poly(vinylsulfate) (PVS, MW = 170 kDa), 3:1 poly(styrene-*co*-maleic acid) (31PSSM, MW = 20 kDa) and 1:1 poly(styrene-*co*-maleic acid) (11PSSM, MW = 20 kDa) to form salts with TTF^+.

A typical synthesis proceeds as follows. $(TTF)_3(BF_4)_2$ was synthesized following reported procedure.[54] 0.1 gm (0.127 mmol) of $(TTF)_3(BF_4)_2$ was dissolved in distilled acetonitrile. A solution of 50 mg (0.231 mmol of monomer) of the sodium salt of PSS dissolved in 2 ml deaerated water was added to it. A brown colored precipitate separated out immediately. A tentative representation of the reaction is shown in Scheme 4.1. The product was filtered out washed with water and acetonitrile and dried under vacuum.
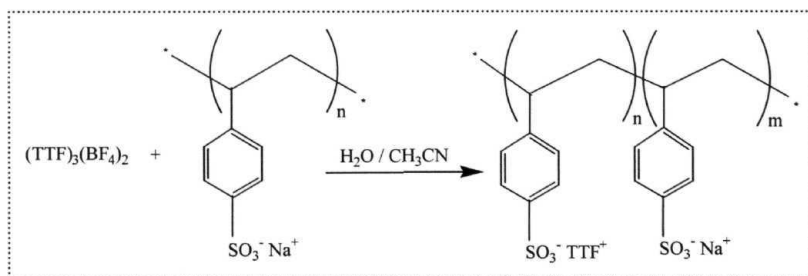
Scheme 4.1
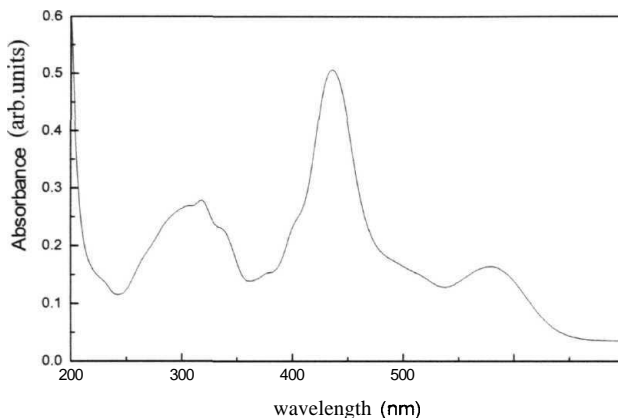
Figure 4.4 *Absorption spectrum of TTF-PSS-70.*

M.P. = 250-260°C (dec); FT-IR (KBr) : ν/cm^{-1} = 3418.1, 2926.3, 1352.2, 1122.6, 1032.0, 1005.0, 827.5. Fig. 4.4 shows the absorption spectrum of PSS salt of TTF (TTF-PSS-70). The spectrum shows the presence of neutral TTF (λ_{max} = 306 nm) as well as the cation, TTF$^+$ (λ_{max} = 581, 435, 340 nm). Similar results were obtained with the other polyanions mentioned above. We have made extensive efforts to obtain reproducible compositional analysis of the materials prepared. However no satisfactory consistency could be achieved in this regard. We believe that this may be due to the randomness in the final composition of the polyanion and alkali metal counterions which comes with the polyanion. We have carried out 2-probe resistivity measurements on powder compactions of the final TTF complexes (see Appendix D for details). The resistivities show good consistency between several batches which were measured. The values obtained for the different polyanion complexes are collected in Table 4.3. The consistent decrease of the resistivity of the TTF$^+$ complexes on incorporation of the polyanions points to the likelihood of improved stacking assembly of the TTF moiety in these materials.

Table 4.3 *Resistivity of various polyelectrolyte complexes of TTF.*

Complex	p (Ω cm)
$(TTF)_3(BF_4)_2$	10^7- 10^6
TTF-PSS-100	10^5
TTF-PSS-70	10^3- 10^2
TTF-PVS	10^4
TTF-31PSSM	10^4
TTF-11PSSM	10^4

Structure and conductivity of $(TTF)_3(PMC)_2$

$(TTF)_3(PMC)_2$ was synthesized as reported earlier.[55] We have characterized the elemental composition and crystal structure of this material.[4] Stoichiometeries like $(TTF)_3X_2$ with X being a monoanion ' and $(TTF)_3X$ with X being a dianion are well known among TTF complexes. The stoichiometry implies an average partial ionicity of +0.67 on TTF which leads to metallic conductivity in the case of $TTFCl_{0.67}$[28] and $TTF(SCN)_{0.67}$.[57] However, in several cases, trimerized TTF stacks are formed with concomitant localization of charge and reduced conductivity. The crystal structure analysis of $(TTF)_3(PMC)_2$ indicates that it belongs to the latter case. The crystallographic data are collected in Table 4.4. The C atoms were refined isotropically and only the S and O atoms were refined fully anisotropically in this structure. The asymmetric unit consists of three TTF molecules (Fig. 4.5a) and two PMC anions (Fig. 4.5b). The TTF molecules A and B almost eclipse each other and B and C are in the 'ring-over-bond' conformation. The molecules are nearly flat and parallel with average interplanar angle of 2.4° between A and B and 2.8° between B and C. The average interplanar distance between A and B is 3.435 A and that between B and C is 3.427 A; these distances are slightly shorter than the interplanar distance of 3.47 A in TTF-TCNQ.[40] The shortest S....S distances between A and B is 3.335 A and that between B and C is 3.659 A. The average interplanar distance between C and its neighboring A in the stack is 3.402 A. The three interplanar distances indicate that the stack deviates only slightly from a

Table 4.4 *Crystallographic data for (TTF)$_3$(PMC)$_2$.*

Compound	(TTF)$_3$(PMC)$_2$
Molecular Formula	C$_{48}$H$_{42}$O$_{20}$S$_{12}$
Formula Weight	1323.54
Crystal System	Monoclinic
Space group	Cc
a *Ik*	16.017(10)
b/A	14.307(12)
c/A	25.091(8)
a/deg	90.0
β / deg	92.11(3)
γ / deg	90.0
Z	4
μ / cm^{-1}	5.3
ρ$_{calc}$ / g cm$^{"3}$	1.530
ρ$_{meas}$ / g cm^{-3}	1.559
Number of independent reflections	5029
Number of reflections with I > 2σ$_I$	2562
Number of parameters	490
R	0.0514
wR^{2}	0.1247

regular segregated stacking motif; it is probably best described as a weakly alternating stack of C-A dimers and B (Fig. 4.6). The stacking clearly suggests the likelihood of localization of charge on the TTF molecules.

The TTF stacks form layers parallel to the *ab* plane. The stacks in one layer run along the [110] directions while the stacks in the adjacent layers run in an orthogonal direction, namely [1̄10] forming a square grid structure. PMC form columns running along the [110] and [1̄10] directions. The spacing between the mean planes of adjacent pentagons within the column is 10.738 A ruling out any kind of π-stacking. The PMC columns running parallel to the TTF stacks and the layer of PMC with their molecular planes in perpendicular orientation together provide a sheath structure around the TTF stacks. Superposition of the core structure of TTF and the sheath structure of PMC ions leads to the 'core and sheath' architecture of the (TTF)$_3$(PMC)$_2$ crystal shown in Fig. 4.7.
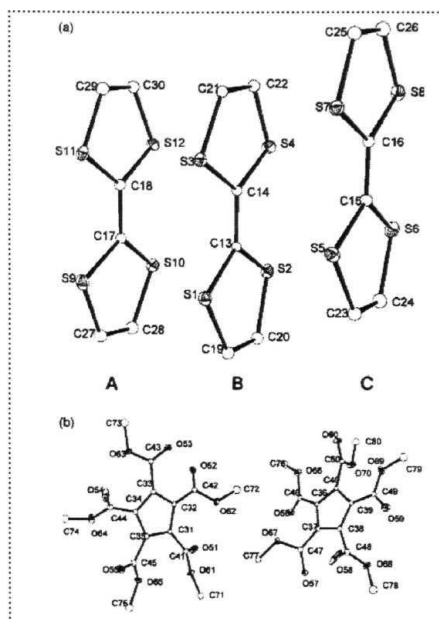
Figure 4.5 *Molecular structures of (a) TTF trimer unit and (b) PMC dimer unit in (TTF)₃(PMC)₂ from single crystal X-ray analysis showing 10% probability ellipsoids on S and O atoms; H atoms are omitted for clarity.*
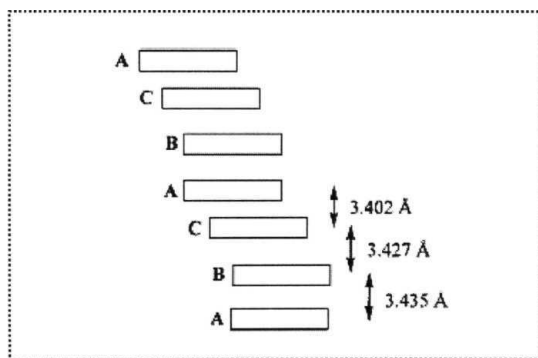
Figure 4.6 *Schematic representation of the TTF stacks in (TTF)₃(PMC)₂.*
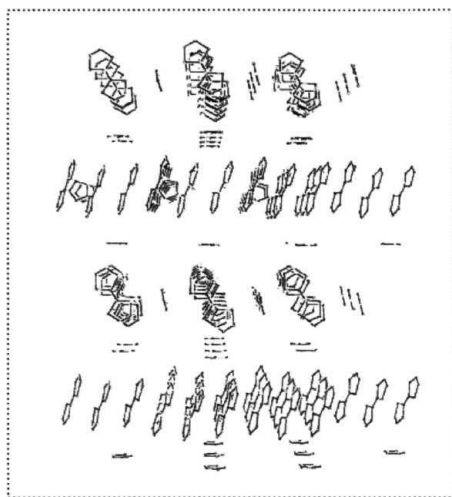
Figure 4.7 *View of the 'core and sheath' structure of (TTF) ₃(PMC) ₂ along the [110] direction; only the pentagonal ring C atoms of PMC are shown for clarity.*

Some of the short interatomic distances observed between the core and sheath structures are the following : $S1...O68 = 3.117$ A, $C19...O68 = 3.122$ A, $C22...O58 = 3.200$ A, $C26...O60 = 3.264$ A, $C24...O70 = 3.266$ A and $C21...O58 = 3.275$ A. The sheath of counterions around the TTF stack precludes interstack interactions and the 2-dimensional character which normally supports the formation of a metallic state. However, the novel case of TTF stacks running in orthogonal directions in $(TTF)_3(PMC)_2$ leads to a new kind of two-dimensional structural motif.

The 2-dimensional character of the grid network is reflected in the unusual resistivity anisotropy. DC resistivity measurements were carried out on single crystals in the form of rectangular plates. Measurements were made in the $[1\overline{1}0]$ and [110] directions which were found to be along the long and short axes of the rectangular face respectively and in the [001] direction, perpendicular to the rectangular face. The measured values are, $p[1\overline{1}0] = 6.7$ x 10^4 Ω cm, $p[1\,10] = 2.3$ x 10^5 Ω cm and $p[001] = 2.4$ x 10^6 Ω cm. The resistivity anisotropy in the orthogonal directions in the *ab* plane is about 3.4 whereas the anisotropy between the axes in the *ab* plane and the *c* axis are

respectively 10 and 36. The semiconducting nature of $(TTF)_3(PMC)_2$ results from the small but definite trimerization present in the stack. ESR experiments carried out on a microcrystalline sample of $(TTF)_3(PMC)_2$ showed weak triplet exciton signals. This is consistent with the presence of neighboring localized TTF^+ radicals in the stack.

4.4   SUMMARY

We have developed novel semiconducting polymeric and molecular materials of polyaniline and tetrathiafulvalene by employing new synthetic strategies involving polyelectrolytes as templates for organizing the molecular assembly. In Sec. 4.2 we have presented the detailed synthetic protocol for (i) the preparation of stable colloidal solutions of PANI using the environmentally friendly aqueous route and (ii) the formation of good quality polyelectrolyte templated PANI films. The morphological characterization reveals interesting features at the submicro and nano levels and their sensitive dependence on the amount of the PVA additive. The investigation also reveals the correlation between the morphology and the electrical conductivity of the films. Preliminary studies in our laboratory suggest that these PANI-PSS films exhibit sensitive and fast resistivity change responses to the presence of ammonia vapors. Its sensor capabilities are currently under exploration.

In Sec. 4.3 we have demonstrated the enhancement of conductivity by $\sim 10^2$ -10^4 in various polyelectrolyte complexes of TTF over the precursor salt $(TTF)_3(BF_4)_2$. This suggests the possible symbiotic interaction between the π-donor molecular ions and the polyionic polymer that leads to improved polymer chain alignment and π-stacking. Detailed characterization of these new materials is yet to be achieved. We have also presented the unusual square grid structure in $(TTF)_3(PMC)_2$ crystals, formed from the TTF stack cores and the PMC sheaths. The flat structure of the anions and their non-stacking nature has led to this new packing motif in the TTF complex. The trimerization observed in the TTF stacks is not very strong. Incorporation of suitable derivatives of the cyclopentadienide ion which support interaction between the cores of TTF stacks, could lead to complexes with similar architecture exhibiting novel 2-dimensional metallic conductivity.

REFERENCES

1.   (a) Bernier, P.; Lerant, S.; Bidan, G. *Advances in synthetic metals: Twenty Years of Progress in Science and Technology,* Elsevier Science, Switzerland, 1999; (b) Nalwa, H. S. (Ed) *Handbook of Organic Conductive Molecules and Polymers, Vols. 1-4,* John Wiley, Chichester, 1997; (c) Ishiguro, T.; Yamaji, K. *Organic Superconductors,* Springer Series in Solid-State Sciences, Vol. 88, Berlin, 1990.

2. (a) Cowie, J. M. G. *Polymers : Chemistry & Physics of Modern Materials,* 2nd Edn, Chapman and Hall, London, 1991; (b) Chandrasekhar, P. *Conducting Polymers : Fundamentals and Applications,* Kluwer Academic publishers, Norwell, 1999.

3.   Jayanty. S.; Radhakrishnan, T. P. *Polymer* (*in press*).

4.   Jayanty. S.; Radhakrishnan, T. P. *J. Mater. Chem*. **1999,** *9,* 1707.

5. (a) Trivedi, D. C. in *Handbook of Organic Conductive Molecules and Polymers, Vol. 2,* Nalwa H. S. (Ed.), John Wiley, London, 1997. pp. 509-511; (b) Metzger, R. M.; Day, P.; Papavassilou, G. C. (Eds.) *Low Dimensional Metals and Molecular Electronics,* NATO ASI Series, Plenum Press, New York, 1990.

6.   Huang, J.; Virji, S.; Weiller, B. H.; Kaner, R. B. *J. Am. Chem. Soc.* **2003,** *125,* 314.

7.   (a) Rowley, N. M.; Mortimer, R. J. *Science Progress* **2002,** *85,* 243; (b) Gazotti W. A.; Faez, R.; De Paoli, M. A. *J. Electroanal. Chem.* **1996,** *415,* 107; (c) Cao, Y.; Treacy, G. M.; Smith, P.; Heeger, A. J. *Appl. Phys. Lett.* **1992,** *60,* 2711.

8.   (a) Su, S. J.; Takeishi, M; Kuramoto, N. *Macromolecules* **2002,** *35,* 5752; (b) Falcao, E. H. L.; Azevedo, W. M. *Synth. Met.* **2002**, *128*, 149; (c) Rao, P. S.; Subrahmanya, S.; Sathyanarayana, D. N. *Synth. Met.* **2002,** *128*, **311;** (d) Han, C; Hong, S.; Yang, K.; Bai, M.; Lu, C; Huang C. *Macromolecules* **2001,** *34,* 587.

9.   (a) Hopkins, A. R.; Reynolds, J. R. *Macromolecules* **2000,** *33,* 5221; (b) Kosonen, H.; Ruokolainen, J.; Knaapila, M.; Torkkeli, M.; Jokela, K.; Serimaa, R.; Brinke, G. T.; Bras, W.; Monkman, A. P.; Ikkala, O. *Macromolecules* **2000,** *33,* 8671.

10.   (a) Chen, S.; Hwang, G. *Polymer* **1997,** *38,* 3333; (b) Chen, S.; Hwang, G. *J. Am. Chem. Soc.* **1995,** *117,* 10055; (c) Chan, H. S. O.; Ho, P. K. H.; Ng, S. C; Tan B. T. G.; Tan, K. L. *J. Am. Chem. Soc.* **1995,** *117,* 8517.

11. (a) Yin W, Ruckenstein E. *Macromolecules* **2000,** *33,* 1129; (b) Lin, H.; Chen, S. *Macromolecules* **2000,** *33,* 8117; (c) Geng, Y. H.; Sun, Z. C; Li, J.; Jing, X. B.; Wang, X. H.; Wang, F. S. *Polymer* **1999,** *40,* 5723; (d) Chen, S.; Hwang, G. J. *Am. Chem. Soc.* **1994,***116,* 7939.

12. (a) Sudhakar, M.; Stoecker, P. W.; Viswanathan T. *Recent Res. Dev. Polym. Sci.* **1998,** 2, 173; (b) Sun, L.; Liu, H.; Clark, R.; Yang, S. C. *Synth. Met.* **1997,** *84,* 67; (c) Geng, Y.; Li, J.; Ling, X.; Wang, F. *Synth. Met.* **1997,** *84,* 81.

13. (a) Langer, J. J.; Framski, G.; Golczak, S. *Synth. Met.* **2001,** *121,* 1319; (b) Langer, J. J.; Framski, G.; Joachimiak, R. *Synth. Met.* **2001,** *121,* 1281; (c) Bergman, B.; Hanks, T. W. *Macromolecules* **2000,** *33,* 8035.

14. (a) Gangopadhyay, R.; De A. *Synth. Met.* **2002,** *132,* 21; (b) Su, M. C; Hong, J. L. *Polymer* **2001,** *42,* 3297.

15. Wei, Z.; Zhang, Z.; Wan, M. *Langmuir* **2002,** *18,* 917.

16. (a) Zhang, Z.; Wei, Z.; Wan, M. *Macromolecules* **2002,** *35,* 5937; (b) Zhang, Z.; Wan, M. *Synth. Met.* **2002,** *128,* 83.

17. (a) Takahashi, K.; Nakamura, K.; Yamaguchi, T.; Komura, T.; Ito, S.; Aizawa, R.; Murata, K. *Synth. Met.* **2002,** *128,* 27; (b) Roy, B. C; Gupta, M. D.; Bhowmik, L.; Ray, J. K. *Synth. Met.* **1999,** *100,* 233; (c) Wang, X. H.; Li, J.; Wang, L. X.; Jing, X. B.; Wang, F. S. *Synth. Met.* **1995,** *69,* 147; (d) Yue, J.; Wang, Z. H.; Cromack, K. R.; Epstein, A. J.; MacDiarmid, A. G. *J. Am. Chem. Soc.* **1991,** *113,* 2665; (e) Yue, J.; Epstein, A. J. *J. Am. Chem. Soc.* **1990,** *112,* 2800.

18. (a) Trivedi, D. C. *J. Solid State Electrochem.* **1998,** *2,* 85; (b) Kuramoto, N.; Tomita, A. *Polymer* **1997,** *38,* 3055.

19. Nagarajan, R.; Tripathy, S.; Kumar, J.; Bruno, F. F.; Samuelson L. *Macromolecules* **2000,** *33,* 9542.

20. Yang, S. M.; Chen, W. M; You, K. S. *Synth. Met.* **1997,** *84,11.*

21. Liu, W.; Cholli, A. L.; Nagarajan, R.; Kumar, J.; Tripathy, S.; Bruno, F. F.; Samuelson, L. *J. Am. Chem. Soc.* **1999,** *121,* 11345.

22. Liu, J.; Yang, S. C. *J. Chem. Soc. Chem. Commun.* **1991,** 1529.

23. Sun, L.; Yang, S. C. *Mat. Res. Soc. Symp. Proc.* **1994,** *328,* 209.

24. Innis, P. C; Norris, I. D.; Kane-Maguire, L. A. P.; Wallace, G. G. *Macromolecules* **1998,** *31,* 6521.

25. (a) Kim, D.; Choi, J.; Kim, J.; Han, Y.; Sohn, D. *Macromolecules* 2002, *35,* 5314. (b) Roichman, Y.; Titelman, G. I.; Silverstein, M. S.; Siegmann, A.; Narkis, M. *Synth. Met.* 1999, PS, 201.

26. (a) Bryce, M. R. *Chem. Soc. Rev.* 1991, *20,* 355. (b) Bryce, M. R. *J. Mater. Chem.* 1995, 5, 1481. (c) Day, P.; Kurmoo, M. *J. Mater. Chem.* 1997, 7, 1291. (d) Coronado, E.; Gómez-García, C. J. *Chem. Rev.* 1998, *98,* 273. (e) Bryce, M. R.*Adv. Mater.* 1999, 77, 11.

27. (a) Cooper, W. F.; Kenny, N. C; Edmonds, J. N.; Nagel, A.; Wudl, F.; Coppens, P. *J. Chem. Soc. Chem. Commun.* 1971, 889. (b) Cooper, W. F.; Edmonds, J. W.; Wudl, F.; Coppens, P. *Cryst. Struct. Commun.* 1974, *3,* 23. (c) Ellern, A.; Bernstein, J.; Becker, J. Y.; Zamir, S. ; Shahal, L.; Cohen, S. *Chem. Mater.* 1994, *6, 1378*.

28. Williams, R.; Lowe Ma, C; Samson, S.; Khanna, S. K.; Somoano, R. B. *J. Chem. Phys.* 1980, 72, 3781.

29. Teitelbaum, R. C; Marks, T. J.; Johnson, C. K. *J. Am .Chem. Soc.* 1980, 702, 2986.

30. Scott, B. A.; La Placa, S. J.; Torrance, J. B.; Silverman, B. D.; Welber, B. *J. Am. Chem. Soc.* **1977**, *99*, 6631.

31. Kathirgamanathan, P.; Mazid, M. A.; Rosseinsky, D. R. *J. Chem. Soc. Perkin Trans. 2.* 1982, 593.

32. Kobayashi, H.; Kobayashi, K. *Bull. Chem. Soc. Jpn.* 1977, 50, 3127.

33. Kasper, J. S.; Interrante, L. V. *ActaCryst.* 1976, *B32, 2914*.

34. Bousseau, M.; Valade, L.; Legros, J.; Cassoux, P.; Garbauskas, M.; Interrante, L. V. *J. Am.Chem. Soc.* **1986**, *108*, 1908.

35. Yan, Y.; Mingos, D. M. P.; Kurmoo, M.; Li, W.; Scowen, I. J.; Mc Partlin, M.; Coomber, A. T.; Friend, R. H. *J. Chem. Soc. Chem. Commun.* 1995, 997.

36. Yan, Y. K.; Mingos, D. M. P.; Kurmoo, M.; Li, W.; Scowen, I. J.; Mc Partlin, M.; Coomber, A.T.; Friend, R. H. *J. Chem. Soc. Dalton Trans.* 1995, 2851.

37. Matsubayashi, G.; Yokoyama, K.; Tanaka, T. *J. C S. Dalton Trans.* 1988, 253.

38. Berger, P. A.; Dahm, D. J.; Johnson, G. R.; Miles, M. G.; Wilson, J. D. *Phys. Rev.* 1975, 572, 4085.

39. Mori, T.; Inokuchi, H. *Bull. Chem. Soc. Jpn.* 1992, *65, 1460*.

40. Kistenmacher, T. J.; Phillips, T. E.; Cowan, D. O. *Acta Cryst.*, 1974, *B30, 763.*

41. Peierls, R. E. *Quantum Theory of Solids.* Oxford University Press, London, **1955,** p.108.

42. Emge, T. J.; Wiygul, F. M; Ferraris, J. P.; Kistenmacher, T. J. *Mol. Cryst. Liq. Cryst.* **1981,** *78,* 295.

43. Geiser, U.; Schultz, A. J.; Wang, H. H.; Beno, M. A.; Williams, J. M. *Acta. Cryst.*, *19S8, C44,* 259.

44. Triki, S.; Ouahab, L.; Halet, J.; Peña, O.; Padiou, J.; Grandjean, D.; Garrigou-Lagrange, C. Delhaes, P. *J. Chem. Soc. Dalton Trans.* **1992,** 1217.

45. Attanasio, D.; Bellitto, C; Bonamico, M.; Fares, V.; Imperatori, P. *Gazz. Chim. Ital.* **1991,** *121*, 155.

46. Matsubayashi, G.; Akiba, K.; Tanaka, T. *Inorg. Chim. Acta,* **1989,** *157*, 195.

47. (a) Bryce, M. R.; Davies, S. R.; Hursthouse, M. B.; Motevalli, M. *J. Chem. Soc. Perkin Trans. 2,* **1988,** 1713. (b) Yamaguchi, S.; Hanafusa, T.; Tanaka, T.; Sawada, M.; Tatemitsu, H.; Sakata, Y.; Misumi, S. *Chem. Exp.* **1992,** 7, 9. (c) Frankenbach, G. M.; Beno, M. A.; Williams, J. M. *Acta. Cryst.* **1991,** *C47,* 762. (d) Mahadevan, C. *J. Crystall. Spectr. Res.* **1986,** *16*, 159. (e) Mayerle, J. J.; Torrance, J. B.; Crowley, J. I. *Acta.Cryst.* **1979,** *B35,* 2988.

48. Philip, D.; Slawin, A. M. Z.; Spencer, N.; Stoddart, J. F.; Williams, D. J. *J. Chem. Soc. Chem. Commun.* **1991,** 1584.

49. Matsubayashi, G.; Ueyama, K.; Tanaka, T. *J. C. S. Dalton Trans.* **1985,** 465.

50. (a) Ueyama, K.; Matsubayashi, G.; Shimizu, R.; Tanaka, T. *Polyhedron,* **1985,** *4,* 1783. (b) Ueyama, K.; Matsubayashi, G.; Tanaka, T. *Inorg. Chim. Acta* **1986,** *112*, 135.

51. Naito, K.; Okamato, M. *Synth. Met.* **1987,** *18,* 417.

52. Kristenmacher, T. T.; Ross, M.; Chiang, C. C; Van Duyana, R. P.; Cape, T.; Siedel, A. R. *J. Am. Chem. Soc.* **1987,** *100*, 1958.

53. Trauz, A.; Ulahski. J.; Kryszeuski. *Polym. J.* **1983,** *15*, 635.

54. Wudl, F. *J. Am. Chem. Soc.* **1975,** *97,* 1962.

55. Radhakrishnan, T. P. *Ph. D. Thesis,* Princeton University, 1987.

56. Legros, J. -P.; Bousseau, M.; Valade, L.; Cassoux, P. *Mol. Cryst. Liq. Cryst.* **1983,** *100*, 181.

57. Pyrka, G. J.; Fernando, Q.; Inoue, M. B.; Inoue, M.. *Inorg. Chim. Acta* **1989,** *156*, 257.

CHAPTER 5

Overview of the Present Work
and Future Prospects

5.1   OVERVIEW OF THE WORK PRESENTED IN THE THESIS

Molecular materials afford great flexibility in their design and fabrication. Development of novel molecular materials requires the knowledge and control of the structure at the molecular level and organization at the bulk level. The latter involves recognition of the relative significance of a wide range of noncovalent intermolecular interactions and continues to be a challenging problem. Though molecular materials afford great many advantages over other classes of materials such as the facility to fine tune the material properties through molecular design, their thermal and mechanical stability are still not optimal for device applications. Therefore search for molecular materials with increased efficiency, thermal and mechanical stability as well as the exploration of novel ways of organizing them to achieve desired attributes continues to be a fascinating and challenging task. Each new class of molecular materials provides important insight into fundamental structure/property correlations, opening avenues for the design and development of further generations of materials.

We have presented in this thesis, investigations of several new classes of molecular materials based on remote functionalized diaminodicyanoquinodimethanes (DADQ's) and polyelectrolyte templated polymers and their optical, nonlinear optical and semiconducting properties. Sec. 1.5 provides a summary of the studies carried out. Here we wish to present an overview of the insights we have gained through these investigations and demonstrate some common links between the different phenomena explored.

We have made extensive use of the semiempirical computational method, AMI/COSMO to model several features of the 'molecule-in-a-crystal', using the solvation subroutine to mimic the molecular microenvironment in the crystal. The studies we have presented in this thesis along with other investigations carried out in our laboratory on polymorphism and intermolecular interactions at the air-water interface, establish the utility of this simple approach for analyzing the structure and organization of molecules as they exist in bulk materials. During our studies we have modeled significant molecular structural features, charge distribution and electronic states of DADQ's relevant to their materials attributes. In Sec. 2.2 we have studied the molecular

dihedral twist of DADQ's which has important consequences for their optical and nonlinear optical characteristics. The dielectric constant used in the solvation routine could be qualitatively correlated to intermolecular interactions arising from dispersion, H-bonding and electrostatic forces. The modeling was extended to the analysis of charge distribution and charge transfer complexation problem in Sec. 2.3. Computational investigation of the full molecular structure and analysis of charge distribution in the case of the unusual zwitterionic molecule presented in Sec. 3.3 provided insight into the origin of the intermolecular electrostatic interactions leading to helical supramolecular assembly. The evolution of the electronic energy states of typical remote functionalized DADQ's as a function of the imposed dielectric constant in the computation was investigated in Sec. 2.4. This led to a semi-quantitative model for the origin of enhanced fluorescence of these systems in the solid state and doped polymer films.

The utilization of remote functionalities on the chromophores and NLO-phores, in the assembly of optical and nonlinear optical molecular materials is another significant theme developed by us. The remote functionality provides a convenient handle to influence the molecular assembly without disturbing the desired properties at the molecular level. The remote functionality on a DADQ molecule (Sec. 2.2) allowed us to establish a highly ionic crystal lattice and probe the influence of the ionic environment on the molecular twist and subsequently model it using computations. This was a significant step in the development of the idea of 'molecule-in-a-crystal' discussed above. In Sec. 2.3 we have shown that the remote functionality acts as an anchoring agent and leads to the formation of charge transfer complex exclusively in the solid state. Remotely connected amino and hydroxy groups facilitate specific and directed intermolecular interactions promoting extended assembly in the molecular materials discussed in Sec. 2.4; they play a positive role in the fluorescence enhancement by effectively inhibiting structure relaxation in the excited state. A comprehensive survey of the different DADQ's studied by us and earlier by others in our laboratory and elsewhere, show that the presence of the remote functionality makes the DADQ's soluble not only in organic solvents, but also in water, without undesirable hydrolysis problems; this is an important advantage for the fabrication of doped polymer films based on these compounds. In Sec. 3.2 we have described the role of the remote functionality on a DADQ molecule in steering the molecular dipoles from a centrosymmetric to a noncentrosymmetric and

SHG active lattice structure, providing a simple chemical route to a novel NLO material. All these examples demonstrate the utility of the remote functionality approach in the design and fabrication of novel molecular materials.

The utilization of polyelectrolytes in the organization of polyaniline as well as tetrathiafulvalene discussed in chapter 4, is a logical extension of the remote functionality approach. Here, instead of remote groups covalently bound to the active molecule, we have a template structure that assists in the molecular organization. In the case of polyaniline (Sec. 4.2), the polyionic template serves as a new design element controlling the solubility of the final material, its submicro/nano level morphology and finally the electrical conductivity. With tetrathiafulvalene (Sec. 4.3), though we could not establish the structural aspects, it appears that the polyionic framework helps to organize the conducting stacks leading to enhanced conductivities. The remote functionalities on the DADQ's as well as the polyelectrolyte templates thus serve to fashion the assembly of small molecules and polymers leading to the realization of significant optical, nonlinear optical and conducting properties.

5.2   FUTURE PROSPECTS

The basic idea of modeling the molecular environment in crystals using solvation routines and semiempirical computational methods has been demonstrated in the various explorations we have undertaken. This concept has wide ramifications which need to be probed further. The methodology is very general and therefore, the computations can be extended to higher levels such as *ab initio* methods and more sophisticated solvation models. A wide range of molecular properties including dipole moments which are often strongly modified in the bulk state needs to be addressed. An important aspect that requires detailed experimental investigation is the question of correlating the dielectric constant used in the computational model to analyze structural or electronic features and the value measured in the bulk materials.

It would be interesting to explore more remote functionalized DADQ's as well as other chromophores and NLO-phores to test the generality of the concepts we have developed. The formation of charge transfer complexes exclusively in the solid state and enhanced fluorescence in the aggregated state are interesting phenomena. Based on the systems we have studied, novel materials can be developed in these areas. Establishment of the model we have presented for the enhanced fluorescence phenomenon requires detailed investigations of the excited state dynamics and variable temperature photophysical studies. Exploration of possible electroluminescence in these materials would be another important avenue for further work. Since molecular aggregation not only does not quench the light emission, but enhances it in these systems, they are promising new candidates for such applications. A fundamental aspect that needs to be investigated is the level of supramolecular aggregation at which the enhanced light emission sets in. The role of remote functionality and complexation in the formation of noncentrosymmetric SHG active lattices needs to be analyzed further and exploited to achieve optimal NLO-phore orientations and strong SHG. Based on their size and symmetry we believe that cyclic systems such as squaric acid dianions would be interesting complexing partners for the DADQ based NLO-phores.

The active role of remote groups and polyelectrolyte templates in molecular organization can be extended by incorporating the functionalized molecules as pendant groups on the polyelectrolyte framework. This may be achieved either through covalent bonds or more conveniently through ionic interactions. Typical cases that can be envisaged are the DADQ's with remote ionic functionalities which may be incorporated in polyelectrolyte matrices. The polyelectrolytes facilitate good thin film fabrication and the NLO-phore orientations, if not favorable, can be tuned through electric field poling techniques. The remote functionalized molecules can also be incorporated in coordination polymers through coordination to the metal centers leading to interpenetrating networks and interchelated compounds which can form novel optical or nonlinear materials. Such materials would be very promising from the viewpoint of applications, since the DADQ's we have described in the thesis possess, in addition to strong nonlinear responses, good thermal stability and laser damage thresholds. The DADQ's possessing remote functionality are also appropriate systems to fabricate Langmuir-Blodgett films, since amphiphilic chains can be attached through ionic or

covalent interactions with the remote groups without perturbing the significant **chromophore** properties.

Our investigations of the polyionic complexes of tetrathiafulvalene are preliminary and need further work for consolidation. Single crystal growth and structural characterization are of utmost priority to assess the validity of the mutually supportive structural model we have proposed. In addition to the popular TTF which we have explored, it would be interesting to incorporate other systems such as free base porphyrins or metalloprophyrins that can form columnar structures based on ionic complexes with the polyions and exhibit low dimensional conductivity. Since this approach to molecular assembly is quite general other materials attributes such as magnetism and NLO properties may also be targeted with appropriate molecular systems. The polyelectrolyte templated polymers are promising candidates for developing efficient sensors, because of the aqueous solubility and the scope for fabrication of high quality films. Preliminary studies in our laboratory reveal fast, efficient and reversible ammonia sensing with these materials. Detailed exploration of their sensor capability is under way.

We believe that the novel developments in the field of molecular materials presented in this thesis pave the way for further exciting research in future.

Appendices

APPENDIX A

Instrumentation for Characterization of New Materials

Melting temperatures of solids were determined using capillary melting point apparatus (Superfit, India); values reported are uncorrected. Infra red spectra were recorded on a Jasco5300 FTIR spectrometer. All the spectra were calibrated against polystyrene absorption at 1601 cm^{-1}. Solid samples were recorded as KBr pellets. Electronic absorption (UV-Vis) spectra were recorded on a Shimadzu UV 3101 PC spectrophotometer. Specular reflectance (8° incidence) or diffuse reflectance spectra of solid pellets were recorded on the same spectrometer using the integrating sphere (ISR 3100) attachment. Circular dichroism spectra were recorded on a Jasco Spectropolari-meter Model J-810. ^{1}H and ^{13}C NMR spectra were recorded on Bruker AC200 NMR spectrometer. ^{1}H NMR (200 MHz) spectra were measured with TMS (8 = 0) as internal standard. ^{13}C NMR (50 MHz) spectra were recorded using the solvent peaks as the internal standard. Elemental analysis was carried out on a Perkin Elmer Model - 2400 CHNS/O, AD2B or 240 CHN analyzer. Sartorius BP211D balance was used for high precision weighing.

Morphology of films coated on glass/aluminum foil substrates using a photoresist spinner was examined using a Philips XL 30 ESEM Scanning Electron Microscope. Gold coating was provided on the films prior to examination. X-ray photoelectron spectroscopy was carried out on a Kratos Axis 165 Spectrometer with a Mg K_α x-ray source (1253.6 eV). The x-ray power supply was run at 15 kV and 5 mA. The pressure in the analysis chamber during the scans was ~ 10^{-9} Torr. The peak positions are based on calibration with respect to the C1s peak at 284.6 eV.

APPENDIX B

<u>X-ray **Crystallography**</u>

X-ray diffraction data were collected on an Enraf-Nonius MACH3 diffractometer. MoK_α radiation *(X* = 0.71073 A) with a graphite crystal monochromator in the incident beam. Standard CAD4 centering, indexing and data collection programs were used. The general routine used for the data collection is as follows; minor variations in settings were done in specific cases. The unit cell dimensions were obtained by a least square fit of 24 centered reflections in the neighborhood of $\theta = 10^o$. Intensity data were collected using the ω scan method at a scan speed of 4.12^o/min to a maximum 20 of 50°. The scan width A0, for each reflection was 0.80 + 0.35 tan0. During data collection the intensities of three standard reflections were monitored every 1.5 hour of x-ray exposure. In all the cases we have studied, no decay was observed. In addition three orientation standards were monitored every 250 reflections to check the effects of crystal movement. Data was reduced using Xtal 3.4;[1] Lorentz and polarization corrections were included. All non-hydrogen atoms were found using the direct method analysis in SHELX-97[2] and after several cycles of refinement the positions of the hydrogen atoms were calculated and added to the refinement process. Empirical absorption correction was applied in the relevant cases, using ψ scan data. Refinement proceeded to convergence by minimizing the function $\sum \mathbf{w} (F_0^2 - F_c^2)$. A final difference Fourier synthesis map showed the largest difference peak and hole to be acceptably small. The R indices were calculated as

$$R = \sum \left| \left(|F_0| - |F_c| \right) \right| / \sum |F_0| \ \ \text{and} \ \ wR^2 = \left[\sum w (F_0^2 - F_c^2)^2 / \sum (F_0^2)^2 \right]^{1/2}.$$

Graphics were handled using ORTEX6a[3] and Platon.[4]

Table B.1 lists the space groups and REFCODE (Cambridge Crystallographic Database) or deposition number from Cambridge Crystallographic Data Centre[5] for the new crystal structures presented in this thesis. The fractional atomic coordinates (x 10^4) and isotropic displacement parameters, U_{eq} (A^2 x 10^3) are provided in Tables B.2-B.11. U_{eq} is defined as one third of the trace of the orthogonal U_{ij} tensor. Estimated standard deviations (e.s.d) are given in paranthesis.

References

1. *Xtal 3.4,* Hall, S. R.; King, G. S. D.; Stewart, J. M. (Eds.), University of Western Australia, Perth, Australia, **1995.**

2. *SHELX-97,* Sheldrick, G. M. University of Gottingen, Gottingen, Germany, 1997.

3. McArdle, P. *J. Appl. Cryst.* **1995,** *28,* 65.

4. Spek, A. L. Utretcht University, The Netherlands, **2000.**

5. Cambridge Structural Database, Version 5.24 (November 2002 Update).

Table B.1 *Space groups and the REFCODE / deposition number from CSD and the reference in the thesis.*

Compound	Space Group	REFCODE / Deposition No.	Page no.
$9(Tos)_2$	P2/c	ICOWAY	**56**
$9(Pic)_2$	P $\bar{1}$	-	**65**
10	$P2_1/c$	181468	100
11(TPA)	Cc	181469	100
12	$P2_1/n$	206354	**82**
13	Pbca	206355	**82**
$18(Iod)_2$	$P2_1/c$	216261	111
19	$P2_12_12_1$	216262	111
$19.H_2O$	$P2_12_12_1$	216263	111
$(TTF)_3 (PMC)_2$	Cc	MAJXAW	150

Atom	x	y	z	U_{eq}
H(12A)	9846	9816	3849	47
H(12B)	8769	10251	4242	47
H(2)	7017	7382	2367	48
H(3)	7009	5600	2351	56
H(10A)	6319	10777	3316	47
H(10B)	6060	10545	2336	47
H(11A)	8352	9870	2529	50
H(11B)	8480	10990	2937	50
H(13A)	8881	8512	4503	50
H(13B)	8614	8301	3520	50
H(14A)	6461	8097	3910	45
H(14B)	6606	9218	4316	45
H(16)	9438	6737	1538	96
H(17)	9541	4954	1297	148
H(19)	6250	5171	-667	264
H(20)	6109	6947	-458	191
H(21A)	7085	3406	207	408
H(21B)	8749	3415	550	408
H(21C)	8066	3579	-423	408
H(26A)	10940(5)	11740(4)	3640(3)	125(17)
H(26B)	12170(4)	11140(3)	3970(2)	88(12)
H(27)	10370(8)	3000(5)	2140(4)	210(3)
H(28A)	5869(16)	11632(13)	1008(9)	0(3)
H(28B)	4850(6)	11030(4)	260(3)	157(18)

Table B.2 Compound **9(Tos)₂**

Atom	x	y	z	U_{eq}
N(8)	7224(4)	3258(3)	2395(3)	122(1)
N(12)	8904(2)	9836(2)	3820(1)	39(1)
O(23)	6218(2)	8633(2)	644(1)	67(1)
O(24)	8612(2)	8601(1)	1516(1)	54(1)
O(25)	8207(2)	8854(2)	11(1)	62(1)
O(26)	11245(2)	11191(2)	3953(2)	65(1)
O(27)	10000	2481(3)	2500	85(1)
O(28)	5810(3)	10798(3)	852(2)	92(1)
S(22)	7696(1)	8378(1)	693(1)	40(1)
N(9)	6053(2)	9244(1)	3037(1)	34(1)
C(1)	5000	7589(2)	2500	35(1)
C(2)	6204(2)	7024(2)	2418(1)	40(1)
C(3)	6200(2)	5955(2)	2413(2)	46(1)
C(4)	5000	5379(3)	2500	46(1)
C(5)	5000	8725(2)	2500	32(1)
C(6)	5000	4252(3)	2500	58(1)
C(7)	6209(4)	3689(2)	2442(3)	78(1)
C(10)	6544(2)	10301(2)	2900(1)	39(1)
C(11)	8143(2)	10284(2)	2987(1)	41(1)
C(13)	8399(2)	8770(2)	3943(1)	42(1)
C(14)	6806(2)	8800(2)	3858(1)	38(1)
C(15)	7775(3)	7021(2)	545(2)	58(1)
C(16)	8793(4)	6428(2)	1082(3)	80(1)
C(17)	8847(7)	5356(3)	936(4)	124(2)
C(18)	7919(10)	4887(3)	284(4)	160(3)
C(19)	6909(11)	5486(4)	-222(4)	220(5)
C(20)	6819(8)	6555(3)	-100(3)	159(3)
C(21)	7959(14)	3713(4)	141(5)	272(7)

Table B.3   Compound **9(Pic)₂**

Atom	x	y	z	U_{eq}
N(10)	-6784(5)	7650(4)	3369(3)	50.6(12)
N(16)	-0923(4)	2689(4)	5270(3)	41.9(11)
N(22)	2792(5)	1277(4)	0650(3)	51.9(13)
O(31)	1546(4)	2880(3)	5467(3)	54.9(11)
O(39)	0295(4)	1210(4)	6372(3)	82.1(15)
O(47)	3857(5)	3120(4)	7537(3)	80.9(14)
O(55)	5842(5)	1183(4)	-0079(3)	75.2(13)
O(56)	7881(7)	1134(5)	-0833(5)	155(3)
N(12)	-3732(5)	8937(4)	1291(3)	58.8(14)
N(13)	-0050(4)	3260(3)	3503(2)	33.2(9)
N(19)	0943(4)	2914(4)	2006(3)	40.2(11)
N(32)	4282(6)	3067(6)	4545(4)	86(2)
O(33)	5215(9)	3434(8)	4440(6)	201(5)
O(34)	3551(8)	3405(9)	4149(7)	235(6)
N(35)	6251(6)	-0026(5)	6075(4)	64.5(15)
O(36)	7415(5)	-0024(4)	5585(5)	75.9(14)
O(37)	6060(5)	-0632(4)	6690(4)	91.8(17)
N(38)	1148(5)	1253(4)	6756(4)	61.8(14)
O(40)	0934(6)	1193(5)	7537(3)	98.3(18)
N(48)	3071(6)	5311(5)	-0494(4)	58.2(13)
O(49)	2175(6)	5096(5)	0086(5)	131(2)
O(50)	2836(6)	6200(5)	-0821(4)	111(2)
N(51)	7774(7)	4473(5)	-2554(4)	61.7(14)
O(52)	7451(6)	5428(5)	-2790(3)	97.0(17)
O(53)	8896(5)	3791(5)	-2922(3)	79.2(14)
N(54)	6645(6)	1619(5)	-0569(4)	66.8(15)
C(1)	-1108(5)	4506(4)	2573(3)	34.4(12)
C(2)	-0782(5)	5309(4)	1983(3)	40.5(13)
C(3)	-1788(5)	6255(4)	1910(3)	37.4(12)
C(4)	-3204(5)	6433(4)	2414(3)	33.4(11)
C(5)	-3545(5)	5593(4)	2997(3)	37.6(12)
C(6)	-2511(5)	4664(4)	3072(3)	37.2(12)

Atom	x	y	z	U_{eq}
C(7)	-0040(5)	3535(4)	2694(3)	33.5(11)
C(8)	-4285(5)	7418(4)	2348(3)	35.4(12)
C(9)	-5678(6)	7571(4)	2902(3)	35.4(12)
C(11)	-3989(5)	8255(5)	1773(3)	38.7(12)
C(14)	-0477(5)	4116(4)	4223(3)	39.6(13)
C(15)	-1520(5)	3839(4)	5018(3)	41.7(13)
C(17)	-0541(5)	1827(4)	4532(3)	43.5(13)
C(18)	0523(5)	2120(4)	3747(3)	40.8(13)
C(20)	2414(5)	2389(4)	1982(3)	43.7(14)
C(21)	2948(6)	1205(5)	1543(3)	52.2(15)
C(23)	1288(6)	1749(5)	0696(4)	57.6(16)
C(24)	0730(6)	2916(5)	1131(3)	48.2(15)
C(25)	2598(5)	2213(4)	5603(3)	40.8(13)
C(26)	4028(6)	2218(4)	5161(4)	43.8(13)
C(27)	5189(6)	1498(5)	5307(4)	50.8(15)
C(28)	5009(6)	0720(4)	5922(4)	44.3(14)
C(29)	3675(6)	0678(5)	6407(3)	47.9(14)
C(30)	2533(5)	1373(5)	6238(4)	44.6(14)
C(41)	4754(7)	3417(5)	-0450(4)	52.3(15)
C(42)	4465(6)	4530(5)	-0814(4)	47.7(14)
C(43)	5452(6)	4857(5)	-1481(3)	48.2(14)
C(44)	6773(6)	4137(5)	-1822(3)	45.8(14)
C(45)	7146(6)	3091(5)	-1509(4)	49.6(14)
C(46)	6171(6)	2751(5)	-0852(3)	48.0(14)
N(57)	8193(11)	11674(7)	2770(6)	148(4)
C(58)	7570(11)	11624(8)	2347(6)	110(3)
C(59)	6749(17)	11571(12)	1797(9)	244(9)

Atom	x	y	z	U_{eq}
H(2)	0147	5202	1626	49
H(3)	-1527	6790	1519	45
H(5)	-4481	5674	3333	45
H(6)	-2755	4127	3466	45
H(14A)	-0897	4847	4037	48
H(14B)	0359	4178	4372	48
H(15A)	-1716	4395	5495	50
H(15B)	-2404	3866	4896	50
H(16A)	-1565	2508	5732	50
H(16B)	-0145	2685	5428	50
H(17A)	-1388	1801	4381	52
H(17B)	-0142	1082	4707	52
H(18A)	1399	2087	3881	49
H(18B)	0732	1573	3262	49
H(20A)	2476	2353	2575	52
H(20B)	3015	2859	1671	52
H(21A)	3937	0894	1511	63
H(21B)	2404	0710	1875	63
H(22A)	3316	1724	0341	62
H(22B)	3112	0579	0375	62
H(23A)	0730	1258	1020	69
H(23B)	1197	1774	0111	69
H(24A)	1216	3428	0775	58
H(24B)	-0274	3187	1190	58
H(27)	6097	1537	4989	61
H(29)	3556	0175	6848	57
H(43)	5224	5568	-1701	58
H(45)	8054	2618	-1741	60
H(59A)	5953	11289	2104	365
H(59B)	7315	11070	1293	365
H(59C)	6415	12317	1614	365

Table B.4   Compound **10**

Atom	x	y	z	U_{eq}
N(1)	2625(2)	292(3)	3889(2)	69(1)
N(2)	3021(2)	2408(3)	4384(2)	62(1)
N(3)	8062(3)	-1148(4)	3110(3)	91(1)
N(4)	7163(3)	2726(4)	1803(3)	99(1)
N(5)	721(2)	2172(4)	3909(2)	82(1)
N(6)	2449(3)	4542(3)	5362(2)	74(1)
C(7)	4211(3)	1246(3)	3748(2)	51(1)
C(8)	4820(3)	94(3)	3876(2)	57(1)
C(9)	5675(3)	-20(3)	3575(2)	52(1)
C(10)	5966(2)	1001(3)	3112(2)	50(1)
C(11)	5345(3)	2157(3)	2982(2)	60(1)
C(12)	4494(3)	2268(3)	3286(2)	58(1)
C(13)	3254(3)	1333(4)	4026(2)	54(1)
C(14)	6841(3)	882(3)	2775(2)	55(1)
C(15)	7514(3)	-232(4)	2950(3)	63(1)
C(16)	7038(3)	1884(4)	2245(3)	68(1)
C(17)	1724(3)	102(4)	4212(3)	87(1)
C(18)	681(3)	819(6)	3628(3)	107(2)
C(19)	237(4)	2333(5)	4604(3)	107(2)
C(20)	191(4)	3046(7)	3125(4)	161(3)
C(21)	3748(3)	3531(4)	4761(3)	77(1)
C(22)	3563(3)	4093(4)	5578(3)	87(1)
C(23)	2248(4)	4681(5)	6227(3)	117(2)
C(24)	2222(4)	5768(5)	4848(4)	129(2)

Atom	x	y	z	U_{eq}
H(1)	2758	-340	3578	83
H(2)	2373	2458	4397	74
H(8)	4642	-614	4173	68
H(9)	6071	-799	3682	62
H(11)	5516	2865	2681	72
H(12)	4096	3046	3181	69
H(17A)	1955	402	4852	104
H(17B)	1567	-829	4205	104
H(18A)	587	776	2976	129
H(18B)	54	393	3696	129
H(19A)	261	3241	4773	160
H(19B)	642	1822	5145	160
H(19C)	-512	2041	4354	160
H(20A)	236	3933	3346	242
H(20B)	-567	2801	2822	242
H(20C)	553	2981	2690	242
H(21A)	3609	4197	4283	92
H(21B)	4507	3253	4948	92
H(22A)	3737	3432	6063	104
H(22B)	4062	4824	5821	104
H(23A)	1510	4981	6085	175
H(23B)	2755	5305	6626	175
H(23C)	2348	3847	6537	175
H(24A)	1476	6025	4720	194
H(24B)	2330	5654	4272	194
H(24C)	2711	6435	5213	194

Table B.5   Compound **11(TPA)**

Atom	x	y	z	U$_{eq}$
N(1)	3583(4)	2642(4)	7611(3)	57(2)
N(2)	4998(4)	3671(4)	7489(3)	44(1)
N(3)	5102(6)	-1819(5)	4445(5)	87(2)
N(4)	8094(5)	-1122(6)	5739(4)	78(2)
N(5)	2281(5)	2847(4)	9210(4)	59(2)
N(6)	5549(4)	5257(4)	5952(3)	45(1)
O(25)	2561(3)	1043(3)	8343(3)	50(1)
O(26)	2553(3)	382(3)	9675(3)	57(1)
O(27)	4188(4)	-3782(4)	6791(3)	72(2)
O(28)	4319(5)	-4435(4)	8118(3)	90(2)
C(7)	4969(4)	1831(4)	6979(3)	36(1)
C(8)	4399(5)	1313(5)	6300(4)	41(1)
C(9)	4769(5)	470(5)	5859(4)	44(2)
C(10)	5767(4)	129(5)	6067(3)	39(1)
C(11)	6334(5)	622(5)	6748(4)	43(2)
C(12)	5943(4)	1459(5)	7210(4)	41(1)
C(13)	4524(4)	2764(5)	7386(4)	41(2)
C(14)	6202(5)	-722(5)	5564(4)	48(2)
C(15)	5606(6)	-1316(6)	4945(5)	62(2)
C(16)	7251(6)	-947(5)	5656(4)	54(2)
C(17)	2936(7)	3505(6)	7849(6)	91(3)
C(18)	2833(9)	3650(6)	8716(6)	119(4)
C(19)	1177(6)	2960(8)	9150(6)	99(3)
C(20)	2727(7)	2887(6)	10130(5)	88(3)
C(21)	5960(5)	3949(5)	7145(4)	50(2)
C(22)	5867(5)	4165(5)	6176(4)	49(2)
C(23)	6387(6)	6035(5)	6172(5)	66(2)
C(24)	5210(5)	5327(6)	5016(4)	66(2)
C(29)	3108(5)	-732(5)	8567(4)	38(1)
C(30)	3046(4)	-1666(5)	9036(3)	41(2)
C(31)	3382(5)	-2623(5)	8728(4)	48(2)
C(32)	3779(4)	-2665(5)	7927(4)	37(1)
C(33)	3853(5)	-1738(5)	7458(4)	49(2)
C(34)	3541(5)	-781(5)	7768(4)	46(2)
C(35)	2725(4)	306(5)	8907(4)	42(2)
C(36)	4147(5)	-3717(5)	7603(4)	46(2)

Atom	x	y	z	U$_{eq}$
H(1)	3342	2006	7615	68
H(2)	4719	4151	7787	53
H(5)	2421	2194	8996	71
H(6)	5019	5429	6264	54
H(8)	3744	1549	6140	49
H(9)	4359	127	5424	53
H(11)	6992	390	6902	52
H(12)	6335	1769	7673	49
H(17A)	3195	4160	7621	109
H(17B)	2266	3391	7556	109
H(18A)	2497	4329	8776	142
H(18B)	3509	3718	9007	142
H(19A)	889	2392	9465	149
H(19B)	914	2932	8549	149
H(19C)	1002	3630	9397	149
H(20A)	3450	2815	10146	132
H(20B)	2456	2317	10454	132
H(20C)	2563	3556	10385	132
H(21A)	6436	3371	7268	60
H(21B)	6236	4575	7448	60
H(22A)	6516	4031	5950	58
H(22B)	5379	3673	5892	58
H(23A)	6604	5989	6783	99
H(23B)	6149	6743	6036	99
H(23C)	6947	5874	5838	99
H(24A)	4663	4837	4880	100
H(24B)	5764	5152	4679	100
H(24C)	4983	6037	4879	100
H(30)	2771	-1648	9571	49
H(31)	3341	-3238	9059	57
H(33)	4121	-1763	6919	58
H(34)	3617	-163	7448	55

Table B.6 Compound **12**

Atom	x	y	z	U_eq
N(9)	7933(1)	4595(1)	8327(1)	39(1)
N(10)	5672(2)	4062(1)	7696(1)	41(1)
N(13)	12217(3)	1168(1)	9279(2)	77(1)
N(14)	11049(2)	1090(1)	5558(1)	56(1)
N(17)	9401(2)	5866(1)	8531(1)	44(1)
N(23)	2797(2)	3949(1)	6458(1)	55(1)
C(1)	8057(2)	3427(1)	7882(1)	40(1)
C(2)	8960(2)	3197(1)	8814(1)	46(1)
C(3)	9826(2)	2628(1)	8707(1)	45(1)
C(4)	9865(2)	2270(1)	7646(1)	37(1)
C(5)	8977(2)	2516(1)	6714(1)	41(1)
C(6)	8072(2)	3076(1)	6833(1)	42(1)
C(7)	7181(2)	4049(1)	7987(1)	38(1)
C(8)	10799(2)	1679(1)	7533(1)	41(1)
C(11)	11582(2)	1400(1)	8492(1)	49(1)
C(12)	10946(2)	1352(1)	6449(2)	40(1)
C(15)	7249(2)	5126(1)	9042(1)	41(1)
C(16)	7710(2)	5800(1)	8590(2)	45(1)
C(18)	10036(2)	5347(1)	7784(2)	49(1)
C(19)	9640(2)	4664(1)	8241(2)	45(1)
C(20)	9810(2)	6522(1)	8096(2)	56(1)
C(21)	4833(2)	4655(1)	7295(2)	49(1)
C(22)	3889(2)	4484(1)	6219(2)	54(1)
C(24)	3667(2)	3357(1)	6791(2)	55(1)
C(25)	4640(2)	3489(1)	7864(2)	49(1)
C(26)	1822(3)	3821(1)	5432(2)	85(1)

Atom	x	y	z	U_eq
H(2)	8975	3431	9517	55
H(3)	10398	2476	9346	54
H(5)	8999	2297	5996	49
H(6)	7465	3220	6207	50
H(15A)	7596	5078	9847	50
H(15B)	6122	5086	9030	50
H(16A)	7268	5866	7815	54
H(16B)	7292	6140	9103	54
H(18A)	11160	5394	7744	58
H(18B)	9622	5396	6997	58
H(19A)	10052	4329	7715	55
H(19B)	10109	4600	9007	55
H(20A)	10924	6562	8057	84
H(20B)	9403	6853	8617	84
H(20C)	9374	6583	7328	84
H(21A)	5570	5005	7111	59
H(21B)	4148	4813	7911	59
H(22A)	3320	4873	5961	64
H(22B)	4586	4352	5592	64
H(24A)	4337	3223	6149	66
H(24B)	2947	2997	6949	66
H(25A)	3960	3572	8527	59
H(25B)	5262	3100	8040	59
H(26A)	1099	3471	5608	128
H(26B)	2468	3691	4785	128
H(26C)	1257	4216	5230	128

Atom	x	y	z	U$_{eq}$
H(2)	3203	3107	6643	112
H(3)	3135	4886	6872	96
H(5)	4154	5543	4928	114
H(6)	4161	3751	4645	115
H(15A)	3341	115	5843	135
H(15B)	4282	-119	5902	135
H(16A)	3283	502	7078	120
H(16B)	3638	-662	6960	120
H(18A)	5130	1742	7469	153
H(18B)	4180	1960	7426	153
H(19A)	5181	1383	6247	123
H(19B)	4811	2529	6366	123
H(20A)	4831	238	8343	251
H(20B)	4269	-712	8078	251
H(20C)	3884	414	8263	251
H(21A)	4319	477	4507	177
H(21B)	3490	-115	4723	177
H(22A)	3819	1040	3417	251
H(22B)	3243	31	3498	251
H(23A)	2245	947	3837	256
H(23B)	2676	1764	3300	256
H(24A)	3053	2814	4191	160
H(24B)	2312	2265	4609	160

Table B.7　Compound **13**

Atom	x	y	z	U$_{eq}$
N(9)	4021(3)	1492(5)	5936(4)	87(2)
N(10)	3392(5)	1605(7)	4843(5)	116(3)
N(13)	3218(5)	7208(5)	7366(4)	125(3)
N(14)	4326(6)	7916(5)	5260(6)	145(4)
N(17)	4471(6)	394(8)	7289(4)	124(3)
C(1)	3681(5)	3241(5)	5602(5)	84(3)
C(2)	3382(5)	3599(6)	6290(5)	93(3)
C(3)	3360(4)	4661(6)	6427(5)	80(2)
C(4)	3652(5)	5447(7)	5948(5)	87(3)
C(5)	3953(4)	5053(6)	5272(5)	95(3)
C(6)	3963(4)	3980(6)	5100(4)	96(3)
C(7)	3694(3)	2041(8)	5419(6)	115(4)
C(8)	3637(5)	6576(6)	6099(5)	84(3)
C(11)	3354(5)	6945(5)	6802(3)	89(3)
C(12)	4019(6)	7298(6)	5607(7)	130(5)
C(15)	3841(6)	320(8)	6096(5)	112(3)
C(16)	3747(5)	99(6)	6888(5)	100(3)
C(18)	4628(6)	1547(8)	7216(6)	128(4)
C(19)	4701(6)	1765(7)	6424(5)	103(3)
C(20)	4353(6)	54(9)	8060(5)	168(5)
C(21)	3726(6)	520(6)	4494(6)	148(5)
C(22)	3398(10)	712(11)	3720(8)	209(7)
C(23)	2736(10)	1373(13)	3761(9)	213(8)
C(24)	2831(7)	2133(8)	4364(6)	134(4)

Atom	x	y	z	U_{eq}
H(2)	1876	-852	7264	16
H(3)	1308	181	5990	23
H(5)	4075	100	5307	35
H(6)	4637	-1020	6656	13
H(15A)	3920	-2618	9538	20
H(15B)	3730	-3391	8759	20
H(16A)	2417	-3413	9607	32
H(16B)	2041	-2518	9191	32
H(18A)	715	-3096	6428	34
H(18B)	877	-2354	7238	34
H(19A)	2570	-3083	6641	39
H(19B)	2132	-2181	6357	39
H(20A)	2362	-4268	7457	125
H(20B)	1113	-4505	6984	125
H(20C)	1817	-4683	8217	125
H(21A)	563	-4015	8766	113
H(21B)	-162	-3846	7536	113
H(21C)	86	-3131	8397	113
H(22A)	5232	-2812	8929	33
H(22B)	5680	-2286	10018	33
H(23A)	7278	-2578	9414	25
H(23B)	6636	-2169	8271	25
H(25A)	6464	-572	8249	47
H(25B)	6781	-158	9405	47
H(26A)	5272	-648	9666	25
H(26B)	4810	-422	8417	25
H(27A)	6943	-1423	10951	85
H(27B)	7948	-857	11050	85
H(27C)	8069	-1818	11040	85
H(28A)	8751	-1679	9624	46
H(28B)	8588	-720	9600	46
H(28C)	8106	-1232	8514	46

Table B.8   Compound **18(Iod)₂**

Atom	x	y	z	U_{eq}
I(29)	4770(8)	-1490(8)	11570(8)	50(5)
I(30)	4840(8)	-3520(6)	6670(7)	60(4)
N(9)	3170(7)	-2310(5)	7900(6)	18(17)
N(10)	4920(7)	-1620(5)	8690(7)	18(18)
N(13)	450(13)	1630(9)	4570(12)	60(4)
N(14)	3110(13)	1440(9)	3450(11)	50(3)
N(17)	1390(8)	-3400(6)	7960(8)	40(2)
N(24)	7220(8)	-1350(6)	9490(8)	20(2)
C(1)	3350(9)	-1030(6)	7050(9)	20(2)
C(2)	2310(9)	-670(7)	6880(9)	10(2)
C(3)	1990(9)	-60(7)	6140(10)	20(2)
C(4)	2690(9)	240(6)	5570(8)	20(2)
C(5)	3640(9)	-80(7)	5690(8)	30(2)
C(6)	3960(9)	-770(7)	6520(8)	10(2)
C(7)	3970(9)	-1570(6)	8010(8)	10(2)
C(8)	2100(10)	880(6)	4650(9)	30(2)
C(11)	1170(12)	1310(7)	4520(10)	40(3)
C(12)	2870(11)	1160(7)	4120(9)	40(3)
C(15)	3410(9)	-2880(7)	8880(8)	20(2)
C(16)	2300(9)	-3030(7)	9000(9)	30(2)
C(18)	1220(9)	-2850(8)	7100(9)	30(2)
C(19)	2300(9)	-2610(7)	6910(8)	30(2)
C(20)	1700(15)	-4310(8)	7620(12)	80(4)
C(21)	380(13)	-3620(14)	8180(15)	80(6)
C(22)	5570(9)	-2290(6)	9240(9)	30(2)
C(23)	6760(9)	-2150(7)	9050(10)	20(2)
C(25)	6480(9)	-660(7)	8990(9)	40(2)
C(26)	5300(9)	-790(6)	8960(9)	20(2)
C(27)	7580(12)	-1360(9)	10750(10)	60(3)
C(28)	8260(10)	-1230(9)	9290(12)	30(3)

Table B.9 Compound **19**

Atom	x	y	z	U_{eq}
O(10)	9251(3)	6302(3)	1890(2)	42(1)
N(9)	11098(3)	7336(3)	2049(2)	33(1)
N(13)	9594(5)	9222(6)	7733(4)	83(2)
N(14)	6302(4)	10716(4)	6003(3)	59(1)
N(17)	12294(3)	8950(3)	550(3)	36(1)
C(1)	9494(4)	7554(4)	3369(3)	30(1)
C(2)	10223(4)	7538(4)	4244(3)	33(1)
C(3)	9801(4)	8053(4)	5154(3)	35(1)
C(4)	8640(4)	8687(4)	5201(3)	29(1)
C(5)	7890(4)	8649(4)	4326(3)	33(1)
C(6)	8292(4)	8096(4)	3440(3)	34(1)
C(7)	9913(4)	7022(4)	2374(3)	29(1)
C(8)	8260(5)	9344(4)	6125(3)	39(1)
C(11)	8970(5)	9297(5)	7020(4)	50(1)
C(12)	7173(5)	10101(4)	6085(4)	41(1)
C(15)	11582(4)	6818(4)	1097(3)	37(1)
C(16)	11554(4)	7785(4)	260(3)	37(1)
C(18)	11810(4)	9436(4)	1557(3)	38(1)
C(19)	11809(4)	8445(4)	2383(3)	35(1)
C(20)	13670(4)	8688(5)	578(4)	49(1)
C(21)	12044(5)	9928(5)	-263(4)	58(2)

Atom	x	y	z	U_{eq}
H(2)	11022	7170	4221	40
H(3)	10294	7976	5741	42
H(5)	7089	9012	4345	39
H(6)	7757	8081	2875	40
H(15A)	11072	6100	898	44
H(15B)	12445	6531	1198	44
H(16A)	10682	8014	118	45
H(16B)	11910	7427	-359	45
H(18A)	10954	9747	1466	45
H(18B)	12335	10134	1775	45
H(19A)	12674	8207	2541	42
H(19B)	11428	8784	2999	42
H(20A)	13956	8460	-93	73
H(20B)	13833	8010	1044	73
H(20C)	14114	9426	803	73
H(21A)	12324	9618	-915	88
H(21B)	12497	10684	-99	88
H(21C)	11153	10104	-292	88

Table B.10   Compound $19.H_2O$

Atom	x	y	z	U_{eq}
O(10)	948(5)	2962(4)	1187(3)	60(1)
N(9)	-234(5)	1365(4)	751(4)	51(1)
N(17)	-1808(5)	-312(5)	1775(4)	56(2)
N(14)	-2747(8)	6938(7)	-2518(6)	93(3)
N(13)	-1243(9)	4031(8)	-4324(5)	100(3)
C(1)	-329(6)	3125(5)	-221(4)	39(1)
C(2)	-210(6)	2625(5)	-1129(5)	45(2)
C(3)	-577(6)	3257(6)	-1928(4)	43(2)
C(4)	-1104(6)	4370(6)	-1871(5)	45(2)
C(5)	-1198(7)	4869(6)	-962(5)	55(2)
C(6)	-812(6)	4264(6)	-150(5)	53(2)
C(7)	164(6)	2480(6)	635(4)	43(2)
C(8)	-1569(7)	4994(6)	-2725(6)	55(2)
C(11)	-1412(8)	4476(8)	-3597(6)	65(2)
C(12)	-2214(8)	6058(8)	-2621(6)	66(2)
C(15)	356(7)	634(7)	1496(5)	70(2)
C(16)	-578(7)	293(7)	2199(5)	68(2)
C(18)	-2340(7)	433(7)	979(6)	71(2)
C(19)	-1390(7)	799(7)	295(6)	68(2)
C(20)	-2828(8)	-349(9)	2546(6)	88(3)
C(21)	-1525(11)	-1535(7)	1469(6)	92(3)
O(22)	-3407(19)	8066(8)	-614(7)	215(7)

Atom	x	y	z	U_{eq}
H(2)	116	1866	-1195	55
H(3)	-463	2919	-2525	52
H(5)	-1528	5627	-900	67
H(6)	-877	4622	443	64
H(15A)	734	-63	1208	84
H(15B)	1073	1064	1799	84
H(16A)	-859	982	2551	82
H(16B)	-152	-237	2644	82
H(18A)	-3032	-4	654	85
H(18B)	-2750	1125	1253	85
H(19A)	-1802	1347	-144	82
H(19B)	-1092	125	-68	82
H(20A)	-2509	-825	3061	133
H(20B)	-3636	-676	2300	133
H(20C)	-2993	432	2772	133
H(21A)	-1186	-1974	1999	139
H(21B)	-877	-1527	967	139
H(21C)	-2329	-1893	1243	139
H(22A)	-3000(2)	7500(16)	-1120(10)	323
H(22B)	-3900(2)	7560(15)	-120(13)	323

Table B.11   Compound (TTF)₃(PMC)₂

Atom	x	y	z	U_eq
S(1)	3792	6210(2)	16007(14)	44.0(8)
S(2)	4831(3)	7516(3)	22112(15)	48.2(9)
S(3)	3594(3)	4960(2)	26774(14)	44.5(8)
S(4)	4700(3)	6250(3)	32523(13)	47.4(9)
S(5)	5357(3)	4347(3)	17238(14)	49.8(9)
S(6)	6436(3)	5664(3)	23360(17)	53.4(10)
S(7)	5234(3)	3033(3)	27559(14)	46.5(8)
S(8)	6315(3)	4326(3)	33811(15)	51.8(9)
S(9)	2011(3)	7400(3)	18939(16)	54.0(10)
S(10)	3083(3)	8762(3)	24349(14)	47.5(9)
S(11)	1913(3)	6208(3)	29672(15)	50.9(9)
S(12)	2973(3)	7561(3)	35266(14)	46.5(9)
C(13)	4254(8)	6502(8)	2211(5)	38(3)
C(14)	4197(8)	5940(9)	2660(5)	39(3)
C(15)	5880(9)	4604(10)	2333(5)	42(3)
C(16)	5823(8)	4075(9)	2773(5)	40(3)
C(17)	2544(9)	7734(10)	2475(6)	41(3)
C(18)	2490(9)	7224(10)	2942(5)	44(3)
C(19)	4210(9)	7145(10)	1261(6)	53(4)
C(20)	4695(9)	7734(11)	1546(6)	52(4)
C(21)	3849(8)	4701(10)	3333(5)	47(3)
C(22)	4367(9)	5277(10)	3597(6)	49(3)
C(23)	5792(10)	5267(11)	1393(6)	57(4)
C(24)	6258(11)	5849(12)	1666(7)	63(4)
C(25)	5441(9)	2764(11)	3416(6)	53(4)
C(26)	5926(10)	3351(12)	3691(7)	60(4)
C(27)	2314(10)	8334(12)	1528(7)	59(4)
C(28)	2807(10)	8959(12)	1776(7)	64(4)
C(29)	2125(10)	6018(12)	3642(6)	57(4)
C(30)	2607(9)	6657(11)	3896(6)	53(4)
C(31)	5359(8)	0340(8)	-2062(5)	36(3)
C(32)	6051(8)	0869(8)	-2201(5)	37(3)
C(33)	6188(8)	0724(9)	-2746(5)	37(3)
C(34)	5568(8)	0100(9)	-2948(5)	41(3)
C(35)	5059(8)	-0129(9)	-2528(5)	43(3)
C(36)	5891(7)	4684(8)	0009(4)	33(2)
C(37)	5031(8)	4542(9)	0006(5)	42(3)
C(38)	4645(8)	5416(9)	0015(5)	40(3)
C(39)	5287(8)	6111(8)	0019(5)	35(3)
C(40)	6059(7)	5637(8)	0018(4)	31(2)

Atom	x	y	z	U_eq
C(41)	5017(9)	0245(10)	-1533(5)	47(3)
C(42)	6582(9)	1437(9)	-1850(5)	45(3)
C(43)	6816(8)	1226(9)	-3060(5)	44(3)
C(44)	5482(9)	-0239(11)	-3504(6)	53(4)
C(45)	4305(9)	-0752(10)	-2603(6)	49(3)
C(46)	6546(8)	3945(9)	0088(5)	40(3)
C(47)	4600(9)	3666(10)	-0035(6)	47(3)
C(48)	3719(9)	5553(10)	-0028(6)	53(3)
C(49)	5142(8)	7103(9)	-0003(5)	44(3)
C(50)	6919(8)	6073(9)	0055(5)	41(3)
O(52)	5429(7)	0095(9)	-1134(4)	73(3)
O(52)	7321(7)	1485(8)	-1850(5)	65(3)
O(53)	6973(8)	2043(7)	-3020(5)	75(4)
C(54)	5413(12)	0246(9)	-3889(4)	110(6)
O(55)	3865(7)	-0775(9)	-29874	72(3)
C(56)	6457(7)	3202(6)	0286(4)	59(3)
C(57)	3976(11)	3453(11)	0175(8)	156(9)
O(58)	3321(9)	544(2)	-0421(7)	211(14)
O(59)	4455(8)	7473(9)	-0044(6)	89(4)
C(60)	7277(7)	6409(8)	-0312(4)	62(3)
O(61)	4197(6)	0355(7)	-1528(4)	50(2)
O(62)	6146(7)	1949(8)	-1515(4)	72(3)
C(63)	7203(8)	06811(7)	-3397(5)	71(3)
C(64)	5476(7)	-1166(8)	-3522(4)	63(3)
O(65)	4199(6)	-1259(7)	-2166(4)	58(3)
C(66)	7277(6)	4237(7)	-0097(5)	66(3)
O(67)	4924(6)	3089(7)	-0396(4)	58(3)
C(68)	3377(6)	5844(9)	0395(4)	67(3)
C(69)	5835(7)	7586(7)	0027(5)	69(3)
O(70)	7214(6)	6035(9)	0543(4)	62(3)
C(71)	3780(11)	0062(13)	-1061(7)	67(5)
C(72)	6612(14)	2523(16)	-1147(9)	98(7)
C(73)	7775(13)	1160(15)	-3739(9)	90(6)
C(74)	5301(12)	-1586(13)	-4032(7)	77(5)
C(75)	3434(12)	-1819(14)	-2169(8)	81(5)
C(76)	7988(11)	3623(12)	0017(7)	72(5)
C(77)	4610(10)	2175(11)	-0448(6)	58(4)
C(78)	2470(13)	5956(15)	0345(9)	91(6)
C(79)	5770(13)	8589(14)	-0031(8)	85(6)
C(80)	8073(12)	6346(14)	0639(8)	79(5)

| Atom	x	y	z	U_eq
H(19)	4101	7233	0898	64
H(20)	4949	8242	1387	62
H(21)	3631	4176	3497	56
H(22)	4542	5164	3949	59
H(23)	5695	5346	1028	68
H(24)	6493	6362	1500	75
H(25)	5223	2231	3571	64
H(26)	6056	3240	4050	72
H(27)	2142	8405	1172	71
H(28)	2996	9484	1598	77
H(29)	1915	5501	3818	68
H(30)	2737	6609	4259	63
H(71A)	3770	-0609	-1046	100
H(71B)	3218	0297	-1074	100
H(71C)	4073	0301	-0749	100
H(72A)	7026	2150	-0959	147
H(72B)	6242	2791	-0896	147
H(72C)	6882	3013	-1336	147
H(73A)	7477	1630	-3942	135
H(73B)	8014	0718	-3978	135
H(73C)	8211	1448	-3525	135
H(74A)	5746	-1447	-4266	116
H(74B)	4785	-1341	-4181	116
H(74C)	5254	-2251	-3991	116
H(75A)	2969	-1427	-2089	122
H(75B)	3491	-2305	-1906	122
H(75C)	3340	-2094	-2515	122
H(76A)	8016	3473	0390	108
H(76B)	8494	3933	-0077	108
H(76C)	7924	3058	-0187	108
H(77A)	4844	1792	-0167	87
H(77B)	4758	1923	-0787	87
H(77C)	4012	2187	-0428	87
H(78A)	2336	6437	0089	136
H(78B)	2258	6126	0684	136
H(78C)	2221	5378	0227	136
H(79A)	5524	8736	-0375	128
H(79B)	6317	8862	0003	128
H(79C)	5427	8836	0241	128
H(80A)	8439	5979	0429	118
H(80B)	8227	6271	1010	118
H(80C)	8119	6993	0543	118

APPENDIX C

Powder Second Harmonic Generation Measurement

We have measured the second harmonic generation from microcrystalline powders of compounds **11(TPA)** (Sec. 3.2) and **19.H$_2$O** (Sec. 3.3) using the Kurtz and Perry[1] method with minor modifications of the original layout. Particle sizes were graded using standard sieves; sizes ranging from 50 - 420 μm were studied. Samples were loaded in glass capillaries having an inner diameter of 600 μm. Fundamental beam (1064 nm) of a Q-switched ns-pulsed (6 ns, 10 pps) Nd:YAG laser (Spectra Physics, Model INDI 40) was used. The beam was split and approximately 10% was passed through a 200 μm thick powder sample of N-4-nitrophenyl-(*S*)-prolinol, NPP (average particle size ~ 175 μm) to monitor pulse to pulse fluctuation of the beam. The main beam was split further into two halves and focused onto the sample from opposite directions. The scattered SHG signal was collected using a concave mirror and lens combination with a 45° disposition to the incident beams (Fig. C.1). The second harmonic signal from reference and the sample were collected using appropriate optics and detected using a monochromator (Jobin-Yvon Model HRS–2), PMT (Hamamatsu, Model C956-06/131) and oscilloscope (Tektronix, Model TDS 210, 60MHz). Calibrated neutral density filters were used when needed, so that the signal measured on the oscilloscope was in the same range for all samples and the reference; this ensures that readings are taken in a linear region of the PMT. Microcrystalline urea having particle sizes 150 - 350 μm was used as the reference in all SHG measurements. The measured SHG signal from the sample is first corrected for the background noise and the fluctuation in reference before comparing with similarly corrected signal of the standard, urea. Measurements for the sample and the standard were carried out for different particle sizes. Our setup is calibrated by measurements on urea and NPP. The SHG measured for NPP is 138 U (1U = SHG of urea) at saturation. The errors in the measurements are ~ 10 - 15 %.

The compounds we have studied showed good stability under laser irradiation and no sign of decomposition was detected, even on continuous irradiation with a laser power of 1GW cm^{-2}. Each measurement was repeated at least three times over a period of time and the value of SHG reported is the average of such measurements. In all cases we have

studied, the SHG saturated at higher particle sizes, indicating phase matchable behavior of the **materials.**
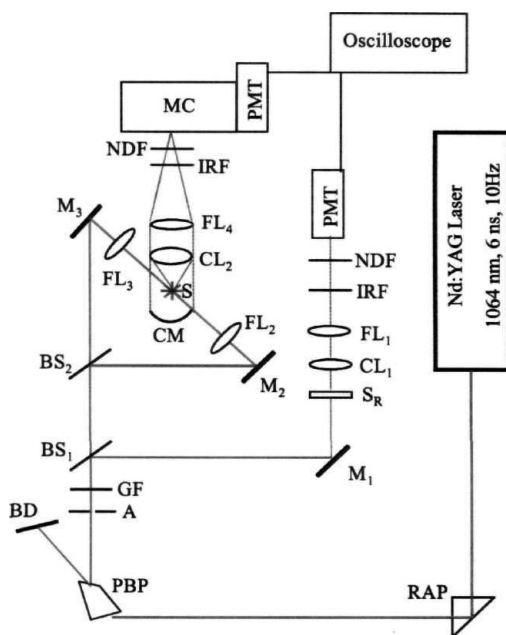
*A: Aperture, BD: Beam Dump, BS,, **BS₂:** Beam Splitters, CL1, CL2: Collecting Lenses, CM: Concave Mirror, **FLₙ:** Focussing Lenses, GF: Green Filter, **IRF: IR** Filter, **Mₙ:** Mirrors, MC: Monochromator, NDF: Neutral Density, Filters, PBP: Pellin-Broca prism, PMT: **Photomultiplier** Tube, RAP: Right angle prism, S: Sample, **Sᵣ:** Reference Sample.*

Figure C.1 *Setup for measurements of **SHG** from microcrystalline powders.*

Reference

1.   Kurtz, S. K.; Perry, T. T. *J. **Appl.** Phys.* **1968, 39,** 3798.

APPENDIX D

Powder and Thin Film Conductivity Measurements

The 2-probe powder conductivity measurements on PANI-PSS (Sec. 4.2) as well as the polyanion salts of TTF (Sec. 4.3) were carried out using the pressed pellet technique in a home-built stainless steel cell' based on a modification of the apparatus described by Wudl and Bryce.[2] 4-probe measurements of the PANI-PSS films (Sec 4.2) were carried out on 15-layer films coated on glass. Samples were mounted on a Perspex platform; electrical connections were made either through equally spaced thin wire press contacts or sublimed aluminum strips. In the case of the $(TTF)_3(PMC)_2$ single crystals, contacts were established by attaching thin wires with conducting silver paint. All conductivity measurements were carried out at room temperature. A Keithly Model 224 Constant Current Source and Keithly Model 175 Multimeter were used. Typically, currents in the range 1 - 4 mA were employed where Ohmic behavior was observed.

References

1. Prasanna, S.; Sastry, B. S. S.; Radhakrishnan, T. P. *Indian. J. Pure. Appl. Phys.* **1998,** *36,* 748.
2. Wudl, F.; Bryce, M. R. *J. Chem. Edn.* **1990,** *67,* 717.

Publications and Presentations

PUBLICATIONS

1. Jayanty, S.; Radhakrishnan, T. P. *J. Mater. Chem.* **1999,** *9,* 1707.
   'Core and Sheath' Structure of a TTF Complex Forming a Square Grid.

2. Jayanty, S.; Kumar, D. B. K.; Radhakrishnan, T. P. *Synth. Metals* **2000,** *114,* 37.
   Structure and Magnetism of a Phenazinium Cyclopentadienide Salt.

3. Jayanty, S.; Radhakrishnan, T. P. *Chem. Mater.* **2001**, *13*, 2072.
   Solid State Charge Transfer Promoted by an Anchoring Agent : A 2-component Analog of Kofler's Ternary Complex.

4. Jayanty, S.; Radhakrishnan, T. P. *Chem. Mater.* **2001**, *13*, 2460.
   Modeling Molecule-in-a-Crystal : The Case of Push-pull Quinonoids.

5. Jayanty, S.; Gangopadhyay, P.; Radhakrishnan, T. P. *J. Mater. Chem.* **2002,** *12,* 2792.
   Steering Molecular Dipoles from Centrosymmetric to Noncentrosymmetric and SHG Active Assembly Using Remote Functionality and Complexation.

6. Jayanty, S.; Radhakrishnan, T. P. *Chem. Eur. J.* (*in press*).
   Enhanced Fluorescence of Remote Functionalized Diaminodicyanoquino-dimethanes in the Solid State and Fluorescence Switching in a Doped Polymer by Solvent Vapors.

7. Jayanty, S.; Prasad, G. K.; Sreedhar, B.; Radhakrishnan, T. P. *Polymer* (*in press*).
   Polyelectrolyte Templated Polyaniline - Film Morphology and Conductivity.

8. Jayanty, S.; Radhakrishnan, T. P. *(submitted)*
   Spontaneous Resolution through Helical Assembly of a Conformationally Chiral Molecule With an Unusual Zwitterionic Structure.

PRESENTATIONS

1. Poster presented at the National Laser Symposium, Hyderabad, December, **1999.**
   Jayanty, S.; Ravi, M.; Rao, D. N.; Radhakrishnan, T. P. "A Rigorous Test of the Salt Model for SHG Active Molecular Materials."

2. Lecture presented on receiving the Third Annual Dr. K. V. Rao Research Award-2003, Hyderabad, March, **2003.**
   Jayanty, S. "Linear and Nonlinear Optical properties of Novel Organic Molecular Materials Based on Diaminodicyanoquinodimethanes."